Termination of Replication Stress Signaling in *Saccharomyces cerevisiae*

A Dissertation

Presented to the Faculty of the Graduate School of Cornell University

In Partial Fulfillment of the Requirements for the Degree of Doctor of Philosophy

By

Carolyn Marie Jablonowski

February 2016

Termination of Replication Stress Signaling in *Saccharomyces cerevisiae*

Carolyn Marie Jablonowski, Ph. D.

Cornell University 2016

During DNA replication, replication forks are prone to stall and collapse. To prevent genomic instability, DNA damage checkpoint (DDC) kinases are activated and coordinate various cellular responses. In *S. cerevisiae*, the key DDC kinase Rad53 plays crucial roles in the regulation of transcription, dNTP levels, fork stability, cell cycle progression and origin firing. As part of the checkpoint response, Rad53 activation results in a major arrest in the cell cycle, which is thought to be important to increase the time in which DNA repair systems can function before the onset of mitosis, therefore preserving the faithful transmission of the genetic material to daughter cells. Although checkpoint signaling is beneficial for preventing genomic instability, Rad53 signaling needs to be turned off following repair to allow for resumption of cell proliferation. Similarly, in humans, activation of checkpoint kinases CHK1 and CHK2 must also be under stringent control to allow for cell proliferation. While different mechanisms for down-regulation have been identified, how they function together to efficiently control checkpoint signaling is not known. In particular, it is not clear how these mechanisms function locally at lesions or in diffused nuclear pools of Rad53 and how they are coordinated. Work from my thesis, summarized in the next paragraph, has elucidated important aspects of the spatio-temporal coordination of checkpoint down-regulation by multiple, distinct mechanisms.

In yeast, several phosphatases have been implicated in regulating checkpoint deactivation. Recently, our group uncovered a phosphatase-independent mechanism for

down-regulating Rad53 signaling named DAMP (Dampens Adaptor Mediated-Phosphosignaling). DAMP relies on the Slx4 scaffold protein competing with the checkpoint adaptor Rad9 at sites of lesions to counteract Rad53 activation. Here, I show that DAMP functions in parallel with canonical phosphatase mechanisms for Rad53 down-regulation. I show that *slx4Δ* cells phenocopy cells lacking the main Rad53 phosphatase, Pph3. Both *pph3Δ* and *slx4Δ* cells show selective sensitivity to methyl methanesulfonate (MMS), accumulate chromosomal defects and hyperactivate Rad53. Both Slx4 and Pph3 seem to converge to the regulation of the Mus81 nuclease, which is necessary for downstream repair. Interestingly, deletion of both *SLX4* and *PPH3* leads to a synergistic increase in MMS sensitivity and Rad53 activation, suggesting that efficient down-regulation of DDC signaling requires the coordinated action of DAMP and phosphatases. I propose that these mechanisms operate in distinct spatio-temporal modes, with Slx4 dampening Rad53 activation at lesions, and Pph3 functioning on free, active pools of Rad53 to turn off the checkpoint response. Collectively, the results from my thesis reveal that checkpoint control is tightly regulated by multiple coordinated mechanisms to allow for cell proliferation following DNA damage. Furthermore, given that checkpoint regulation is highly conserved from yeast to humans, this work contributes to better understanding the importance of checkpoint control and provides rationale to manipulate checkpoint signaling in human systems and particularly in cancer research.

BIOGRAPHICAL SKETCH

Carolyn Marie Jablonowski was born in Carbondale, PA, a small town in northeastern Pennsylvania. While attending high school at Carbondale Area Jr/Sr High School, Carolyn was among the top of her class. She graduated in the top 3 graduating seniors and earned a prestigious GPA of 101.4% and having taken 4 Advanced Placement classes during her senior year.

After completing high school, Carolyn attended East Stroudsburg University of Pennsylvania where she dual majored in Biochemistry and Chemical Biotechnology. As an undergraduate at ESU, she performed research in a small lab with Dr. Paul Wilson. Her project was investigating the phylogeny and biodiversity of species populations by studying the DNA sequences of mitochondrial cytochrome *b* gene from small darter fish from the Ozarks collected earlier by Dr. Wilson. During the summer between her junior and senior years, Carolyn was awarded into the Research Experience for Undergraduates (REU) program where she worked under Dr. Wenwan Zhong in a bioanalytical chemistry lab at the University of California Riverside. Her research project was innovating a method using rolling circle amplification combined with capillary electrophoresis coupled with laser-induced fluorescence to detect minute amounts of a target siRNA (small interfering RNA) from *Arabidopsis* plants (Li, Jablonowski, *et al.* 2009). During that intense 10-week program, Carolyn got a taste for what being a science graduate student was like, and decided to pursue a PhD in biochemistry.

After graduating from ESU with Summa cum laude, Carolyn bridged her undergraduate year by working as a vaccine formulation technician at Sanofi Pasteur, a

major pharmaceutical company in the United States. There, she learned valuable laboratory skills including proper aseptic technique, good documentation, and analytical consistency.

In 2010, Carolyn joined the Molecular Biology and Genetics department at Cornell University in the field of Biochemistry, Molecular and Cell Biology to pursue her PhD. Eventually, Carolyn joined the lab of Dr. Marcus Smolka with the goal of further understand life. In the initial years of her thesis work, Carolyn investigated how enzymes that control protein acetylation contribute to the DNA damage response. Later, she studied how the DNA damage checkpoint pathway is modulated by concerted actions of the major phosphatase Pph3 and the scaffold protein Slx4 during replication stress to prevent hyper-checkpoint signaling. During her time at Cornell, she made many memories and life-long friends to which she will be eternally grateful for.

This dissertation is dedicated to
my father, Edward Jablonowski,
for his unconditional love and support.

ACKNOWLEDGEMENTS

This dissertation represents an incredible milestone in my life. It has been an incredible and fulfilling journey to partake on. Though the road was not always easy, well-laid out, or predictable, it has been my own path. I have made it through an incredible experience, to which I will always cherish.

First of all, I would like to thank Marcus Smolka, for taking me into the lab. Marcus is an incredible advisor and Professor. Marcus has been everything I've ever wanted in a mentor; he's enthusiastic and engaged in my research and inspires me to go above and beyond what I ever thought possible. Though we occasionally butted heads, he always had my best interests in mind. His constant support and mentorship is a key factor in allowing me the possibility to pursue a PhD.

I would also like to thank the immense support of my committee members: Eric Alani and Haiyuan Yu. In particular, I would like to express my gratitude to both Eric Alani and Bill Brown, our current Director of Graduate Studies, for their emotional support during graduate school. Both Eric and Bill were supportive and understanding when I was having rough times and helped me work through issues during grad school. I could not be here without them.

My fellow lab members made my time at Cornell really wonderful. I spent innumerable hours with them and I couldn't have asked for better people to have spent time with. Specifically, I would like to thank Zé Cussiol, Laura Nemeth Jaramillo, Patrice Ohouo, DS Kim, Mike Lanz, Susannah Oberly, Francisco Bastos de Oliviera, Yi Liu, and Jennie Sims. These wonderful people picked me up when I was down and also were

very enjoyable to be around. I couldn't have spent these last several years with a better group of people.

My father, Ed Jablonowski, has been an immeasurable support system my entire life. Recently, life has gotten in the way, which almost caused me to leave graduate school. Fortunately, I have wonderful individuals in my life that helped me along and prosper. In addition to my dad, I would like to thank my best friends Amy Larson, Maggie Gustafson, Jeney Wierman, Adam Moody, and Casey Inman. They were the ones that kept me going through difficult times by persistently encouraging me. I can't thank them enough for everything they've done for me.

TABLE OF CONTENTS

LIST OF FIGURES

LIST OF TABLES

CREDITS

All material in chapters 3 and 4 are published as a manuscript in *Genetics*[1]. FACS (Fluorescence Activated Cell Sorting) in figures 3C, 3.5D, and 3.8A, was performed by Dr. José Cussiol, a post doc in the lab. The sensitivity assay in figure 4.5 was performed by Dr. José Cussiol. ChIP-seq experiments in figure 4.6 was carried out by Dr. Grant Brown's laboratory in the University of Toronto. Fluorescence microscopy experiments in figure 4.4 was also performed by members of the Brown laboratory. Model figures 4.3 and 4.8 were created by Dr. Marcus Smolka. All other experiments in this work were done by Carolyn Jablonowski.

1. Jablonowski, C.M.; Cussiol, J.R.; Oberly, S.; Yimit, A.; Balint, A.; Kim, T.; Zhang, Z.; Brown, G.W.; Smolka, M.B. (2015). Termination of replication stress signaling via concerted action of the Slx4 scaffold and the PP4 phosphatase. Genetics *201,* 937-949.

CHAPTER 1

INTRODUCTION

Accurate transmission of genetic material is vital for optimal cell and organismal survival. Prior to cell division, cells must coordinate many highly complicated processes such as cell growth, DNA replication, chromatin condensation, and chromosome segregation. These processes need to be performed accurately and be tightly controlled to generate viable progeny. Failure to properly regulate these processes has the potential to result in genomic instability.

Cells are constantly exposed to many types of endogenous and exogenous sources of stress that can potentially lead to genomic instability, a hallmark of cancer (Hoeijmakers 2009; Phillips *et al.* 1988). Stalled DNA replication forks and collisions between replication and transcriptional machinery are examples of endogenous sources of replication stress, which can be deleterious to the cells. Additionally, genotoxins can modify DNA, can negatively impact genomic stability by causing DNA gaps, mutations, and breaks. If left unchecked, DNA damage can cause genomic sequence loss and sequence rearrangements, which is detrimental to preserving genomic integrity. Loss of genomic integrity is a driving force for tumorigenesis (Burell *et al.* 2013; Hanahan & Weinberg 2011). This is supported by the observation that genomic instability allows cancer cells to circumvent the checkpoint surveillance system and cell death mechanisms and promotes a significant proliferative advantage by deregulating tumor suppressing genes (Beckman & Loeb 2006; Lowe et al. 2004).

Fortunately, cells are equipped with a highly sophisticated surveillance mechanism, called the DNA Damage Checkpoint (DDC), to monitor for abnormal DNA structures and elicit a variety of cellular responses to preserve genomic integrity. Therefore, proper checkpoint signaling constitutes a barrier to cancer transformation by preventing genomic instability (Bartkova *et al.* 2005; Bartkova *et al.* 2006). Although the DDC signaling pathway is necessary for genome integrity and cellular survival, aberrant hyper-DDC signaling is deleterious for cells. Therefore, DDC signaling needs to be kept in-check. My graduate work focused on how DDC signaling is down-regulated and coordinated by two distinct, but complementary mechanisms.

The Checkpoint Signaling Pathway as a Genome Surveillance Mechanism

To protect genomic integrity, the DDC monitors and protects the genome. The DDC is composed of a kinase signaling network that senses DNA damage and elicits a series of responses that promote proper cell survival. In the budding yeast *Saccharomyces cerevisiae*, the apical kinase Mec1 (ATR in humans) plays an essential role in the checkpoint pathway by initiating a phosphorylation cascade to downstream effector kinases (see **Figure 1.1**; Ma *et al.* 2006; Pellicioli *et al.* 1999; Cortez *et al.* 2001; Friedel *et al.* 2009; Harrison & Haber 2006). This signaling cascade regulates several cellular responses that include regulation of cell cycle progression, replication fork stability, transcription, and DNA repair with the goal of preserving genomic integrity (see **Figure 1.1**; Cobb *et al.* 2003; Cobb *et al.* 2005; Desany *et al.*1998; Lopes *et al.* 2001; Tourrière *et al.* 2005). At the onset of DNA damage or replication stress, the checkpoint

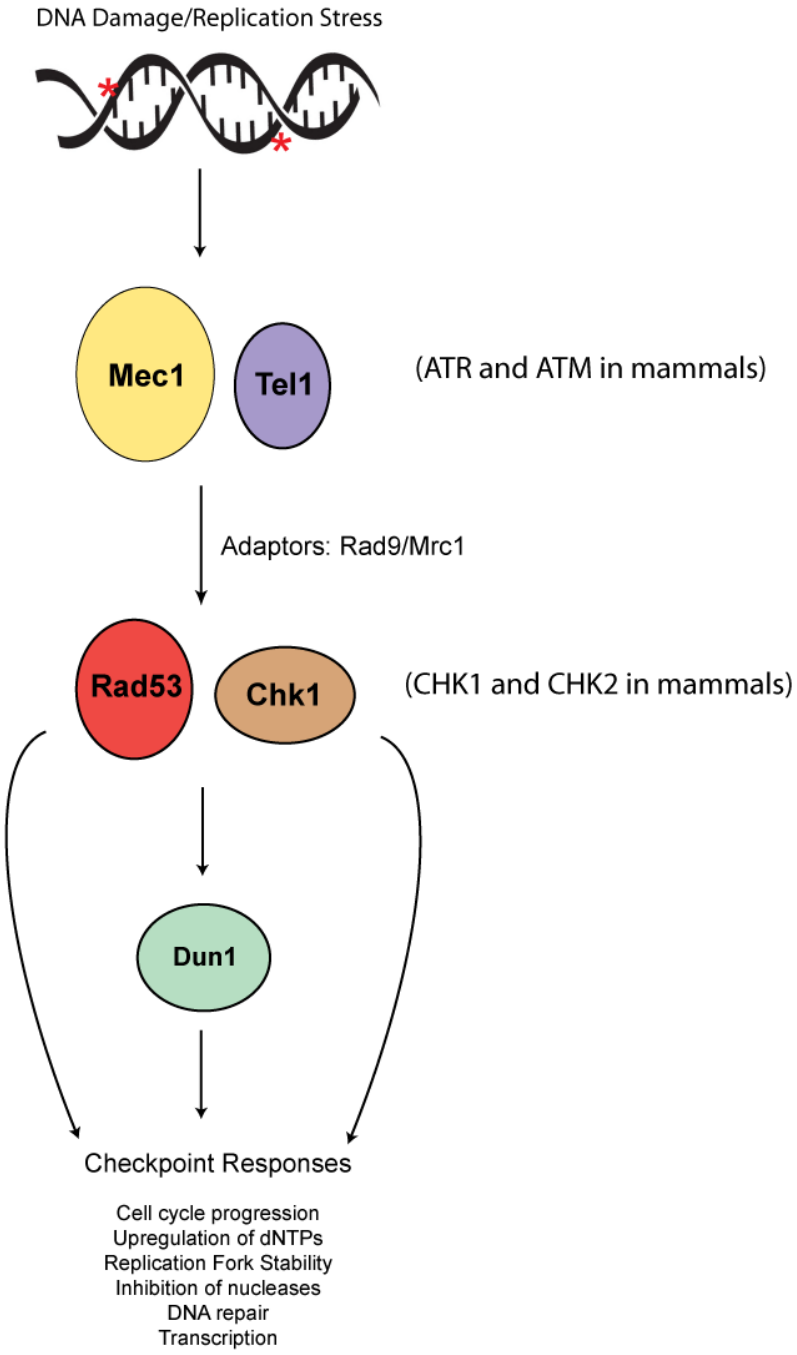
DNA Damage/Replication Stress
Mec1
Tel1
(ATR and ATM in mammals)
Adaptors: Rad9/Mrc1
Rad53
Chk1
(CHK1 and CHK2 in mammals)
Dun1
Checkpoint Responses
Cell cycle progression
Upregulation of dNTPs
Replication Fork Stability
Inhibition of nucleases
DNA repair
Transcription

Figure 1.1. Central components of the *S. cerevisiae* checkpoint signaling pathway. Upon DNA damage or replication stress, the apical kinases Mec1 and Tel1 (human ATR and ATM) sense damage and signal to effector kinases Rad53 and Chk1 (human CHK1 and CHK2). The signal transduction from the sensor kinases to the effector kinases requires the help of checkpoint adaptor proteins, Rad9 and/or Mrc1. Effector kinases elicit a wide range of cellular responses (indicated) as well as activating another down-stream kinase, Dun1, to preserve genomic integrity.

has a major role in delaying mitosis to allow enough time for repair before resuming cellular division. Importantly, cells with mutations in checkpoint pathway components cause increased genomic instability and correlate with an increased predisposition to cancers (Myung *et al.* 2001a; Myung *et al.* 2001b; Chen & Kolodner 1999). Thus, proper checkpoint control is necessary to prevent genomic instability and cellular survival, as described later below.

In this introduction, I will discuss key concepts central to my thesis work, focusing on the importance of DDC during DNA replication. Following this, I will discuss how the checkpoint pathway is activated, what cellular processes it regulates, and how the checkpoint is deactivated.

DNA Replication is an Inherent Source of Genomic Instability

DNA duplication (replication) is an essential event that is required for transmission of genetic information to daughter cells. It is a highly dynamic process that needs to be carefully regulated and maintained to ensure accurate transmission of genetic material. However, DNA replication can compromise genomic integrity (Myung *et al.* 2001; Tercero *et al.* 2003; Katou *et al.* 2003; Lopes *et al*. 2001). DNA replication is initiated by the recruitment of an extensive network of proteins, termed the “replisome”, to DNA replication origins. These replication origins are designated sites for the initiation of DNA duplex unwinding and DNA synthesis that is highly regulated with regard to whether and when an origin is “fired” (initiated). At each origin, the replisome machinery unwinds and replicates the two parental DNA strands generating two replication “forks” in opposing directions. Although DNA damage can occur during any cell cycle stage, cells are

particularly vulnerable during S phase, when the DNA is unwound. Single-strand DNA is generated during DNA replication and is intrinsically more labile than double-stranded DNA (Lindahl 1993). Because replication forks generate regions of ssDNA, they are vulnerable structures that are prone to fork stalling or collapse, providing an inherent source of genomic instability. Additionally, upon collapse, the exposed fork structures can be further processed into double-strand breaks (DSBs) by structure specific nucleases (Costanzo *et al* 2003). Thus, during DNA replication, the DDC has a vital role in monitoring and maintaining the integrity of the genome (Desany *et al.* 1998; Foiani *et al.* 2000; Lopes *et al.* 2001; Myung & Kolodner, 2002).

Although DNA replication provides a potential source for genomic stability, DNA replication can be a useful target for anti-cancer drugs. Cancer cells are highly proliferative and more prone to stress during DNA replication. Currently, many anti-cancer therapy drugs target components of DNA replication. For instance, camptothecin inhibits topoisomerase 1 (reviewed in Wang 2002), which is important for alleviating torsional stress generated by DNA replication, and cisplatin is a DNA crosslinker. Additionally, doxorubicin is both a DNA polymerase and topoisomerase II inhibitor, and gemcitabine is a toxic cytidine nucleoside analog (Tacar *et al.* 2013; Mose *et al.* 2002). Furthermore, because checkpoint proteins prevent cells from deleterious collapse during replication stress, inhibitors of checkpoint proteins have started to be explored as novel anti-cancer therapies. For example, inhibitors of the human checkpoint kinase ATR selectively kill cancer cells with heightened replication stress, while normal cells with normal DNA replication and relatively low levels of DNA lesions are left generally

unaffected (Murga *et al.* 2011; Toledo *et al.* 2011 (a); Hoglund *et al.* 2011; Toledo *et al.* 2011 (b); Reaper *et al.* 2011).

In the next section, I will address how the DNA Damage Checkpoint becomes activated in response to DNA replication stress.

Checkpoint Activation

DNA damage checkpoints are a critical system in eukaryotic cells. Checkpoints sense DNA damage, delay the cell cycle prior to mitosis, and control a wide range of cellular processes with the end goal of preserving genomic integrity (Friedel *et al.* 2009). Checkpoints rely on the actions of key PI3K-like kinases (PI3KK) Mec1 (Mitosis Entry Checkpoint 1) and Tel1 (Telomere Maintenance 1) in budding yeast and ATM (Ataxia telangiectasia mutated) and ATR (Ataxia telangiectasia mutated and Rad3-related) in human cells (Cimprich & Cortez, 2008; Sanchez *et al.* 1996). Tel1 (human ATM) and Mec1 (human ATR) are phosphoinositide 3-kinase (PI3K)-related kinases (PIKKs) that share significant sequence homology and phosphorylate an overlapping set of protein substrates (Smolka *et al* 2007; Bastos de Oliveira *et al* 2015). Both preferentially phosphorylate serine or threonine residues that are followed by glutamine residue (S/T-Q motifs) (Kim *et al.* 1999; Chan *et al.* 1999; Cortez *et al.* 1999; and Sweeney *et al.* 2005). Often, these target sites are found in clusters in substrates or SQ/TQ cluster domains (SCDs) (Traven 2005). All PIKKs have a common structure in which their kinase domain is flanked by both FRAPP, ATM, TRRAP (FAT) and FAT C-terminal (FATC) domains, which is likely important for scaffolding or protein binding surfaces to proteins (Cimprich

& Cortez 2008; Bosotti *et al.* 2000; Zhao *et al.* 2001). Tel1/ATM is primarily activated in response to DNA double strand breaks (DSBs), while Mec1/ATR can sense a wide variety of DNA lesions (Cimprich & Cortez 2008). Mec1 is widely thought to be a sensor of DNA damage (Carr, 2002; Melo & Toczyski 2002), but has roles in unperturbed S phase, as it regulates dNTP levels and DNA replication origin firing (Zhao *et al.* 2001; Randall *et al.* 2010).

During the DNA damage checkpoint response, the Mec1 and Tel1 kinases in budding yeast sense stress and activate the effector kinases Rad53 and Chk1, as well as the down-stream kinase Dun1 (**Figure 1.1**) to elicit the checkpoint response. The activation and signal transduction of this signaling pathway is highly coordinated and regulated at several keys steps and will be discussed below.

Single-Stranded DNA as the Upstream Signal for Checkpoint Activation

Single-stranded DNA (ssDNA) is a major signal for checkpoint activation. Exposed ssDNA occurs only transiently in the cell, because it is rapidly coated with the single-stranded DNA binding protein complex RPA (for Replication Protein A) (Wold 1997). During unchallenged replication, the amount of ssDNA is limited. However, during replication stress, the stalling of polymerases uncouples the activities of polymerase and helicases, leading to the exposure of extensive amounts of ssDNA-RPA complex formation (**Figure 1.2a**; Majka *et al* 2006; Wold 1997; Zou & Elledge 2003). Alternatively, ssDNA can be generated by resection through the action of nucleases (Majka *et al* 2006; Wold 1997; Zhu *et al* 2008). RPA-bound ssDNA interacts

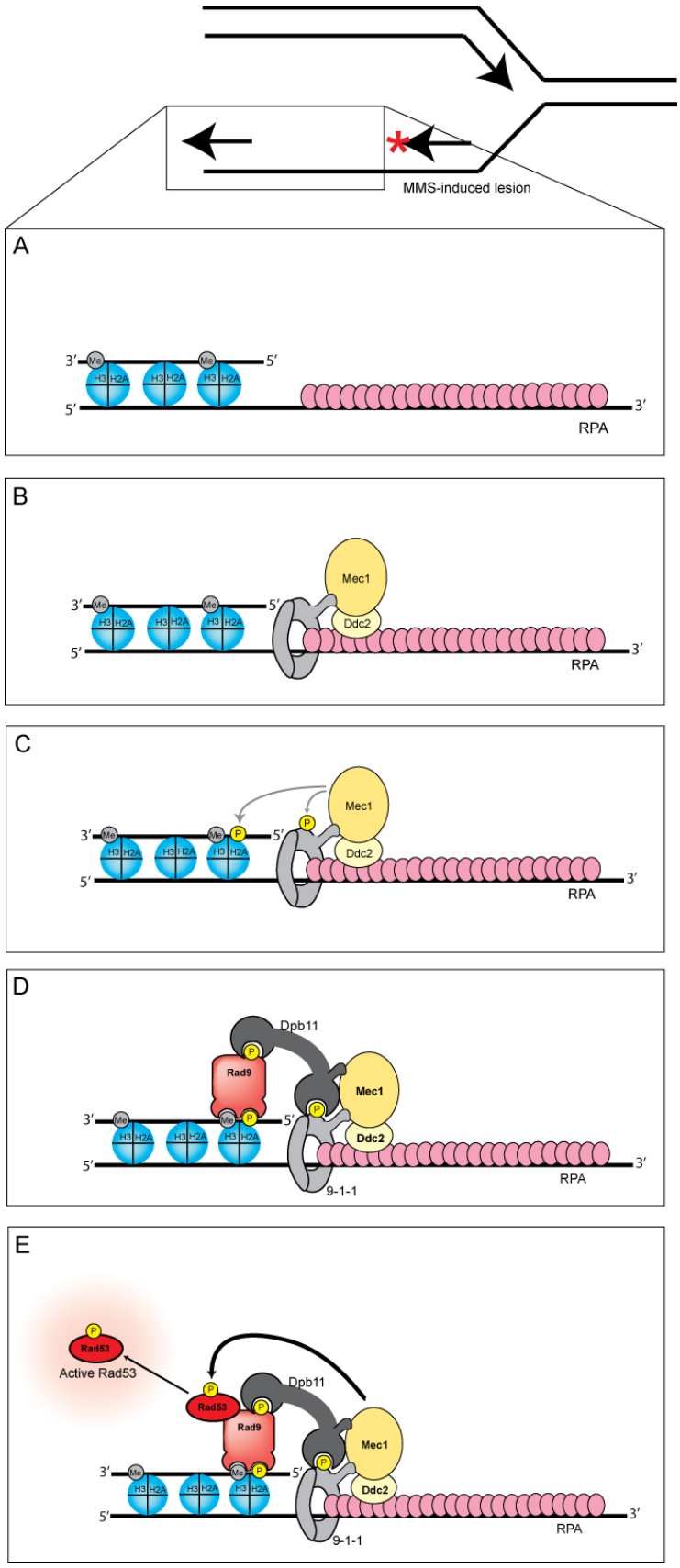
MMS-induced lesion
A
3′
5′
Me
H3
H2A
RPA
B
Mec1
Ddc2
C
P
D
Dpb11
Rad9
9-1-1
E
Rad53
Active Rad53

Figure 1.2. Mec1-to-Rad53 checkpoint signal transduction after methyl methanesulfonate (MMS, a DNA-alkylating drug)-induced replication stress. Low doses of MMS generate bulky adducts on DNA bases, preventing the passage of DNA polymerases during S-phase. Regions of ssDNA are left behind moving DNA replication forks. Exposed ssDNA is rapidly coated with the ssDNA-binding protein RPA (shown as pink spheres) (a). The sensor kinase Mec1-Ddc2 recognizes ssDNA. Independently, the 9-1-1 checkpoint clamp complex (composed of yeast Ddc1-Mec3-Rad17) recognize 5' recessed ends at ds/ssDNA junctions (b). The Ddc1 subunit stimulates and activates Mec1. Mec1 then phosphorylates Ddc1 on Thr601 and histone H2A on Ser129 (c). These phosphorylated residues create chromatin docking sites for Dpb11 and Rad9 checkpoint proteins. Dpb11's unstructured C-terminal further stimulates Mec1 activity (d). Rad9 provides a docking site for Rad53 molecules in the vicinity of active Mec1. Rad53 associated with Rad9 increases the local concentration of Rad53 and allows it to undergo *in trans* autophosphorylation. Mec1 then phosphorylates and activates Rad53. Active Rad53 rapidly diffuses from chromatin where it phosphorylates several substrates in the nucleus to elicit the checkpoint response (e).

with the Mec1 subunit, Ddc2 (ATRIP in humans), which is an essential player in Mec1-dependent checkpoint activation (**Figure 1.2b**; Zou & Elledge 2003; Ball & Myers 2005).

Most Mec1/ATR activation is generated by the exposure of ssDNA, while Tel1/ATM is activated primarily by double-strand breaks. Once activated, however, either kinase can initiate a signaling cascade, with the help of mediator proteins, to activate the effector kinases Rad53 (human CHK2) and Chk1 (human CHK1). At DSBs, the kinase Tel1 (human ATM) is recruited and activated by the Mre11-Rad50-Xrs2 (MRE11-RAD50-NBS1 in humans) complex. Loading of this complex promotes resection of the double strand break, which generates a ss/dsDNA junction, providing a platform to activate Mec1(ATR) (Jazayeri *et al.* 2006; Shiotai & Zou 2009; Costanzo *et al.* 2001; Myers & Cortez 2006).

The "9-1-1" Checkpoint Clamp in Checkpoint Activation

In addition to exposure of ssDNA, a double-stranded DNA junction with a free 5' end is also required for full checkpoint activation (MacDougall *et al.* 2007). This structure is recognized by the "9-1-1" (Ddc1-Mec3-Rad17 in *S. cerevisiae*, and RAD9-RAD1-HUS1 in humans) checkpoint clamp protein (**Figure 1.2b**). The 9-1-1 checkpoint clamp is structurally related to the proliferating cell nuclear antigen (PCNA) complex, which functions as a processivity factor during DNA replication. This ds/ssDNA junction can arise from various methods, including lagging strand DNA synthesis, nucleotide excision repair, or from DNA resection (Huang *et al.* 1992). At these ds/ssDNA junctions, the 9-1-1 clamp is recruited by the Rad24-RFC clamp loader complex (Ellison & Stillman 2003). *In vitro* work showed that 9-1-1 can be loaded at either 3' or 5' junctions, but once RPA

is bound to ssDNA, 9-1-1 has a preference for 5' junctions (Majka *et al.* 2006 (a); MacDougall *et al.* 2007). In *S. cerevisiae,* Mec1 phosphorylates the 9-1-1 component Ddc1 on Thr602, which can then recruit the checkpoint protein Dpb11 (**Figure 1.2c; Figure 1.2d**; Puddu *et al.* 2008). The role of Dpb11 in checkpoint signaling will then be discussed further below.

Recruitment of the Dpb11 Checkpoint Protein

Dpb11(human TopBP1) is an essential multi-BRCT (BRCA1 C-terminal) domain protein that functions as a scaffold protein to coordinate several checkpoint proteins (see Wardlaw *et al.* 2014 for a review). BRCT domains are thought to work in pairs to recognize phosphorylated motifs, but some recent work suggests a single BRCT domain is able to recognize phospho-sites independently, but perhaps cooperatively (Qu *et al.* 2013). In addition, Dpb11 has an essential role in the initiation of DNA replication by coordinating the initiator proteins Sld3 and Sld2 at origins (Masumoto *et al.* 2002; Tak *et al.* 2006; Zegerman & Diffley 2010). Dpb11 is recruited to Ddc1, which is phosphorylated on Thr602 by Mec1 (Puddu *et al.* 2008). Through the association with Ddc1, the yeast scaffold protein Dpb11 is recruited to the vicinity of Mec1-Ddc2-RPA bound to ssDNA (**Figure 1.2d**; Wang & Elledge 2002).

The recruitment of Dpb11 to lesions plays two main roles in checkpoint activation. First, Dpb11 stimulates Mec1 activity through its C-terminal tail. Second, Dpb11 helps to recruit the checkpoint protein Rad9, which then helps to recruit the effector kinase Rad53 in the vicinity of Mec1 (**Figure 1.2d**; Pfander & Diffley 2011). This allows Mec1 to

phosphorylate and activate Rad53, promoting full checkpoint activation. Both of these points will be discussed in further detail below.

Mec1 Activators

Following recruitment to chromatin, Mec1 needs to be stimulated to initiate checkpoint signaling. Both Dpb11 and Ddc1 can further activate Mec1 (**Figure 1.2d**; Navadgi-Patil & Burgers 2009; Navadgai-Patil *et al.* 2011; Pfander & Diffley 2011). Dpb11 has a C-terminal ATR Activating Domain, or AAD, which can further stimulate Mec1 activity (Delacroix *et al.* 2007; Lee *et al.* 2007; Furuya *et al.* 2004; Mordes *et al.* 2008 (a); Mordes *et al.* 2008 (b); Puddu *et al.* 2008; Paciotti *et al.* 1998). Furthermore, the Ddc1 subunit has been shown to be capable of activating Mec1 *in vitro*, and artificially positioning Ddc1 and Ddc2-Mec1 in close proximity is sufficient to activate Mec1 (Majka *et al.* 2006 (b); Navadgi-Patil & Burgers 2009; Bonilla *et al.* 2008). This highlights an important point to which, although Mec1 can become localized to sites of replication stress (specifically ssDNA), Mec1/ATR requires external activation from other factors, like Dpb11 and Ddc1.

Mec1 activation by Ddc1 and Dpb11 both function to promote checkpoint activation, though how they are coordinated is not completely understood. It is suggested that the way Ddc1 and Dpb11 activate Mec1 is cell-cycle dependent. The 9-1-1 subunit Ddc1 is likely responsible for Mec1 activation in G1, while both the 9-1-1 and Dpb11 cooperate to activate Mec1 in G2/M (Navadgi-Patil *et al.* 2011; Navadgi-Patil & Burgers 2011). In S phase cells, several redundant mechanisms exist to activate Mec1. The 9-1-1 complex is recruited to stalled replication forks and enables activation of Rad53

(Katou *et al.* 2003; Bjergbaek *et al.* 2005). However, mutants of *dpb11* or *ddc1* only show mild defects in Rad53 activation, suggesting that Mec1/Rad53 can be activated redundantly in S phase (Navadgi-Patil & Burgers 2009; Navadgi-Patil *et al.* 2011; Berens & Toczyski 2012). In addition to the ability of Ddc1 and Dpb11 to activate Mec1, the Burger's lab identified Dna2, an endonuclease/helicase with a predominant role in Okazaki fragment maturation, also plays a role in Mec1 activation (Kumar & Burgers 2013). The three Mec1 activators Dpb11, Ddc1, and Dna2, stimulate Mec1 by two aromatic residues in their unstructured AADs (Navadgi-Patil & Burgers 2009; Navadgi-Patil *et al.* 2011; Kumar & Burgers 2013). Moreover, in addition to the role of Dna2's AAD to activate Mec1, Dna2 also binds to the helicase Sgs1, which is also implicated in stress-dependent checkpoint activation (Bjergbaek *et al.* 2005; Frei & Gasser 2000; Hegnauer *et al.* 2012). Rather than Sgs1 generating structures to which Mec1 activation can be facilitated, it has been shown that Sgs1 is regulated in a Mec1-dependent manner, which helps to recruit Rad53 to the vicinity of stalled replication forks (Hegnauer *et al.* 2012). This suggests that Dna2 plays a role in both activating Mec1 via its AAD, as well as its role to recruit Sgs1 for further checkpoint activation.

Checkpoint Adaptors Rad9 and Mrc1

Once Mec1/ATR and Tel1/ATM have been activated, they transduce this signal to the downstream effector kinases Rad53 and Chk1 in budding yeast. In response to replication stress, Mec1-to-Rad53 signaling is the primary guardian. The Rad53 protein structure contains a kinase domain that is flanked by two Forkhead Associated (FHA)

domains, which are important for binding phosphorylated proteins (Durocher & Jackson 2002).

Rad53 activation is facilitated by the assistance of two adaptor proteins, Rad9 and Mrc1, during replication stress. The DNA alkylating agent, methyl methanesulfonate (MMS), induces replication stress by halting polymerases and leaving ssDNA gaps behind moving replication forks, activating Rad53 in a Rad9-dependent manner. Rad9 is a checkpoint adaptor protein necessary for Mec1-to-Rad53 signal transduction during the DNA damage checkpoint response. Rad9 is recruited to sites of lesions via its Tudor and BRCT domains. Rad9's Tudor domain recognizes methylated histone H3 on Lysine (K) 79 (Grenon *et al.* 2007). This histone modification is constitutively found throughout the genome by the yeast histone methyltransferase Dot1 (van Leeuwen *et al.* 2002). Additionally, Rad9's BRCT domains recognize histone H2A phosphorylated on serine 129 (Hammet *et al.* 2007). This modification is mediated by both Mec1 and Tel1 near sites of DNA damage (Downs *et al.* 2000; Cobb *et al.* 2005; Van Attikum *et al.* 2004). Thus, both H3K79 methylation and phosphorylated H2A are thought to help recruit Rad9 to damaged sites on chromatin (Grenon *et al.* 2007; Hammet *et al.* 2007; Giannattasio *et al.* 2005; Wysocki *et al.* 2005).

Once Rad9 is recruited to chromatin via it's Tudor and BRCT domains, Rad9 interacts with Dpb11-9-1-1 (**Figure 1.2d**). CDK-dependent phosphorylation of Rad9 is required for the interaction between Rad9 and Dpb11. Dpb11's BRCT domains 1 and 2 interact with CDK-phosphorylated Rad9 (Schwartz *et al.* 2002; Pellicioli & Foiani 2005; Pfander & Diffley 2011; Wang *et al* 2012). Here, Dpb11 bridges Rad9 with the 9-1-1 complex in the vicinity of active Mec1. Once Rad9 is recruited in the vicinity of active

Mec1, Rad9 becomes phosphorylated by Mec1/Tel1. This phosphorylation allows Rad53 to associate with Rad9, preferentially through Rad53's FHA2 domain (Sweeney *et al.* 2005; Emili 1998; Schwartz *et al.* 2003; Schwartz *et al.* 2002; Sun *et al.* 1998; Pike *et al.* 2003). Rad9-dependent recruitment of Rad53 is thought to facilitate full Rad53 activation by local concentration, allowing Rad53 to autophosphorylate itself *in trans* (**Figure 1.2e**; Gilbert *et al.* 2001; Ma *et al.* 2006). Furthermore, now that Rad53 is in the vicinity of active Mec1, Mec1 can now phosphorylate Rad53 at several S/T-Q motifs to fully activate Rad53 and allow it to disassociate and phosphorylate its own targets (Smolka *et al.* 2005; Sweeney *et al.* 2005).

In response to stress induced by stalled replication forks, Mrc1 is the primary activator of Rad53 (Alcasabas *et al.* 2001; Osborn & Elledge 2003; Tanaka & Russell 2001). Mrc1 is a component of the replisome, and thus it travels along with a moving replication fork (Katou *et al.* 2003; Osborn & Elledge 2003). The ribonucleotide reductase (RNR) inhibitor hydroxyurea (HU) causes replication stress by depleting dNTPs pools. This causes replication forks to stall. In order to protect replication fork stability, the checkpoint is activated near the stalled fork. Mrc1, CLASPIN in human cells, activate Rad53 (Alcasabas *et al.* 2001). During replication stress, Mrc1 helps to recruit Rad53 to a stalled replication fork in the vicinity of Mec1 (Chen & Zhou 2009). Other than checkpoint activation, Mrc1 has a role in stabilization of the replication fork. Mrc1 binds to the replisome via the proteins Tof1 and Csm3 (Bando *et al.* 2009). It has been suggested that Mrc1 bridges both the helicase and polymerase functions of a functional replisome. Replisome stability and checkpoint functions of Mrc1 can be teased apart utilizing a mutant of Mrc1, *mrc1-AQ,* in which all Mec1-dependent phosphorylation sites

Homologs of the Central Components of the DNA Damage Checkpoint		
S. cerevisiae	***H. sapiens***	**Function**
Mec1-Ddc2	ATR-ATRIP	PIKK kinase complex; involved in sensing DNA damage and transducing the checkpoint signal
Tel1	ATM	PIKK kinase; partially overlapping with Mec1 in DNA damage response
Mre11-Rad50-Xrs2	MRE11-RAD50-NBS1	Complex involved in sensing DSBs.
Rad24-Rfc2-5 (RFC)	RAD17-RFC2-5	Checkpoint clamp loader
Ddc1-Rad17-Mec3 (PCNA-like complex; called "9-1-1")	RAD9-RAD1-HUS1 (9-1-1)	Heterotrimeric checkpoint clamp complex; structurally similar to PCNA
Dpb11	TopBP1	Replication intiator protein and checkpoint sensor recruited to sites of damage by 9-1-1
Rad9	53BP1; BRCA1; MDC1	Adaptor protein required for DNA damage signal transduction.
Mrc1	Claspin	Replisome-associated checkpoint adaptor protein
Rad53	CHK2	Effector kinase in DNA damage checkpoint response
Chk1	CHK1	Effector kinase in DNA damage checkpoint response
Sae2	CtIP	Endonuclease that functions with MRX complex in the first step of DNA resection
Exo1	EXO1	5'-3' exonuclease involved in recombination and DNA repair
Sgs1	BLM	RecQ-like helicase that functions with Dna2 to process DSBs
Dna2	DNA2	5' flap endonuclease/helicase that functions with Sgs1 to resect DSBs

Table 1. Homologs of the central components of the DNA damage checkpoint in eukaryotes. DNA damage checkpoint proteins and protein complexes involved in the early steps of checkpoint activation in *Saccharomyces cerevisiae* and their structural or functional homologues in *Homo sapiens.*

are mutated to AQ. In this mutant, checkpoint activation is impeded, but replication progression is not (Alcasabas *et al.* 2001; Osborn *et al.* 2003; Naylor *et al.* 2009). However, in replication stress, Rad9 can compensate for loss of Mrc1 in checkpoint activation (Alcasabas *et al.* 2001).

Checkpoint Activation: Yeast vs Mammals

Checkpoint signaling relies on several classes of checkpoint and repair genes, which are evolutionarily conserved in vertebrates (Lisby & Rothstein 2009). Similar to yeast, PI3K kinases are central to recognizing DNA damage and activating the checkpoint response. In mammals, ATM and ATR are the central kinases that sense DNA damage, homologous to Tel1 and Mec1, respectively (see **Table 1**). In yeast, Mec1 is often considered to be the principal PIKK involved in the DDC response, while Tel1 is primarily responsive to DSBs (Mantiero *et al.* 2007). However, in reality, both Tel1 and Mec1 have important roles in DSB signaling, which is more apparent in higher eukaryotes.

Initially, upon DSBs, the MRN (MRE11-RAD50-NBS1) complex competes with the Ku (Ku70/Ku80) complex for DNA end binding. The Ku complex, normally found at telomeres, associates with dsDNA ends, holding them together to ensure they are properly aligned for rejoining (Martin *et al,* 1999; Walker *et al.* 2001; Gravel *et al.* 1998). In vertebrates, this Ku complex recruits DNA-PKcs, functioning as a DNA end-bridging factor (Gottlieb & Jackson 1993; Spagnolo *et al.* 2006; Weterings *et al.* 2003). However, although DNA-PKcs is not conserved in *S. cerevisiae*, the yeast MRX complex seems to carry out this DNA bridging function alone (Smith *et al.* 1999; Chen *et al.* 2001).

In mammals, ATM functions in response to DSBs while ATR and its associated subunit ATRIP (ATR Interacting Protein) are recruited to RPA-coated ssDNA, which often occurs at DSBs that have undergone resection (Zou & Elledge 2003; Dart *et al.* 2004; Cuadrado *et al.* 2006; Jazayeri *et al.* 2006; Adams *et al.* 2006). Therefore, upon DSBs, both ATM and ATR eventually become activated. Like yeast, ATM is activated by DSBs that are recognized by the MRN complex. Here, MRN functions as a sensor of DNA ends and recruits and activates ATM. Active ATM can then phosphorylate substrates such as CHK2, p53, and H2AX nearby. Phosphorylated H2AX on Ser139 (γ-H2AX) can be recognized by MDC1 (a Rad9 ortholog), creating a feedforward loop that spreads activated ATM and γ-H2AX along chromatin (reviewed in Finn *et al.* 2012).

In *S. cerevisiae,* the 9-1-1 complex associates with Mec1 and helps to promote Mec1-dependent phosphorylation of its targets and stimulates Mec1 kinase activity. However, unlike *S. cerevisiae,* evidence that vertebrate 9-1-1 can similarly stimulate ATR kinase activity is lacking. Instead in vertebrates, the 9-1-1 clamp functions to recruit TopBP1 to sites of damage through the interaction with phosphorylated RAD9 and TopBP1. Casein kinase 2 (CK2) stimulates this interaction by phosphorylating RAD9 at Ser387 to which TopBP1 recognizes through its first two BRCT domains (reviewed in Finn *et al.* 2012). Recently, a novel protein in the ATR-mediated checkpoint signaling, RHINO (Rad9, Rad1, Hus1 interacting nuclear orphan), has been identified (Cotta-Ramusino *et al.* 2011). Recruitment of RHINO is dependent on 9-1-1 and also independently associates with TopBP1. Recruitment of TopBP1-RHINO is suggested to promote TopBP1 to sites of damage and currently the precise role of RHINO remains to be determined (Cotta-Ramusino *et al.* 2011). Once recruited, the TopBP1-RAD9

interaction then promotes activation of ATR through its AAD (ATR activation domain) and helps to facilitate ATR-dependent CHK1 activation (Kumagai *et al.* 2006; Mordes *et al.* 2008a).

In higher eukaryotes, there is no single Rad9 ortholog. Instead, a family of tandem BRCT domain-containing proteins that function in the checkpoint response take over the functionality of Rad9 in the checkpoint response. These Rad9 homologs are BRCA1, 53BP1, and MDC1, and similar to Rad9, these mediators localize to sites of DNA damage, are substrates for PIKKs, and help to propagate the DNA damage signal (Finn *et al.* 2012). Analogous to *cerevisiae,* 53BP1 functions as a molecular adaptor at sites of damage. 53BP1 is recruited to chromatin via binding of its Tudor domain to methylated H3K79 and/or H4K20 (Huyen *et al.* 2004; Botuyan *et al.* 2006; Pei *et al.* 2011). Unlike budding yeast, RNF8-RNF168-UBC13-dependent polyubiquitination of H2A may also play a role in 53BP1 recruitment (Mailand *et al.* 2007; Huen *et al.* 2007; Kolas *et al.* 2007; Stewart *et al.* 2009; Doil *et al.* 2009). Stable retention of 53BP1 recruits the MDC1 checkpoint protein and allows for full checkpoint activation.

In *S. cerevisiae,* Mec1 activates both Rad53 and Chk1, while in vertebrates, ATM primarily activates CHK2 and ATR activates CHK1 (Stracker *et al.* 2009; Sanchez *et al.* 1999). In vertebrates, CHK1 is the primary effector kinase, whereas CHK2 plays a more central role in response to DSBs (Stracker *et al.* 2009). CHK1 activation is mediated by ATR-dependent phosphorylation Ser317 and Ser345. This phosphorylation reportedly promotes CHK1 activation by inducing a conformation change that relieves the inhibition of the kinase domain from the C-terminal regulatory domain (Katsuragi & Sagata 2004; Oe *et al.* 2001; Chen *et al.* 2000; Walker *et al.* 2009). Similar to Mec1-Rad53 signal

transduction, it is proposed that the ATR-CHK1 signal transduction occurs through the adaptors Claspin, 53BP1, and MDC1. Once active, CHK1 dissociates from chromatin and phosphorylates several downstream targets to elicit the checkpoint response (reviewed in Finn *et al.* 2012).

Checkpoint Signaling Controls Various Cellular Processes

Once the checkpoint has been activated, effector kinases phosphorylate many substrates to coordinate a wide variety of cellular responses upon replication stress. Here, I describe the major cellular responses governed by DDC activation.

Cell Cycle Regulation

In eukaryotes, checkpoint kinases play a crucial role in delaying cell cycle progression upon checkpoint activation. In fission yeast and higher eukaryotes, entry into mitosis at the G2/M boundary is governed by the regulation and timing of phosphorylation status of tyrosine residues on Cdc2. Tyrosine phosphorylation at Tyr15 in fission yeast (Tyr15 and Thr14 in humans) is inhibitory and is dependent on the fission yeast kinases Wee1 and Mik1. Thus Wee1 and Mik1 phosphorylation of Cdc2 prevents entry into mitosis until dephosphorylation via the Cdc25 phosphatase (See **figure 1.3a**)(Enoch & Nurse 1990; Rhind *et al.* 1997; Rhind & Russel 1998; Baber-Furnari *et al.* 2000; McGowan & Russel 1993; Gould & Nurse 1989; Lundgreen *et al.* 1991). During G2 in fission yeast, Cdc2 is bound to cyclin B and is phosphorylated on Thr167. However, its activity is low due to the phosphorylation of Tyr15, and mitosis is prevented (Gould & Nurse 1989; Gould

et al. 1991). At the G2/M transition, Tyr15 on Cdc2 is dephosphorylated and cells continue through mitosis.

The DNA damage checkpoint has been investigated in a variety of systems, yet the mechanisms for arrest are not conserved. In fission yeasts and higher eukaryotes, checkpoint kinases Chk1/CHK1 and Cds1/CHK2 negatively regulate Cdc25/CDC25 phosphatases, which remove the inhibitory phosphorylation on cyclin-dependent kinases (CDK) (**Figure 1.3a**; Sanchez *et al*. 1997; Rhind & Russell 1998; Karlsoon-Rosenthal & Millar 2006; Sorensen & Syljuasen 2012). CDC25 is needed to dephosphorylate CDK, and checkpoint-dependent phosphorylation of CDC25 allows the binding and sequestration by 14-3-3 proteins. These 14-3-3 proteins are nuclear-cytoplasmic shuttling proteins that, upon association with CDC25, change its nuclear localization to cytoplasmic localization, and facilitating its degradation via SCF/BTrcp ubiquitin ligase complex (Peng *et al*. 1997; Busino *et al.* 2003; Jin *et al.* 2003). In this fashion, the CDK cell cycle progression is stopped, thereby blocking cells at the G2/M transition.

In *Saccharomyces cerevisiae*, the Wee1 kinase homolog and Cdc25 phosphatase homolog Swe1 and Mih1, respectively, regulate the inhibitory phosphorylation on Cdc28 (or Cdk1), the Cdc2 homolog (**Figure 1.3a**). However, it has been shown that checkpoint is independent of Cdc28 tyrosine phosphorylation on the equivalent tyrosine (Tyr19) as mutations in that tyrosine do not change entry dynamics into mitosis (Sorger & Murray 1992). This suggests that the tyrosine phosphorylation of Cdc28 does not play a major role in control mitosis in DNA damage (Amon *et al.* 1992; Sorger & Murray 1992). Supporting this, cells that carry a non-phosphorylatable Cdc28 allele are still able to block progression into mitosis (Sorger & Murray 1992; Amon *et al.* 1992; Stueland *et al.* 1993).

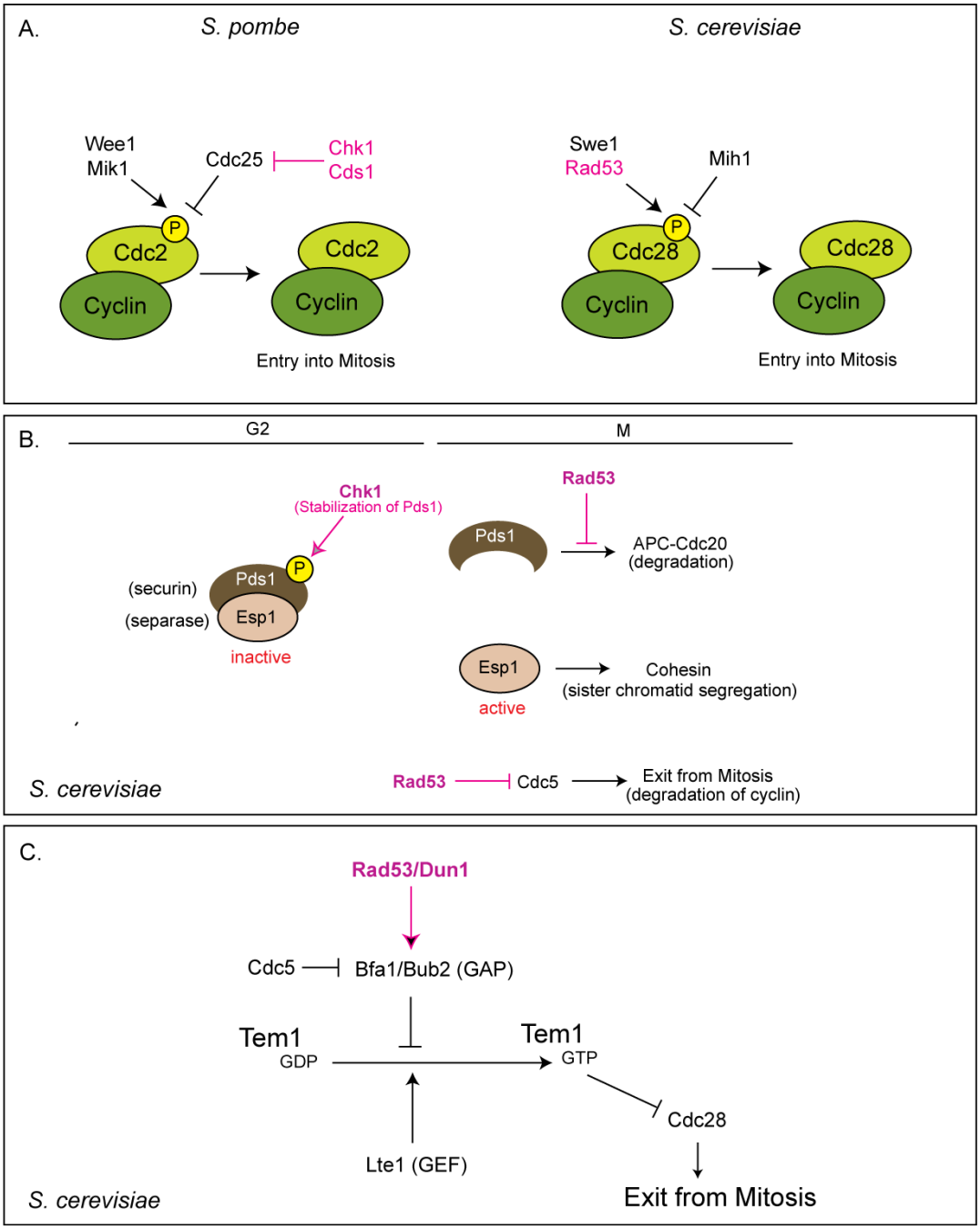
A.
S. pombe
S. cerevisiae
Wee1
Mik1
Cdc25
Chk1
Cds1
P
Cdc2
Cyclin
Cdc2
Cyclin
Entry into Mitosis
Swe1
Rad53
Mih1
P
Cdc28
Cyclin
Cdc28
Cyclin
Entry into Mitosis
B.
G2
M
Chk1
(Stabilization of Pds1)
Rad53
Pds1
APC-Cdc20
(degradation)
P
(securin)
Pds1
(separase)
Esp1
inactive
Esp1
active
Cohesin
(sister chromatid segregation)
S. cerevisiae
Rad53
Cdc5
Exit from Mitosis
(degradation of cyclin)
C.
Rad53/Dun1
Cdc5
Bfa1/Bub2 (GAP)
Tem1
GDP
Tem1
GTP
Cdc28
Lte1 (GEF)
S. cerevisiae
Exit from Mitosis

Figure 1.3. Mechanisms of checkpoint control on cell cycle regulation in *S. cerevisiae*. Different mechanisms of checkpoint control on preventing mitotic exit from *S. pombe* and *S. cerevisiae.* In *S. pombe,* checkpoint kinases inhibit the Cdc25 phosphatase, which is necessary for mitotic exit, which is not conserved in *S. cerevisiae* (a). Checkpoint kinases Chk1 and Rad53 stabilize Pds1 securin, preventing sister chromatid segregation required for mitosis (b). Another mechanism of checkpoint control in inhibiting mitosis in *S. cerevisiae* is through the inhibitory action of the GAP complex Bfa1/Bub2 on the spindle pole-associated GTP-binding protein Tem1 (c).

Additionally, cells lacking the CDC25 homolog Mih1 are viable when exposed to DNA damage (Sorger & Murray 1992; Amon *et al.* 1992), either suggesting that budding yeast is the exception with respect to other eukaryotes regarding CDK control, or redundant mechanisms are in place to downregulate CDK. Instead, *S. cerevisiae* have three different, yet partially redundant pathways with which to prevent chromosome segregation in the presence of DNA damage or replication stress. A recent study showed that both Swe1 phosphatase and Rad53 checkpoint kinase redundantly inhibit CDK(Cdc28) activity, explaining the dispensability of Swe1 in budding yeast and solving a long-sought answer as to why the Wee1 homolog Swe1 is dispensable in response to DNA damage (Palou *et al*. 2015).

Another well studied mechanism *S. cerevisiae* utilize to prevent entry into mitosis during DNA damage is by stabilizing the securin Pds1 along with inhibiting mitotic CDK activity (**Figure 1.3b**). Pds1 inhibits the metaphase to anaphase transition by sequestering the Esp1/separase, a protease that serves to promote sister chromatid separation by cleaving the Mcd1 subunit of cohesion (Yamamoto *et al.* 1996; Ciosk *et al.* 1998; Uhlmann *et al.* 1999). Cohesin binds to sister chromatids during S phase, and prevents premature separation during G2/M phase. Prior to mitosis, cohesin is removed by Esp1 and degraded by the ubiquitin-dependent anaphase-promoting complex (APC/Cdc20) during the metaphase-anaphase transition (Michaelis *et al.* 1997). Upon DNA damage and checkpoint activation, both Chk1 and Rad53 inhibit APC-Cdc20-dependent degradation of Pds1, but at different steps of the process. Chk1 phosphorylates Pds1, preventing ubiquitination and stabilizing Pds1, while Rad53 inhibits

the Pds1-Cdc20 interaction, thereby preventing chromosome segregation and mitosis (**Figure 1.3b**; Sanchez *et al*. 1999; Cohen-Fix & Koshland 1997; Agarwal *et al.* 2003).

Polo-like kinases have been suggested to play various roles in mitosis (Glover et al. 1998; Nigg 1998). Cdc5, a polo-like kinase in budding yeast, indeed promotes anaphase by phosphorylating Scc1, a component of cohesion. Phosphorylation of Scc1 promotes Esp1 cleavage and entry into mitosis (Alexandru *et al.* 2001). Although Cdc5 is not required for degradation of Pds1, Cdc5 is necessary for Cdc28/cyclin B degradation to exit from mitosis. In support of this, *cdc5* mutants arrest cells with elevated Cdk1 activity (Shirayama *et al.* 1998; Sanchez *et al.* 1999). This suggests that Cdc5 plays a role in inactivating CDK that is required for mitotic exit (**Figure 1.3b**). In response to DNA damage, Cdc5 has been shown to be phosphorylated in a Mec1-dependent and Rad53-dependent manner, which results in an inhibitory function of Cdc5 (Sanchez *et al.* 1999; Cheng *et al.* 1998). This suggests that Rad53 plays a major role by phosphorylating and inhibiting Cdc5 function to control both anaphase entry and mitotic exit. However, Cdc5 plays very complex roles in cell cycle progression that are still not very well understood.

Another key regulator of mitotic exit is through the GTP binding protein Tem1. Exit from mitosis after sister chromatid segregation is triggered when the spindle pole body protein Tem1 converts from the GDP-bound state to the GTP-bound state (**Figure 1.3c**; Morgan 1999). Active GTP-bound Tem1 protein activates a signal transduction pathway that inhibits Cdc28 activity and ensures mitotic exit. Tem1 is kept in its inactive Tem1(GDP) form when it is bound by the Bfa1/Bub2 GAP complex, but when the spindle pole body moves into the daughter cell, where the GEF Lte1 is located, Tem1 exchanges GDP for GTP and exits mitosis (Bardin *et al.* 2000; Pereira *et al.* 2000). Bfa1 and Bub2

have been implicated in checkpoint control in preventing mitosis, because checkpoint-dependent mitotic arrest depends on a functional Bfa1/Bub2 GAP complex (Hoyt *et al.* 1991; Bloecher *et al.* 2000; Pereira *et al.* 2000; Wang *et al.* 2000). Bfa1/Bub2 is important for preventing mitotic exit in response to spindle damage and misorientation, and is regulated by the Rad53- and Dun1-dependent checkpoint response (**Figure 1.3c;** Hu *et al.* 2001). Bfa1 has been shown to be phosphorylated by the polo kinase Cdc5, which promotes mitotic exit (Hu *et al.* 2001). In response to DNA damage, Bfa1 phosphorylation by Cdc5 still occurs, but is further modified in a Rad53/Dun1-dependent manner, potentially negating the inhibitory effect of Cdc5 toward Bfa1. In this sense, once the nucleus and spindle poles are properly matured, Cdc5 phosphorylates and inhibits Bfa1/Bub2 which activates Tem1 to allow mitotic exit. Checkpoint regulation of Bfa1/Bub2 prevents Tem1 activation by stabilizing Bfa1 activity, and thus preventing mitotic exit (Weinreich & Stillman 1999: Wang *et al.* 2000).

Controlling Firing of Replication Origins

DNA replication requires a sequential series of steps that needs to be carefully regulated in order to ensure that DNA content is replicated exactly one time per cell cycle. Failure to carefully regulate this process can lead to under-replication leading to a loss of genomic content, as well as over-replication that can be detrimental for genes that need to be expressed in vary precise quantities (Nielson & Løbner-Olesen 2008). In the first step of DNA replication, the pre-replicative complex (pre-RC) is loaded onto DNA at the origins of replication. This step, called “licensing”, is restricted to G1 when CDK activity is low. This pre-RC complex is composed of ORC, Cdt1, Mcm2-7 helicases, and Cdc6.

Next upon S phase, the helicase components Cdc45 and GINS along with DNA polymerases are recruited to the pre-RC complexes. This recruitment to licensed pre-RCs is bridged by Sld3-Sld7 and Dpb11-Sld2 components in a CDK- and DDK- (Dbf4 dependent kinase) dependent manner (Tanaka & Araki 2010; Zegerman & Diffley 2009). Additionally, the unwinding of DNA requires Mcm10 together with the CMG (Cdc45-MCM-GINS) helicase complex to initiate DNA replication (Watase *et al.* 2012; Van Deursen *et al.* 2012; Kanke, *et al.* 2012). In contrast to prokaryotes, eukaryotes have multiple replication origins. These origins are not initiated, or "fired", at the same time. Instead, initiation of DNA replication events is temporally regulated (Gilbert *et al.* 2010; Barberis *et al.* 2010). The temporal regulation of origin firing depends on the limited abundance of replication factors, which are recycled and allow for a cascade of origins fired (Tanaka *et al.* 2011; Manteiro *et al.* 2011).

In response to DNA damage, the checkpoint slows DNA replication by inhibiting late origins from firing (Santocanale & Diffley 1998; Shirahige *et al.* 1998). Upon DNA damage, Rad53 phosphorylates and inhibits the replication initiation protein Sld3 and the Cdc7 kinase regulatory subunit Dbf4 to block late origin firing in *S. cerevisiae*. Phosphorylation of Sld3 by Rad53 in DNA damage conditions prevents CDK-phosphorylated Sld3 from binding to Dpb11, which is necessary for replication initiation (Lopez-Mosqueda *et al.* 2010). In the case of Dbf4, Dbf4 is the regulatory subunit for DDK (Dbf4-dependent kinase), which is responsible for phosphorylating and activating Mcm2-7 for replication initiation. It's protein abundance changes throughout the cell cycle, and Rad53-dependent phosphorylation of Dbf4 inactivates DDK, targets it for degradation, preventing it from firing late origins (Weinreich & Stillman 1999).

Transcriptional control and upregulation of dNTPs.

Mec1 and Rad53 are necessary for cell proliferation, but this role is not due to their checkpoint function in controlling cell cycle progression (Desany *et al.* 1998; Zhao *et al.* 1998; Brown & Baltimore 2000; De Klein & Muijtjns 2000; Liu *et al.* 2000; and Takai *et al.* 2000). An essential function of Mec1-Rad53 signaling is to upregulate the pools of dNTPs to counteract replication stress. In response to DNA damage, the checkpoint upregulates ribonucleotide reductase (RNR) activity, providing a 6-8- fold increase in dNTP concentrations (Chabes *et al.* 2003). The checkpoint upregulates dNTPs by transcriptionally inducing ribonucleotide reductase genes (Allen *et al.* 1994; Huang *et al.* 1998). Additionally, in *Saccharomyces cerevisiae,* the lethality of *mec1* or *rad53* mutants can be rescued by the deletion of *SML1* (Desany *et al.* 1998; Zhao *et al.* 1998). Rad53 activates the downstream kinase Dun1, which in turn, targets the RNR inhibitors Sml1 and Dif1 to be degraded (Nordlund & Reichard 2006; Zhao & Rothstein 2002; Lee *et al.* 2008; Zhao *et al.* 2001; Zhao *et al.* 1998). Dun1 also induces RNR gene transcription by inhibiting the transcriptional repressor Crt1 (Huang *et al.* 1998). Taken together, the observation that failure to regulate dNTP levels is lethal, suggests that these pathways are vital to the survival of budding yeast.

In addition to regulating the transcriptional control of RNR genes, DNA damage triggers significant changes in the transcriptional regulation of many genes in budding yeast. In addition to *RNR2* and *RNR4*, Mec1 signaling inducts an “environmental stress response” (ESR), which involves hundreds of genes, upon a variety of cellular stresses (Gasch *et al.* 2001; Jelinsky & Samson 1999; Benton *et al.* 2006). Checkpoint signaling-

dependent transcriptional responses are primarily triggered by the Rad53 and Rad53-Dun1 pathways (Huang *et al.* 1998; Travesa *et al.* 2012; Bastos de Oliveira *et al.* 2012). Dun1 phosphorylates and inhibits Crt1, which recruits the repressor proteins Ssn6 and Tup1 to the promoters of DNA damage response genes (Huang *et al.* 1998; Gasch *et al.* 2001). Also, checkpoint signaling has an important role in regulating the transcriptional activity of many genes at the G1/S bounder under replication stress conditions. Under normal conditions, SBF (Swi4-Swi6 cell-cycle boc (SCB) binding factor) transcription factors activate transcription of over 200 genes in G1, while MBF (*MluI* cell-cycle box (MCB) binding factor) transcription factors down-regulate these genes outside G1 due to the transcriptional repressor Nrm1. However, under replication stress, the MBF target genes are upregulated though Rad53-dependent yet Dun1-independent regulation of the repressor Nrm1 (Travesa *et al.* 2012; Bastos de Oliveira *et al.* 2012).

Stability of Replication Forks

DNA damage checkpoint signaling has an essential role in replication fork stability. This is supported by the observation that checkpoint mutants fail to resume DNA replication after transient genotoxin exposure (Desany *et al.* 1998; Lopes *et al.* 2001; Tercero *et al.* 2003). Additionally, replisome components are not found at early origins via ChIP in cells that lack *MEC1* (Cobb *et al.* 2005; Tercero *et al.* 2003; Cobb *et al.* 2003; Lucca *et al.* 2004). Also, checkpoint mutants accumulate aberrant DNA structures, such as reversed replication forks which resemble a “chicken foot”, and accumulate stretches of ssDNA (Sogo *et al.* 2002; Lopes *et al.* 2001). These observations suggest that checkpoint signaling plays a vital role in maintaining the integrity of replication forks and

their associated components and prevent the accumulation of aberrant fork structures that might compromise genome integrity.

Checkpoint signaling protects replication forks during replication stress by inhibiting enzymes that might process stalled forks, such as nucleases. In budding yeast, the MMS lethality of *rad53* cells can be alleviated by the deletion of the exonuclease *EXO1* (Segurado & Diffley 2008). This suggested that a necessary function of Rad53-dependent signaling relied on its ability to down-regulate Exo1 at stalled forks. In this fashion, Rad53 prevents aberrant processing of abnormal replication fork structures by Exo1 upon replication stress. Importantly, *exo1* does not rescue the MMS sensitivity of *mec1* cells, highlighting that Mec1 and Rad53 are not equivalent and that Mec1 has alternative functions that are critical for cell survival in MMS (Segurado & Diffley 2008; Morin *et al.* 2008). Deletion of EXO1 in checkpoint-deficient mutants has also been shown to prevent the accumulation of ssDNA at stalled forks upon HU treatment (Cotta-Ramusino *et al.* 2005). Additionally, human EXO1 is degraded in response to HU, which is dependent on both ATR signaling and ubiquitin-mediated degradation (El-Shemerly *et al.* 2008), suggesting that inhibition of nucleases during stress conditions is a conserved role of checkpoint signaling.

Activated Rad53 targets several substrates that result in the protection of stalled forks. For example, the nuclease-helicase Dna2 is phosphorylated by the checkpoint pathway, which was shown to facilitate its association to DNA in response to HU. This is thought to prevent the accumulation of ssDNA by clipping of ssDNA tails from regression forks (Hu *et al.* 2012). The Mus81-Eme1 structure-specific nuclease was shown to be a target of Cds1 (the Rad53 homolog in *S. pombe*) during stalled forks (Kai *et al.* 2005).

Also, the helicase Sgs1, which has roles in maintaining the stability of replication forks, has also been shown to be a target of Mec1, and this role is dependent on Sgs1's helicase activity (Cobb *et al.* 2005; Frei & Gasser 2000; Hegnauer *et al.* 2012; Cobb *et al.* 2003). Moreover, mammalian homologs of Sgs1 helicase (BLM and WRN) are also phosphorylated by ATR and ATM (Davies *et al.* 2004; Davies *et al.* 2007; Ammazzalorso *et al.* 2010).

Checkpoint signaling has been shown to regulate fork-associated proteins, such as enzymes that modify long-range chromatin organization. The budding yeast chromatin remodelers Ino80 and Isw2 have been shown to be targets of the DNA damage checkpoint (Chen *et al.* 2010; Morrison *et al.* 2007). These chromatin remodelers have been shown to be recruited to stalled replication forks upon stress conditions and promote replication fork recovery (Shimada *et al.* 2008; Vincent *et al.* 2008; Falbo *et al.* 2009). The proposed model is that these remodelers remove nucleosomes to allow fork progression as well as altering fork structure (Shen *et al.* 2000). However, it remains poorly understood how checkpoint signaling protects fork integrity.

DNA Repair

Checkpoint signaling has a less clearly understood role in regulating DNA repair. In budding and fission yeasts, studies have shown that checkpoint activity prevents the initiation and processing events that are required for homologous recombination-directed repair (Alabert et a 209; Barlow & Rothstein 2009; Meister *et al.* 2005). Checkpoint kinases negatively regulate the Exo1 endonuclease, which is important for DNA resection in homologous recombination (HR) (Bolderson *et al.* 2010; Morin *et al.* 2008; El-

Shermerly *et al.* 2008). Mec1 also regulates the repair functions of the Sae2 nuclease and Rtt107 repair scaffold proteins (Baroni *et al.* 2004; Flott *et al.* 2007; Rouse 2004). Additionally, chromatin-modifying enzymes are suggested to be targeted by checkpoint kinases. Mec1 regulates the phosphorylation of histone H2A (γ-H2A), which can recruit chromatin remodelers such as Ino80 (reviewed in van Attikum & Gasser 2009 and Thiriet & Hayes 2005). However, the mechanisms by which chromatin-remodelers and DNA repair factors help cells survive is not understood.

Checkpoint signaling has recently been implicated in regulation of post-replicative repair proteins. Upon MMS-induced replication blocks, lesions are commonly bypassed by template-switching mechanisms that utilizes the newly synthesized sister chromatid as a homologous recombination template. This type of repair, although error-free, leaves joint DNA molecules (JMs) behind that need to be separated prior to mitosis. The processing of these physically linked DNA molecules is repaired by either 'dissolved' by the topoisomerase-helicase complex Sgs1-Top3-Rmi1 complex or 'resolved' by the structure-specific nuclease complex Mus81-Mms4 (Hickson & Mankouri 2011; Sarbajna & West 2014). The actions of CDK and Cdc5 cell cycle kinases restrict the activity of Mus81-Mms4 to G2/M, presumably to avoid premature processing of non-JM structures prior to G2/M. Checkpoint activity is proposed to negatively regulate Mus81-Mms4 activity to avoid aberrant nuclease activity (Zhang *et al.* 2009; Szakal & Branzei 2013; Kai *et al.* 2005).

The Importance of Checkpoint Down-Regulation

Cells are always facing endogenous sources of DNA damage, and the ability to respond to threats via checkpoint activation is important for maintaining the integrity of the genomic material. After successful repair of lesions after induction of the checkpoint signaling cascade, the checkpoint presumably must be down-regulated in order for the cell to resume cell cycle progression and cell proliferation. This down-regulation of checkpoint activity following repair is known as checkpoint recovery. Although the detailed mechanisms for checkpoint recovery are not fleshed out, several genes have been implicated in being important for checkpoint inactivation following recovery from DNA damage (Vaze *et al.* 2002; Leroy *et al.* 2003). Moreover, the checkpoint response may also be deactivated despite the presence of persistent DNA damage, a process known as checkpoint adaptation. The ability of cells to either recover from or adapt to checkpoint signaling suggests that checkpoint down-regulation may be regulated in a variety of mechanisms, presumably tailored to each type of need for checkpoint down-regulation. Although the mechanisms for checkpoint activation are vastly studied, the mechanisms for checkpoint down-regulation are considerably less understood.

Cancer cells find mechanisms to prevent checkpoint activity from halting cell proliferation. Therefore, understanding how to up-regulate checkpoint activity in these cells could serve as a potential anti-cancer strategy. Because the checkpoint signaling pathway is highly conserved in eukaryotes, budding yeast provide an ideal model organism with which to investigate mechanisms for regulating checkpoint activity as well as the biological consequences for checkpoint hyperactivation with respect to genome instability.

Checkpoint Deactivation via Phosphatases

As mentioned above, checkpoint deactivation is necessary for cell proliferation following DNA repair. In budding yeast, checkpoint deactivation requires the deactivation of Rad53. During an irreparable DSB, the disappearance of phosphorylated Rad53 closely correlates with checkpoint adaptation (Pellicioli *et al.* 2001). Importantly, this disappearance of phosphorylated Rad53 is not dependent on protein degradation of active Rad53, suggesting that Rad53 must be dephosphorylated by one or more protein phosphatases during adaptation (Tercero *et al.* 2003). Furthermore, this highlights an important aspect of the roles of Ser/Thr phosphatases necessarily for checkpoint deactivation during recovery and adaptation. Several Ser/Thr phosphatases have been implicated in checkpoint recovery and adaptation in budding yeast. In *Saccharomyces cerevisiae,* those known to date are Ptc2, Ptc3, Pph3, and Glc7 (Leroy *et al.* 2003; Guillermain *et al.* 2007; Keough *et al.* 2006; Bazzi *et al.* 2010). Other Ser/Thr phosphatases, such as PP1 (den Elzen *et al.* 2004), PP2A (Dozier *et al.* 2004, Liang *et al.* 2006, Li *et al.* 2007, and Leung-Pineda *et al.* 2006), PP2C (Lu *et al.* 2005 (b), Fujimoto *et al.* 2006, and Oliva-Trastoy *et al.* 2007), and PP5 (Yong, *et al.* 2007, Zhang *et al.* 2005, Ali *et al.* 2004, Zuo *et al.* 1998, and Lavin *et al.* 2007) have been shown to be involved in checkpoint regulation in other organisms.

Ser/Thr phosphatases are important for many aspects of cellular function, including DNA replication, pre-mRNA splicing, DNA damage response, transcription, and growth factor-dependent signaling (Archambault *et al.* 1998; Cho *et al.* 1999; Yeo etal 2005; Thompson *et al.* 2006; Moorhead *et al.* 2007). Ser/Thr protein phosphatases are

generally grouped into the PPP (phosphoprotein phosphatase) family. This is further subdivided into the metal-independent classes PP1, PP2A, PP4, PP5 and PP6 phosphatases, the Ca+2-dependent PP7 and PP2B phosphatases, and the Mn2+/Mg2+-dependent PPM (protein phosphatase magnesium-dependent) family which primarily contains PP2C phosphatases. Of these phosphatase families, the PP2A, PP4, and PP6 phosphatases have the highest homology and make up the 2A subgroup.

Originally, the consensus was that phosphatases acted with little specificity. However, it seems that phosphatases may be very specific *in vivo* due to post-translational modifications (PTMs), cellular localization and compartmentalization, or associations with regulatory adapter subunits (Virshup & Shenolikar 2009). The observation that yeast have several PP2C family phosphatases (Ptc1-7) and humans have reported at least 15 isoforms further suggests how phosphatases can be specific in what substrates they regulate. These different PP2C phosphatase isoforms are highly conserved, yet contain different N- and C-terminal extensions (Stern *et al.* 2007). These isoform-specific extensions are believed to contain membrane-targeting motifs, kinase-interaction domains, and other regulatory sites that might regulate protein-protein interactions (Mustelin 2007). For example, CK2-mediated phosphorylation of the C-terminal extension of Ptc2 and Ptc3 assists the ability of the enzyme to recognize Rad53 (Guillermain *et al.* 2007). Additionally, most phosphatases rely on association with regulatory subunits. In *Saccharomyces cerevisiase,* the PP2A phosphatase utilizes the subunits Pph21, Pph22, the scaffold Tpd3, and either Cdc55 or Rts1. Furthermore, in higher eukaryotes, human PP2A can contain one of four distinct classes of subunits,

denoted as B, B', B'', and B''', which we can extrapolate to a way to provide the whole complex with a way to tailor its specificity to a variety of substrates (Andreas *et al.* 2006).

Ptc2 and Ptc3 Phosphatases

The two PP2C phosphatases, Ptc2 and Ptc3, have been shown to be required for dephosphorylating Rad53 after a programmed DSB (Leroy *et al.* 2003). They were the first phosphatases to be implicated in the regulation of the yeast DNA damage checkpoint. Ptc2 and Ptc3 are paralogs that arose by whole genome duplication, and they share 62% amino acid sequence identity. CK2-dependent phosphorylation of Ptc2 at Thr376 allows constitutively interaction with Rad53's FHA1 domain (Leroy *et al.* 2003; Guillemain *et al.* 2007). Cells lacking *PTC2* and *PTC3* are unable to adapt to an irrepairable HO-induced DSB, and are also defective in recovering from a repairable DSB (Leroy *et al.* 2003). In many cases, Ptc2 and Ptc3 act redundantly with the PP4 (a PP2A-like) phosphatase Pph3 in budding yeast. Triple mutants lacking these three phosphatases are hypersensitive to a variety of genotoxins (Kim *et al.* 2011).

The human Ptc2/3 homolog, Wip1/PPM1D has been shown to bind Chk2 and dephosphorylate Chk2 on Thr68 (Fujimoto *et al*. 2006; Oliva-Trastoy *et al*. 2007). Phosphorylation of Chk2 on Thr68 is ATM-dependent and allows Chk2 dimerization and activation by autophosphorylation of the T-loop upon DNA damage (Matsuoka *et al.* 2000; Melchionna *et al.* 2000; Xu *et al.* 2002; Schwarz *et al.* 2003). Wip1 was originally identified due to its p53-dependent transcriptional induction after ionizing radiation (Fiscella *et al.* 1997). In response to stress, Wip1 has been suggested to play a role in several checkpoint pathways, such as preventing p53 stabilization by dephosphorylating

p38 MAP kinase, dephosphorylating p53 on Ser15, and inhibiting Chk1 by dephosphorylating Ser345 (Lu *et al.* 2005 (b); Takekawa et al. 2000).

Pph3 Phosphatase

In *S. cerevisiae,* a central checkpoint kinase is Pph3, a PP4 family phosphatase. *PPH3* encodes the catalytic subunit for the yeast phosphatase complex with its subunits Psy2 and Psy4. While Psy2 and Psy4 provide substrate specificity for Pph3, Pph3-Psy2 can form a stable phosphatase complex with or without Psy4 (O'Neil *et al.* 2007). Human PP4 is composed of Pp4c with one of two regulatory subunits, R1 (Psy4 homolog) or R2 (Psy2 homolog). Adding to this complexity, Pp4c-R1 or Pp4c-R2 can associate with another variable subunit. Pp4c-R1 has been shown to interact with histone deacetylase 3, while Pp4c-R2 can associate with other regulatory subunits R3, Gemin3, Gemin4 and others (Zhang *et al.* 2005; Gingras *et al.* 2005; Carnegie *et al.* 2003; Yeh *et al.* 2004; and Hu *et al.* 1998).

Pph3 has a major role in checkpoint deactivation by dephosphorylating Rad53 (O'Neill *et al.* 2007). Yeast cells that lack *PPH3* are sensitive to both the DNA alkylating agent MMS as well as the topoisomerase inhibitor camptothecin (CPT) (Kim *et al.* 2011). Importantly, deletion of *PPH3* suppresses the MMS sensitivity of cells that lack genes important for proper checkpoint activation, such as *MEC1, RAD9, RAD17*, and *RAD24* (O'Neill *et al.* 2007), suggesting that a major function for Pph3 is checkpoint regulation. The Psy2 subunit interacts with phosphorylated Rad53 through its kinase domain (O'Neill *et al.* 2007). *In vitro* studies have shown that Pph3 does dephosphorylate hyperphosphorylated Rad53, and deletion of *PPH3* incompletely restores Rad53

phosphorylation in *rad9* and *mec1* cells after exposure to MMS. Also, cells lacking *PPH3* progress more slowly through S-phase after MMS treatment, and dephosphorylation of Rad53 is delayed in cells after transient exposure to MMS (O'Neill *et al.* 2007).

In addition to Rad53, Pph3-Psy2 also has a role in dephosphorylating histone H2A on Serine 129 in yeast, termed γH2A. Dephosphorylation of γH2A is dependent on the variable subunit Psy4 in addition to Pph3-Psy2, as indicated that the genetic and biochemical profiles of both *PPH3* and *PSY2* are indistinguishable, whereas Psy4 is dispensable for Rad53 dephosphorylation. Rad53 dephosphorylation in *psy4* cells during checkpoint recovery after MMS proceeds normally. Additionally, cells lacking *PSY4* are not sensitive to MMS, and do not affect the MMS sensitivity of various checkpoint mutants (O'Neill *et al.* 2007). In contrast, *pph3, psy2,* and *psy4* cells all show identical defects in dephosphorylating γH2A (Keogh *et al.* 2006). In parallel, the Psy2 regulatory subunit, human R3 subunit, was first implicated in the DNA damage checkpoint based on the sensitivity of *psy2* cells to cisplatin, a DNA crosslinker used as a chemotherapy drug (Huang *et al.* 2005) and genetic interactions between *PSY2* and genes involved in the stability of stalled replication forks (O'Neill *et al.* 2004). Thus, it is generally well-accepted that Pph3-Psy2 dephosphorylates Rad53, while the Pph3-Psy2-Psy4 complex dephosphorylates γH2A. The idea that Pph3 dephosphorylates both Rad53 and γH2A suggests that Pph3 is involved in many aspects of the checkpoint response.

Glc7 Phosphatase

Until recently, the Ser/Thr phosphatases Ptc2, Ptc3, and Pph3 were found to be the only phosphatases important for checkpoint recovery (Keogh *et al.* 2006; Leroy *et al.*

2003). Additionally, Pph3 and Ptc2 have been shown to deactivate the checkpoint during recovery from MMS exposure (O'Neill *et al.* 2007; Szyjka *et al.* 2008). Interestingly, none of those phosphatases was shown to be important for Rad53 inactivation following exposure to hydroxyurea (HU), and the triple mutant *pph3Δ ptc3Δ ptc2Δ* does not show sensitivity to HU exposure, suggesting the involvement of another phosphatase here (Szyjka *et al.* 2008; Travesa *et al.* 2008). Indeed, the Longhese group showed that the essential PP1 protein phosphatase Glc7 is important for checkpoint recovery upon exposure to HU and DSB induction, but not to MMS. Also, these authors show that Glc7 can also dephosphorylate γH2A following HU or treatment with phleomycin (Bazzi *et al.* 2010). It is likely that, Glc7 and the other Rad53 phosphatases have some level of redundancy in checkpoint deactivation in different conditions.

Glc7 is an essential gene coding for the catalytic subunit of yeast PP1 protein phosphatase. Glc7 is involved in many cellular processes including glucose/glycogen metabolism, cell polarity, chromatin remodeling and segregation, transcription, meiosis, cell wall organization, and others (Virshup & Shenolikar 2009; Tan *et al.* 2003; Peggie *et al.* 2002; Williams-Hart *et al.* 2002). On its own, Glc7 has little substrate specificity (Lenssen *et al.* 2005). Instead, several regulatory subunits assist Glc7 to target various substrates in different conditions (Cui *et al.* 2004). For example, Bni4 targets Glc7 to the bud neck, while Gac1 helps Glc7 target Gsy2 (the glycogen synthase), which is required for accumulation of glycogen (Larson *et al.* 2008; Sanz *et al.* 2004; Williams-Hart *et al.* 2002). Although Glc7's function has been characterized as an important factor in many cellular processes previously, its role in the DNA damage checkpoint response and recovery is recent and considerably less understood.

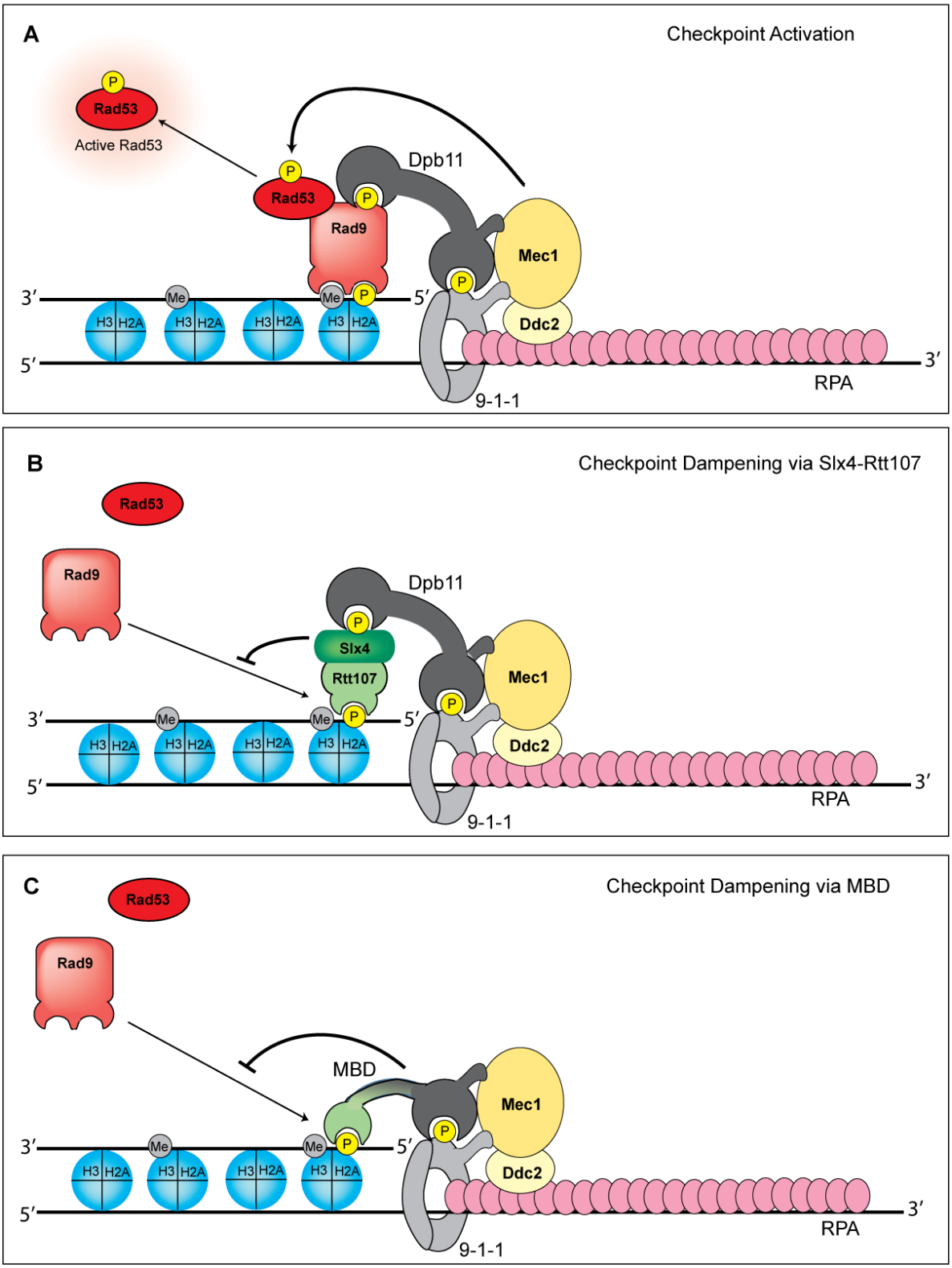
A
Checkpoint Activation
Rad53
Active Rad53
P
Rad53
Rad9
Dpb11
Mec1
Ddc2
9-1-1
RPA
3′
5′
Me
H3
H2A
B
Checkpoint Dampening via Slx4-Rtt107
Rad53
Rad9
Dpb11
Slx4
Rtt107
Mec1
Ddc2
9-1-1
RPA
C
Checkpoint Dampening via MBD
Rad53
Rad9
MBD
Mec1
Ddc2
9-1-1
RPA

Figure 1.4. A phosphatase-independent mechanism for down-regulating checkpoint activation. Checkpoint activation is mediated by the recruitment of the Rad9 adaptor to sites of lesions by interacting with both Dpb11-9-1-1 and with methylated H3K79 and γ-H2A (a). Slx4-Rtt107 competes with Rad9 binding to Dpb11 and to γ-H2A, preventing Rad9 from recruiting Rad53 in the vicinity of Mec1 (b). An engineered chimeric protein (MBD, Minimal multi-BRCT domain) composed of BRCT domains of both Rtt107 and Dpb11 recapitulate the checkpoint dampening function as Slx4-Rtt107 (c).

A Phosphatase-Independent Mechanism of Checkpoint Deactivation

Scaffold proteins are essential to the coordination of a variety of cellular processes. In particular, the budding yeast scaffold proteins Slx4 and Rtt107 are important for proper checkpoint dampening and subsequent repair of damaged DNA. Rtt107 and Slx4 are extensively phosphorylated by Mec1 and are important for recovery from replication stress (Flott & Rouse 2005; Rouse 2004). These proteins stably interact and are important for resistance to MMS-induced replication stress (Roberts *et al.* 2006; Rouse 2004). Recently, our lab identified the Slx4-Rtt107 scaffold complex as an important mechanism for down-regulating Rad53-dependent checkpoint activity, which will be discussed below (Ohouo *et al.* 2013; Ohouo *et al.* 2010).

Rtt107, also known as Esc4, was originally identified in a genetic screen for increased mobility of the Ty transposon (Scholes *et al.* 2001). It is a multi-BRCT domain protein with several cellular responsibilities (Ohouo *et al.* 2010; Rouse 2004). Rtt107 interacts, in a mutually exclusive manner with components of different repair processes, such as with ubiquitin ligase complex components Rtt101, Mms1, and Mms22, which are suggested to regulate bypass of DNA lesions and direct homologous recombination-directed repair (Duro *et al.* 2008). Through its C-terminal BRCT domains (BRCT 5 & 6), Rtt107 binds to γ-H2A and helps to recruit repair factors to the damaged site (Li *et al.* 2012). Our lab also showed that Rtt107 also interacts with the Smc5-Smc6 sumo ligase complex, which is important for the structural maintenance and repair of chromosomes (Ohouo *et al.* 2010; Zhao & Blobel 2005). Importantly, cells lacking certain Rtt107-associated components show different genotoxin sensitivities, indicating that Rtt107 is involved in several distinct repair complexes (Roberts *et al.* 2008).

Slx4 is an evolutionarily conserved scaffold protein. Slx4 has a well-documented role in interacting with structure-specific endonucleases. In *S. cerevisiae,* Slx4 associates with Slx1 and the Rad1/Rad10 nucleases (*SLX1* and XPF/ERCC1 in humans, respectively) (Coulon *et al.* 2004; Fricke & Brill 2003). Even though Slx4 lacks an obvious nuclease domain, Slx4 enhances the nuclease activity of Slx1 *in vitro* (Fricke & Brill 2003; Coulon *et al.* 2004). The ability of Slx4 to coordinate nucleases suggests it has critical roles in DNA repair. This is supported by the observation that *SLX4* is one of 6 genes (including *MMS4, MUS81, SLX1, SLX5,* and *SLX8*) that were shown to be lethal when combined with a mutation that lacks the RecQ helicase Sgs1 (Mullen *et al.* 2001; Tong *et al.* 2001; Coulon *et al.* 2004). Presumably, Slx4 is needed to recruit nucleases to cleave stalled replication forks that are unable to be resolved by the Sgs1-Top3 helicase/topoisomerase complex (Fricke & Brill, 2003; Coulon *et al.* 2004), thus making the loss of both pathways inviable. Recently, Slx4 was suggested to form a complex with the Mus81 endonuclease complex through interactions between Dpb11 and Mms4, the regulatory subunit with Mus81. The Rtt107-Slx4-Dpb11-Mms4-Mus81 complex forms specifically in G2/M, and is proposed to directly regulate the action of Mus81-Mms4 for the resolution of DNA repair intermediates formed in response to MMS (Gritenaite *et al.* 2014).

Furthermore, human SLX4 interacts with three distinct nucleases: SLX1, ERCC4/XPF-ERCC1, and MUS81-EME1 (Fekairi *et al.* 2009; Muñoz *et al.* 2009; Svendsen *et al.* 2009). Interaction with these nuclease complexes is implicated in the resolution of Holliday junctions and processing of DNA interstrand crosslinks (ICLs). Additionally, SLX4 (also designated as FANCP) has been classified as a protein involved

in the Fanconi Anemia (FA) pathway. Fanconi anemia is a rare genetic disease that is characterized by congenital abnormalities, high instance of bone marrow failure, and increased cancer susceptibility. FA proteins are known to function against ICLs, and SLX4/FANCP is thought to function in downstream homologous recombination-directed repair of ICLs (Ciccia *et al.* 2008).

Although Slx4 was traditionally only thought to function as a nuclease with Slx1/Rad1/10, our lab proposed that Slx4 plays nuclease independent roles. For instance, ***slx4Δ*** mutants are more sensitive to MMS- or CPT-induced DNA damage than ***slx1Δ, rad1Δ, or slx1Δrad1Δ*** double mutants (Ohouo *et al.* 2013; Fricke & Brill 2003; and Deng *et al.* 2005, respectively). Interestingly, *slx4* mutants show phenotypes similar to that seen in ***rtt107Δ*** mutants, including prolonged checkpoint activation and S phase delay, suggesting a common role for Slx4 with Rtt107 that is independent of Slx1 nuclease (Roberts 2006). Indeed, through its N-terminal BRCT domains, Rtt107 forms a physical complex with Slx4 upon DNA damage that is independent of Slx1 (Roberts 2006).

It has become evident that the roles Slx4 and Rtt107 are not interchangeable. Although ***slx4Δ*** and ***rtt107Δ*** mutants show similar DNA damage response phenotypes, the phenotypes shown for ***rtt107Δ*** mutants were more severe compared with *slx4* cells and ***slx4Δ rtt107Δ*** double mutants were slightly more sensitive to MMS when compared with either single mutant (Roberts 2006). This could suggest that Rtt107 has Slx4-independent roles in the DNA damage response. In support of an Slx4-independent role for Rtt107 is the observation that, although ***slx4Δ*** cells combined with ***sgs1Δ*** are lethal, ***rtt107Δ sgs1Δ*** cells are viable (Mullen *et al.* 2001; Tong *et al.* 2001, 2004).

Our lab recently identified a novel nuclease-independent role for the Slx4-Rtt107 scaffold complex as and adaptor-mediated mechanism to counteract DDC signaling. Slx4-Rtt107 counteracts the checkpoint adaptor protein Rad9 by physically interacting with Dpb11 and γ-H2A (see **Figure 1.4a-b**). Slx4-Rtt107 binding to Dpb11 and γ-H2A at sites of lesions prevents Rad9 from interacting with Dpb11, and thus preventing the recruitment of Rad53 in the vicinity of Mec1. We named this adaptor-mediated mechanisms DAMP for Dampens Adaptor Mediated-Phosphosignaling. (see **figure 1.4b** and Ohouo *et al.* 2013). Additionally, our lab identified the molecular requirements for this mechanism and engineered a minimal multi-BRCT domain (MBD) module that mimics the action of the Slx4-Rtt107 complex in checkpoint down-regulation (**Figure 1.4c**). This MBD is a chimeric fusion protein composed of the BRCT domains 5/6 of Rtt107 with the BRCT domains 3/4 of Dpb11 that recognize γ-H2A and phosphorylated T602 in the 9-1-1 component Ddc1, respectively (Williams *et al.* 2010; Li *et al.* 2012; Puddu *et al.* 2008). This fusion protein recapitulates the "two-site-docking" mechanism that Dpb11-Slx4-Rtt107 uses to displace Rad9 (see **figure 1.4c;** Cussiol *et al.* 2015).

During my thesis, I investigated the consequences of checkpoint hypersignaling in response to MMS-induced replication stress. I specifically compared the phenotypes of cells lacking the main Rad53 phosphatase, Pph3, and cells lacking DAMP function, and found that cells lacking *PPH3* phenocopy defects seen in ***slx4Δ*** cells. These cells show hyper-Rad53 activation, specific sensitivity to MMS, and chromosomal defects. My work presented here suggests that defects seen in hypercheckpoint signaling converge to the regulation of the Mus81 nuclease, which is necessary for downstream repair of MMS-induced lesions. Additionally, I found that Pph3 and Slx4-Rtt107 function in parallel

mechanisms, as double mutants show more dramatic defects compared with single mutants. This suggests that the actions of Pph3 and Slx4-Rtt107 coordinate to down-regulate DDC signaling. Interestingly, I also show that although Pph3 and Slx4-Rtt107 function cooperatively, they do not compensate for one another. Here, I propose a model that DAMP functions to down-regulate Rad53 activation at sites of lesions, while Pph3 dephosphorylates diffuse nuclear pools of active Rad53.

CHAPTER 2

MATERIALS AND METHODS

Yeast strains and plasmids.

Strains generated in this study were derived either from MBS164 or MBS191 (both congenic to S288C) or W303 (where indicated). All yeast strains and plasmids used in this study are described in **Tables 4** and **5**, respectively. Additional strains generated are listed in **Table 6**. Strains were constructed using standard genetic protocols for knockout and epitope tagging (Bähler *et al.* 1998; Longtine *et al.* 1998). All yeast transformations were performed using the lithium acetate method (Gietz *et al.* 1992). Deleted genes were screened using PCR for presence of marker in the the place of the gene ORF. Yeast strains carrying the *rad53-R605A* allele were generated by linearizing a plasmid carrying *rad53-R605A-kanMX6* (pMBS 362) and integrating it at the endogenous *RAD53* locus. Integration was selected on rich medium (YPD) in the presence of G418 (300µg/mL). Individual colonies were selected for DNA extraction and *rad53-R605A* allele confirmed by DNA sequencing of the *RAD53* gene.

All tags were integrated by homologous recombination at the C-terminus of the gene's original chromosomal loci unless otherwise stated (tagged genes on plasmids are indicated). Endogenously-tagged proteins were verified by western blotting. To ensure epitope-tagging of genes did not disrupt protein function, tagged cells were checked for sensitivity to genotoxins and cell doubling time and compared with wildtype cells (not shown).

Genes containing an *ADH1* promotor were generated by fusing the *ADH1* promoters (800 base pairs upstream of the start codon) to the corresponding reading frame. This fusion was performed by stitch PCR using a PCR product of the *ADH1* promotor with 50bp of sequence homology. This 50bp of homology overlapped with the first 50bp of the gene. The resulting PCR product was combined with the KanMX6 marker upstream of the *ADH1* promoter and directly integrated upstream of the target loci, where indicated.

Western blot analysis.

For western blotting, about 50mg of frozen yeast cell pellet (grown in either YPD or drop out media) was lysed by bead beating at 4^{o}C in lysis buffer (50mL Tris-HCl, pH7.5, 0.2% Tergitol, 150mM NaCl, 5mM EDTA, 1mM phenylmethylsulphonyl (PMSF), Complete phosphatase inhibitor, and EDTA-free Protease inhibitor cocktail (Roche). SDS loading buffer was supplemented with 60mM dithiothreitol (DTT). Samples were separated by standard SDS-polyacrylamide gel electrophoresis (SDS-PAGE). Rad53 and phosphorylated histone H2A proteins were probed using specific antibodies: anti-Rad53 (clone Mab EL7, gift from Dr. Achille Pellicioli, 1:30 dilution), anti-γ-H2A (Ab17353-Abcam, 1:5000 dilution), ECL HRP-Linked secondary antibody (NA931-GE, 1:10000 dilution).

Cell Cycle Synchronization.

Yeast cells were grown in yeast peptone dextrose (YPD) medium or drop-out medium at 30°C until log phase. For arrest of cells in G1, α-factor (Zymo Research) was added to a final concentration of 50 ng/ml (for *bar1Δ* background strains) and incubated for 2 hours. To release cells from G1 arrest, cells were centrifuged and resuspended in fresh warm medium in the presence of pronase (50 ng/ml, Sigma P5147) and methyl methanesulfonate (MMS) (where indicated).

Genotoxin Sensitivity.

Cells were grown until log-phase and normalized to an optical density (OD) of 0.8. Fourfold serial dilutions were spotted on YPD or synthetic complete medium lacking uracil (SC –URA) plates and grown for 2–3 days at 30°C in the presence or absence of drugs as indicated.

Cell Collection and Fluorescence Activated Cell Sorting (FACS).

Cells were grown in liquid YPD to and OD600 of 0.2 before addition of α-factor for 2 hours. G1 samples were collected and remaining cultures were washed with warm fresh YPD before being released into MMS-containing medium. At each indicated time-point, 1 mL of log phase yeast cultures were collected, harvested, resuspended in 1 mL of 70% ethanol and incubated for 15 minutes at RT or overnight at 4^{o}C. Cells were then centrifuged, supernatant was removed and residual ethanol was dried in a speed-vac. After that, samples were solubilized in sodium citrate buffer (50mM, pH 7.2) and sonicated (3 cycles of 3 seconds, amplitude 30%) to break up cell clumps. Samples were then

incubated with 200µg of RNAse A (Qiagen™) for 2 hours at 37°C followed by incubation with 500µg of Proteinase K (Invitrogen™) for 1 hour at 42°C. Finally, 1µL of SYTOX Green (Life Technologies™) was added to the samples and incubated for 2 hours at 4°C protected from the light. Data was acquired using a BD™ Accuri C6 Flow Cytometer.

Pulse Field Gel Electrophoresis (PFGE).

Yeast cells were allowed to reach log phase in 200mL of YPD medium. An untreated, asynchronous sample (ASY) was taken for control. Cells were then treated with MMS for 2 hours, then centrifuged and recovered in fresh, MMS-free medium for up to 6 hours. For a detailed protocol please see (Appendix iii or Cussiol *et al.* 2015). Briefly, 50mg of cell pellet was isolated for each time point and yeast strain being tested. To each 50mg pellet, 450uL of low melting point (LMP) agarose and 20uL of zymolyase was used to resuspend the cell pellet before transferring to the genomic plug mold. Once the plug mold is completely solidified, each plug was gently pushed into a 2mL snapcap tube with ZYM solution (500mM EDTA, 10mM Tris, pH7.5) overnight at 37°C for complete digestion of the yeast cell wall. The next day, proteinase K (5% Sarcosyl, 5mg/ml proteinase K in 500mM EDTA pH7.5) was added to digest proteins at 50°C for at least 5 hours, followed by several days of washing with Wash solution (20mM Trish, 50mM EDTA, pH8.0) at room temperature.

The pulse-field gel was set up so that each plug was cut to an appropriate size, placed on a gel comb (see detailed protocol), and a gel was poured around each plug using 1% pulse field certified agarose in 0.5% TBE buffer. The pulse field gel was allowed to completely solidify at 4°C for at least 4 hours in a Bio-Rad gel cast system with a cast

iron plate. Once, the gel is completely set, the gel with the cast iron plate was removed from the cast and place in a Bio-Rad CHEF mapper reservoir with 3.5L of 0.5X TBE buffer chilled to 14^{o}C. The running conditions for the Bio-Rad CHEF mapper pulse-field set up were: 2 state mode; 6.0v/cm gradient for 24 hours; 120^{o} included angle; 60 second initial switch time; 120 second final switch time; linear ramping factor. Once the chromosomes are separated on the pulse-field gel, the gel was stained with ethidium bromide for 20 minutes and then destained with fresh water for 2X 20 minutes at room temperature before imaging.

Confocal fluorescence microscopy.

Co-localization of Pph3-GFP and Slx4-yEmCherry was analyzed by growing yeast cultures (AYY183: *MAT*a *SLX4-yEmCherry::CaURA3, Pph3-GFP::HIS3MX STE2pr-LEU2 lyp1*Δ *ura3*Δ*0 leu2*Δ*0 his3*Δ*1 met15*Δ*0*) to saturation in YPD, diluting into fresh YPD to OD_{600} = 0.1, and growing for 2 h at 30°C before treating with 0.03% MMS. Eleven z slices with a 0.4 µm step size were acquired using Volocity imaging software (PerkinElmer) controlling a Leica DMI6000 microscope with the fluorescein isothiocyanate, Texas Red and differential interference contrast filter sets (Quorum Technologies). Slx4-yEmCherry foci, Pph3-GFP foci, and co-localizing foci were counted in >500 cells total, in 2 independent experiments.

Chromatin Immunoprecipitation (ChIP) and deep sequencing.

ChIP-seq analysis was performed as previously described (Balint *et al.* 2015). Briefly, cells were synchronously released into 0.04% MMS for 60 min, cross-linked with

formaldehyde, and subjected to chromatin immunoprecipitation. Sequencing libraries were generated from immunoprecipitated (IP) and input (IN) DNA using the Nextera™ XT DNA Sample Preparation Kit (Illumina) with custom Index primers, and sequenced using the HiSeq 2500 (Illumina). Data are presented for chromosome ten as a log2 ratio of normalized read counts for each IP:input pair. Enrichment values for 1 kb bins across 50 kb upstream and downstream of each replication origin were extracted to visualize median (± standard error) protein enrichment across all early origins. Replication profiles were generated using VarScan 2 [version 2.3.5; default settings (Koboldt *et al.* 2012)] by comparing sequencing read counts from the input samples with sequencing read counts from a reference sample from a G1-arrested strain (BY4741). All sequencing data were deposited in the Sequence Read Archive (http://www.ncbi.nlm.nih.gov/sra; Study accession SRP062915).

Analysis of Pph3-dependent targets upon MMS treatment using quantitative mass spectrometry.

The strains MBS164 (wildtype) and MBS2191 (*pph3Δ*) were grown to OD_{600} 0.2 in 400mL of –Arg –Lys dropout media ("light" media is completed with normal arginine and lysine, while "heavy" media is complemented with L-Lysine $^{13}C^{6}$, $^{15}N^{2}$.HCl and L-Arginine $^{13}C^{6}$, $^{15}N^{4}$.HCl). Cells were synchronized in G1 using the pheromone α-factor for 2 hours (see cell synchronization). After cells were checked for uniform arrest in G1 via microscropy, cells were released into fresh medium with 0.015% MMS. After 45 minutes, cells were collected and mixed evenly. Cells were then centrifuged and kept at -80C prior to cell lysis. Approximately 0.6g of cell pellet of each strain was lysed by beat beating at

4°C in lysis buffer (50mM Tris-HCl pH8.0, 0.2% Tergitol, 150mM NaCl, 5mM EDTA, 10mM B-glycerol-phosphate (phosphatase inhibitor)). Proteins were extracted by solubilizing in 1% SDS and reducing disulfide bonds using 5mM DTT. Cysteines were alkylated using 15mM Iodoacetamide to prevent disulfide bond reformation. Proteins were precipated by adding 3 volumes of PPT solution (50% acetone, 49.9% ethanol, 0.1% acetic acid) on ice for at least 10 minutes, followed by centrifugation. Protein pellets were allowed to dry and resolubilzed by adding 8M urea, 100mM Tris-HCl (pH 8) to the protein pellet and using a douncer to homogenize the solution. Tris/NaCl solution (50mM Tris-HCl (pH 8.0), 150mM NaCl) was added to the protein solution to dilute the final concentration of urea to 2M. TPCK-treated trypsin (400ug) was added to the protein solution and allowed to digest overnight at 37°C under constant rotation. The next morning, 10% formic acid and 10% TFA were added to the trypsinized solution to a final concentration of 0.2% each to inactivate tryspin. Samples were desalted up using Sep-Pak C18 columns (Waters), dried using a speed-vac, and reconstituted in 85uL of a solution containing 80% acetonitrile and 1% formic acid.

Phospho-peptide enrichment via immobilized metal affinity chromatography (IMAC)

Phosphopeptides were purified using agarose immobilized metal affinity chromatography (IMAC). IMAC columns are packed as described in Appendix iii. Each column, was equilibrated with 1% acetic acid. Then, trypsin-digested peptides were added to each column using gravity and washed with IMAC wash solution 1 (0.1M NaCl, 0.1% acetic acid, 25% acetronitrile), IMAC wash solution 2 (1% acetic acid), and

deionized water. Phosphopeptides were eluted directly in silanized flat bottom glass tubes using 3 volumes of IMAC eluting solution (12% ammonia, 10% acetronitrile) and dried in a speed-vac. Before further analysis, dried phospho-peptides were then resuspended in formic acid and acetonitrile prior to HILIC (Hydorphilic Interaction Liquid Chromatography) fractionation. Each HILIC fraction was then dried and resuspended in 0.1 picomole angiotension as a standard before LC-MS/MS analysis.

Database search and data analysis

Database search was performed using the Sorcerer system (Sagen) running Sequest program. Peptides identified by mass spectrometry were searched against a yeast protein database as well as a target-decoy budding yeast database to determine false identification rate. Results were filtered based on the probability score to achieve 1% or less fasle positive rate. Quantitation of the “heavy” to “light” peptide isotope ratios were performed using the Xpress program (Smolka *et al.* 2007). Additionally, results were manually inspected.

CHAPTER 3

PP4 AND SLX4-RTT107 FUNCTION IN PARALLEL TO DOWN-REGULATE CHECKPOINT SIGNALING AND ALLOW RESOLUTION OF JOINT CHROMOSOMES.

This work was published in Jablonowski, C.M.; Cussiol, J.R.; Oberly, S.; Yimit, A.; Balint, A.; Kim, T.; Zhang, Z.; Brown, G.W.; Smolka, M.B. (2015). Termination of replication stress signaling via concerted action of the Slx4 scaffold and the PP4 phosphatase. Genetics *201,* 937-949.

Introduction

Replication stress is one of the main sources of genomic instability that has been associated with the onset of cancers (Branzei & Foiani 2009; Kastan & Bartek 2004; Myung *et al.* 2001). To cope with stress during DNA replication, cells rely on the DNA damage checkpoint (DDC), a surveillance mechanism that senses abnormal DNA structures and elicits signaling responses that coordinate multiple cellular processes. With the goal of preserving genome integrity and cell viability, DDC signaling triggers cell cycle arrest (Weinert & Hartwell 1988), inhibition of replication origin firing (Santocanale & Diffley 1998; Zegerman & Diffley 2010) and replication fork protection mechanisms that include an increase of dNTP pools (Davidson *et al.* 2012; Zhao *et al.* 2001; Zhou & Elledge 1993) and inhibition of nucleases such as Exo1 (Morin *et al.* 2008). In *Saccharomyces cerevisiae*, the DDC is orchestrated mainly by the action of the apical PI3K-like kinase (PI3KK) Mec1 (ATR in humans) that senses the damage as exposure of single-stranded DNA (ssDNA) and transduces the signal to the downstream effector kinase Rad53 (human CHK2/CHK1), which will then enforce most of the responses that characterize a canonical DDC (Sanchez *et al.* 1996; Sun *et al.* 1996).

A critical step in the activation of the DDC is the recruitment of Rad53 to sites of DNA lesions. While Mec1 is rapidly recruited to regions of ssDNA via a direct interaction of its cofactor Ddc2 with ssDNA-coated RPA (Zou & Elledge 2003), the recruitment of Rad53 is subject to extensive regulation and requires the involvement of DDC adaptors (a.k.a. mediators) Rad9 or Mrc1. Mrc1 is a component of the replisome and is mostly involved in recruiting Rad53 to stalled replication forks (Alcasabas *et al.* 2001). Rad9 mediates Rad53 recruitment and activation in response to a broader variety of DNA lesions, including double strand breaks (DSBs) and DNA lesions induced by replication stress in which replication forks bypass the lesion, leaving ssDNA gaps behind (Branzei & Foiani 2010; Gilbert *et al.* 2001; Schwartz *et al.* 2002; Sun *et al.* 1998). Rad9 is recruited to DNA lesions by direct recognition of chromatin marks, including histone H2A phosphorylated at serine 129 (γH2A) and methylated histone H3K79 (Giannattasio *et al.* 2005; Grenon *et al.* 2007; Hammet *et al.* 2007), via its BRCT and Tudor domains, respectively. Rad9 is also recruited to DNA lesions via interaction with the Dpb11 scaffold, which binds to a Mec1-phosphorylated site in the 9-1-1 clamp loaded at ss/dsDNA junctions (Granata *et al.* 2010; Pfander & Diffley 2011; Puddu *et al.* 2008). Recruitment of Rad9 via multiple partially redundant mechanisms is believed to increase opportunities for regulating Rad53 recruitment and activation, therefore helping to fine-tune DDC activation levels (Ohouo & Smolka 2012).

Once Rad9 is recruited, it is extensively phosphorylated by Mec1, creating docking phospho-sites that are recognized by the FHA-domains (forkhead-associated domains) of Rad53, enabling Rad53 to be recruited in the vicinity of Mec1 (Grenon *et al.* 2001; Schwartz *et al.* 2002; Sweeney *et al.* 2005). Mec1 then phosphorylates and activates

Rad53, which undergoes further autophosphorylation *in trans* to reach its full activation state (Gilbert *et al.* 2001). Once activated, Rad53 is believed to quickly diffuse throughout the nucleus to phosphorylate its physiological substrates eliciting a global checkpoint response [for review see (Pellicioli & Foiani 2005)].

Despite the key roles for Rad53 signaling in the replication stress response, it is imperative that its activity is precisely regulated. Because checkpoint signaling represses DNA replication and cell cycle progression, down-regulation of Rad53 activity is essential for the resumption of cell proliferation once the DNA damage is repaired or bypassed. Although activation of DDC has been extensively studied, less is understood about its down-regulation. The PP2C phosphatases, Ptc2 and Ptc3, were first characterized as important for Rad53 dephosphorylation and checkpoint recovery following DSB induction (Leroy *et al.* 2003). Later on, the PP4 phosphatase complex Pph3-Psy2 was shown to be important for Rad53 dephosphorylation following treatment with the DNA alkylating agent methyl methanesulfonate (MMS), which generates replication blocks that are readily bypassed by moving replication forks (O'Neill *et al.* 2007). In addition to phosphatase-mediated mechanisms, our lab has recently uncovered a new mechanism of Rad53 down-regulation involving direct displacement of Rad9 from DNA lesions (Cussiol *et al.* 2015; Ohouo *et al.* 2013). In this phosphatase-independent mechanism, named DAMP (for Dampens Adaptor Mediated-Phosphosignaling), a complex formed by the DNA repair scaffolds Slx4 and Rtt107 competes with Rad9 by interacting with two proteins required for Rad9 recruitment, namely γH2A and Dpb11. As a consequence, Rad9 is displaced from DNA lesions, prohibiting further transduction of Mec1 signaling to Rad53, thus dampening the DDC. Interestingly, Slx4 has an established role as a scaffold for the

coordination of structure-specific nucleases (Mullen *et al.* 2001; Rouse 2009), so the identification of a nuclease-independent function for Slx4 in DDC regulation suggests an intricate mechanism for the crosstalk and coordination of DDC signaling control and DNA repair.

Here I show that proper termination of DDC signaling following the bypass of replication blocks imposed by alkylated DNA adducts requires the concerted and highly complementary actions of Slx4 and the PP4 phosphatase. I show that cells lacking both *SLX4* and the *PPH3* subunit of PP4 display a synergistic increase in Rad53 signaling and are exquisitely sensitive to MMS. Rad53 hyperactivation in these mutants seems to indirectly converge to cause repression of Mus81-Mms4, a nuclease involved in the resolution of sister chromatid linkages that are byproducts of replication fork bypass events. These results support a model in which checkpoint down-regulation via the scaffold complex Slx4-Rtt107 or PP4 phosphatase Pph3 allows for the timely activation of the structure-specific endonuclease Mus81 to resolve joint DNA molecules following DNA repair.

Results

Cells lacking *PPH3* or *SLX4* display similar defects upon MMS-induced replication blocks

Rad53 is activated in response to a wide range of genotoxins and types of replication stress (Pellicioli *et al.* 1999; Sun *et al.* 1996). Notably, *pph3Δ* cells and *slx4Δ* cells display hypersensitivity to replication stress induced by the DNA alkylating agent MMS but not to replication stress induced by the ribonucleotide reductase (RNR) inhibitor hydroxyurea (HU) (**Figure 3.1A**). A distinct feature of MMS-induced DNA lesions is the extensive generation of adducts, mostly N7-guanine methylation on one of the DNA strands, which are readily bypassed by moving replication forks (Branzei & Foiani 2010). Upon exposure to MMS, both *pph3Δ* cells and *slx4Δ* cells display hyperactivation of Rad53 and an intra-S delay (**Figs. 3.1B** and **3.1C**), consistent with previous reports (Chang *et al.* 2002; O'Neill *et al.* 2007; Ohouo *et al.* 2013; Roberts *et al.* 2006).

Furthermore, both *pph3Δ* cells and *slx4Δ* cells exhibit MMS-induced chromosomal defects visualized by PFGE [(**Figure 3.2**), see also (Roberts *et al.* 2006) for *slx4Δ*], a defect often attributed to either incomplete chromosomal replication or improper processing of joint chromosomal structures (Hennessy *et al.* 1991; Saugar *et al.* 2013). Consistent with these findings, checkpoint signaling has been shown to counteract DNA replication, S-phase progression and timely resolution of joint chromosomes (Santocanale & Diffley 1998; Szakal & Branzei 2013; Szyjka *et al.* 2008).

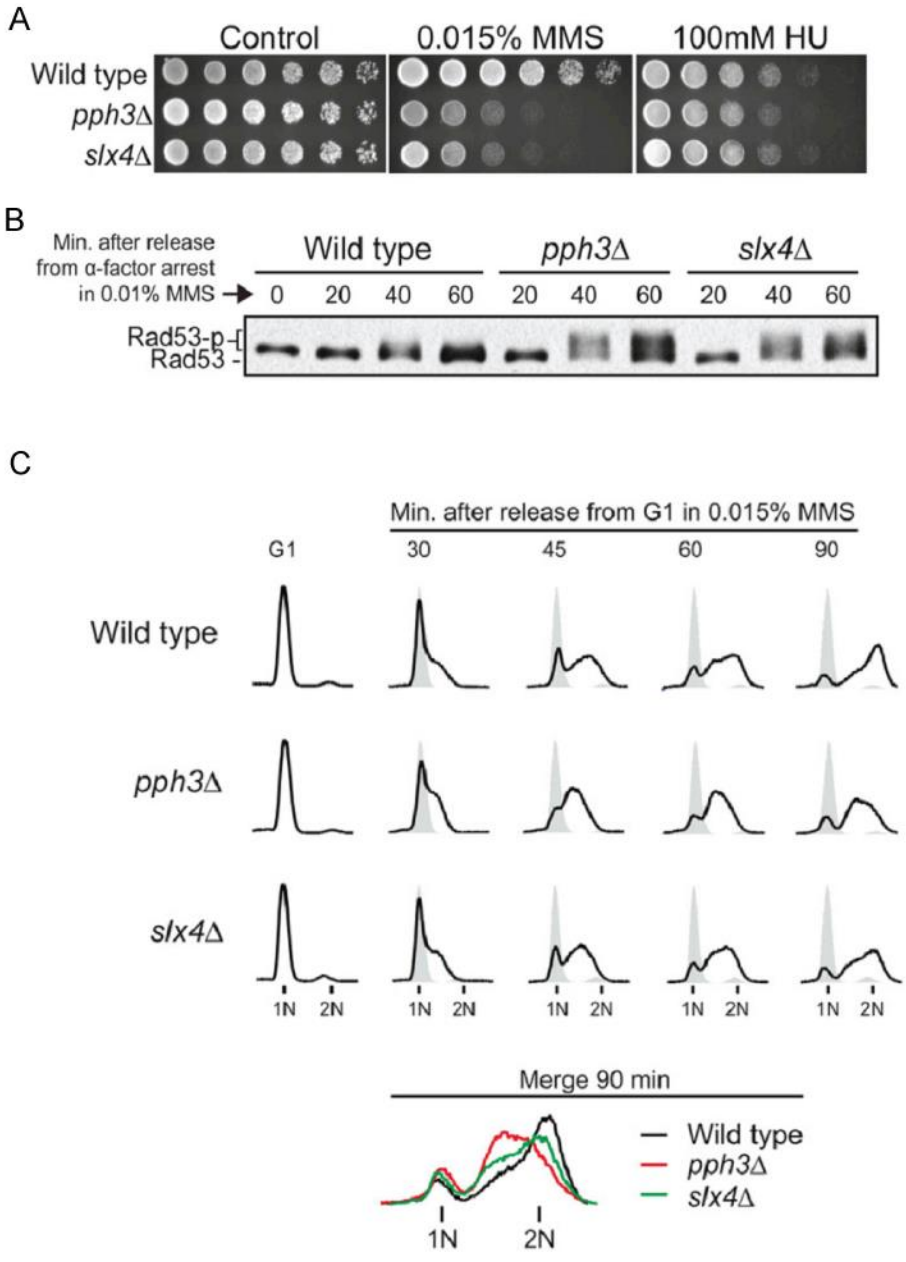
A
Control
0.015% MMS
100mM HU
Wild type
pph3Δ
slx4Δ
B
Min. after release from α-factor arrest in 0.01% MMS
Wild type
pph3Δ
slx4Δ
0 20 40 60 20 40 60 20 40 60
Rad53-p
Rad53
C
Min. after release from G1 in 0.015% MMS
G1 30 45 60 90
Wild type
pph3Δ
slx4Δ
1N 2N
Merge 90 min
Wild type
pph3Δ
slx4Δ
1N 2N

Figure 3.1. Cells lacking either *PPH3* or *SLX4* show similar defects upon replication stress induced by MMS. (A). Serial dilution assays showing the effect of genotoxin treatment upon the sensitivity of wild-type, ***slx4Δ***, and ***pph3Δ*** cells. Four-fold serial dilutions were spotted on YPD plates and grown for 2–3 days at 30^{o}C. (B) Anti-Rad53 immunoblots of wild-type, ***slx4Δ***, and ***pph3Δ*** strains showing Rad53 phosphorylation status after MMS treatment. (C) S phase progression analysis of wild-type, ***slx4Δ***, and ***pph3Δ*** strains. For B and C, cells were arrested in G1 with α-factor and then released in medium containing MMS. Samples were collected in G1 and at different time points following release. FACS analysis was completed with the help of Dr. José Cussiol.

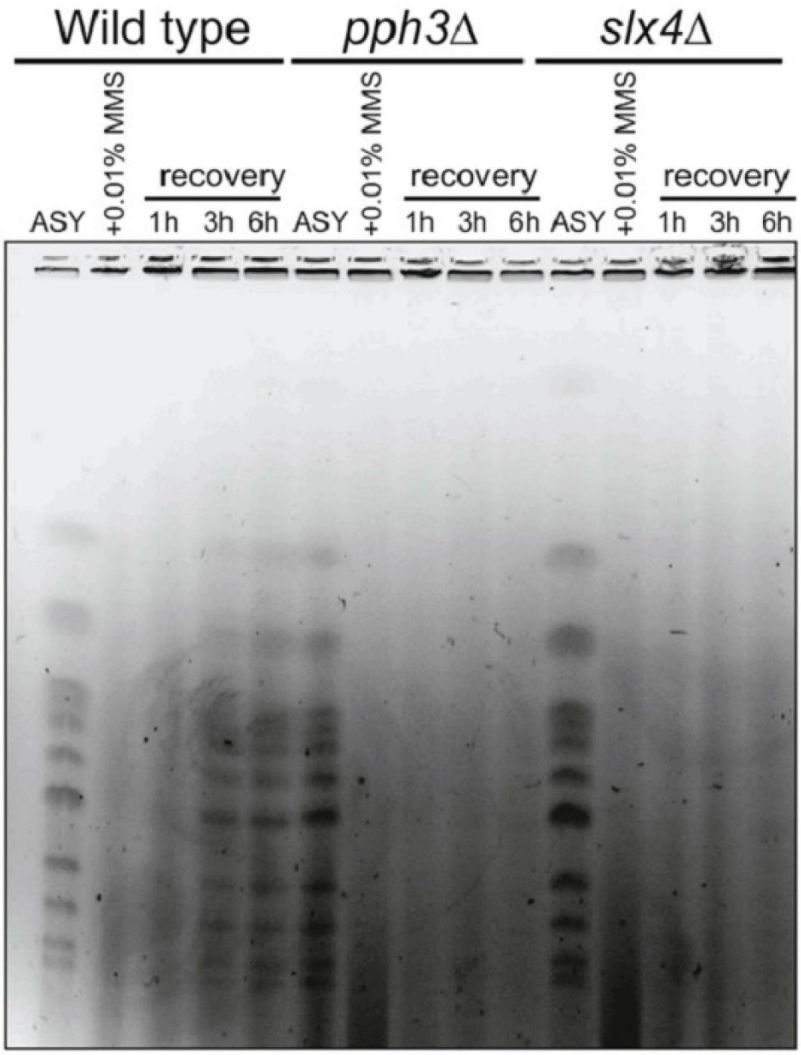

Figure 3.2. Cells lacking either *PPH3* or *SLX4* show similar defects in pulse-field gel electrophoresis (PFGE) upon MMS-induced replication stress. Analysis of fully replicated chromosomes measured by PFGE in wild-type, ***slx4Δ***, and ***pph3Δ*** strains. Asynchronous (ASY) cells were treated with 0.01% MMS for 2 hr and then released in MMS-free medium for up to 6 hr. See appendix iii for details.

Of importance, the MMS sensitivity of both *pph3Δ* cells and *slx4Δ* cells could be rescued by a hypomorphic allele of *RAD53* (*rad53-R605A*) that we have previously shown to lower Rad53 activation levels (Ohouo *et al.* 2013) (**Figure 3.3**). Taken together, these results show that *pph3Δ* cells display similar defects as *slx4Δ* cells upon exposure to MMS-induced replication stress, and that in both cases the observed defects are caused by improper regulation of Rad53 signaling.

Pph3 and Slx4 represent complementary mechanisms for Rad53 down-regulation following MMS-induced replication stress

To better understand the functional interplay between the phosphatase-mediated (via Pph3) and the DAMP-mediated (via Slx4) mechanisms for Rad53 down-regulation, I analyzed cells lacking both *PPH3* and *SLX4*. When compared to the single mutants, *pph3Δ slx4Δ* cells display significant increase in Rad53 activation, which was accompanied by a dramatic increase in MMS sensitivity and chromosomal defects visualized by PFGE (**Figs. 3.4A-C**). Strikingly, these abnormalities, as well as the intra-S-phase delay observed by Fluorescence-Activated Cell Sorting (FACS), could be rescued in cells expressing the *rad53-R605A* allele (**Figs. 3.5A-D**). Of importance, the *slx4* mutant bearing the S486A mutation, which encodes a protein that is specifically unable to interact with Dpb11 and promote DAMP (Ohouo *et al.* 2013), behaved similarly to the full deletion of *SLX4* in our analysis of Rad53 activation, MMS sensitivity and PFGE (See Appendix i.). Collectively, these results support the notion that *PPH3* and *SLX4* function in parallel, representing two complementary mechanisms for down-regulating

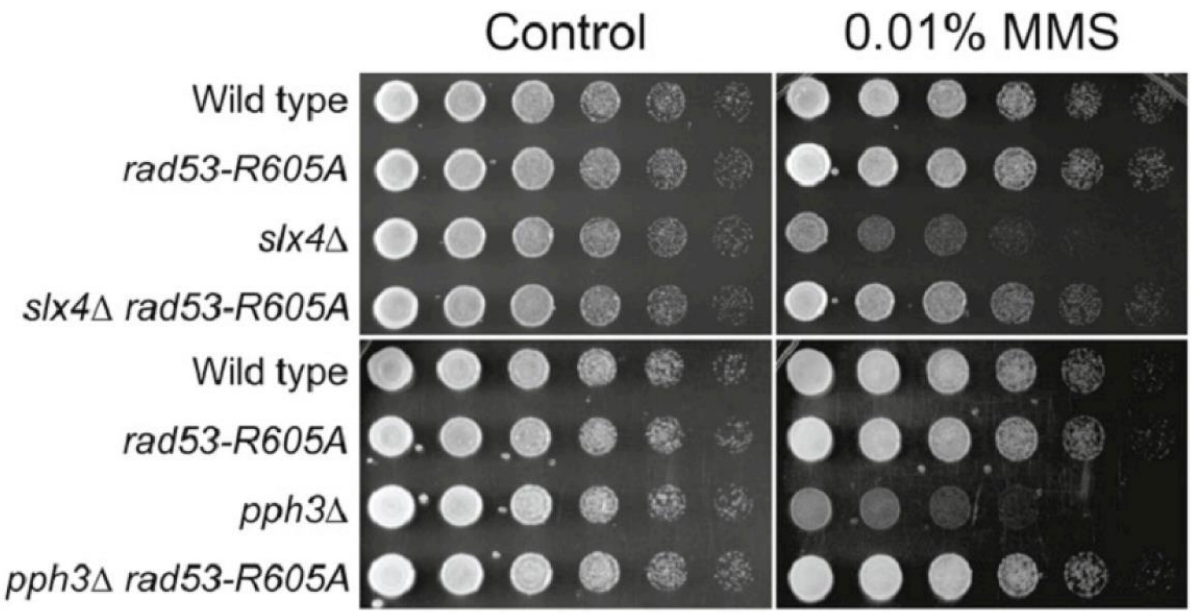

Figure 3.3. A *RAD53* hypomorphic mutant rescues the MMS sensitivity of *pph3Δ* or *slx4Δ* cells. Serial dilution assay showing the effect of a hypomorphic *RAD53* allele (*rad53-R605A*) on MMS sensitivity of wild-type, *slx4Δ*, and *pph3Δ* strains. Four-fold serial dilutions were spotted on YPD plates and grown for 2–3 days at 30^{o}C.

A

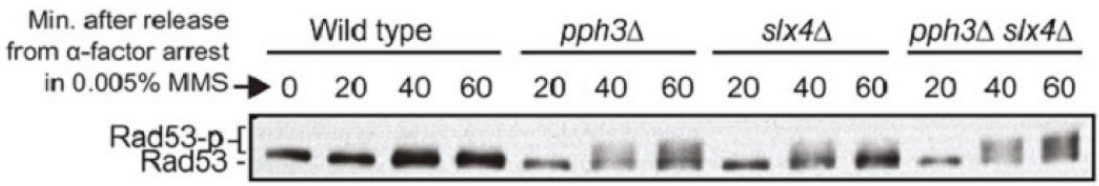
Min. after release
from α-factor arrest
in 0.005% MMS
Wild type
pph3Δ
slx4Δ
pph3Δ slx4Δ
0 20 40 60 20 40 60 20 40 60 20 40 60
Rad53-p
Rad53

B

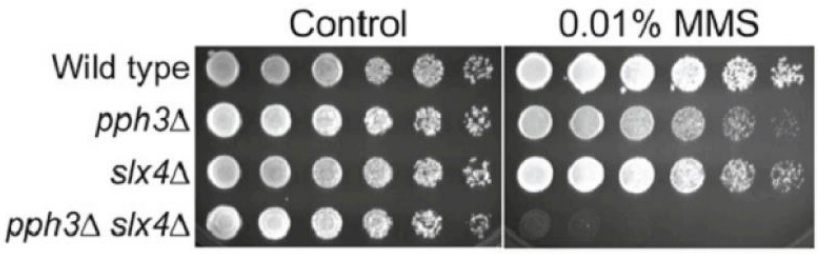
Control
0.01% MMS
Wild type
pph3Δ
slx4Δ
pph3Δ slx4Δ

C

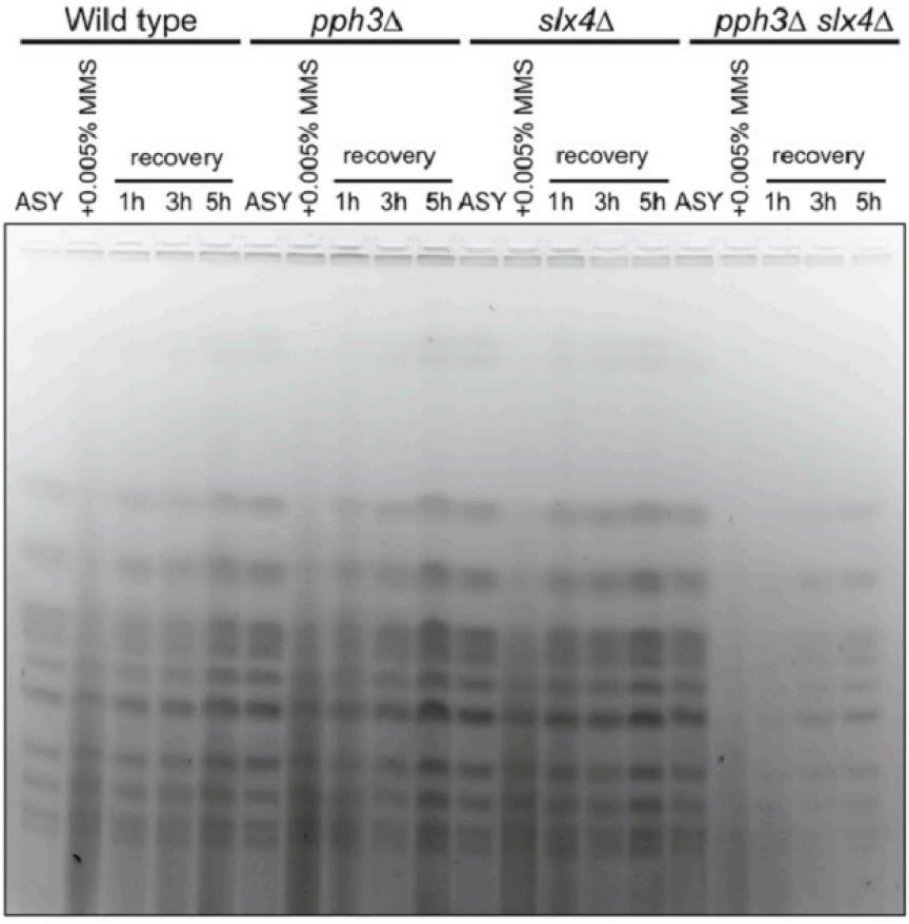
Wild type
pph3Δ
slx4Δ
pph3Δ slx4Δ
ASY
+0.005% MMS
recovery
1h 3h 5h

Figure 3.4. Slx4 and Pph3 function in a complementary manner in the regulation of Rad53 signaling. (A–C) Wild-type, *slx4Δ*, and *pph3Δ* single mutants were compared against a *pph3Δ slx4Δ* strain. (A) Anti-Rad53 immunoblots of wild-type*, slx4Δ*, *pph3Δ*, and *pph3Δ slx4Δ* strains showing Rad53 phosphorylation status after MMS treatment. (B) Serial dilutions assay showing the MMS sensitivity of indicated strains. Four-fold serial dilutions were spotted on YPD plates and grown for 2–3 days at 30^{o}C. (C) Analysis of fully replicated chromosomes by PFGE. Asynchronous (ASY) cells were treated with 0.005% MMS for 2 hr and then released in MMS-free medium for up to 5 hr. For detailed protocol, see Appendix iii.

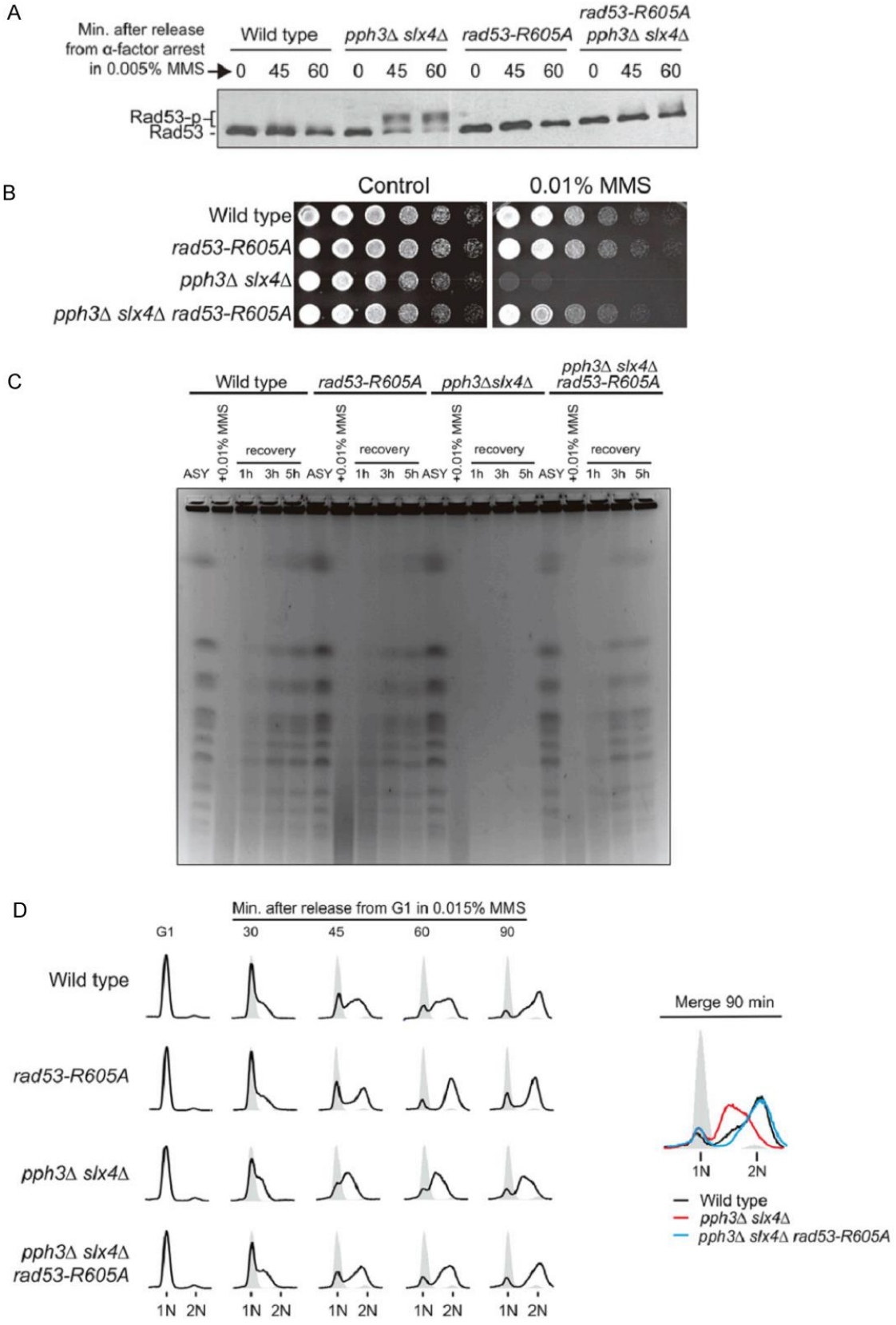
A
Min. after release from α-factor arrest in 0.005% MMS
Wild type
pph3Δ slx4Δ
rad53-R605A
rad53-R605A pph3Δ slx4Δ
0 45 60 0 45 60 0 45 60 0 45 60
Rad53-p
Rad53
B
Control
0.01% MMS
Wild type
rad53-R605A
pph3Δ slx4Δ
pph3Δ slx4Δ rad53-R605A
C
Wild type
rad53-R605A
pph3Δslx4Δ
pph3Δ slx4Δ rad53-R605A
+0.01% MMS
recovery
ASY 1h 3h 5h
D
Min. after release from G1 in 0.015% MMS
G1 30 45 60 90
Wild type
rad53-R605A
pph3Δ slx4Δ
pph3Δ slx4Δ rad53-R605A
1N 2N
Merge 90 min
Wild type
pph3Δ slx4Δ
pph3Δ slx4Δ rad53-R605A

Figure 3.5. The defects observed in *pph3Δ slx4Δ* cells can be alleviated with a hypomorphic allele of *RAD53.* The hypomorphic allele, *rad53-R605A,* decreases Rad53 phosphorylation status (A), rescues the MMS sensitivity (B), defects seen in PFGE-monitored chromosomes (C), and delay of S-phase progression of *pph3Δ slx4Δ* cells (D). FACS analysis was completed with the help of Dr. José Cussiol.

Rad53. These two mechanisms and their concerted action seem particularly important for regulating Rad53 signaling following the bypass of replication blocks.

Rad53 hyper-signaling in *slx4Δ* or *pph3Δ* cells impairs proper cell cycle-dependent regulation of the Mus81-Mms4 nuclease

Replication forks typically bypass MMS-induced replication blocks via template switching mechanisms, resulting in physical linkages between sister chromatids, also known as joint molecules (JMs) (Branzei *et al.* 2008). Processing of these linkages is crucial for chromosome segregation and occurs mainly through two parallel mechanisms, either dissolution via the Sgs1-Top3-Rmi1 complex or resolution via the Mus81-Mms4 structure-specific endonuclease (Hickson & Mankouri 2011; Sarbajna & West 2014). The Mus81-Mms4 pathway is under strict cell cycle regulation, being activated in G2/M by action of the CDK and Cdc5 kinases and presumably antagonized by DDC-mediated cell cycle arrest (Szakal & Branzei 2013; Zhang *et al.* 2009). Because MMS treatment induces massive amounts of JMs, it seems likely that repression of Mus81-Mms4 activation imposed by the strong cell cycle arrest is perhaps a major deleterious effect of Rad53 hyperactivation in *slx4Δ* and *pph3Δ* mutants, and could explain why these cells are hyper-sensitive to MMS. To test the hypothesis that temporal mis-regulation of Mus81-Mms4 activation accounts for the reason why cells lacking *SLX4* and *PPH3* are hyper-sensitive to MMS-induced replication blocks, I performed genetic analysis with *sgs1Δ* or *mus81Δ* cells. As cells lacking both *SLX4* and *SGS1* are inviable due to the checkpoint-independent role of Slx4 controlling the activity of the Slx1 nuclease (Fricke

& Brill 2003), I utilized the *slx4-S486A* allele that we have previously shown to disrupt the checkpoint dampening function of Slx4 (Ohouo *et al.* 2013). Cells lacking *SGS1* and expressing the *slx4-S486A* allele are viable, but display a significant increase in MMS sensitivity compared to the single mutants. In addition, cells lacking *MUS81* and expressing the *slx4-S486A* mutant display MMS sensitivity similar to the *mus81Δ* single mutant [**Figure 3.6A**, see also (Gritenaite *et al.* 2014)]. As for Pph3, a *pph3Δ sgs1Δ* strain also showed enhanced MMS sensitivity compared to single mutants and deletion of *PPH3* did not significantly increase the sensitivity of *mus81Δ* cells to MMS (**Figure 3.6B**). Taken together, these results are consistent with the model in which a major cause of MMS sensitivity in both *pph3Δ* cells and *slx4Δ* cells is related to the inability of these cells to trigger the timely activation of Mus81-Mms4. While Rad53 hyper-signaling in these mutants likely has a broad impact on other events linked to cell cycle progression, the fact that these cells are selectively sensitive to MMS suggests that Mus81-Mms4 activation likely becomes the major limiting factor upon extensive accumulation of JMs.

If a crucial role of *PPH3*-dependent or *SLX4*-dependent down-regulation of Rad53 signaling is to promote Mus81-Mms4 activation, the *rad53-R605A* allele would rescue the MMS sensitivity of either *slx4Δ* or *pph3Δ* cells but not the sensitivity of cells lacking *MUS81*. Indeed, swapping the endogenous copy of *RAD53* for the *rad53-R605A* allele failed to rescue the MMS sensitivity of *mus81Δ*, *mus81Δ pph3Δ* or *mus81Δ slx4Δ* cells (**Figure 3.7** and Appendix ii). Interestingly, while *rad53-R605A* allele could rescue the strong intra-S delay observed in *mus81Δ pph3Δ slx4Δ* cells (**Figure** 3.8A), there was no observable rescue of the chromosome defects seen by PFGE (**Figure** 3.8B). This finding strongly suggests that the chromosome defects seen by PFGE

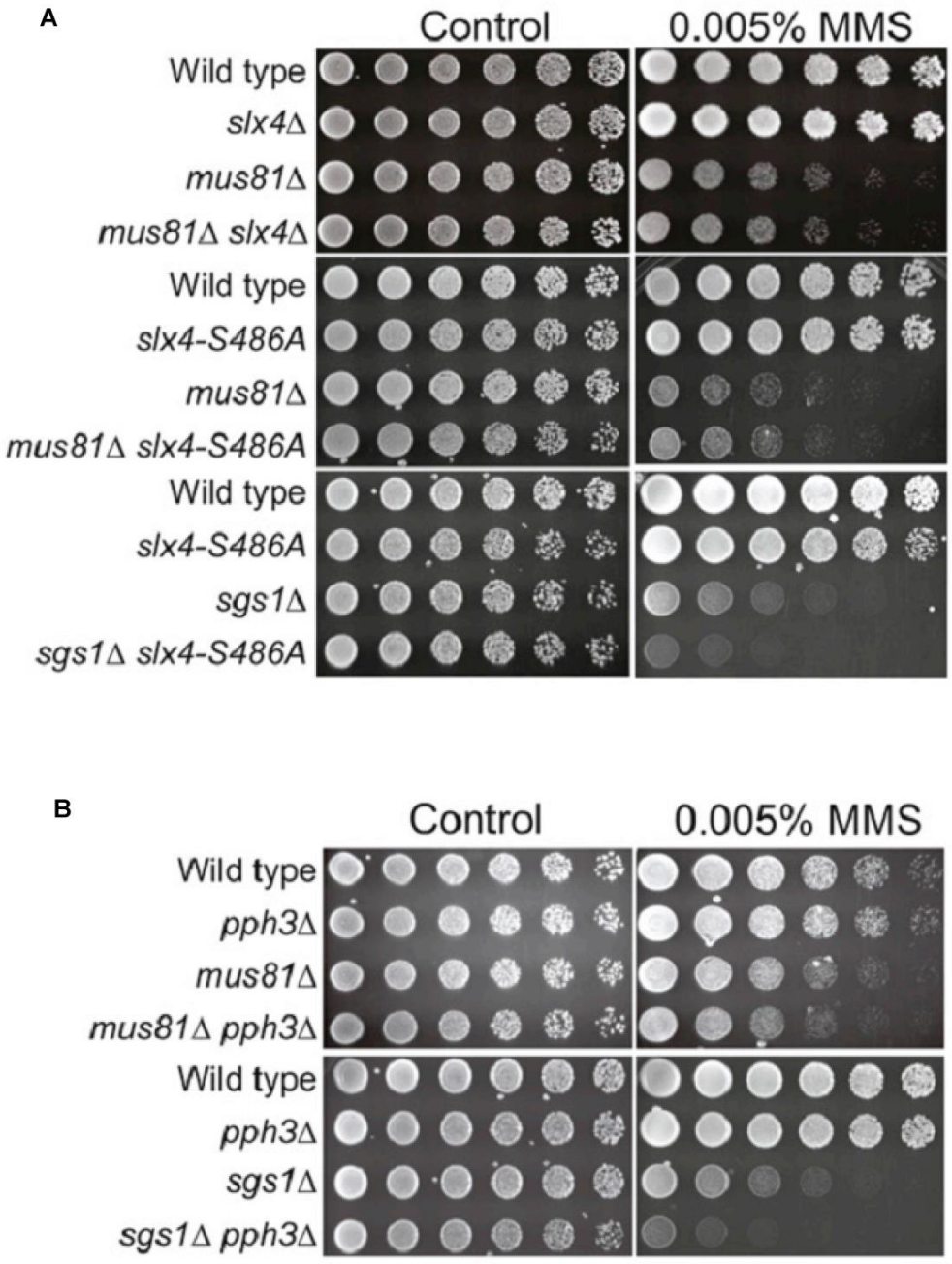

Figure 3.6. Genetic interaction of either *PPH3* or *SLX4* with mutations in either the *SGS1* helicase or *MUS81* endonuclease. (A and B) Serial dilution assay showing the effect of *MUS81* or *SGS1* deletion on the MMS sensitivity of the indicated strains. Four-fold serial dilutions were spotted on YPD plates and grown for 2–3 days at 30ºC.

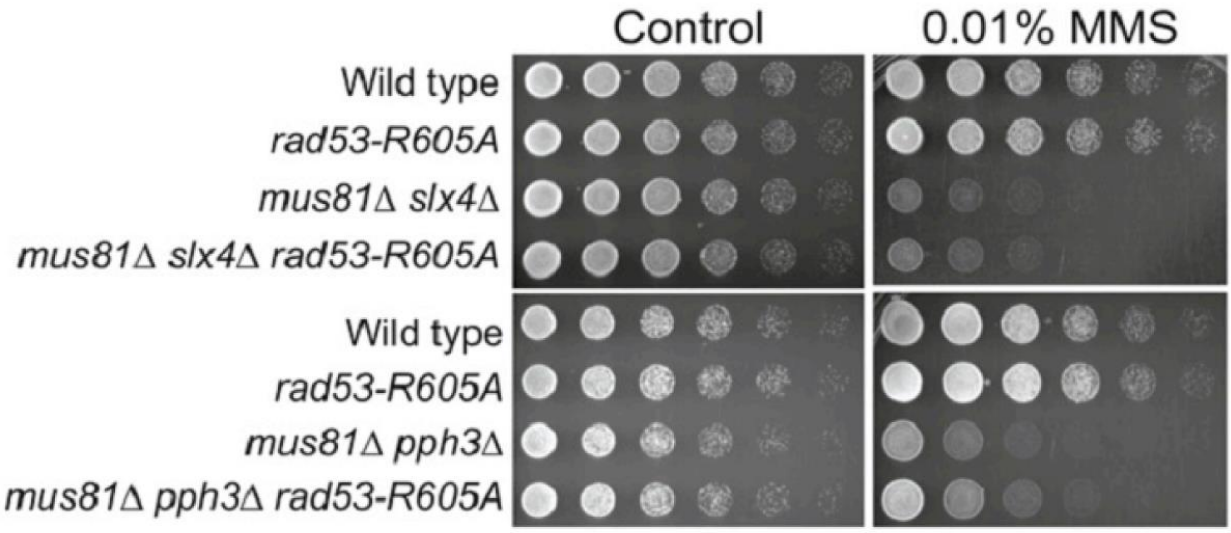

Figure 3.7. A hypomorphic allele of *RAD53* does not rescue the MMS sensitivity of *mus81Δ slx4Δ* or *mus81Δ pph3Δ* cells. Four-fold serial dilutions were spotted on YPD plates and grown for 2–3 days at 30^{o}C.

A

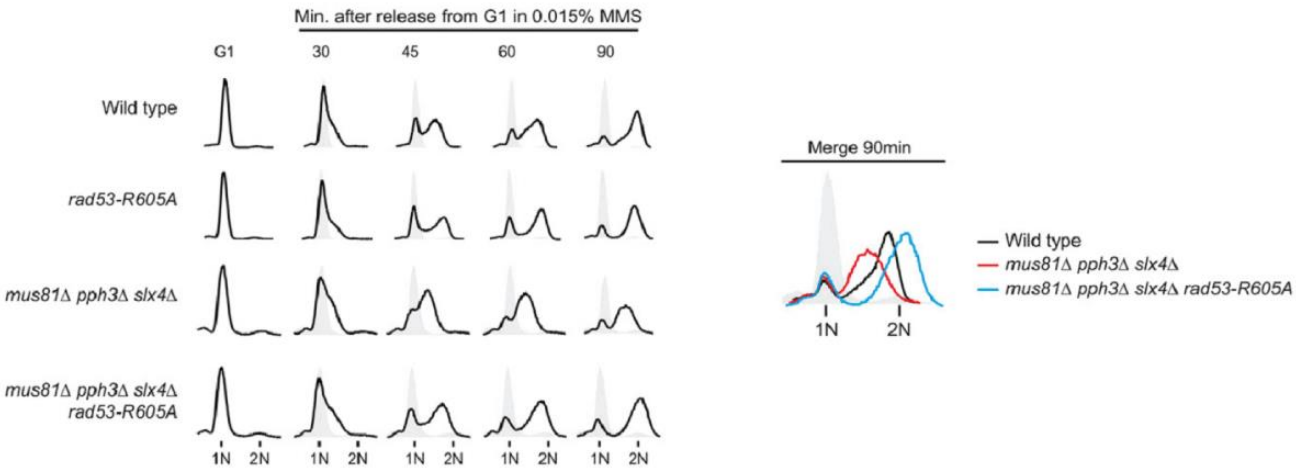
Min. after release from G1 in 0.015% MMS
G1
30
45
60
90
Wild type
rad53-R605A
mus81Δ pph3Δ slx4Δ
mus81Δ pph3Δ slx4Δ rad53-R605A
1N
2N
Merge 90min
Wild type
mus81Δ pph3Δ slx4Δ
mus81Δ pph3Δ slx4Δ rad53-R605A

B

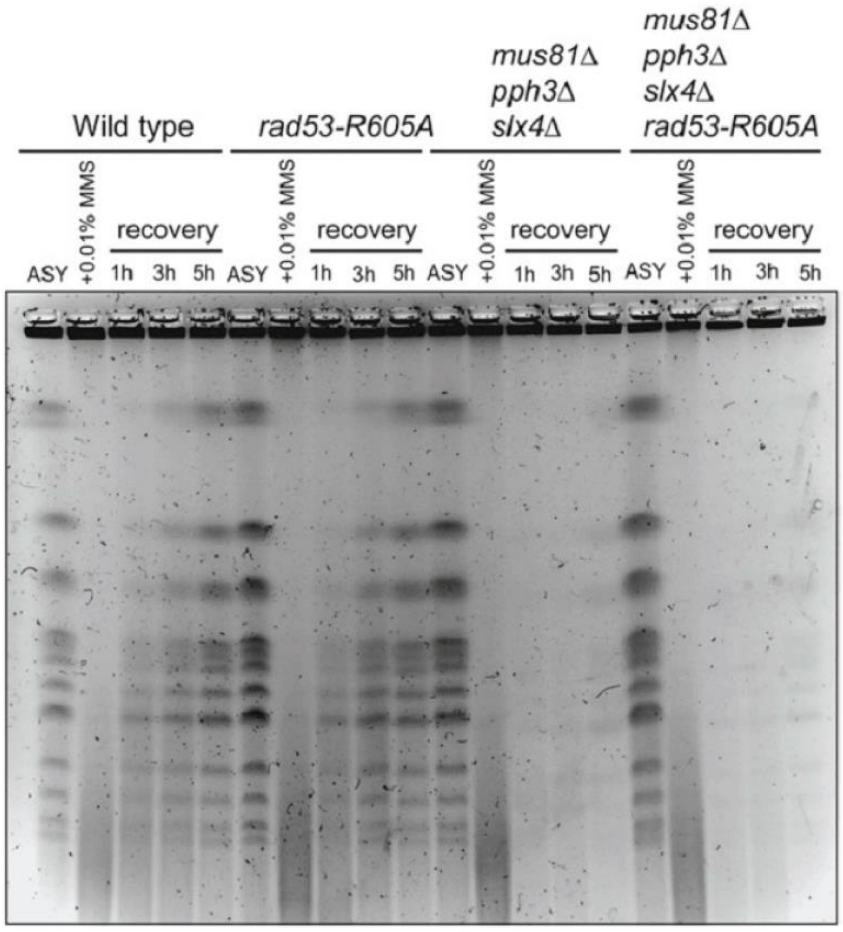
Wild type
rad53-R605A
mus81Δ pph3Δ slx4Δ
mus81Δ pph3Δ slx4Δ rad53-R605A
ASY
+0.01% MMS
recovery
1h
3h
5h

Figure 3.8. A hypomorphic allele of *RAD53* rescues the S phase delay of cells lacking *mus81Δ pph3Δ slx4Δ* but not the PFGE defect upon MMS-induced replication stress. (A) Indicated strains were arrested in G1 using α-factor and then released into S phase with 0.015% MMS for indicated time points. (B) PFGE-monitored chromosomes of the indicated strains lacking *MUS81*. Asynchronous cells were treated with 0.01% MMS for 2 hr and released into MMS-free medium for up to 5 hr. Samples were taken at each indicated time point.

in *slx4Δ* and *pph3Δ* cells are not due to the negative impact of Rad53 signaling on bulk DNA synthesis, but most likely due to the negative impact of Rad53 signaling on the ability of cells to resolve joint chromosomes via Mus81-Mms4 action. This interpretation is consistent with a previous report showing that these MMS-induced chromosomal defects observed by PFGE can be attributed to defective Mus81 action after completion of DNA replication (Saugar *et al.* 2013). Finally, cells lacking both *SGS1* and *MUS81* are inviable (Mullen *et al.* 2001) and *sgs1Δ pph3Δ slx4-S486A* cells display a dramatic hyper-sensitivity to minimal doses of MMS (**Figure 3.9**), underscoring the key role of PP4 and DAMP for proper regulation of the Mus81-Mms4 pathway. Based on the results presented above, I propose that upon replication blocks that promote extensive template switching events and formation of chromosomal linkages, cells strongly rely on the concerted action of Pph3 and Slx4 to down-regulate Rad53 signaling for proper cell cycle progression and timely Mus81-Mms4 activation.

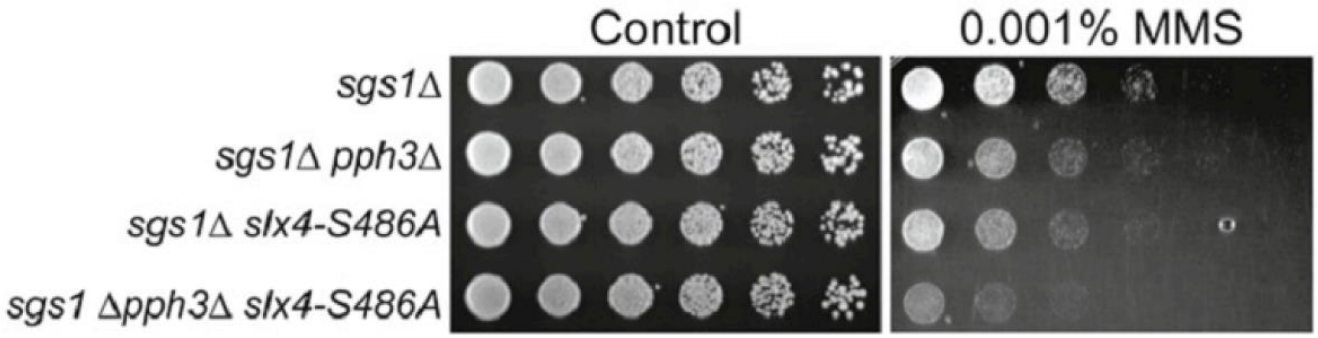

Figure 3.9. Deletion of *SGS1* helicase increases the MMS sensitivity of *pph3Δ slx4-S486A* cells. Indicated strains were serially diluted on either YPD plates with or without 0.001% MMS. Four-fold serial dilutions were spotted on YPD plates and grown for 2–3 days at 30^{o}C.

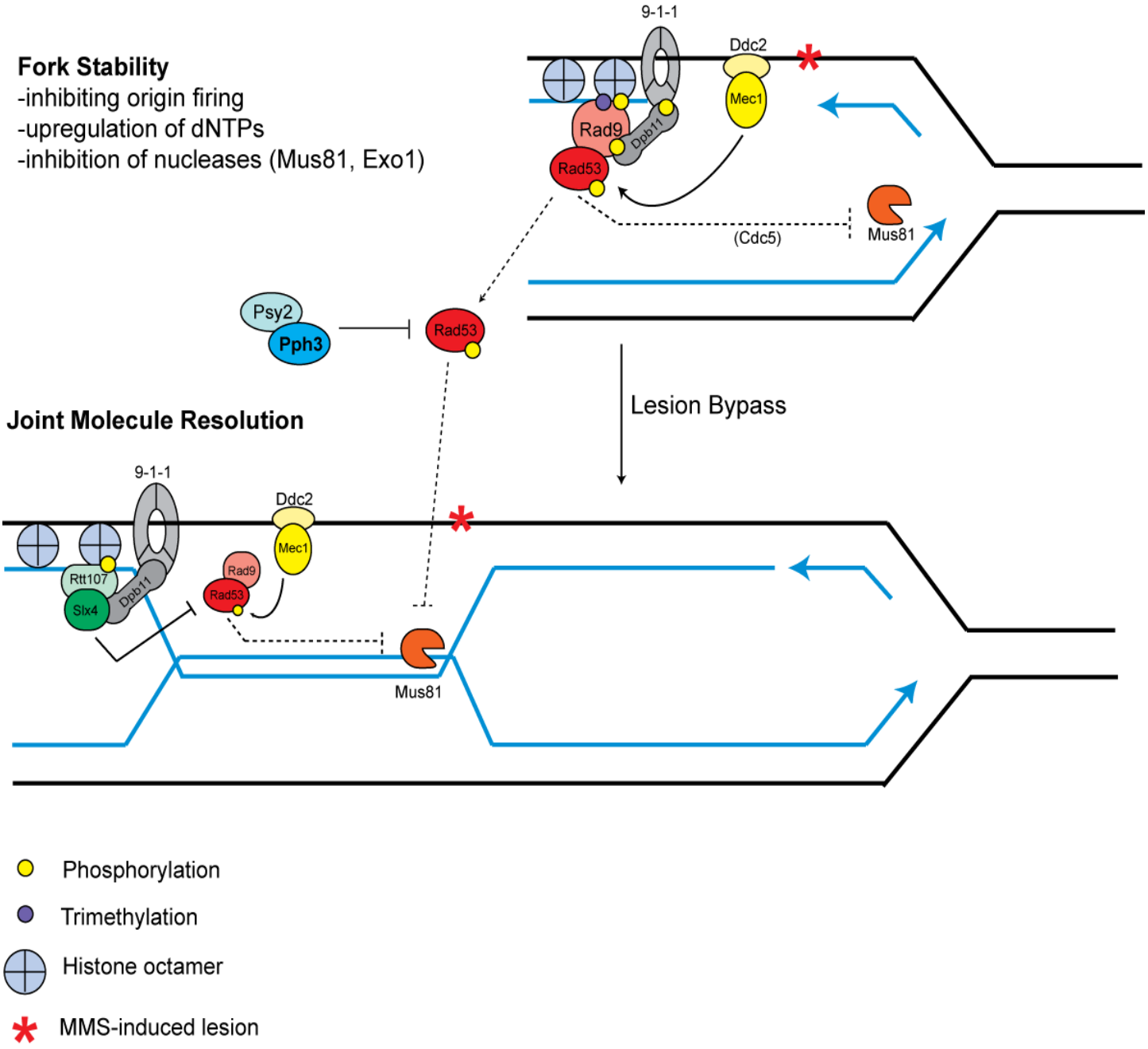
Fork Stability
-inhibiting origin firing
-upregulation of dNTPs
-inhibition of nucleases (Mus81, Exo1)
9-1-1
Ddc2
Mec1
Rad9
Dpb11
Rad53
(Cdc5)
Mus81
Psy2
Pph3
Rad53
Lesion Bypass
Joint Molecule Resolution
9-1-1
Ddc2
Mec1
Rtt107
Slx4
Dpb11
Rad9
Rad53
Mus81
Phosphorylation
Trimethylation
Histone octamer
MMS-induced lesion

Figure 3.10. Model: Down-regulation of checkpoint activity is necessary for proper resolution of joint DNA molecules. Upon MMS-induced DNA lesions, Mec1 becomes activated and further activates Rad53 through the help of the adaptor Rad9. Lesions are eventually bypassed via template-switching mechanisms, leaving behind joint DNA molecules. These joint molecules are substrates of both the Sgs1 helicase and the Mus81-Mms4 nuclease. Rad53 activation has a primary role in preventing aberrant Mus81-Mms4 endonuclease action on fork structures. However, in late G2/M, Rad53 activity needs to be down-regulated to allow for timely Mus81-Mms4 action on persistent joint DNA structures. Hyperactivation of Rad53 signaling causes persistent inhibition of Mus81-Mms4 and thus persistent joint molecules in G2/M.

DISCUSSION

Upon replication stress, DNA damage checkpoint signaling plays crucial roles in preserving cell viability mainly by protecting the integrity of replication forks, but this benefit comes at the expense of a strong repression of cell cycle progression and DNA synthesis. Mechanisms for termination of checkpoint signaling are therefore required to maintain the proliferative capacity of cells. Using budding yeast as a model system, I have shown that proper termination of Rad53 signaling following the bypass of replication blocks requires the concerted action of two fundamentally distinct mechanisms for checkpoint down-regulation. In this manner, the Pph3 phosphatase functions in a highly complementary manner to the mechanism of checkpoint dampening mediated by the Slx4-Rtt107 repair scaffolds.

Joint molecule (JM) accumulation likely explains why cells lacking *PPH3* and/or *SLX4* are particularly sensitive to MMS-induced replication stress

MMS is a monofunctional DNA alkylating agent that primarily methylates DNA on N^7-deoxyguanine and N^3-deoxyadenine (Pegg 1984), generating adducts that block the progression of DNA polymerases. A distinct feature of MMS-induced replication stress, when compared to hydroxyurea (HU) or camptothecin (CPT)-induced replication stress, is that DNA adducts generated by MMS are readily bypassed by moving replication forks so DNA synthesis proceeds, albeit slower, and cells eventually replicate their chromosomes in a timely manner, especially with the low doses of MMS used in the

experiments presented here. However, because replication fork bypass is achieved through, or results in, template-switching events, completion of replication is accompanied by extensive formation of chromosomal linkages (joint molecules, JMs) (Boiteux & Jinks-Robertson 2013). Therefore, the massive accumulation of JMs in MMS treated cells is likely the main reason behind the strong sensitivity of *slx4Δ* and/or *pph3Δ* cells to MMS. Consistent with this notion, checkpoint signaling arrests the cell cycle, preventing activation of Mus81-Mms4 (Szakal & Branzei 2013), the main nuclease involved in resolution of JMs, and deletion of *SLX4* and/or *PPH3* does not further sensitize *mus81Δ* cells to MMS treatment (**Figure 3.7**). Interestingly, drugs that result in other types of replication stress that do not induce extensive JM formation also lead to cell cycle arrest, but do not cause growth sensitivity in *slx4Δ* and/or *pph3Δ* cells. However, while other cell cycle-dependent events are probably executable with low levels of CDK and/or Cdc5 activity, JM resolution seems to require robust and timely activation of these cell cycle kinases. In addition, it is possible that if activation of Mus81-Mms4 is delayed for too long, aberrant JM processing can compromise chromosomal integrity and cell viability.

Transitioning from fork protection to JM resolution

In the proposed model (**Figure 3.10**), Rad53 is rapidly activated as replication forks encounter MMS-induced DNA adducts. Rad53 activation in response to MMS treatment is mostly mediated by the Rad9 adaptor (Ohouo *et al.* 2013) and is thought to occur proximal to replication fork regions mainly to protect the integrity of replication forks. This

fork protection function likely relies on the local action of Rad53 in inhibiting nucleases, such as Exo1, from processing fork structures (Morin *et al.* 2008). In addition, the global action of Rad53 in inhibiting origin firing, increasing dNTP levels and halting cell cycle progression supposedly have an overall positive impact on fork integrity. However, as forks bypass the lesions and JMs are formed, the importance of fork protection transitions to JM processing. Such transition requires down-regulation of Rad53 signaling mainly because resolution of JMs via Mus81-Mms4 is tightly coupled to activation of the cell cycle kinases Cdc5 and CDK, which are thought to be inhibited by checkpoint signaling (Saugar *et al.* 2013; Gallo-Fernández *et al.* 2012; Kai *et al.* 2005; Szakal & Branzei 2013). Of importance, the mechanism by which Rad53 inhibits Cdc5 and CDK in budding yeast remains incompletely understood. Taken together, this model implies that, in a first moment, *slx4Δ* and *pph3Δ* cells suffer from a recovery defect due to the inability to properly down-regulate Rad53 after the bypass of replication blocks. Given the strong dependency on Mus81 to resolve MMS-induced JMs, the recovery defect results in a subsequent repair defect due to hyper-inhibition of Mus81-Mms4.

CHAPTER 4

THE PP4 PHOSPHATASE AND SLX4 SCAFFOLD WORK IN COORDINATED SPATIO-TEMPORAL MODES TO DOWN-REGULATE RAD53 SIGNALING

This work was published in Jablonowski, C.M.; Cussiol, J.R.; Oberly, S.; Yimit, A.; Balint, A.; Kim, T.; Zhang, Z.; Brown, G.W.; Smolka, M.B. (2015). Termination of replication stress signaling via concerted action of the Slx4 scaffold and the PP4 phosphatase. Genetics *201,* 937-949.

Introduction

Down-regulation of the DDC requires the dephosphorylation of Rad53 and other targets. In addition to phosphatases, our lab has identified a novel mechanism for down-regulating checkpoint kinase activity. In this mechanism, the scaffold protein Slx4 dampens Rad53 signaling by competing with Rad9 for Dpb11 binding. As a consequence, Rad9 is displaced from the DNA lesion site, reducing the levels of Rad53 activation (Cussiol *et al.* 2015). Cells that lack *SLX4* show hypersensitivity to MMS, and this is correlated with an increase in Rad53 hyperactivation levels (Ohouo *et al.* 2013).

The presence of different mechanisms to down-regulate the DDC demonstrates the importance to keep Rad53 activation levels tightly regulated. However, although both mechanisms have been explored independently, nothing is known about whether these mechanisms overlap and how these mechanisms coordinate together to deactivate the DDC. Here, I describe how these two mechanisms act in parallel to tightly regulate Rad53 activation levels. Although cells lacking either *SLX4* or *PPH3* show very similar phenotypes, as shown in Chapter 3, they do not compensate for one another. In the previous chapter, I suggested that down-regulate Rad53 activity is necessary for proper resolution of joint DNA molecules via regulation of the Mus81 nuclease following repair.

Here, I propose that Slx4 and Pph3 function in distinct spatial mechanisms. Specifically, I propose that Slx4 functions to down-regulated Rad53 activation behind a moving replication fork, in order to repair lesions on chromatin, while Pph3 likely has a predominant role to dephosphorylate free nuclear pools of active Rad53.

Results

Antagonistic roles of H2A phosphorylation in checkpoint regulation provide insights into the mechanism of coordinated action of Slx4-Rtt107 and Pph3

So far, I have shown that the Pph3 phosphatase and the Slx4-Rtt107 scaffold complex down-regulate Rad53 activation in *cerevisiae.* I sought to investigate the molecular purpose for both of these mechanisms. I proposed that Pph3 and Slx4-Rtt107 function to down-regulate Rad53 signaling in spatially-distinct mechanisms. Because Slx4-Rtt107 associates with chromatin marks (meH3K79 and γ-H2A) as well as chromatin-associated 9-1-1 (through Dpb11), Slx4-Rtt107 likely functions on chromatin at sites of lesions. However, no such role is evident for Pph3. I sought to investigate where bulk Pph3 functions by investigating another well-documented substrate, histone H2A at serine 129 (γ-H2A).

Upon replication stress, the sensor kinase Mec1 extensively phosphorylates γ-H2A to form a platform of γ-H2A surrounding the site of lesion (Balint *et al.* 2015; Shroff *et al.* 2004). This γ-H2A platform recruits Rad9, via BRCT domains, and therefore contributes to promote Rad53 activation (Hammet *et al.* 2007; Ohouo *et al.* 2013). Unexpectedly, previous work from the Haber lab found that the non-phosphorylatable S129A mutation in H2A does not rescue, but slightly increases, the MMS sensitivity of *pph3Δ* cells (Kim *et al.* 2011). Here, elucidation of the complementary actions of Pph3 and Slx4 provides important insight into the roles of γ-H2A in the response to MMS treatment. As shown in **Figure 4.1A**, the *hta-S129A* mutation does not provide any rescue of the MMS sensitivity of *pph3Δ* cells, but confers substantial, albeit incomplete, rescue

of *slx4Δ* cells. The apparent antagonistic roles of γ-H2A in each of these mutants may be explained by the fact that the Slx4-Rtt107 complex strictly relies on γ-H2A for recruitment (Balint *et al.* 2015) and enforcement of DAMP (Ohouo *et al.* 2013), whereas Rad9 can be recruited via either γ-H2A or methylated H3K79 (Giannattasio *et al.* 2005; Toh *et al.* 2006; Wysocki *et al.* 2005). A likely scenario is that in the absence of *PPH3* there is an increased dependency on the Slx4-Rtt107 complex for counteracting Rad53 activation, and γ-H2A becomes crucial for checkpoint down-regulation, while not essential for checkpoint activation (Rad9 can still be recruited via methylated H3K79). Therefore, *hta-S129A* will mostly result in less checkpoint dampening

A

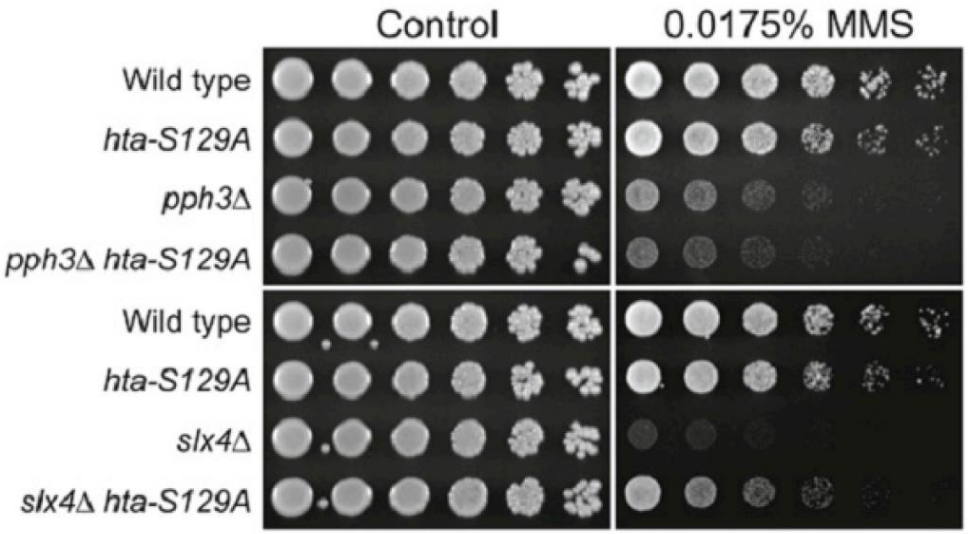
Control
0.0175% MMS
Wild type
hta-S129A
pph3Δ
pph3Δ hta-S129A
Wild type
hta-S129A
slx4Δ
slx4Δ hta-S129A

B

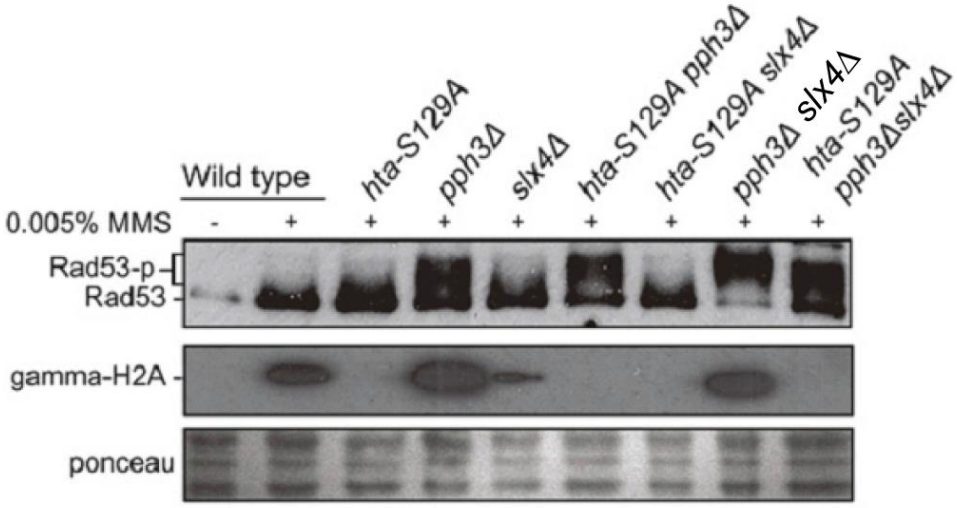
Wild type
hta-S129A
pph3Δ
slx4Δ
hta-S129A pph3Δ
hta-S129A slx4Δ
pph3Δ slx4Δ
hta-S129A
pph3Δslx4Δ
0.005% MMS
- + + + + + + + +
Rad53-p
Rad53
gamma-H2A
ponceau

Figure 4.1. Antagonistic roles for γ-H2A in DDC control. Effect of an H2A phospho-mutant (*hta-S129A)* on the MMS sensitivity (A) and Rad53 phosphorylation status (B) of ***slx4Δ*** and ***pph3Δ*** strains. (A) Four-fold serial dilutions of indicated strains were spotted on YPD plates and grown for 2-3 days at 30^{o}C in the presence or absence of MMS. (B) Asynchronous cells were treated with 0.005% MMS for 2 hr and samples were collected. Western blots were probed with either anti-Rad53 antibody (EL7 from Pellicioli) for Rad53 phosphorylation and anti-γ-H2A antibody as indicated in *Materials and Methods.* Ponceau staining is present as a loading control.

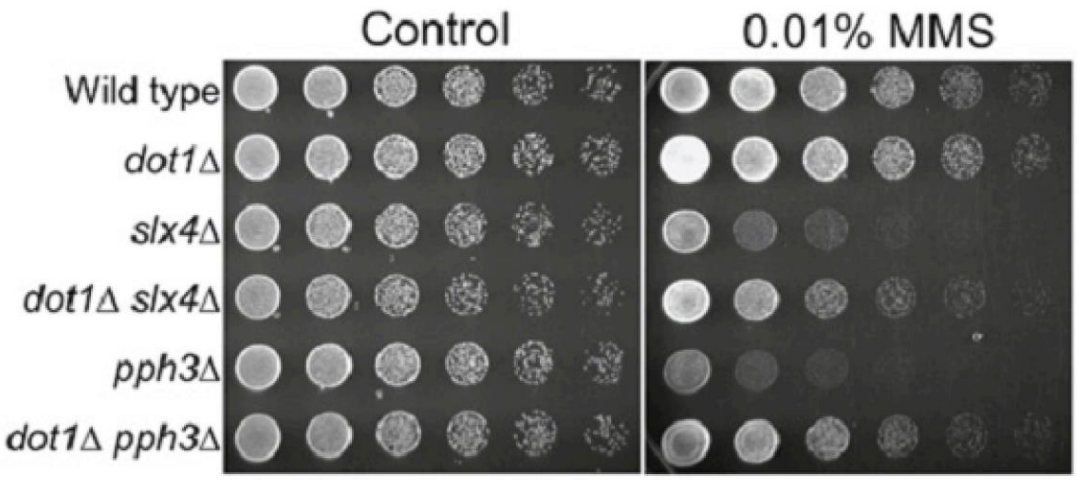

Figure 4.2. Deletion of the H3K79 methyltransferase *DOT1* rescues the MMS sensitivity of *pph3Δ* or *slx4Δ* cells. Four-fold serial dilutions of indicated strains were spotted on YPD plates and grown for 2–3 days at 30ºC in the presence or absence of MMS.

and increased checkpoint activation in *pph3Δ* cells. On the other hand, in the absence of *SLX4*, as γ-H2A serves mainly for checkpoint activation, *hta-S129A* will lead to reduced checkpoint activation. Indeed, I observed that expression of the *hta-S129A* mutant increased activation of Rad53 in *pph3*Δ cells, but reduced Rad53 activation in *slx4*Δ cells (**Figure 4.1B**).

Finally, I predicted that elimination of H3K79 methylation, important for Rad9 recruitment but not for Slx4-Rtt107 recruitment, would cause an opposite effect than the *hta-S129A* mutation, resulting in rescue of MMS sensitivity of *pph3Δ* cells. To test this idea, I deleted *DOT1,* the methyltransferase responsible for methylation of H3K79 (van Leeuwen *et al.* 2002), in *pph3Δ* cells and in *slx4Δ* cells and monitored MMS sensitivity. As predicted, *dot1Δ* rescued the MMS sensitivity of *pph3Δ* cells as well as of *slx4Δ* cells (**Figure 4.2**). These results elucidate the apparent antagonistic roles of γ-H2A in checkpoint control (**Figure 4.3**) and highlight the elaborate coordination of the actions of Pph3 and Slx4 during the response to MMS. Interestingly, γ-H2A is itself a target of Pph3 (Keogh *et al.* 2006), adding an additional level of complexity to the coordinated action of Pph3 and Slx4-Rtt107.

Slx4-Rtt107 and PP4 function in spatially distinct modes

Single mutant cells lacking either *PPH3* or *SLX4* display hyperactive Rad53 activation (**Figure 3.1B**, Chapter 3), revealing that these mechanisms of Rad53 down-regulation are not redundant and cannot be fully compensated by each other. I hypothesized that DAMP functions in a more localized fashion, as it requires interaction of Slx4-Rtt107 with γ-H2A and the Dpb11 scaffold (Cussiol *et al.* 2015; Ohouo *et al.* 2013), which are both

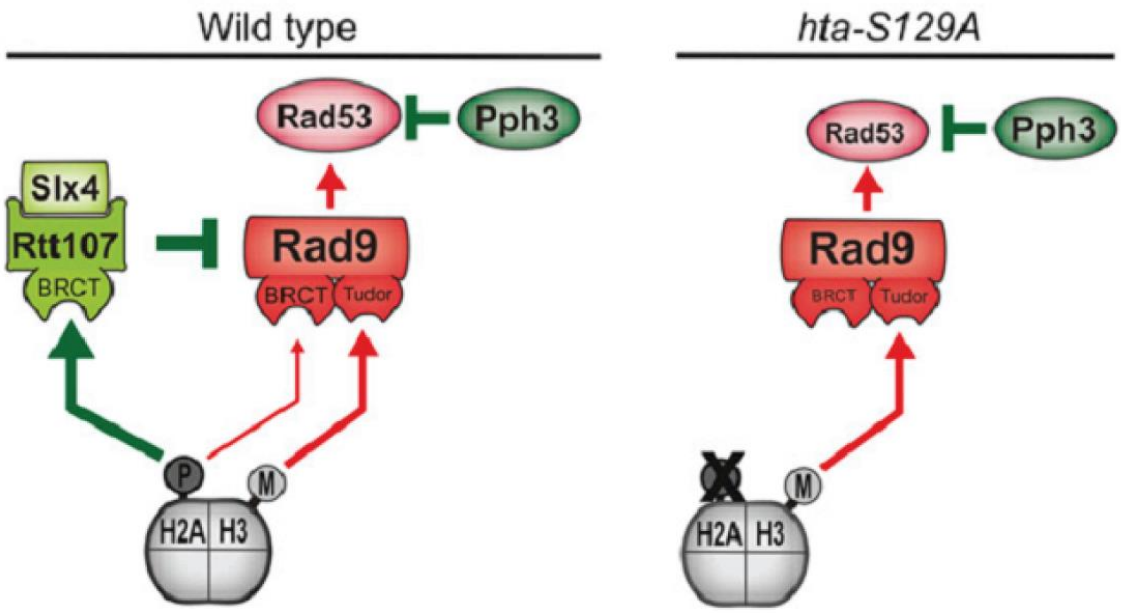

Figure 4.3. Proposed model illustrating the antagonistic roles of γ-H2A on DDC regulation. Here, in wildtype cells, Rad9 promotes recruitment of Rad53 to chromatin by two chromatin anchoring points, phospho-S129 on H2A and methylation of H3K79, via its BRCT and Tudor domains, respectively. Therefore, in the *hta-S129A* mutant, Rad9 can still recruit Rad53 to chromatin via its Tudor domain to methylated H3K79. However, Slx4-Rtt107 recruitment to chromatin to displace Rad9 is entirely dependent on its BRCT domain to γ-H2A. Therefore, in the *hta-S129A* mutant, Slx4-Rtt107 can no long compete with Rad9, while Rad9 can still be recruited.

specifically located at sites of lesions (Balint *et al.* 2015). In support of a model in which Slx4-Rtt107 function at sites of DNA lesions, recent work form the Brown lab using ChIP-seq has shown that Slx4-Rtt107 robustly localize to chromatin as replication forks traverse regions of MMS-alkylated DNA (Balint *et al.* 2015). On the other hand, a previous report on the action of Pph3 in response to DSBs showed that chromatin bound γ-H2A is not affected by Pph3 action (Keogh *et al.* 2006), suggesting that Pph3 mostly functions on free pools of γ-H2A, and by extension, Rad53. In this scenario, precise down-regulation of Rad53 activation would only be achieved through the coordinated local and global actions of Pph3 and Slx4, respectively. Interestingly, while both Slx4 and Pph3 form nuclear foci upon MMS treatment [**Figure 4.4A**, see also (Tkach *et al.* 2012)], Slx4 and Pph3 foci do not co-localize (**Figure 4.4B**), further supporting the model that Pph3 and Slx4 act in spatially-distinct manners. Also congruent with this notion, I found that expression of a minimal multi-BRCT-domain (MBD) module, previously shown to strongly reduce Rad53 activation by counteracting the Rad9 adaptor at sites of lesions (Cussiol *et al.* 2015), could fully rescue the MMS sensitivity of cells lacking *SLX4* but not the sensitivity of cells lacking *PPH3* (**Figure 4.5**). In contrast to MBD, the *rad53-R605A* hypomorphic allele can fully rescue the MMS sensitivity of *pph3Δ* cells (see **Figure 3.3**, Chapter 3), which suggests that *PPH3* is crucial to deactivate even low levels of activated Rad53 that have diffused from the site of lesion. It is important to mention that the MBD module only docks at the lesion site after an initial bout of Mec1 activation that creates the γ-H2A and phospho-Ddc1 anchoring points for the BRCT domains of Rtt107 and Dpb11, respectively (Cussiol *et al.* 2015). In this manner, some population of active

A

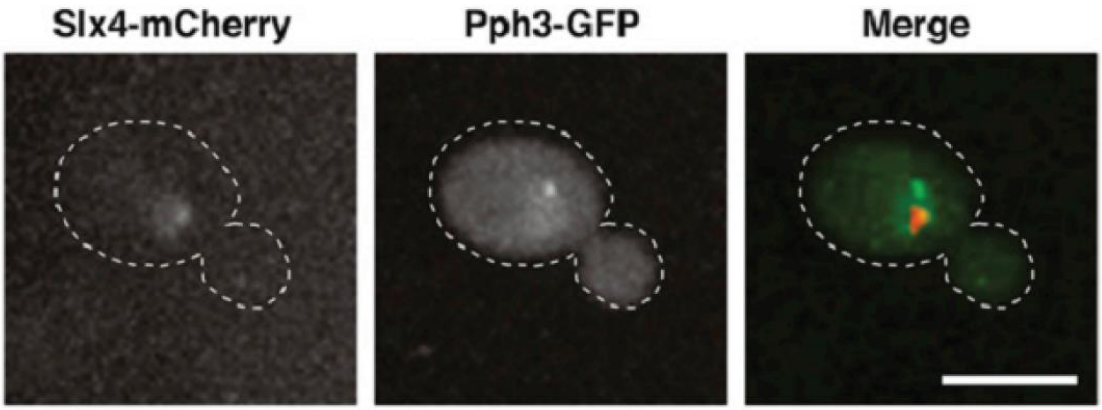
Slx4-mCherry
Pph3-GFP
Merge

B

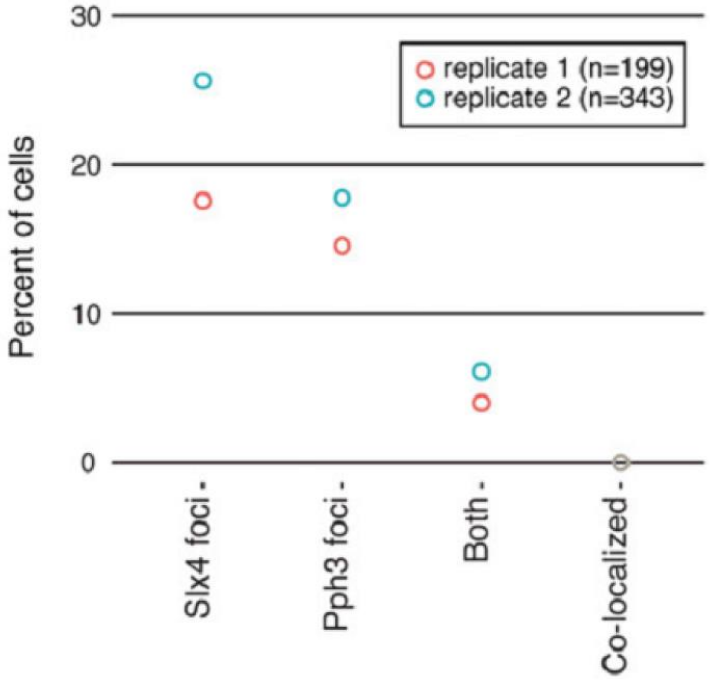
30
20
10
0
Percent of cells
replicate 1 (n=199)
replicate 2 (n=343)
Slx4 foci -
Pph3 foci -
Both -
Co-localized -

Figure 4.4. Microscopy analysis of the localization of Pph3 and Slx4. (A) Representative images showing the intracellular localization of Slx4 and Pph3 proteins. (B) Slx4-yEmCherry and Pph3-GFP foci were measured by confocal microscopy after treatment with 0.03% MMS for 2 hours. The percentage of cells with Slx4-yEmCherry, Pph3-GFP, and both Slx4-yEmCherry/Pph3-GFP foci is plotted. This work was completed with the help of Grant Brown's lab in Toronto, Canada.

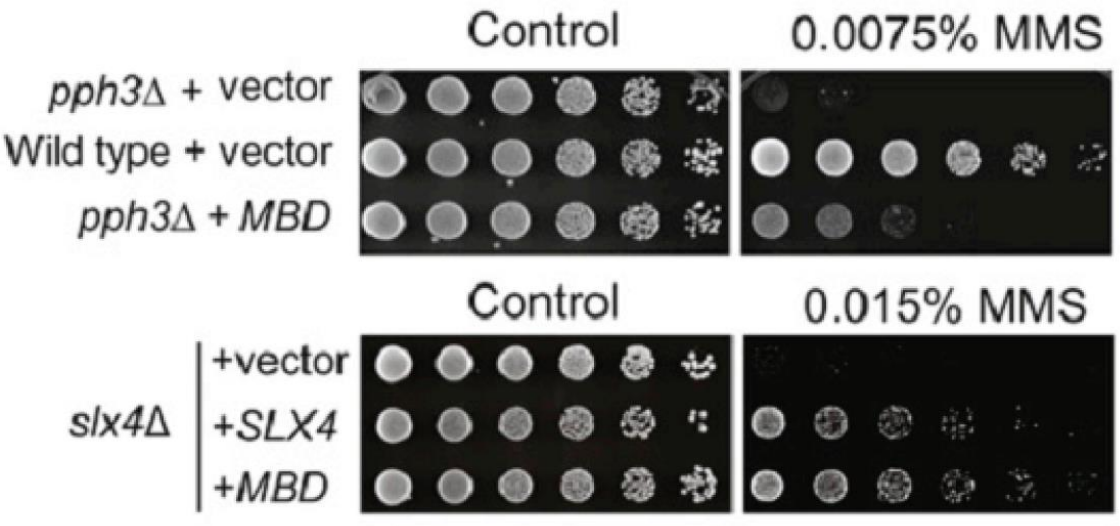

Figure 4.5. An engineered Multi-BRCT Domain module mimicking the role of Slx4 in checkpoint dampening rescues the sensitivity of *slx4Δ* cells, but not *pph3Δ* cells. Serial dilution assay showing the effect of MBD expression on the MMS sensitivity of the selected strains. *MBD* and *SLX4* were expressed from a *pRS416* plasmid (for details see Table 5) in SC –URA. This work was completed with the help of Dr. José Cussiol.

Rad53 would be quickly generated, even upon expression of MBD. But once diffused, active Rad53 molecules would be unable to be properly de-activated in *pph3Δ* cells.

To better spatially define the action of Pph3, and specifically address the question of whether it acts on chromatin or on free pools of histone H2A during replication stress, I decided to use ChIP-seq to monitor γ-H2A, another Pph3 target (Keogh *et al.* 2006). Because γ-H2A can be robustly detected on chromatin, even in the absence of DNA damage (Szilard *et al.* 2010), it provides a convenient substrate to address whether Pph3 acts or not on chromatin. With the help of our collaborators at the University of Toronto (Grant Brown's lab), ChIP-seq analysis of γ-H2A was performed comparing wild type, *pph3Δ* and *slx4Δ* cells in S-phase treated with MMS. Cells were arrested in G1 with alpha-factor and then released into S-phase in medium containing MMS. As shown in **Figures 4.6A-E**, γ-H2A accumulated near early origins of replication (represented by green marks) in wild-type and *slx4Δ* cells, consistent with the idea that H2A is phosphorylated upon movement of replication forks over regions of alkylated DNA, while regions not yet replicated are mostly devoid of strong γ-H2A signal. In cells lacking *PPH3* (**Figure 4.6B**) there was no detectable accumulation of γ-H2A at those same origin-proximal regions, and the overall detected signal is de-localized and appears across the entire chromosome, with concurrent accumulation of massive amounts of total γ-H2A (**Figure 4.7**). Of note, the differential accumulation of γ-H2A at early origins in wild type and *slx4Δ* cells compared with *pph3Δ* cells (**Figure 4.6D**) is not due to differences in the replication timing between these strains (**Figure 4.6E**). We interpret this result as Pph3 acting mainly on free pools of γ-H2A, before they are recycled back onto chromatin, consistent with previous work showing that Pph3 does not act on chromatin γ-H2A upon

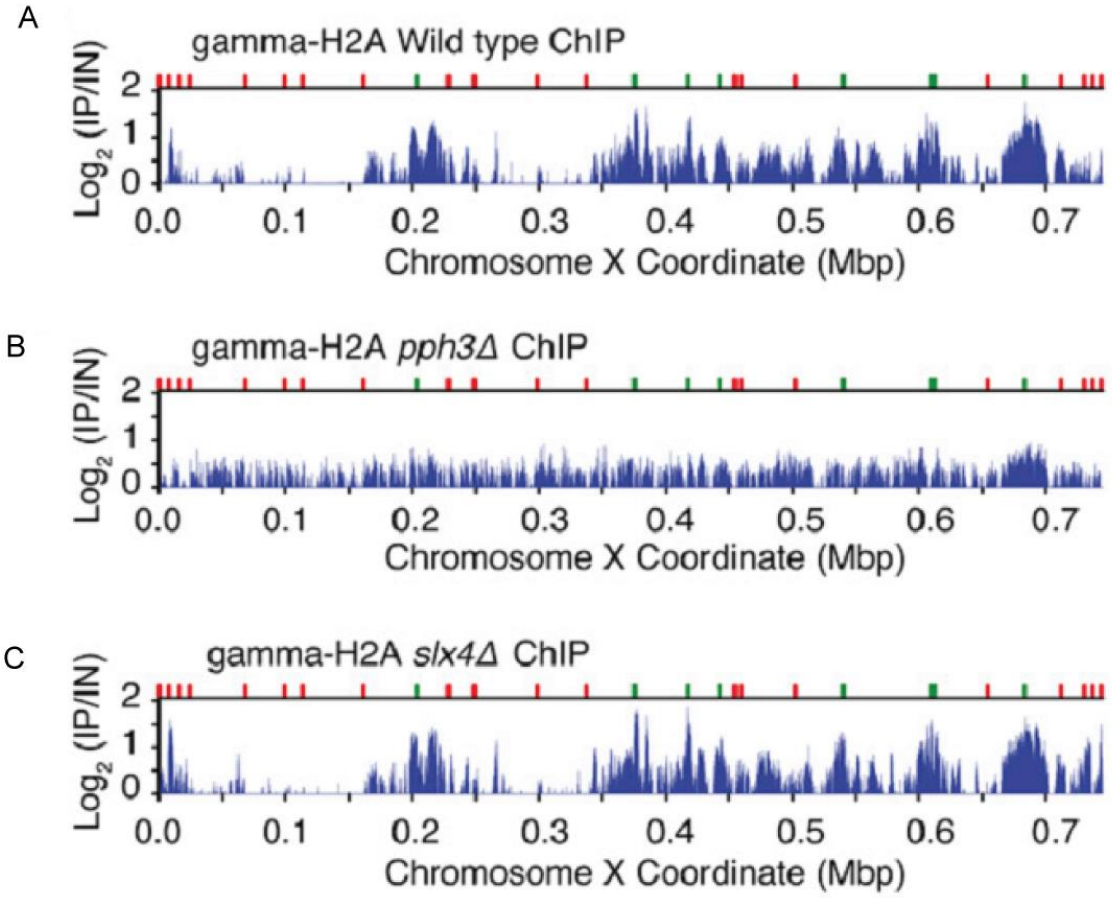
A
gamma-H2A Wild type ChIP
Log2 (IP/IN)
2
1
0
0.0
0.1
0.2
0.3
0.4
0.5
0.6
0.7
Chromosome X Coordinate (Mbp)
B
gamma-H2A pph3Δ ChIP
Log2 (IP/IN)
2
1
0
0.0
0.1
0.2
0.3
0.4
0.5
0.6
0.7
Chromosome X Coordinate (Mbp)
C
gamma-H2A slx4Δ ChIP
Log2 (IP/IN)
2
1
0
0.0
0.1
0.2
0.3
0.4
0.5
0.6
0.7
Chromosome X Coordinate (Mbp)

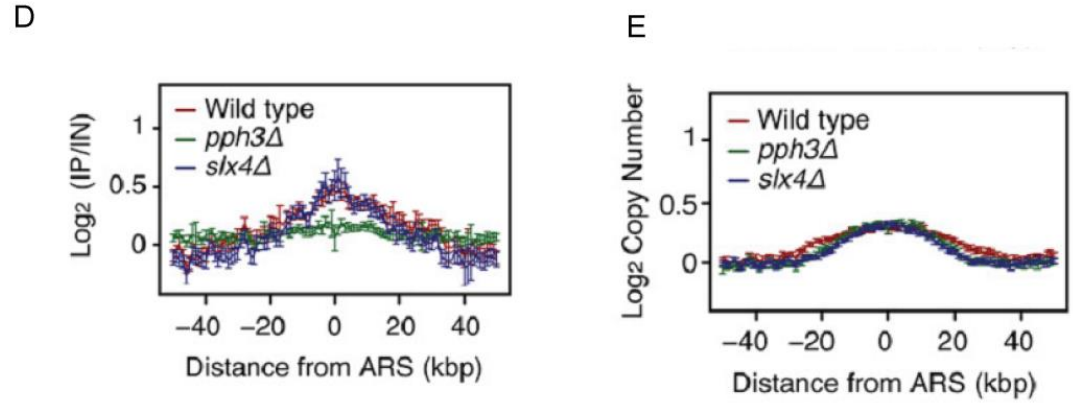
D
Log2 (IP/IN)
Wild type
pph3Δ
slx4Δ
1
0.5
0
−40
−20
0
20
40
Distance from ARS (kbp)
E
Log2 Copy Number
Wild type
pph3Δ
slx4Δ
1
0.5
0
−40
−20
0
20
40
Distance from ARS (kbp)

Figure 4.6. Pph3 functions on free nuclear pools of histone H2A. ChIP-seq analysis was performed following synchronous release of wild-type (A), *pph3Δ* (B), and *slx4Δ* (C) cells into S phase in the presence of 0.04% MMS for 60 minutes. γ-H2A (phospho-S129) enrichment scores on chromosome X are shown. Early origins are indicated by green bars and late origins by red bars. This work was completed with the help of our collaborators in Grant Brown's lab located in Toronto, Canada.

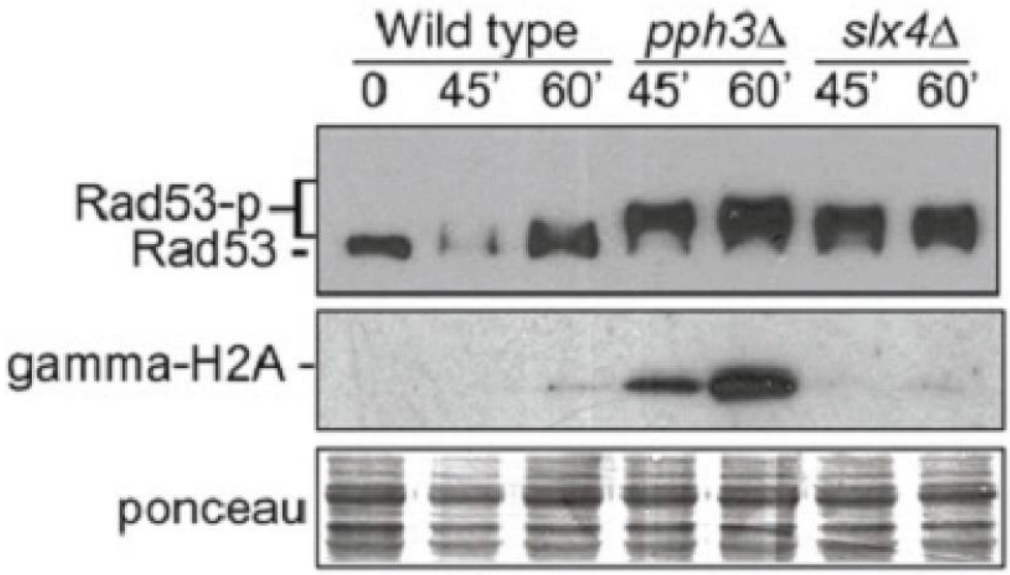

Figure 4.7. Pph3 and Slx4 regulate Rad53 phosphorylation, but γ-H2A levels increase only in *pph3Δ* cells. Immunoblot showing the status of Rad53 and γ-H2A in wild-type, *pph3Δ*, and *slx4Δ* cells after treatment of G1-synchronized cultures with α-factor and release into medium containing 0.01% MMS for the indicated time points. Western blots were probed with either anti-Rad53 antibody (EL7 from Pellicioli) for Rad53 phosphorylation and anti-γ-H2A antibody as indicated in *Materials and Methods*. Ponceau staining is present as a loading control.

DSB induction (Keogh *et al.* 2006). In summary, the microscopy, genetic and ChIP data presented here support the model that Pph3 and Slx4 function in spatially distinct manners. This work supports the model that Slx4-Rtt107 has a primary role in down-regulating Rad53 activation locally, on chromatin, as replication forks bypass lesions, whereas Pph3 likely has a more predominant role in dephosphorylating active Rad53 at diffused nuclear pools (**Figure 4.8**).

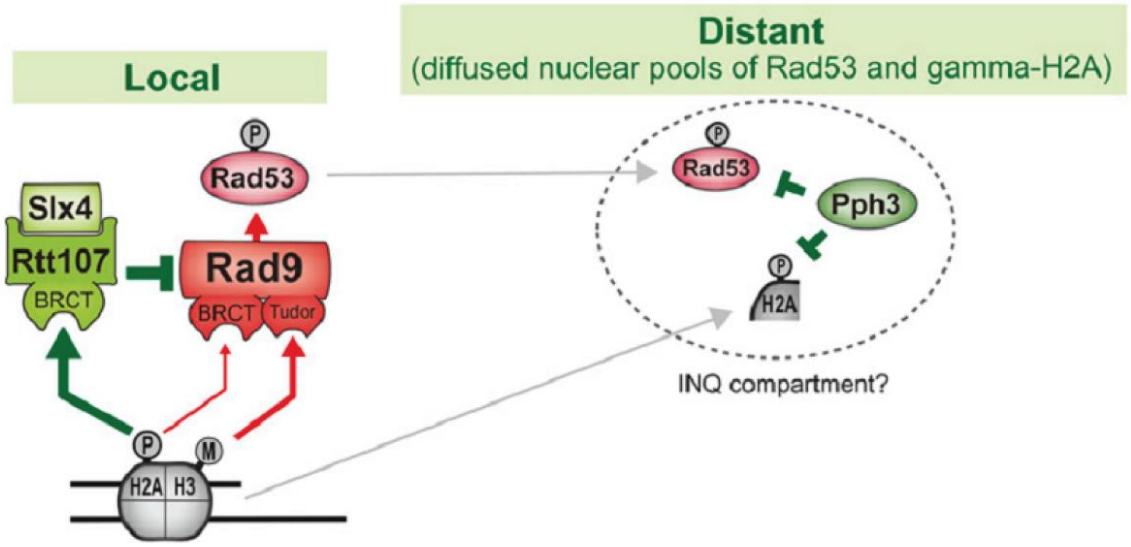

Figure 4.8. Proposed model illustrating how Pph3 and Slx4 coordinate Rad53 down-regulation in spatially distinct manners. Here, Slx4-Rtt107 competes with Rad9 for Dpb11 binding, down-regulating Rad53 activation on chromatin near lesions. Once Rad53 is active, it diffuses throughout the nucleus phosphorylating its targets for proper checkpoint response, where it is eventually dephosphorylated by Pph3 in global nuclear pool to promote checkpoint recovery.

Discussion

I propose a model in which Slx4-Rtt107 act locally to counteract Rad53 activation at sites of DNA lesions bypassed by the replication machinery, while Pph3 de-activates pools of Rad53 that have diffused from the site of lesion. The action of both mechanisms is therefore required for full termination of checkpoint signaling triggered by replication blocks.

Rad53 as a mobile kinase

While Rad53 is activated in a localized manner at sites of DNA lesions (Alcasabas *et al.* 2001; Gilbert *et al.* 2001), the fact that it plays roles in signaling responses that occur distant from those sites, such as transcription and cell cycle control, is consistent with the notion that Rad53 is a highly mobile kinase. While the well-established mode of Rad53 activation following replication stress involves recruitment of Rad53 close to the sensor kinase Mec1 at sites of RPA-coated ssDNA, Rad53 seems to rapidly diffuse from these sites, as inferred by the following negative or indirect observations: (1) Microscopic analysis showed that Rad53 foci are faint and tend to rapidly dissipate (Lisby *et al.* 2004); (2) ChIP experiments have not been able to robustly detect Rad53 on chromatin and a weak Rad53 signal has been detected at replicating regions only after treatment with protein-protein crosslinking agents (Katou *et al.* 2003); (3) CHK2, the mammalian homolog of Rad53, has been shown to form a pan nuclear distribution throughout the nucleus minutes after DNA double strand break formation, and forced immobilization of CHK2 at the DNA lesion site affects phosphorylation of CHK2 targets (Lukas *et al.* 2003).

The realization that Rad53 is a highly mobile kinase has crucial implications for understanding how it is de-activated and is congruent with our finding of two complementary modes of Rad53 de-activation, one acting locally to prevent new Rad53 molecules from being activated and another acting globally to de-activate pools of active Rad53 that have diffused form the site of lesion. Interestingly, a recent report has shown that Pph3 foci co-localize with an intranuclear quality control compartment (INQ) proposed to be involved in the recovery from genotoxic stress (Gallina *et al.* 2015). It is tempting to speculate that global pools of active Rad53 and phosphorylated H2A are eventually sequestered into these INQ compartments for de-phosphorylation.

A spatial model for termination of Rad53 signaling following the bypass of DNA lesions

I propose a model in which the proper down-regulation of Rad53 signaling requires the concerted action of the Slx4-Rtt107 scaffold and the PP4 phosphatase. The Slx4-Rtt107 complex functions at sites of lesions to prevent continued Rad53 activation via the Rad9 adaptor. As previously reported in Ohouo *et al. 55*2013, this is achieved by the ability of Slx4-Rtt107 to interact with the Dpb11 scaffold and lesion-specific phospho-sites in histone H2A and on the Ddc1 component of the 9-1-1 complex. However, this DAMP mechanism is unable to deal with the pools of activated Rad53 that have diffused from the site of lesion. In this manner, proper termination of Rad53 signaling also requires the action of the PP4 phosphatase, which should presumably be capable of de-activating the pools of Rad53 that have diffused. Consistent with this notion, localization data reveal that Pph3 is evenly distributed throughout the nucleoplasm or at the specialized INQ

compartment (Gallina *et al.* 2015) and ChIP data show that the γ-H2A is likely not dephosphorylated by Pph3 on chromatin, but in the nucleoplasm as it is being recycled back to chromatin. Interestingly, the recent finding that Pph3 physically interacts with Mec1 (Hustedt *et al.* 2015) raises new possibilities as to how Pph3 may strategically localize to more efficiently target the pools of Rad53 emanating from sites of activation.

CHAPTER 5

PERSPECTIVES

In this thesis, I investigated the mechanisms of how Rad53-dependent checkpoint signaling is down-regulated. I showed that the PP4 protein phosphatase Pph3 and the scaffold protein complex Slx4-Rtt107 work in a concerted mechanism to down-regulate Rad53 signaling to control appropriate levels of active Rad53 upon replication stress. Both *pph3Δ* and *slx4Δ* cells show similar phenotypes when exposed to MMS-induced replication stress, and double mutants show exaggerated phenotypes in each case. Interestingly, I have shown that although these mutants display similar phenotypes, they differ in several ways. First, *slx4Δ* and *pph3Δ* cells show different dependencies of phosphorylated histone H2A (γ-H2A) (**Figure 4.1**). This supports the model that Slx4-Rtt107 depends on γ-H2A for chromatin association and checkpoint dampening, while Pph3 localizes in global nuclear pools. Secondly, an engineered chimeric protein that mimics Slx4's checkpoint dampening function rescues the MMS sensitivity of *slx4Δ* cells but not *pph3Δ* cells, further supporting the local versus global regulation model (**Figure 4.5**). Moreover, Slx4 and Pph3 do not colocalize together in the nucleus upon MMS treatment, further supporting that they are functionally distinct in the mechanisms to down-regulate Rad53 signaling (**Figure 4.4**).

In a recent report, Gallina *et al.* (2015) showed that Pph3 focus formation colocalizes with a newly characterized intranuclear protein quality control compartment (INQ) that sequesters misfolded, phosphorylated, ubiquitinated, and sumolyated proteins

in response to genotoxic stress. How this INQ-dependent role for Pph3 functions is not understood. In particular, I would like to further distinguish Pph3's role in checkpoint recovery from the perspective of its role in INQ function. In Gallina *et al.*, the authors identify two genes that are required for INQ formation, *HSP42* and *BTN2.* In future work, I would like to investigate Pph3's INQ-dependent role by disrupting INQ formation. To do this, I will test the genetic interaction of double mutants yeast strains *pph3Δhsp42Δ* and *pph3Δbtn2Δ* in response to MMS. In these cells, INQ-formation would be abrogated but leave other pathways that Pph3 functions in intact. It will be interesting to see if mutation in *HSP42* or *BTN2* rescue MMS sensitivity, which would suggest Pph3's primary role is to function in INQ upon MMS, or whether deletion of these genes in combination with *pph3Δ* further sensitizes cells.

Furthermore, I would like to investigate the specific INQ-dependent role of Pph3. It is tempting to speculate whether Pph3 dephosphorylates active Rad53 or other targets in the INQ specifically to allow checkpoint recovery. If INQ formation is necessary for Pph3 to dephosphorylate a specific set of substrates, cells that are unable to form INQ compartments should show a relative increase in phosphorylation of these targets. I would use SILAC-based (Stable Isotope Labeling of Amino acids in Cell culture) quantitative mass spectrometry and enrich for phosphorylated peptides to directly compare wildtype cells with cells lacking either *HSP42* or *BTN2,* which prevent INQ formation (INQΔ). Phosphorylated peptides enriched in the INQΔ cells would be likely candidates for needing to be dephosphorylated in the INQ compartment.

As mentioned in the introduction, Pph3 is one of four Rad53-specific phosphatases. The other phosphatases Ptc2, Ptc3, and Glc7 are not well characterized

in this present study. In contrast to *ptc2Δ* and *ptc3Δ* cells, *pph3Δ* cells alone are sensitive to MMS and thus was chosen for further characterization in this study. However, cells lacking *PTC2, PTC3,* and *PPH3* are extremely sensitive to a variety of genotoxins (Kim *et al.* 2011; Travesa *et al.* 2008). The relationships between the functions of these phosphatases leaves several unanswered questions. First of all, it is unclear whether these phosphatases regulate specific phosphorylation sites of Rad53. Phosphatases that deactivate different phosphorylation patterns may regulate different aspects of the checkpoint response. It is tempting to speculate that differently phosphorylated isoforms of Rad53 may be generated by the way Rad53 becomes activated, i.e. Rad9 or Mrc1. Different phosphatases may be responsible to dephosphorylate and thus, deactivate, select phospho-forms of Rad53 that have tailored roles in the checkpoint response. This is supported by two studies that found that Rad53 is phosphorylated differently in MMS and in 4-NQO (a UV-mimetic drug) (Smolka *et al.* 2005; Sweeney *et al.* 2005). However, differences found between these two studies may just have occurred from a lack of sensitivity of the instruments or differences in the experimental processing. Furthermore, in humans, CHK2's kinase activity is different when exposed to gamma rays, UV, or HU, suggesting that different types of DNA damage might produce differently phosphorylated CHK2 to produce a more specific checkpoint response (Ahn *et al.* 2004). Therefore, it will be important to clarify whether Rad53 exists in distinct phospho-forms upon different types of DNA damage. To accomplish this, I would immunoprecipitate Rad53 from cells exposed to different genotoxins (for example, MMS, hydroxyurea, camptothecin, phleomycin, etc) and use quantitative mass spectrometry to detect and compare different phosphorylation states in Rad53.

Additionally, cells lacking the different Rad53 phosphatases can have vastly different characteristics. For example, *pph3Δ* cells are sensitive to MMS, while *ptc2Δ ptc3Δ* cells are not (Kim *et al.* 2011; Travesa *et al.* 2008). Also, cells lacking *PTC2* and *PTC3* cannot undergo checkpoint adaptation, while *pph3Δ* cells can adapt to a persistent DSB (personal communication with A. Pellicioli). Also, Pph3-Psy2 and Ptc2/Ptc3 interact with different domains within Rad53. Pph3-Psy2 associates with Rad53's kinase domain, while Ptc2/Ptc3 interacts with the FHA1 domain (O'Neill *et al.* 2007; Guillemain *et al.* 2007). Rad53's FHA1 domain has been shown to be important for regulation of late origin firing (Pike *et al.* 2004). Therefore, it this might suggest that Ptc2/Ptc3 associate with Rad53's FHA1 domain to regulate Rad53's late origin firing functions, while Pph3-Psy2 dephosphorylates Rad53 within its kinase domain to regulate other functions, such as fork stabilization (see Heideker *et al.* 2007). Interestingly, although I have shown that the MMS sensitivity of *pph3Δ* cells can be rescued by the introduction of a hypomorph of *RAD53 (rad53-R605A;* **Figure 3.3***),* this *RAD53* hypomorph only incompletely rescues *pph3Δ ptc2Δ ptc3Δ* cells (**Figure S3**). However, it is unclear whether this triple mutant results in a particular phospho-form of Rad53 to which the *rad53-R605A* allele can no longer compensate for or whether this triple phosphatase mutant merely overwhelms the cell with a hyperphosphorylated form of Rad53. To begin to understand how these phosphatases work together, I would like to address whether deletion of these phosphatases results in specific phospho-forms of Rad53. To do this, I would use quantitative mass spectrometry and compare wildtype cells with phosphatase mutants. Specifically, I would like to directly compare phosphorylation sites in Rad53 immunoprecipated from different mutant cells, treated with genotoxic drugs. Furthermore,

I would specifically like to compare individual phosphatase mutants with *pph3Δ ptc2Δ ptc3Δ* cells to look for overlapping dephosphorylated sites among the phosphatases. Understanding how the roles of the phosphatases differ and how they operate cooperatively can help us understand how checkpoint activation and signaling can lead to the downstream repair of different types of DNA damage.

Overall, the proposed model for the spatial coordination of Rad53 de-activation is supported by the genetic, biochemical, and cell biological data presented here. Mus81 action requires an increase in Cdc5 and CDK activity, and it is plausible that both of these kinases, similar to Rad53, are also highly diffused throughout the nucleus. It is tempting to speculate that Cdc5 itself may be somehow subjected to repression by global pools of activated Rad53, highlighting the importance of full de-activation of the complete pool of Rad53 for proper cell cycle progression and Mus81 activation. In further work, I would like to expand this model into higher eukaryotes. It will be interesting to test whether the human PP4 phosphatase also acts on diffused pools of checkpoint kinases and in coordination with more localized mechanisms of checkpoint down-regulation to properly regulate cell cycle progression and timely processing of repair intermediates, such as JMs.

APPENDIX i.

Supplementary Data Supporting Present Study

The *slx4-S486A* mutant phenocopies cells lacking *SLX4* in the response to MMS-induced replication stress.

In this study, I have investigated the roles of both Slx4 and Pph3 in yeast DNA damage checkpoint down-regulation. Slx4 functions with Rtt107 to down-regulate checkpoint activation by outcompeting Rad9 for Dpb11 binding (Ohouo *et al.* 2013). In addition to checkpoint dampening, Slx4 has important roles in DNA repair by coordinating nucleases Slx1 and Rad1/Rad10 (Mullen *et al.* 2001; Flott *et al.* 2007; Roberts *et al.* 2006; and reviewed in Rouse 2009). I sought to analyze Slx4's function in checkpoint dampening independently of its nuclease-dependent roles. To do this, I generated a separation of function mutant of Slx4 (*slx4-S486A)* that was previously shown to disrupt Slx4 binding to Dpb11 (Ohouo *et al.* 2013). Here, I show that the *slx4-S486A* mutant phenocopies cells lacking *SLX4* in the response to MMS-induced stress, and is independent of Slx4's associated nucleases (**Figure S1**).

A

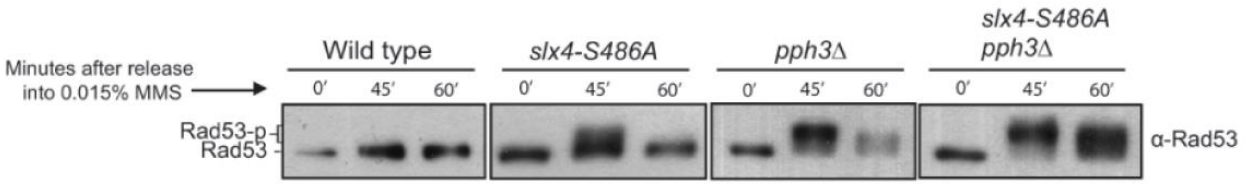
Minutes after release into 0.015% MMS
Wild type
slx4-S486A
pph3Δ
slx4-S486A pph3Δ
0′ 45′ 60′
Rad53-p
Rad53
α-Rad53

B

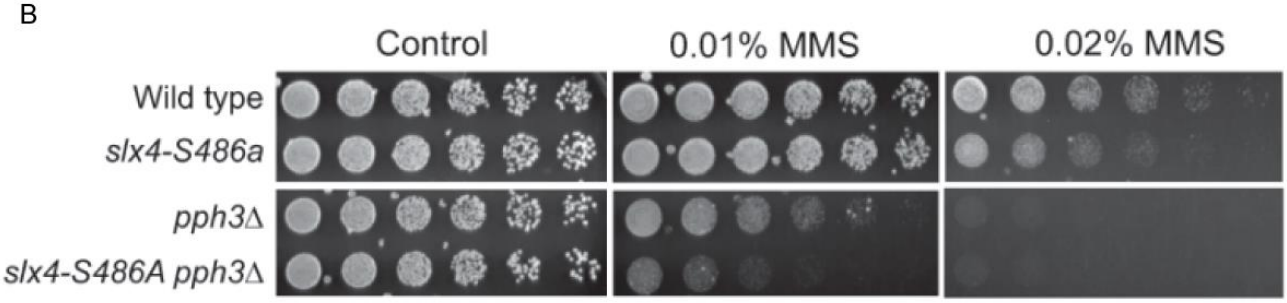
Control
0.01% MMS
0.02% MMS
Wild type
slx4-S486a
pph3Δ
slx4-S486A pph3Δ

C

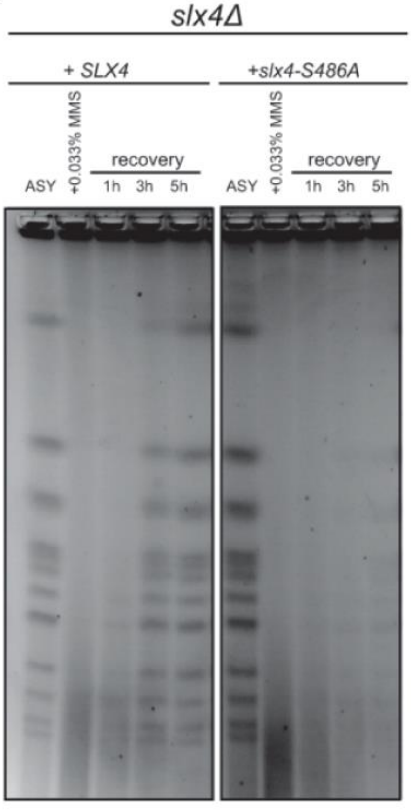
slx4Δ
+ SLX4
+slx4-S486A
ASY
+0.033% MMS
recovery
1h 3h 5h

D

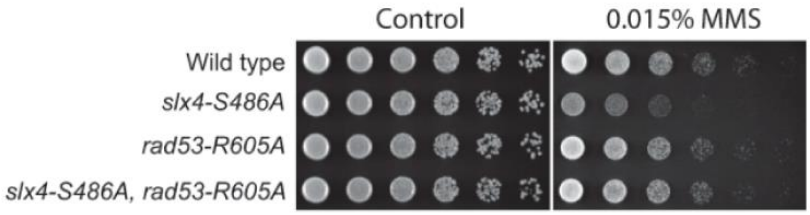
Control
0.015% MMS
Wild type
slx4-S486A
rad53-R605A
slx4-S486A, rad53-R605A

Figure S1 The *slx4-S486A* mutant phenocopies cells lacking *SLX4* in the response to MMS-induced replication stress. (A) Anti-Rad53 immunoblots of WT, *slx4-S486A*, *pph3Δ* and *pph3Δ slx4-S486A* strains showing Rad53 phosphorylation status after MMS treatment. Experiment was performed as described in **Figure 1B.** (B) Serial dilution assays showing the effect of MMS treatment upon the sensitivity of wild type, *slx4-S486A*, *pph3Δ* and *pph3Δ slx4-S486A* strains. Four-fold serial dilutions were spotted on YPD plates and grown for 2–3 days at 30°C. (C) Analysis of fully replicated chromosomes measured by PFGE in wild type and *slx4-S486A* strains. Asynchronous (ASY) cells were treated with 0.033% MMS for 3 hours and then released in MMS-free media at different time points. (D) Serial dilution assay showing the effect of a hypomorphic *RAD53* allele (*rad53-R605A*) on MMS sensitivity of wild type and *slx4-S486A* strains.

Effect of the presence of the *rad53-R605A* allele on the MMS sensitivity of strains lacking *MUS81* or *PPH3*.

In the work presented here, I have shown that cells lacking *PPH3* are sensitive to MMS due to checkpoint hyperactivation. I have suggested a model that suggests the consequences of checkpoint hyperactivation is due to a failure of timely activation of the nuclease Mus81 to resolve joint DNA molecules. In support of this, genetic interactions between *PPH3* and *MUS81* suggest they function together. However, as shown below, a hypomorphic allele of *RAD53, rad53-R605A,* rescues the MMS sensitivity of *pph3Δ* cells but not *mus81Δ* cells, further suggesting the deleterious effects in *pph3Δ* cells are due to a lack of Mus81 function (**Figure S2**).

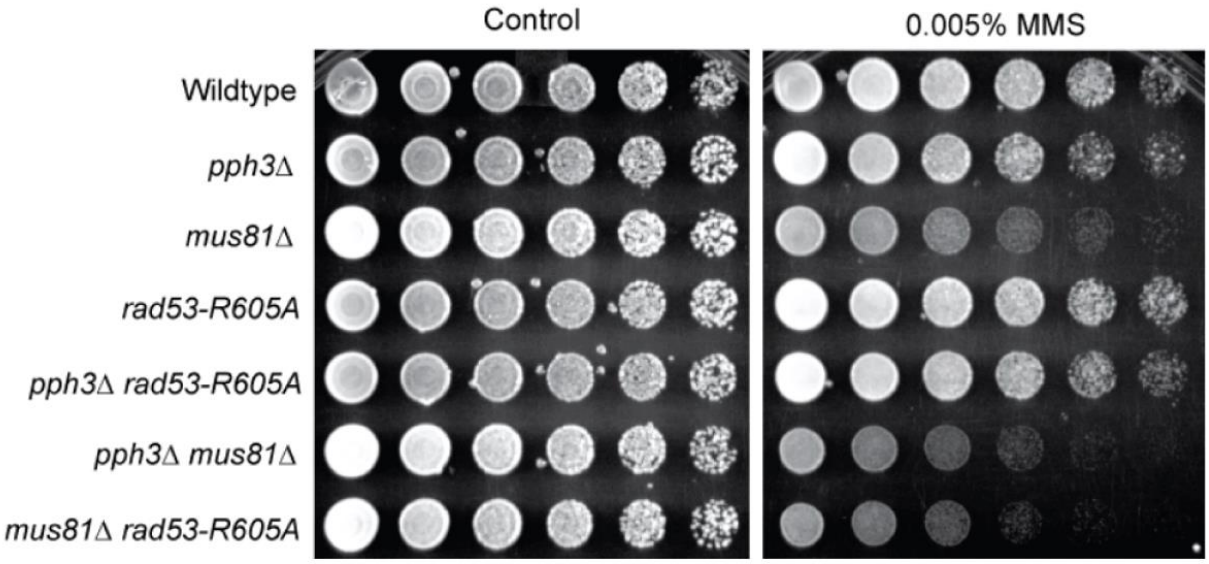

Figure S2. Effect of the presence of the *rad53-R605A* allele on the MMS sensitivity of strains lacking *MUS81* or *PPH3*. Indicated strains were grown in log phase and plated on plates either in the presence or absence of MMS. Four-fold serial dilutions were spotted on YPD plates and grown for 2–3 days at 30°C.

The *rad53-R605A* allele rescues the MMS sensitivity of *pph3Δ* cells, but only incompletely rescues *pph3Δptc2Δptc3Δ* cells.

Pph3, Ptc2, and Ptc3 are three Rad53 phosphatases. In this study, I have shown that Pph3 is important for checkpoint recovery following MMS-induced replication stress. Cells lacking *PPH3* are sensitive to MMS due to Rad53-dependent checkpoint hyperactivation (**Figure 3.1**). In support of this, a hypomorphic allele of *RAD53, rad53-R605A,* rescues the MMS sensitivity of *pph3Δ* cells (**Figure 3.3**). However, cells lacking *PPH3, PTC2,* and *PTC3* are hypersensitive to many genotoxins (Kim *et al.* 2011; Travesa *et al.* 2008). I decided to ask whether the *rad53-R605A* could rescue the MMS sensitivity of *pph3Δptc2Δptc3Δ* cells. Interestingly, although there is a significant rescue in the MMS sensitivity, the *rad53-R605A* allele did not rescue the defects completely (**Figure S3**).

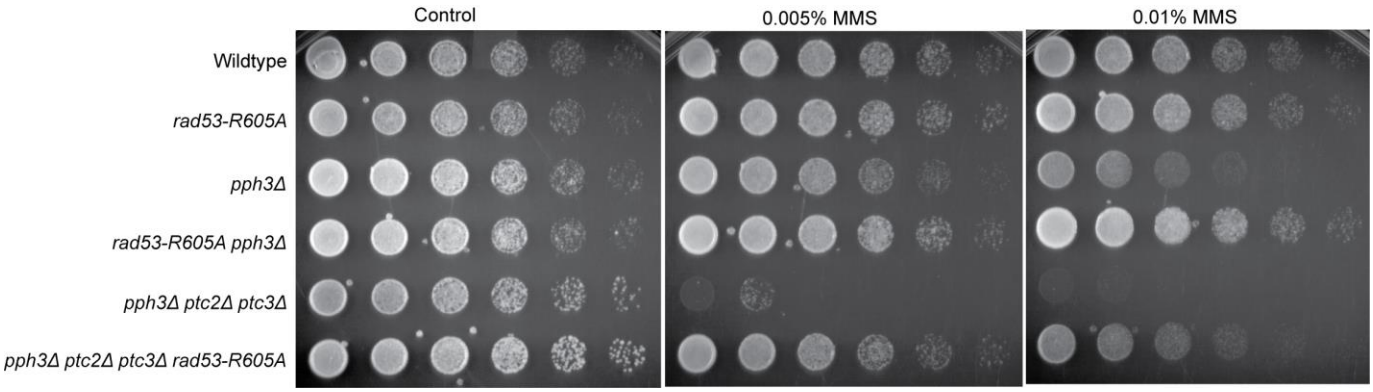

Figure S3. The *rad53-R605A* allele rescues the MMS sensitivity of *pph3Δ* cells, but only incompletely rescues *pph3Δptc2Δptc3Δ* cells. Serial dilution assay showing the effect of a hypomorphic *RAD53* allele (*rad53-R605A*) on MMS sensitivity of the indicated strains. Four-fold serial dilutions were spotted on YPD plates with or without MMS and grown for 2–3 days at 30°C.

APPENDIX ii

Determination of the S-phase Delay in *pph3Δ* Cells Upon MMS Exposure

The MMS sensitivity of cells lacking *PPH3* is independent of a defect in origin firing regulation.

Cells that lack *PPH3* are sensitive to MMS and show a delay in S-phase upon exposure to MMS (**Figure 3.1**). Because Pph3 facilities checkpoint recovery, and checkpoint signaling regulates late origin firing, I sought to address whether the sensitivity of *pph3Δ* cells is due to a misregulation of late origin firing. Checkpoint signaling phosphorylates Sld3 and Dbf4, two components necessary for origin firing, to inhibit late origins from firing. The Toczyski lab generated yeast mutant strains in which the checkpoint-dependent phosphorylation sites are mutated to either prevent phosphorylation (*sld3-m25* or *dbf4-m25*) or mimic phosphorylation (*sld3-m21D)* (Lopez-Mosqueda *et al.* 2010). I deleted *PPH3* in combination with these mutations. If the reason that *pph3Δ* cells are sensitive to MMS is due to misregulation of origin firing, the mutants that prevent checkpoint-dependent phosphorylation should rescue the sensitivity of *pph3Δ* cells. As shown below, these mutants do not rescue *pph3Δ,* indicating that the reason these cells are sensitive to MMS is not due to an inability to inhibit late origins from firing.

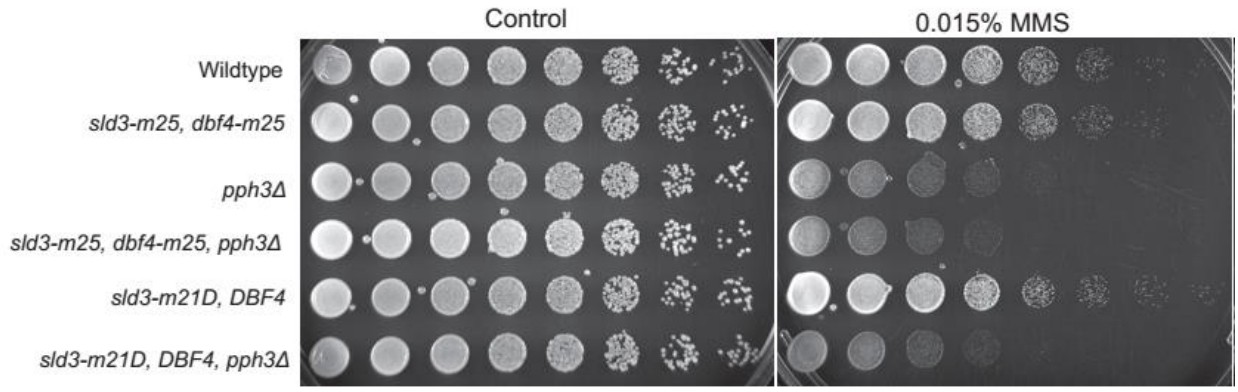

Figure S4. The MMS sensitivity of cells lacking *PPH3* is independent of a defect in origin firing regulation. Genetic interactions between *pph3Δ* cells and mutants of *DBF4* and/or *SLD3* that either prevent or mimic Rad53 regulation. Phospho-mutants, *sld3-m25* and *dbf4-m25,* and a phospho-mimetic of *SLD3*, *sld3-m21D*, were analyzed for their genetic interactions with deletion of *PPH3.* Serial dilution assay showing the MMS sensitivity of the indicated strains. Four-fold serial dilutions were spotted on YPD plates with or without the indicated drugs and grown for 2–3 days at 30°C.

Identifying Pph3-regulated Replication Components using Quantitative Mass Spectrometry.

In order to assess the biological reason for the intra-S phase delay upon MMS treatment in *pph3Δ* cells, I decided to perform an unbiased quantitative mass spectrometry analysis comparing phosphorylated peptides between wildtype and *pph3Δ* cells using SILAC. Here, wildtype and *pph3Δ* cells were grown in media supplemented with either normal ("light") or "heavy" isotopes of Arg and Lys for several generations. Cells were synchronized in G1 and released into S phase with MMS. Cells were evenly mixed and whole cell lysates were enriched for phosphorylated peptides using Immobilized metal ion affinity chromatography (IMAC) (see Appendix iii for details). Quantitative mass spectrometry was used to analyze the relative abundances of specific phosphorylated peptides between wildtype and *pph3Δ* cells. Phosphorylated peptides identified more in their "heavy" counterpart compared with "light" are likely substrates of Pph3. Phosphorylated peptides that were more enrich in *pph3Δ* cells ("heavy") compared with wildtype ("light") cells are shown as log2 values in **Table 2** and on the left side of **Figure S5**. Because I am interested in the mechanism for the MMS-induced S-phase delay in *pph3Δ* cells, replication fork components that are substrates of Pph3 (in red) are particularly interesting candidates to explore in future work. Protein descriptions are listed in **Table 3**.

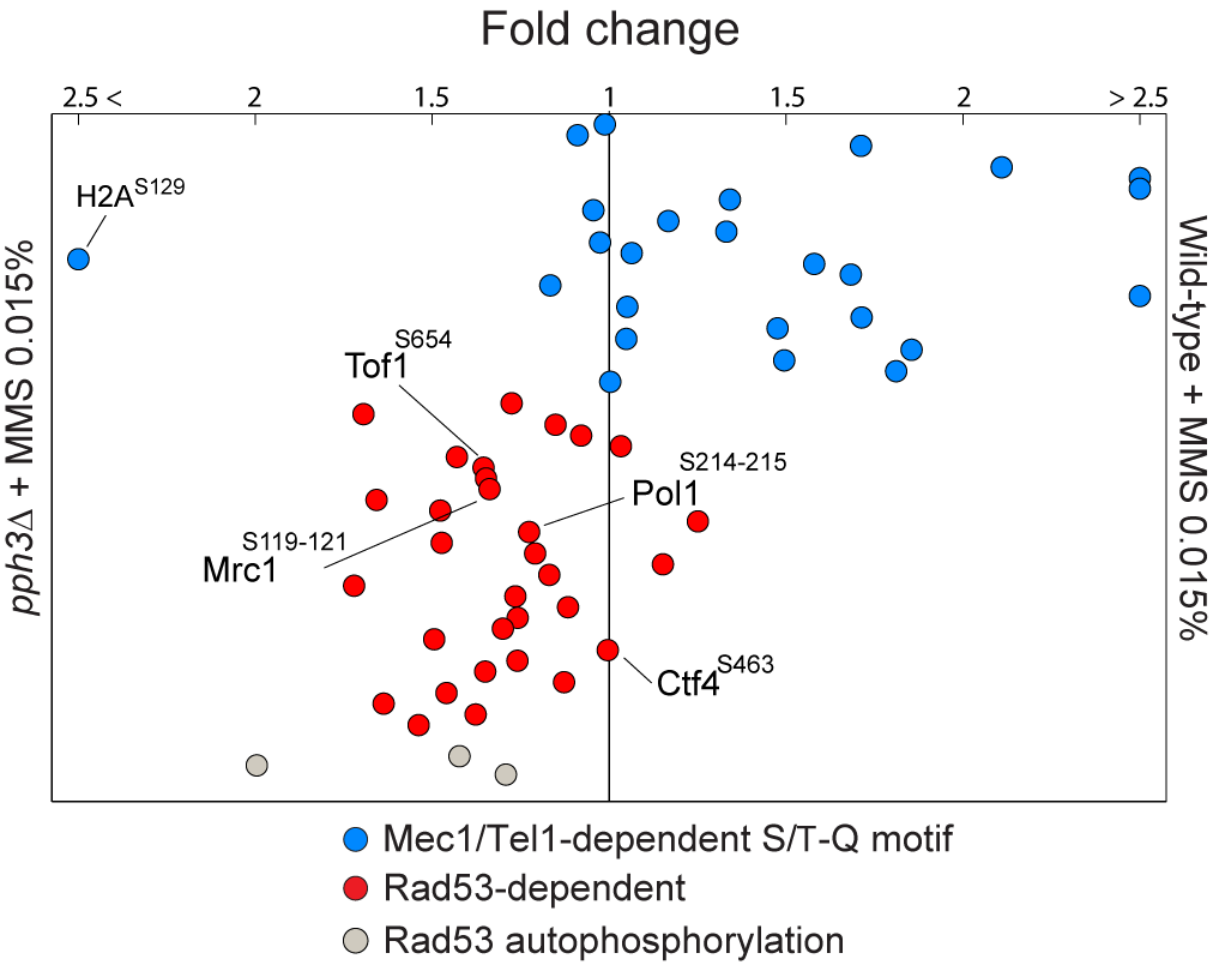
Fold change
2.5 <
2
1.5
1
1.5
2
> 2.5
H2A S129
Tof1 S654
S214-215
Pol1
S119-121
Mrc1
Ctf4 S463
pph3Δ + MMS 0.015%
Wild-type + MMS 0.015%
Mec1/Tel1-dependent S/T-Q motif
Rad53-dependent
Rad53 autophosphorylation

Figure S5. Quantitative mass spectrometry analysis comparing phosphorylated peptides in wildtype and *pph3Δ* cells in MMS-induced replication stress. Wildtype and *pph3Δ* cells were grown in “light” and “heavy” SILAC media, respectively. Cells were grown to an OD600 of 0.2 and arrested in G1 using α-factor pheromone for 2 hours. Cells were then released into fresh media with 0.015% MMS for 45 minutes. Cells were evenly mixed and lysed. IMAC purification was used to enrich for phosphorylated peptides before HILIC fractionation and LC-MS/MS analysis. Each phospho-peptide is shown as a circle, with Mec1-dependent peptides shown as blue circles, Rad53-dependent peptides shown as red circles, and Rad53 autophosphorylation sites shown as gray circles. Phosphorylated peptides that were more abundance in *pph3Δ* cells compared with wildtype are shown on the left side, and ones more enriched in wildtype cells are shown on the right side. Phospho-peptides that did not change in abundance are shown in the middle. Identification of each phospho-peptide and site of modification are shown in **Table 2**.

Table 2. Identification and quantitation of phospho-peptides comparing Wildtype and *pph3Δ* cells in MMS conditions.

Kinase Dependency	GENE	ORF (SGD)	Phosphopeptide sequence	Number of times identified	Relative abundance of phosphopeptides (*pph3* Δ/wildtype, log2)	Phosphorylation site (aa position)
Mec1	MSH6	YDR097C	R.EEPGNFYNETphosQLDSSTIVQK.L	7	-0.01764	451
Mec1	MSH6	YDR097C	K.STTTDEDL(SSS)phosQSRR.N	6	-0.12295	128-130
Mec1	DAD1	YDR016C	K.TLYDGLESLSDEAPIDEQPTLSphosQSK.T	17	0.7757	89
Mec1	HTA2	YBL003C	K.TAKASphosQEL.-	10	-1.32735	129
Mec1	NGG1	YDR176W	K.SEFVVSphosQTLPR.A	5	1.07695	231
Mec1	HPR1	YDR138W	K.SSEV(SS)phosQDPDSGVAGEFAPQNTTAQLENPK.T	7	1.51937	706-707
Mec1	GCD10	YNL062C	K.TV(YS)phosQEKYVNR.K	4	1.43804	174-175
Mec1	TOA2	YKL058W	R.DASphosQNGSGDSQSVISVDKLR.L	7	0.42393	95
Mec1	RFA2	YNL312W	K.GYGSphosQVAQQFEIGGYVK.V	161	-0.06272	122
Mec1	SUM1	YDR310C	R.KTPGDEETTTFVPLENSphosQPSDTIR.K	12	0.22341	712
Mec1	SPN1	YPR133C	K.VVEATPEDGTA(SS)phosQK.S	42	0.41282	22-23
Mec1	SPT7	YBR081C	R.SDDV(SS)phosQTIK.D	5	-0.03638	99-100
Mec1	DPB4	YDR121W	K.TESphosQDVETR.V	18	0.08886	183
Mec1	PRP19	YLL036C	K.(SS)phosQQAVAITR.E	20	0.65965	140-141
Mec1	SPT7	YBR081C	K.SFPLTphosQEEEHHGAVSPAVDTR.S	2	0.75095	78
Mec1	DPB4	YDR121W	K.QKTESphosQDVETR.V	15	-0.22172	183
Mec1	PSY4	YBL046W	R.SEGLLPGDELVSPSM(SSS)phosQEDK.M	13	1.44387	413-415
Mec1	MSH6	YDR097C	R.SDIMHSphosQEPQSDTMLNSNTTEPK.S	26	0.07224	102
Mec1	FES1	YBR101C	K.LLQWSIANSphosQGDKEAMAR.A	4	0.77734	12
Mec1	SGF73	YGL066W	K.VIEEYSLSphosQGSGPSNDSWK.S	7	0.56184	22
Mec1	RTT107	YHR154W	K.RIDSEEISLSphosQDVER.S	5	0.0684	806
Mec1	RFA1	YAR007C	R.KFANENPNSphosQK.T	27	0.89143	178
Mec1	RFA1	YAR007C	K.FANENPNSphosQK.T	28	0.58029	178
Mec1	CBF5	YLR175W	K.EYVPLDNAEQ(STSSS)phosQETKETEEEPK.K	9	0.85699	395-399
Mec1	SOK2	YMR016C	R.(SS)phosQLPISALTSTDTDKIK.T	4	0.00505	718-719
Mec1	NUP60	YAR002W	R.SNLSphosQENDNEGK.H	5	-0.20317	483
Rad53	PLM2	YDR501W	K.FVPVEHSphosPR.T	35	-0.3512	281
Rad53	NET1	YJL076W	K.G(TTS)phosFNEEGNRK.N	9	-0.76085	838-840
Rad53	MBP1	YDL056W	R.SA(STS)phosAIMETK.R	5	-0.11	133-135
Rad53	TOS4	YLR183C	R.TVDP(YS)phosPPNYK.Q	26	0.04676	16-17
Rad53	RLP7	YNL002C	R.EVSphosGFGSLNR.L	39	-0.51598	278
Rad53	TOF1	YNL273W	R.SphosIEVNFQK.V	5	-0.43844	654
Rad53	NUP2	YLR335W	K.(SS)phosFTFGSTTIEK.K	4	-0.43065	316-317
Rad53	MRC1	YCL061C	K.NV(SSS)phosFTQTQR.L	3	-0.41966	119-121
Rad53	USO1	YDL058W	K.TISphosDLEQTKEEIISK.S	14	-0.72881	1032
Rad53	NUP2	YLR335W	K.QA(SS)phosFSFLNR.A	9	-0.56296	65-66
Rad53	DUN1	YDL101C	K.YA(SSSST)phosDIENDDEKVSSESR.S	17	0.32262	139-143
Rad53	POL1	YNL102W	K.IDPDSSTDKYLEIE(SS)phosPLK.L	17	-0.29385	214-215
Rad53	SEC16	YPL085W	R.ELSphosEVASR.L	28	-0.55892	1383
Rad53	DUN1	YDL101C	R.EHSphosGDVTDSSFKR.Q	24	-0.27411	10
Rad53	MMS4	YBR098W	K.FLD(SS)phosDSITTDVLSTPAK.G	8	0.20433	291-292
Rad53	NRM1	YNR009W	K.VATHSKSphosEPLTR.R	13	-0.2254	145
Rad53	NPL3	YDR432W	R.ENSphosLETTFSSVNTR.D	113	-0.78297	224
Rad53	RTT107	YHR154W	K.LTFGSphosFSSSSTNK.H	7	-0.3392	184
Rad53	RFX1	YLR176C	R.SN(SS)phosAYPLSFK.S	11	-0.15867	173-174
Rad53	TAF4	YMR005W	K.QYGWL(TSS)phosVNKPTSLGAK.S	11	-0.33166	319-321
Rad53	RAD9	YDR217C	K.RNSphosDLDAASIK.R	20	-0.37891	729
Rad53	SUM1	YDR310C	K.ALPSphosITDIPVSDDSDIKR.Q	14	-0.57951	55
Rad53	CTF4	YPR135W	K.THSphosFPISLANTGK.F	28	-0.00522	463
Rad53	HPC2	YBR215W	K.KEN(SS)phosLSSIK.A	10	-0.33259	386-387
Rad53	YRB2	YIL063C	R.ENSphosEVKQTAVENPIDKLDGTPK.R	2	-0.43343	14
Rad53	YMR144W	YMR144W	K.MKSphosFSTIDGSIK.D	4	-0.17319	330
Rad53	ULS1	YOR191W	K.EGTLSphosFSTYK.Q	9	-0.54574	634
Rad53	NPL3	YDR432W	K.DLARENSphosLETTFSSVNTR.D	32	-0.71146	224
Rad53	ENP1	YBR247C	R.ILDDGSphosNGEDATR.V	11	-0.4616	404
Rad53	DEF1	YKL054C	K.EISphosDIKKDDQK.S	31	-0.62127	273
Rad53	RAD53	YPL153C	K.LLHSphosNNTENVK.S	3	-0.49425	560
Rad53	RAD53	YPL153C	R.IHSphosVSLSphosQSQIDPSK.K	4	-0.98642	789 793
Rad53	RAD53	YPL153C	K.SphosIEAETR.E	14	-0.35293	547

Table 2. Identification and quantitation of phospho-peptides comparing Wildtype and *pph3Δ* cells in MMS conditions. Phosphorylated peptides from **Figure S4**. are shown here. Phospho-peptides are in descending order as the circles appear in Figure S4. from top down. The kinase target, target gene name, and open reading frame (ORF) for each phospho-peptide are indicated. Phospho-peptide sequence is also shown, and site of phosphorylation is marked as “phos” after the modified residue. In the case where multiple possible phosphorylated residues are possible, these potentially phosphorylated residues are grouped together in parenthesis. The number of times each phospho-peptide was identified in the LC-MS/MS is also shown. Relative abundance between wildtype and *pph3Δ* cells are indicated as either negative or positive log2 values, with the more negative value as found more in *pph3Δ* cells compared with wildtype, and the more positive value being more abundance in wildtype compared with *pph3Δ* cells. The amino acid residue number that is modified in each phospho-peptide in the whole protein is also shown. Potentially interesting replication fork components that are dependent on Pph3 are listed in red.

Table 3. Protein descriptions for phosphorylated peptides found during quantitative mass spectrometry analysis comparing wildtype and *pph3Δ* cells.

GENE	Protein Description
CBF5	Pseudouridine synthase catalytic subunit of box H/ACA small nucleolar ribonucleoprotein particles (snoRNPs), acts on both large and small rRNAs and on snRNA U2
CTF4	Chromatin-associated protein, required for sister chromatid cohesion; interacts with DNA polymerase alpha (Pol1p) and may link DNA synthesis to sister chromatid cohesion
DAD1	Essential subunit of the Dam1 complex (aka DASH complex), couples kinetochores to the force produced by MT depolymerization thereby aiding in chromosome segregation; is transferred to the kinetochore prior to mitosis
DEF1	RNAPII degradation factor, forms a complex with Rad26p in chromatin, enables ubiquitination and proteolysis of RNAPII present in an elongation complex; mutant is deficient in Zip1p loading onto chromosomes during meiosis
DPB4	Shared subunit of DNA polymerase (II) epsilon and of ISW2/yCHRAC chromatin accessibility complex; involved in both chromosomal DNA replication and in inheritance of telomeric silencing
DUN1	Cell-cycle checkpoint serine-threonine kinase required for DNA damage-induced transcription of certain target genes, phosphorylation of Rad55p and Sml1p, and transient G2/M arrest after DNA damage; also regulates postreplicative DNA repair
ENP1	Protein associated with U3 and U14 snoRNAs, required for pre-rRNA processing and 40S ribosomal subunit synthesis; localized in the nucleus and concentrated in the nucleolus
FES1	Hsp70 (Ssa1p) nucleotide exchange factor, cytosolic homolog of Sil1p, which is the nucleotide exchange factor for BiP (Kar2p) in the endoplasmic reticulum
GCD10	Subunit of tRNA (1-methyladenosine) methyltransferase with Gcd14p, required for the modification of the adenine at position 58 in tRNAs, especially tRNAi-Met; first identified as a negative regulator of GCN4 expression
HPC2	Subunit of the HIR complex, a nucleosome assembly complex involved in regulation of histone gene transcription; mutants display synthetic defects with subunits of FACT, a complex that allows passage of RNA Pol II through nucleosomes
HPR1	Subunit of THO/TREX complexes that couple transcription elongation with mitotic recombination and with mRNA metabolism and export, subunit of an RNA Pol II complex; regulates lifespan; involved in telomere maintenance; similar to Top1p
HTA2	Histone H2A, core histone protein required for chromatin assembly and chromosome function; one of two nearly identical (see also HTA1)

	subtypes; DNA damage-dependent phosphorylation by Mec1p facilitates DNA repair; acetylated by Nat4p
MBP1	Transcription factor involved in regulation of cell cycle progression from G1 to S phase, forms a complex with Swi6p that binds to MluI cell cycle box regulatory element in promoters of DNA synthesis genes
MMS4	Subunit of the structure-specific Mms4p-Mus81p endonuclease that cleaves branched DNA; involved in recombination and DNA repair
MRC1	S-phase checkpoint protein required for DNA replication; interacts extensively with Pol2p and stabilizes it at stalled replication forks during replication stress, where it forms a pausing complex with Tof1p and is phosphorylated by Mec1p
MSH6	Protein required for mismatch repair in mitosis and meiosis, forms a complex with Msh2p to repair both single-base & insertion-deletion mispairs; potentially phosphorylated by Cdc28p
NET1	Core subunit of the RENT complex, which is a complex involved in nucleolar silencing and telophase exit; stimulates transcription by RNA polymerase I and regulates nucleolar structure
NGG1	Transcriptional regulator involved in glucose repression of Gal4p-regulated genes; component of transcriptional adaptor and histone acetyltransferase complexes, the ADA complex, the SAGA complex, and the SLIK complex
NPL3	RNA-binding protein that carries poly(A)+ mRNA from the nucleus into the cytoplasm; dissociation from mRNAs is promoted by Mtr10p; phosphorylated by Sky1p in the cytoplasm
NRM1	Transcriptional co-repressor of MBF (MCB binding factor)-regulated gene expression; Nrm1p associates stably with promoters via MBF to repress transcription upon exit from G1 phase
NUP2	Nucleoporin involved in nucleocytoplasmic transport, binds to either the nucleoplasmic or cytoplasmic faces of the nuclear pore complex depending on Ran-GTP levels; also has a role in chromatin organization
NUP60	Subunit of the nuclear pore complex (NPC), functions to anchor Nup2p to the NPC in a process controlled by the nucleoplasmic concentration of Gsp1p-GTP; potential Cdc28p substrate; involved in telomere maintenance
PLM2	Protein required for partitioning of the 2-micron plasmid
POL1	Catalytic subunit of the DNA polymerase I alpha-primase complex, required for the initiation of DNA replication during mitotic DNA synthesis and premeiotic DNA synthesis
PRP19	Splicing factor associated with the spliceosome; contains a U-box, a motif found in a class of ubiquitin ligases
PSY4	Putative regulatory subunit of an evolutionarily conserved protein phosphatase complex containing the catalytic subunit Pph3p and a third subunit Psy2p; required for cisplatin resistance; GFP-fusion protein localizes to the nucleus

RAD53	Protein kinase, required for cell-cycle arrest in response to DNA damage; activated by trans autophosphorylation when interacting with hyperphosphorylated Rad9p; also interacts with ARS1 and plays a role in initiation of DNA replication
RAD9	DNA damage-dependent checkpoint protein, required for cell-cycle arrest in G1/S, intra-S, and G2/M; transmits checkpoint signal by activating Rad53p and Chk1p; hyperphosphorylated by Mec1p and Tel1p; potential Cdc28p substrate
RFA1	Subunit of heterotrimeric Replication Protein A (RPA), which is a highly conserved single-stranded DNA binding protein involved in DNA replication, repair, and recombination
RFA2	Subunit of heterotrimeric Replication Protein A (RPA), which is a highly conserved single-stranded DNA binding protein involved in DNA replication, repair, and recombination
RFX1	Major transcriptional repressor of DNA-damage-regulated genes, recruits repressors Tup1p and Cyc8p to their promoters; involved in DNA damage and replication checkpoint pathway; similar to a family of mammalian DNA binding RFX1-4 proteins
RLP7	Nucleolar protein with similarity to large ribosomal subunit L7 proteins; constituent of 66S pre-ribosomal particles; plays an essential role in processing of precursors to the large ribosomal subunit RNAs
RTT107	Protein implicated in Mms22-dependent DNA repair during S phase, DNA damage induces phosphorylation by Mec1p at one or more SQ/TQ motifs; interacts with Mms22p and Slx4p; has four BRCT domains; has a role in regulation of Ty1 transposition
SEC16	COPII vesicle coat protein required for ER transport vesicle budding and autophagosome formation; Sec16p is bound to the periphery of ER membranes and may act to stabilize initial COPII complexes; interacts with Sec23p, Sec24p and Sec31p
SGF73	Subunit of SAGA histone acetyltransferase complex; involved in formation of the preinitiation complex assembly at promoters; null mutant displays defects in premeiotic DNA synthesis
SOK2	Nuclear protein that plays a regulatory role in the cyclic AMP (cAMP)-dependent protein kinase (PKA) signal transduction pathway; negatively regulates pseudohyphal differentiation; homologous to several transcription factors
SPN1	Protein that interacts with Spt6p and copurifies with Spt5p and RNA polymerase II, probable transcriptional elongation factor; metazoan homologs contain an acidic N terminus; mutations in the gene confer an Spt- phenotype
SPT7	Subunit of the SAGA transcriptional regulatory complex, involved in proper assembly of the complex; also present as a C-terminally truncated form in the SLIK/SALSA transcriptional regulatory complex
SUM1	Transcriptional repressor required for mitotic repression of middle sporulation-specific genes; also acts as general replication initiation factor;

	involved in telomere maintenance, chromatin silencing; regulated by pachytene checkpoint
TAF4	TFIID subunit (48 kDa), involved in RNA polymerase II transcription initiation; potential Cdc28p substrate
TOA2	TFIIA small subunit; involved in transcriptional activation, acts as antirepressor or as coactivator; homologous to smallest subunit of human and Drosophila TFIIA
TOF1	Subunit of a replication-pausing checkpoint complex (Tof1p-Mrc1p-Csm3p) that acts at the stalled replication fork to promote sister chromatid cohesion after DNA damage, facilitating gap repair of damaged DNA; interacts with the MCM helicase
TOS4	Transcription factor that binds to a number of promoter regions, particularly promoters of some genes involved in pheromone response and cell cycle; potential Cdc28p substrate; expression is induced in G1 by bound SBF
ULS1	RING finger protein involved in proteolytic control of sumoylated substrates; interacts with SUMO (Smt3p); member of the SWI/SNF family of DNA-dependent ATPases; plays a role in antagonizing silencing during mating-type switching
USO1	Essential protein involved in intracellular protein transport, coiled-coil protein necessary for transport from ER to Golgi; required for assembly of the ER-to-Golgi SNARE complex
YMR144W	Protein of unknown function
YRB2	Protein of unknown function involved in nuclear processes of the Ran-GTPase cycle; involved in nuclear protein export; contains Ran Binding Domain and FxFG repeats; interacts with Srm1p, GTP-Gsp1p, Rna1p and Crm1p; is not essential

Table 3. Protein descriptions for phosphorylated-peptides found during quantitative mass spectrometry analysis comparing wildtype and *pph3Δ* cells. Protein descriptions from Table 3 are listed as describe from www.yeastgenome.org.

APPENDIX iii

Tables

Table 4. *S. cerevisiae* strains used in this study.

MBS strain number	Background	Relevant Genotype	Reference
164	S288C	*MATa ura3-52 leu2Δ1 trp1Δ63 his3Δ200 lys2ΔBgl hom3-10 ade2Δ1 ade8 arg4Δ sml1Δ::TRP1 bar1Δ::HIS3*	(Ohouo et al 2010)
571	S288C	*MATa ura3-52 leu2Δ1 trp1Δ63 his3Δ200 lys2ΔBgl hom3-10 ade2Δ1 ade8 arg4Δ sml1Δ::TRP1 bar1Δ::HIS3 DPB11-6HIS3-HA::LEU2 SLX4-6HIS3-FLAG::kanMX6*	(Ohouo et al 2010)
626	S288C	*MATa ura3-52 trp1Δ63 his3Δ200 bar1Δ::HIS3*	(Ohouo et al 2010)
662	S288C	*MATa ura3-52 trp1Δ63 his3Δ200*	this study
943 = yDD_705	W303	*MATa ade2-1 trp1-1 can1-100 leu2-3,112 his3-11,15 ura3-1 RAD5*	Durocher lab (Szilard et al 2010)
944 = yDD_1793	W303	*MATa hta1-S129A hta2-S129A leu2-3,112 his3-11,15 ade2-1 ura3-1 trp1-1 can1-100 RAD5*	Durocher lab (Szilard et al 2010)
961	W303	*MATa hta1-S129A hta2-S129A leu2-3,112 his3-11,15 ade2-1 ura3-1 trp1-1 can1-100 RAD5 slx4Δ::HIS3*	this study
1002	W303	*MATa ade2-1 trp1-1 can1-100 leu2-3,112 his3-11,15 ura3-1 RAD5 slx4Δ::HIS3*	this study
1013	S288C	*MATa ura3-52 trp1Δ63 his3Δ200 bar1Δ::HIS3*	(Ohouo et al 2013)
1301	S288C	*MATa ura3-52 leu2Δ1 trp1Δ63 his3Δ200 lys2ΔBgl hom3-10 ade2Δ1 ade8 arg4Δ sml1Δ::TRP1 bar1Δ::HIS3 DPB11-6HIS3-HA::LEU2 slx4-S486A-3XFLAG::kanMX6*	(Ohouo et al 2013)
1437	S288C	*MATa ura3-52 trp1Δ63 his3Δ200 RAD53-6HIS3-FLAG::kanMX6*	(Ohouo et al 2013)
1438	S288C	*MATa ura3-52 trp1Δ63 his3Δ200 RAD53-6HIS3-FLAG::kanMX6 slx4Δ::HIS3*	(Ohouo et al 2013)
1440	S288C	*MATa ura3-52 trp1Δ63 his3Δ200 rad53-R605A-6HIS3-FLAG::kanMX6*	(Ohouo et al 2013)
1442	S288C	*MATa ura3-52 trp1Δ63 his3Δ200 rad53-R605A-6HIS3-FLAG::kanMX6 slx4Δ::HIS3*	(Ohouo et al 2013)
2111	S288C	*MATa ura3-52 his3Δ200 leu2Δ1 met15Δ0 RAD9-6HIS3-10XFLAG::kanMX6*	this study
2161	S288C	*MATa ura3-52 his3Δ200 leu2Δ1 met15Δ0 RAD9-6HIS3-10XFLAG::kanMX6 slx4Δ::URA3*	this study
2191	S288C	*MATa ura3-52 leu2Δ1 trp1Δ63 his3Δ200 lys2ΔBgl hom3-10 ade2Δ1 ade8 arg4Δ sml1Δ::TRP1 bar1Δ::HIS3 pph3Δ::kanMX6*	this study

2285	S288C	*MATa ura3-52 leu2Δ1 trp1Δ63 his3Δ200 lys2ΔBgl hom3-10 ade2Δ1 ade8 arg4Δ sml1Δ::TRP1 bar1Δ::HIS3 sgs1Δ::URA3*	this study
2287	S288C	*MATa ura3-52 leu2Δ1 trp1Δ63 his3Δ200 lys2ΔBgl hom3-10 ade2Δ1 ade8 arg4Δ sml1Δ::TRP1 bar1Δ::HIS3 pph3Δ::kanMX6 sgs1Δ::URA3*	this study
2325	S288C	*MATa ura3-52 leu2Δ1 trp1Δ63 his3Δ200 lys2ΔBgl hom3-10 ade2Δ1 ade8 arg4Δ sml1Δ::TRP1 bar1Δ::HIS3 DPB11-6HIS3-HA::LEU2 SLX4-6HIS3-FLAG::kanMX6 mus81Δ::URA3*	(Ohouo et al 2013)
2326	S288C	*MATa ura3-52 leu2Δ1 trp1Δ63 his3Δ200 lys2ΔBgl hom3-10 ade2Δ1 ade8 arg4Δ sml1Δ::TRP1 bar1Δ::HIS3 DPB11-6HIS3-HA::LEU2 slx4-S486A-3XFLAG::kanMX6 mus81Δ::URA3*	(Ohouo et al 2013)
2362	S288C	*MATa ura3-52 leu2Δ1 trp1Δ63 his3Δ200 lys2ΔBgl hom3-10 ade2Δ1 ade8 arg4Δ sml1Δ::TRP1 bar1Δ::HIS3 dot1Δ::URA3*	this study
2363	S288C	*MATa ura3-52 leu2Δ1 trp1Δ63 his3Δ200 lys2ΔBgl hom3-10 ade2Δ1 ade8 arg4Δ sml1Δ::TRP1 bar1Δ::HIS3 pph3Δ::kanMX6 dot1Δ::URA3*	this study
2422	S288C	*MATa ura3-52 trp1Δ63 his3Δ200 bar1Δ::HIS3 pph3Δ::URA3*	this study
2522	S288C	*MATa ura3-52 leu2Δ1 trp1Δ63 his3Δ200 lys2ΔBgl hom3-10 ade2Δ1 ade8 arg4Δ sml1Δ:TRP1 bar1Δ::HIS3 pph3Δ::natMX*	this study
2524	S288C	*MATa ura3-52 leu2Δ1 trp1Δ63 his3Δ200 lys2ΔBgl hom3-10 ade2Δ1 ade8 arg4Δ sml1Δ::TRP1 bar1Δ::HIS3 rad53-R605A::kanMX6*	this study
2528	S288C	*MATa ura3-52 leu2Δ1 trp1Δ63 his3Δ200 lys2ΔBgl hom3-10 ade2Δ1 ade8 arg4Δ sml1Δ::TRP1 bar1Δ::HIS3 pph3Δ::natMX rad53-R605A::kanMX6*	this study
2597	S288C	*ura3-52 trp1Δ63 his3Δ200*	this study
2600	S288C	*ura3-52 trp1Δ63 his3Δ200 rad53-R605A::kanMX6*	this study
2602	S288C	*ura3-52 trp1Δ63 his3Δ200 pph3Δ::HIS3 mus81Δ::URA3*	this study
2639	W303	*MATa ade2-1 trp1-1 can1-100 leu2-3,112 his3-11,15 ura3-1 RAD5 pph3Δ::TRP1*	this study
2640	W303	*MATa hta1-S129A hta2-S129A leu2-3,112 his3-11,15 ade2-1 ura3-1 trp1-1 can1-100 RAD5 pph3Δ::TRP1*	this study
2642	W303	*MATa ade2-1 trp1-1 can1-100 leu2-3,112 his3-11,15 ura3-1 RAD5 slx4Δ::HIS3 pph3Δ::natMX*	this study
2644	W303	*MATa hta1-S129A hta2-S129A leu2-3,112 his3-11,15 ade2-1 ura3-1 trp1-1 can1-100 RAD5 slx4Δ::HIS3 pph3Δ::TRP1*	this study
2655	S288C	*MATa ura3-52 trp1Δ63 his3Δ200*	this study

		pph3Δ::kanMX6	
2661	S288C	*MATa ura3-52 trp1Δ63 his3Δ200 bar1Δ::HIS3 slx4Δ::kanMX6*	this study
2663	S288C	*MATa ura3-52 trp1Δ63 his3Δ200 bar1Δ::HIS3 pph3Δ::URA3 slx4Δ::kanMX6*	this study
2732	S288C	*MATa ura3-52 trp1Δ63 his3Δ200 bar1Δ::HIS3 rad53-R605A::kanMX6*	this study
2733	S288C	*MATa ura3-52 trp1Δ63 his3Δ200 bar1Δ::HIS3 pph3Δ::URA3 slx4Δ::natMX rad53-R605A::kanMX6*	this study
2738	S288C	*ura3-52 trp1Δ63 his3Δ200 pph3Δ::HIS3 mus81Δ::URA3 rad53-R605A::kanMX6*	this study
2790	S288C	*MATα ura3-52 trp1Δ63 his3Δ200 slx4-S486A::kanMX6*	this study
2791	S288C	*MATa ura3-52 trp1Δ63 his3Δ200 bar1Δ::HIS3 sgs1Δ::natMX*	this study
2793	S288C	*MATα ura3-52 trp1Δ63 his3Δ200 bar1Δ::HIS3 slx4-S486A::kanMX6 sgs1Δ::natMX*	this study
2802	S288C	*MATa ura3-52 trp1Δ63 his3Δ200 bar1Δ::HIS3 sgs1Δ::natMX*	this study
2803	S288C	*MATa ura3-52 trp1Δ63 his3Δ200 bar1Δ::HIS3 pph3Δ::URA3 sgs1Δ::natMX*	this study
2805	S288C	*MATa ura3-52 trp1Δ63 his3Δ200 bar1Δ::HIS3 slx4-S486A::kanMX6 sgs1Δ::natMX*	this study
2807	S288C	*MATa ura3-52 trp1Δ63 his3Δ200 bar1Δ::HIS3 pph3Δ::URA3 slx4-S486A::kanMX6 sgs1Δ::natMX*	this study
2831	S288C	*MATa ura3-52 leu2Δ1 trp1Δ63 his3Δ200 lys2ΔBgl hom3-10 ade2Δ1 ade8 arg4Δ sml1Δ::TRP1 bar1Δ::HIS3 slx4Δ::kanMX6*	this study
2833	S288C	*MATa ura3-52 leu2Δ1 trp1Δ63 his3Δ200 lys2ΔBgl hom3-10 ade2Δ1 ade8 arg4Δ sml1Δ::TRP1 bar1Δ::HIS3 dot1Δ::URA3 slx4Δ::natMX*	this study
2835	S288C	*MATa ura3-52 trp1Δ63 his3Δ200 bar1Δ::HIS3 pph3Δ::TRP1 sgs1Δ::natMX*	this study
2837	S288C	*MATa ura3-52 trp1Δ63 his3Δ200 bar1Δ::HIS3 pph3Δ::TRP1 slx4-S486A::kanMX6 sgs1Δ::natMX*	this study
2838	S288C	*MATa ura3-52 trp1Δ63 his3Δ200 bar1Δ::HIS3 pph3Δ::URA3 slx4Δ::kanMX6 mus81Δ::TRP1*	this study
2840	S288C	*MATa ura3-52 trp1Δ63 his3Δ200 bar1Δ::HIS3 pph3Δ::URA3 slx4Δ::natMX rad53-R605A::kanMX6 mus81Δ::TRP1*	this study
2841	S288C	*ura3-52 trp1Δ63 his3Δ200 mus81Δ::URA3 rad53-R605A::kanMX6 slx4Δ::TRP1*	this study
2842	S288C	*ura3-52 trp1Δ63 his3Δ200 mus81Δ::URA3 slx4Δ::TRP1*	this study

Table 4. *S. cerevisiae* strains used in this study.

Table 5. Plasmids used in this study.					
Plasmid No.	**Vector**	**Gene**	**Mutation**	**Tag**	**Reference**
pMBS148	*pRS416*	-	-	-	Scott Emr lab
pMBS213	*pRS416*	*SLX4*	-	FLAG	(Cussiol et al, 2015)
pMBS362	*pFA6a*	*RAD53*	R605A	-	(Ohouo et al, 2013)
pMBS622	*pRS416*	*SLX4*	S486A	FLAG	(Cussiol et al, 2015)
pMBS810	*pRS416*	*pDPB11-MBD [dpb11(aa292-600)-rtt107(aa742-end) fusion]*	-	HA	(Cussiol et al, 2015)

Table 5. Plasmids used in this study.

Table 6. *S. cerevisiae* strains generated		
MBS Strain Number	**Background**	**Relevant Genotype**
1244	S288C	*MATa, ura3-52, leu2Δ1, trp1Δ63, his3Δ200, lys2ΔBgl, hom3-10, ade2Δ1, ade8, arg4Δ, sml1Δ::TRP1 bar1Δ::HIS3, Nup60-3xHA::KanMX6*
1246	S288C	*ura3-52/ura3-52, trp1-63/trp1-63, his3-200/his3-200, Sml1/sml1Δ::TRP1, RAD53/rad53Δ::HIS3, NUP60/nup60Δ::URA3*
1249	S288C	*MATa, ura3-52, leu2Δ1, trp1Δ63, his3Δ200, lys2ΔBgl, hom3-10, ade2Δ1, ade8, arg4Δ, sml1Δ::TRP1, barΔ::HIS3, rad53Δ::URA3, Nup60-3xHA::KanMX6*
1572	S288C	*ura3-52, trp1-63, his3-200, slx4Δ::KanMX6, hos2Δ::URA3, rpd3Δ::KanMX6*
1584	S288C	*MATa, ura3-52, leu2Δ1, trp1Δ63, his3Δ200, lys2ΔBgl, hom3-10, ade2Δ1, ade8, arg4Δ, sml1Δ::TRP1 bar1Δ::HIS3 rad53Δ::URA3, rpd3Δ::KanMX6*
1590	S288C	*MATa, ura3-52, trp1-63, his3-200, bar1Δ::HIS3, Rad53-HA::natMX, rtt107Δ::KanMX6*
1676	S288C	*MATa, ura3-52, leu2Δ1, trp1Δ63, his3Δ200, lys2ΔBgl, hom3-10, ade2Δ1, ade8, arg4Δ, sml1Δ::TRP1 bar1Δ::HIS3*
1693	S288C	*ura3-52/ura3-52, trp1-63/trp1-63, his3-200/his3-200, hda1Δ::KanMX6*
1704	S288C	*ura3-52/ura3-52, trp1-63/trp1-63, his3-200/his3-200, hda1Δ::URA3, rpd3Δ::KanMX6*
1705	S288C	*MATa, ura3-52, leu2Δ1, trp1Δ63, his3Δ200, lys2ΔBgl, hom3-10, ade2Δ1, ade8, arg4Δ, sml1Δ:TRP1 bar1Δ:HIS3, hda1Δ:URA3, TOP2-3HA(FL):KanMX6*
1706	S288C	*MATa, ura3-52, leu2Δ1, trp1Δ63, his3Δ200, lys2ΔBgl, hom3-10, ade2Δ1, ade8, arg4Δ, sml1Δ:TRP1 bar1Δ:HIS3, hda1Δ:URA3, TOP2-3HA(1220 trunc):KanMX6*
1707	S288C	*ura3-52/ura3-52, trp1-63/trp1-63, his3-200/his3-200, hda1Δ:URA3, TOP2-3HA (full length):: KanMX6*
1708	S288C	*ura3-52/ura3-52, trp1-63/trp1-63, his3-200/his3-200, hda1Δ:URA3, TOP2-3HA (->1220):: KanMX6*
1709	S288C	*MATa, ura3-52, leu2Δ1, trp1Δ63, his3Δ200, lys2ΔBgl, hom3-10, ade2Δ1, ade8, arg4Δ, sml1Δ:TRP1 bar1Δ::HIS3, TOP2-3HA(FL)::KanMX6*
1710	S288C	*MATa, ura3-52, leu2Δ1, trp1Δ63, his3Δ200, lys2ΔBgl, hom3-10, ade2Δ1, ade8, arg4Δ, sml1Δ:TRP1 bar1Δ::HIS3, TOP2-3HA(1220)::KanMX6*
1850	S288C	*MATa, ura3-52, leu2Δ1, trp1Δ63, his3Δ200, lys2ΔBgl, hom3-10, ade2Δ1, ade8, arg4Δ, sml1Δ::TRP1 bar1Δ::HIS3, Top2-HA (FL)::KanMX*

1851	S288C	*MATa, ura3-52, leu2Δ1, trp1Δ63, his3Δ200, lys2ΔBgl, hom3-10, ade2Δ1, ade8, arg4Δ, sml1Δ::TRP1 bar1Δ::HIS3, Top2-HA (1-1220aa)::KanMX*
1852	S288C	*MATa, ura3-52, leu2Δ1, trp1Δ63, his3Δ200, lys2ΔBgl, hom3-10, ade2Δ1, ade8, arg4Δ, sml1Δ::TRP1 bar1Δ::HIS3, Top2-HA (1-1230aa)::KanMX*
1853	S288C	*MATa, ura3-52, leu2Δ1, trp1Δ63, his3Δ200, lys2ΔBgl, hom3-10, ade2Δ1, ade8, arg4Δ, sml1Δ::TRP1 bar1Δ::HIS3, Top2-HA (1-1240aa)::KanMX*
1854	S288C	*MATa, ura3-52, leu2Δ1, trp1Δ63, his3Δ200, lys2ΔBgl, hom3-10, ade2Δ1, ade8, arg4Δ, sml1Δ::TRP1 bar1Δ::HIS3, Top2-HA (1-1250aa)::KanMX*
1855	S288C	*MATa, ura3-52, leu2Δ1, trp1Δ63, his3Δ200, lys2ΔBgl, hom3-10, ade2Δ1, ade8, arg4Δ, sml1Δ::TRP1 bar1Δ::HIS3, Top2-HA (1-1260aa)::KanMX*
1856	S288C	*MATa, ura3-52, leu2Δ1, trp1Δ63, his3Δ200, lys2ΔBgl, hom3-10, ade2Δ1, ade8, arg4Δ, sml1Δ::TRP1 bar1Δ::HIS3, Top2-HA (1-1270aa)::KanMX*
1857	S288C	*MATa, ura3-52, leu2Δ1, trp1Δ63, his3Δ200, lys2ΔBgl, hom3-10, ade2Δ1, ade8, arg4Δ, sml1Δ::TRP1 bar1Δ::HIS3, Top2-HA (1-1320aa)::KanMX*
1858	S288C	*MATa, ura3-52, leu2Δ1, trp1Δ63, his3Δ200, lys2ΔBgl, hom3-10, ade2Δ1, ade8, arg4Δ, sml1Δ::TRP1 bar1Δ::HIS3, Top2-HA (1-1370aa)::KanMX*
2149	S288C	*MATa, ura3-52, trp1-63, his3-200, bar1Δ::HIS3, pADH1-EXO1::KanMX6*
2150	S288C	*MATa, ura3-52, trp1-63, his3-200, bar1Δ::HIS3, pADH1-EXO1::G419*
2151	S288C	*MATa, ura3-52, leu2Δ1, trp1Δ63, his3Δ200, lys2ΔBgl, hom3-10, ade2Δ1, ade8, arg4Δ mec1Δ::URA3, rtt109Δ::KanMX6*
2152	S288C	*MATa, ura3-52, leu2Δ1, trp1Δ63, his3Δ200, lys2ΔBgl, hom3-10, ade2Δ1, ade8, arg4Δ mec1Δ::URA3, rtt109Δ::KanMX6*
2153	S288C	*MATa, ura3-52, leu2Δ1, trp1Δ63, his3Δ200, lys2ΔBgl, hom3-10, ade2Δ1, ade8, arg4Δ mec1Δ::URA3, gcn5Δ::KanMX6*
2154	S288C	*MATa, ura3-52, leu2Δ1, trp1Δ63, his3Δ200, lys2ΔBgl, hom3-10, ade2Δ1, ade8, arg4Δ mec1Δ::URA3, gcn5Δ::KanMX6*
2155	S288C	*MATa, ura3-52, leu2Δ1, trp1Δ63, his3Δ200, lys2ΔBgl, hom3-10, ade2Δ1, ade8, arg4Δ, sml1Δ::TRP1, rtt109Δ::KanMX6*
2156	S288C	*MATa, ura3-52, leu2Δ1, trp1Δ63, his3Δ200, lys2ΔBgl, hom3-10, ade2Δ1, ade8, arg4Δ, sml1Δ::TRP1, rtt109Δ::KanMX6*

2157	S288C	*MATa, ura3-52, leu2Δ1, trp1Δ63, his3Δ200, lys2ΔBgl, hom3-10, ade2Δ1, ade8, arg4Δ, sml1Δ::TRP1, gcn5Δ::KanMX6*
2158	S288C	*MATa, ura3-52, leu2Δ1, trp1Δ63, his3Δ200, lys2ΔBgl, hom3-10, ade2Δ1, ade8, arg4Δ, sml1Δ::TRP1, gcn5Δ:KanMX6*
2159	S288C	*MATa, ura3-52, leu2Δ1, trp1Δ63, his3Δ200, lys2ΔBgl, hom3-10, ade2Δ1, ade8, arg4Δ, sml1Δ::TRP1 bar1Δ::HIS3, rad53Δ::KanMX6*
2160	S288C	*MATa, ura3-52, leu2Δ1, trp1Δ63, his3Δ200, lys2ΔBgl, hom3-10, ade2Δ1, ade8, arg4Δ, sml1Δ::TRP1 bar1Δ::HIS3, rad53Δ::KanMX6*
2185	S288C	*MATa, ura3-52, trp1-63, his3-200, bar1Δ::HIS3, EXO1-HA::TRP*
2186	S288C	*MATa, ura3-52, trp1-63, his3-200, bar1Δ::HIS3, EXO1-HA::TRP*
2187	S288C	*MATa, ura3-52, trp1-63, his3-200, bar1Δ::HIS3, pADH1(KanMX6)-EXO1-HA::TRP*
2188	S288C	*MATa, ura3-52, trp1-63, his3-200, bar1Δ::HIS3, pADH1(KanMX6)-EXO1-HA::TRP*
2189	S288C	*MATa, ura3-52, leu2Δ1, trp1Δ63, his3Δ200, lys2ΔBgl, hom3-10, ade2Δ1, ade8, arg4Δ, sml1Δ::TRP1 bar1Δ::HIS3, Dpb11-6xHis-3xHA::LEU2, Slx4 (S486A)-3xFLAG::natMX, pph3Δ::KanMX6*
2190	S288C	*MATa, ura3-52, leu2Δ1, trp1Δ63, his3Δ200, lys2ΔBgl, hom3-10, ade2Δ1, ade8, arg4Δ, sml1Δ::TRP1 bar1Δ::HIS3, Dpb11-6xHis-3xHA::LEU2, Slx4(S486A)-3xFLAG::natMX, pph3Δ::KanMX6*
2191	S288C	*MATa, ura3-52, leu2Δ1, trp1Δ63, his3Δ200, lys2ΔBgl, hom3-10, ade2Δ1, ade8, arg4Δ, sml1Δ::TRP1 bar1Δ::HIS3, pph3Δ::KanMX6*
2192	S288C	*MATa, ura3-52, leu2Δ1, trp1Δ63, his3Δ200, lys2ΔBgl, hom3-10, ade2Δ1, ade8, arg4Δ, sml1Δ::TRP1 bar1Δ::HIS3, pph3Δ::KanMX6*
2193	S288C	*MATa, ura3-52, leu2Δ1, trp1Δ63, his3Δ200, lys2ΔBgl, hom3-10, ade2Δ1, ade8, arg4Δ, sml1Δ::TRP1 bar1Δ::HIS3, Dpb11-6xHis-3xHA::LEU2, Slx4(7MUT)-3xFLAG::natMX, pph3Δ::KanMX6*
2194	S288C	*MATa, ura3-52, leu2Δ1, trp1Δ63, his3Δ200, lys2ΔBgl, hom3-10, ade2Δ1, ade8, arg4Δ, sml1Δ::TRP1 bar1Δ::HIS3, Dpb11-6xHis-3xHA::LEU2, Slx4(7MUT)-3xFLAG::natMX, pph3Δ::KanMX6*
2195	S288C	*MATa, ura3-52, leu2Δ1, trp1Δ63, his3Δ200, lys2ΔBgl, hom3-10, ade2Δ1, ade8, arg4Δ, sml1Δ::TRP1 bar1Δ::HIS3, rad53Δ::URA3, pph3Δ::KanMX6*

2196	S288C	*MATa, ura3-52, leu2Δ1, trp1Δ63, his3Δ200, lys2ΔBgl, hom3-10, ade2Δ1, ade8, arg4Δ, sml1Δ::TRP1 bar1Δ::HIS3, rad53Δ::URA3, pph3Δ::KanMX6*
2197	S288C	*MATa, ura3-52, leu2Δ1, trp1Δ63, his3Δ200, lys2ΔBgl, hom3-10, ade2Δ1, ade8, arg4Δ, sml1Δ::TRP1 bar1Δ::HIS3, pADH1-TOP1::KanMX6*
2198	S288C	*MATa, ura3-52, leu2Δ1, trp1Δ63, his3Δ200, lys2ΔBgl, hom3-10, ade2Δ1, ade8, arg4Δ, sml1Δ::TRP1 bar1Δ::HIS3, pADH1-TOP1::KanMX6*
2199	S288C	*MATa, ura3-52, leu2Δ1, trp1Δ63, his3Δ200, lys2ΔBgl, hom3-10, ade2Δ1, ade8, arg4Δ, sml1Δ::TRP1 bar1Δ::HIS3, slx4Δ::URA3, pADH1-TOP1::KanMX6*
2200	S288C	*MATa, ura3-52, leu2Δ1, trp1Δ63, his3Δ200, lys2ΔBgl, hom3-10, ade2Δ1, ade8, arg4Δ, sml1Δ::TRP1 bar1Δ::HIS3, slx4Δ::URA3, pADH1-TOP1::KanMX6*
2201	S288C	*MATa, ura3-52, leu2Δ1, trp1Δ63, his3Δ200, lys2ΔBgl, hom3-10, ade2Δ1, ade8, arg4Δ, sml1Δ::TRP1 bar1Δ::HIS3, slx4Δ::URA3, top1Δ::KanMX6*
2202	S288C	*MATa, ura3-52, leu2Δ1, trp1Δ63, his3Δ200, lys2ΔBgl, hom3-10, ade2Δ1, ade8, arg4Δ, sml1Δ::TRP1 bar1Δ::HIS3, slx4Δ::URA3, top1Δ::KanMX6*
2285	S288C	*MATa, ura3-52, leu2Δ1, trp1Δ63, his3Δ200, lys2ΔBgl, hom3-10, ade2Δ1, ade8, arg4Δ, sml1Δ::TRP1 bar1Δ::HIS3, sgs1Δ::URA3*
2287	S288C	*MATa, ura3-52, leu2Δ1, trp1Δ63, his3Δ200, lys2ΔBgl, hom3-10, ade2Δ1, ade8, arg4Δ, sml1Δ::TRP1 bar1Δ::HIS3, pph3Δ::KanMX6, sgs1Δ::URA3*
2288	S288C	*MATa, SLD3-m21D-3xFLAG::HYG*
2289	S288C	*MATa, sld3-25A-3XFLAG::HYG (Y153F, Y154F, S370A, T373A, T451A, S456A, S463A, S466A, S493A, T495A, S497A, S505A, T507A, S521A, S534A, T582A, S591A, T607A, T609A, S618A, T631A, T638A, S639A, T643A, T644A, T646A) his3Δ leu2Δ ura3Δ met15Δ*
2290	S288C	*MATa his3Δ1 leu2Δ0, met15Δ0, ura3Δ, dbf4-m25::LEU2 dbf4Δ::KanMX6*
2291	S288C	*MATa his3Δ1 leu2Δ0, met15Δ0, ura3Δ, sld3-m25-3xFLAG::HYG dbf4-m25A::LEU2 dbf4Δ::KanMX6*
2292	S288C	*MATa his3Δ1 leu2Δ0, met15Δ0, ura3Δ sld3-3xFLAG::HYG*
2293	S288C	*MATa, ura3-52, trp1-63, his3-200, bar1Δ::HIS3, RAD9::rad9(S462A T474A)-HA::KanMX6, pph3Δ::URA3*
2294	S288C	*MATa, ura3-52, trp1-63, his3-200, bar1Δ::HIS3, Rad9-3xHA::TRP1, pph3Δ::URA3*

2295	S288C	*MATa, ura3-52, leu2Δ1, trp1Δ63, his3Δ200, lys2ΔBgl, hom3-10, ade2Δ1, ade8, arg4Δ, sml1Δ::TRP1 bar1Δ::HIS3 rad53Δ::URA3, pph3Δ::KanMX6*
2296	S288C	*MATa, ura3-52, leu2Δ1, trp1Δ63, his3Δ200, lys2ΔBgl, hom3-10, ade2Δ1, ade8, arg4Δ, sml1Δ::TRP1 bar1Δ::HIS3 rad53Δ::URA3, pph3Δ::KanMX6*
2301	S288C	*MATa, SLD3-m21D-3xFLAG::HYG, pph3Δ::KanMX6*
2302	S288C	*MATa, sld3-25A-3XFLAG::HYG (Y153F, Y154F, S370A, T373A, T451A, S456A, S463A, S466A, S493A, T495A, S497A, S505A, T507A, S521A, S534A, T582A, S591A, T607A, T609A, S618A, T631A, T638A, S639A, T643A, T644A, T646A, his3Δ leu2Δ ura3Δ met15Δ, pph3Δ::URA3*
2303	S288C	*MATa his3Δ1 leu2Δ0, met15Δ0, ura3Δ, dbf4-m25::LEU2 dbf4Δ::KanMX6, pph3Δ::URA3*
2304	S288C	*MATa his3Δ1 leu2Δ0, met15Δ0, ura3Δ, sld3-m25-3xFLAG::HYG dbf4-m25A::LEU2 dbf4Δ::KanMX6, pph3Δ::URA3*
2305	S288C	*MATa his3Δ1 leu2Δ0, met15Δ0, ura3Δ sld3-3xFLAG::HYG, pph3Δ::KanMX6*
2316	S288C	*MATa, ura3-52, leu2Δ1, trp1Δ63, his3Δ200, lys2ΔBgl, hom3-10, ade2Δ1, ade8, arg4Δ, sml1Δ::TRP1 bar1Δ::HIS3, Rad27-HA::KanMX6*
2317	S288C	*MATa, ura3-52, leu2Δ1, trp1Δ63, his3Δ200, lys2ΔBgl, hom3-10, ade2Δ1, ade8, arg4Δ, sml1Δ::TRP1 bar1Δ::HIS3, Smc3-HA::KanMX6*
2318	S288C	*MATa, ura3-52, leu2Δ1, trp1Δ63, his3Δ200, lys2ΔBgl, hom3-10, ade2Δ1, ade8, arg4Δ, sml1Δ::TRP1 bar1Δ::HIS3, Sae2-HA::KanMX6*
2321	S288C	*MATa, ura3-52, trp1-63, his3-200, bar1Δ::HIS3, pADH1-(KanMX6)-EXO1-HA::TRP*
2356	S288C	*MATa, ura3-52, leu2Δ1, trp1Δ63, his3Δ200, lys2ΔBgl, hom3-10, ade2Δ1, ade8, arg4Δ, sml1Δ::TRP1 bar1Δ::HIS3, mus81Δ::URA3*
2357	S288C	*MATa, ura3-52, leu2Δ1, trp1Δ63, his3Δ200, lys2ΔBgl, hom3-10, ade2Δ1, ade8, arg4Δ, sml1Δ::TRP1 bar1Δ::HIS3, pph3Δ::KanMX6, mus81Δ::URA3*
2358	S288C	*ura3-52/ura3-52, trp1-63/trp1-63, his3-200/his3-200, MUS81/mus81::Δ::URA3*
2359	S288C	*ura3-52/ura3-52, trp1-63/trp1-63, his3-200/his3-200, MUS81/mus81Δ::URA3, PPH3/pph3Δ::HIS3*
2360	S288C	*MATa, ura3-52, trp1-63, his3-200, bar1Δ::HIS3, mus81Δ::natMX*
2361	S288C	*MATa, ura3-52, trp1-63, his3-200, bar1Δ::HIS3, pph3Δ::natMX*

2362	S288C	*MATa, ura3-52, leu2Δ1, trp1Δ63, his3Δ200, lys2ΔBgl, hom3-10, ade2Δ1, ade8, arg4Δ, sml1Δ::TRP1 bar1Δ::HIS3, dot1Δ::URA3*
2363	S288C	*MATa, ura3-52, leu2Δ1, trp1Δ63, his3Δ200, lys2ΔBgl, hom3-10, ade2Δ1, ade8, arg4Δ, sml1Δ::TRP1 bar1Δ::HIS3, pph3Δ::KanMX6, dot1Δ::URA3*
2364	S288C	*MATa, ura3-52, trp1-63, his3-200, bar1Δ::HIS3, pph3Δ::URA3*
2409	S288C	*MATa, ura3-52, leu2Δ1, trp1Δ63, his3Δ200, lys2ΔBgl, hom3-10, ade2Δ1, ade8, arg4Δ, sml1Δ::TRP1 bar1Δ::HIS3, pph3Δ::KanMX6, ptc2Δ::URA3*
2410	S288C	*MATa, ura3-52, leu2Δ1, trp1Δ63, his3Δ200, lys2ΔBgl, hom3-10, ade2Δ1, ade8, arg4Δ, sml1Δ::TRP1 bar1Δ::HIS3, pph3Δ::KanMX6, ptc2Δ::URA3*
2411	S288C	*MATa, ura3-52, leu2Δ1, trp1Δ63, his3Δ200, lys2ΔBgl, hom3-10, ade2Δ1, ade8, arg4Δ, sml1Δ::TRP1 bar1Δ::HIS3, pph3Δ::KanMX6, ptc2Δ::URA3, ptc3Δ::natMX*
2412	S288C	*MATa, ura3-52, leu2Δ1, trp1Δ63, his3Δ200, lys2ΔBgl, hom3-10, ade2Δ1, ade8, arg4Δ, sml1Δ::TRP1 bar1Δ::HIS3, pph3Δ::KanMX6, ptc2Δ::URA3, ptc3Δ::natMX*
2413	S288C	*ura3-52/ura3-52, trp1-63/trp1-63, his3-200/his3-200, MUS81/mus81Δ::URA3*
2414	S288C	*ura3-52/ura3-52, trp1-63/trp1-63, his3-200/his3-200, MUS81/mus81Δ::URA3, PPH3/pph3Δ::HIS3*
2415	S288C	*ura3-52/ura3-52, trp1-63/trp1-63, his3-200/his3-200, MUS81/mus81Δ::URA3, PPH3/pph3Δ::HIS3, SGS1/sgs1Δ::KanMX6*
2416	S288C	*MATα ura3-52, trp1-63, his3-200*
2417	S288C	*MATa, ura3-52, trp1-63, his3-200, mus81Δ::URA3.*
2418	S288C	*MATa, ura3-52, trp1-63, his3-200, pph3Δ::HIS3*
2419	S288C	*MATa, ura3-52, trp1-63, his3-200, sgs1Δ::KanMX*
2420	S288C	*MATalpha, ura3-52, trp1-63, his3-200, mus81Δ::URA3, pph3Δ:HIS3*
2421	S288C	*MATalpha, ura3-52, trp1-63, his3-200, sgs1Δ::KanMX6, pph3Δ::HIS3*
2422	S288C	*MATa, ura3-52, trp1-63, his3-200, bar1Δ::HIS3, pph3Δ::URA3*
2423	S288C	*MATa, ura3-52, trp1-63, his3-200, bar1Δ::HIS3, pph3Δ::URA3*
2424	S288C	*MATa, ura3-52, leu2Δ1, trp1Δ63, his3Δ200, lys2ΔBgl, hom3-10, ade2Δ1, ade8, arg4Δ, sml1Δ::TRP1 bar1Δ::HIS3, MUS81/mus81Δ::URA3*

2425	S288C	*MATa, ura3-52, leu2Δ1, trp1Δ63, his3Δ200, lys2ΔBgl, hom3-10, ade2Δ1, ade8, arg4Δ, sml1Δ::TRP1 bar1Δ::HIS3, pph3Δ::KanMX6, mus81Δ::URA3*
2426	S288C	*MATa, ura3-52, trp1-63, his3-200, bar1Δ::HIS3, mus81Δ::natMX*
2427	S288C	*MATa, ura3-52, trp1-63, his3-200, bar1Δ::HIS3, mus81Δ::natMX*
2428	S288C	*MATa, ura3-52, trp1-63, his3-200, bar1Δ::HIS3, pph3Δ::natMX*
2429	S288C	*MATa, ura3-52, trp1-63, his3-200, bar1Δ::HIS3, pph3Δ::natMX*
2430	S288C	*MATa, ura3-52, leu2Δ1, trp1Δ63, his3Δ200, lys2ΔBgl, hom3-10, ade2Δ1, ade8, arg4Δ, sml1Δ::TRP1 bar1Δ::HIS3, DOT1/dot1Δ::URA3*
2431	S288C	*MATa, ura3-52, leu2Δ1, trp1Δ63, his3Δ200, lys2ΔBgl, hom3-10, ade2Δ1, ade8, arg4Δ, sml1Δ::TRP1 bar1Δ::HIS3, DOT1/dot1Δ::URA3*
2432	S288C	*MATa, ura3-52, leu2Δ1, trp1Δ63, his3Δ200, lys2ΔBgl, hom3-10, ade2Δ1, ade8, arg4Δ, sml1Δ::TRP1 bar1Δ::HIS3, pph3Δ::KanMX6, dot1Δ::URA3*
2433	S288C	*MATa, ura3-52, leu2Δ1, trp1Δ63, his3Δ200, lys2ΔBgl, hom3-10, ade2Δ1, ade8, arg4Δ, sml1Δ::TRP1 bar1Δ::HIS3, pph3Δ::KanMX6, dot1Δ::URA3*
2434	S288C	*MATa, ura3-52, trp1-63, his3-200, bar1Δ::HIS3, pADH1(KanMX6)-MUS81*
2435	S288C	*MATa, ura3-52, trp1-63, his3-200, bar1Δ::HIS3, pph3Δ::URA3, pADH1(KanMX6)-MUS81*
2436	S288C	*MATa, ura3-52, trp1-63, his3-200, bar1Δ::HIS3, pADH1(natMX)-MMS4*
2437	S288C	*MATa, ura3-52, trp1-63, his3-200, bar1Δ::HIS3, pph3Δ::URA3, pADH1(natMX)-MMS4*
2438	S288C	*MATa, ura3-52, trp1-63, his3-200, bar1Δ::HIS3, pADH1(KanMX6)-MUS81, pADH1(natMX)-MMS4*
2439	S288C	*MATa, ura3-52, trp1-63, his3-200, bar1Δ::HIS3, pADH1(KanMX6)-MUS81, pph3Δ::URA3, pADH1(natMX)-MMS4*
2440	S288C	*MATa, ura3-52, trp1-63, his3-200, bar1Δ::HIS3, pADH1(natMX)-MUS81*
2441	S288C	*MATa, ura3-52, trp1-63, his3-200, bar1Δ::HIS3, pph3Δ::URA3, pADH1(natMX)-MUS81*
2442	S288C	*MATa, ura3-52, leu2Δ1, trp1Δ63, his3Δ200, lys2ΔBgl, hom3-10, ade2Δ1, ade8, arg4Δ, sml1Δ::TRP1 bar1Δ::HIS3, Slx4-FLAG::LEU, Mus81-HA::natMX*
2443	S288C	*ura3-52/ura3-52, trp1-63/trp1-63, his3-200/his3-200 Slx4/slx4Δ:HIS3 Rtt107/rtt107Δ::URA3 Rad53/rad53(R605A)::KanMX6, PPH3/pph3Δ::natMX*

2499	S288C	*MATa, ura3-52, trp1-63, his3-200, bar1Δ::HIS3, rad53(R605A)::KanMX6*
2500	S288C	*MATa, ura3-52, trp1-63, his3-200, bar1Δ::HIS3, pph3Δ::URA3, rad53(R605A)::KanMX6*
2501	S288C	*MATa, ura3-52, trp1-63, his3-200, bar1Δ::HIS3, pph3Δ::URA3, rad53(R605A)::KanMX6*
2502	S288C	*MATa, ura3-52, trp1-63, his3-200, bar1Δ::HIS3, pph3Δ::URA3, ptc3Δ::natMX*
2503	S288C	*MATa, ura3-52, trp1-63, his3-200, bar1Δ::HIS3, pph3Δ::URA3, rad53(R605A)::KanMX6, ptc3Δ::natMX*
2504	S288C	*MATa, ura3-52, trp1-63, his3-200, bar1Δ::HIS3, rad51Δ::natMX*
2505	S288C	*MATa, ura3-52, trp1-63, his3-200, bar1Δ::HIS3, pph3Δ::URA3, rad51Δ::natMX*
2506	S288C	*MATa, ura3-52, trp1-63, his3-200, bar1Δ::HIS3, rad52Δ::natMX*
2507	S288C	*MATa, ura3-52, trp1-63, his3-200, bar1Δ::HIS3, pph3Δ::URA3, rad52Δ::natMX*
2508	S288C	*MATa, ura3-52, trp1-63, his3-200, bar1Δ::HIS3, rdh54Δ::natMX*
2509	S288C	*MATa, ura3-52, trp1-63, his3-200, bar1Δ::HIS3, pph3Δ::URA3, rdh54Δ::natMX*
2510	S288C	*MATa, ura3-52, trp1-63, his3-200, bar1Δ::HIS3, xrs2Δ::natMX*
2511	S288C	*MATa, ura3-52, trp1-63, his3-200, bar1Δ::HIS3, pph3Δ::URA3, xrs2Δ::natMX*
2512	S288C	*MATa, ura3-52, trp1-63, his3-200, bar1Δ::HIS3, sae2Δ::natMX*
2513	S288C	*MATa, ura3-52, trp1-63, his3-200, bar1Δ::HIS3, pph3Δ::URA3, sae2Δ::natMX*
2514	S288C	*MATa, ura3-52, trp1-63, his3-200, bar1Δ::HIS3, tel1Δ::natMX*
2515	S288C	*MATa, ura3-52, trp1-63, his3-200, bar1Δ::HIS3, pph3Δ::URA3, tel1Δ::natMX*
2516	S288C	*MATa, ura3-52, trp1-63, his3-200, bar1Δ::HIS3, exo1Δ::KanMX6*
2517	S288C	*MATa, ura3-52, trp1-63, his3-200, bar1Δ::HIS3, pph3Δ::URA3, exo1Δ::KanMX6*
2518	S288C	*MATa, ura3-52, trp1-63, his3-200, bar1Δ::HIS3, pph3Δ::URA3, ptc3Δ::natMX, ptc2Δ::TRP1*
2519	S288C	*MATa, ura3-52, trp1-63, his3-200, bar1Δ::HIS3, pph3Δ::URA3, rad53(R605A)::KanMX6, ptc3Δ::natMX, ptc2Δ::TRP1*
2520	S288C	*MATa, ura3-52, trp1-63, his3-200, bar1Δ::HIS3, pph3Δ::URA3, rad53(R605A)::KanMX6, ptc3Δ::natMX, ptc2Δ::TRP1*

2521	S288C	*MATa, ura3-52, trp1-63, his3-200, bar1Δ::HIS3, pph3Δ::URA3, ptc3Δ::natMX, ptc2Δ::TRP1*
2522	S288C	*MATa, ura3-52, leu2Δ1, trp1Δ63, his3Δ200, lys2ΔBgl, hom3-10, ade2Δ1, ade8, arg4Δ, sml1Δ::TRP1 bar1Δ::HIS3, pph3Δ::natMX*
2523	S288C	*MATa, ura3-52, leu2Δ1, trp1Δ63, his3Δ200, lys2ΔBgl, hom3-10, ade2Δ1, ade8, arg4Δ, sml1Δ::TRP1 bar1Δ::HIS3, pph3Δ::natMX*
2524	S288C	*MATa, ura3-52, leu2Δ1, trp1Δ63, his3Δ200, lys2ΔBgl, hom3-10, ade2Δ1, ade8, arg4Δ, sml1Δ::TRP1 bar1Δ::HIS3, rad53(R605A)::KanMX6*
2525	S288C	*MATa, ura3-52, leu2Δ1, trp1Δ63, his3Δ200, lys2ΔBgl, hom3-10, ade2Δ1, ade8, arg4Δ, sml1Δ::TRP1 bar1Δ::HIS3, rad53(R605A)::KanMX6*
2526	S288C	*MATa, ura3-52, trp1-63, his3-200, bar1Δ::HIS3, dun1Δ::TRP1*
2527	S288C	*MATa, ura3-52, trp1-63, his3-200, bar1Δ::HIS3, pph3Δ::URA3, dun1Δ::TRP1*
2528	S288C	*MATa, ura3-52, leu2Δ1, trp1Δ63, his3Δ200, lys2ΔBgl, hom3-10, ade2Δ1, ade8, arg4Δ, sml1Δ::TRP1 bar1Δ::HIS3, pph3Δ::natMX, rad53(R605A)::KanMX6*
2529	S288C	*MATa, ura3-52, leu2Δ1, trp1Δ63, his3Δ200, lys2ΔBgl, hom3-10, ade2Δ1, ade8, arg4Δ, sml1Δ::TRP1 bar1Δ::HIS3, pph3Δ::natMX, rad53(R605A)::KanMX6*
2546	S288C	*MATa, ura3-52, trp1-63, his3-200, bar1Δ::HIS3, pph3Δ::KanMX6, ptc3Δ::natMX, ptc2Δ::TRP1*
2547	S288C	*MATa, ura3-52, trp1-63, his3-200, bar1Δ::HIS3, pph3Δ::KanMX6, ptc3Δ::natMX, ptc2Δ::TRP1*
2548	S288C	*MATa, ura3-52, leu2Δ1, trp1Δ63, his3Δ200, lys2ΔBgl, hom3-10, ade2Δ1, ade8, arg4Δ, sml1Δ::TRP1 bar1Δ::HIS3, pph3Δ::natMX, rad53(R605A)::KanMX6, ptc2Δ::URA3*
2549	S288C	*ura3-52/ura3-52, trp1-63/trp1-63, his3-200/his3-200, MUS81/mus81Δ::URA3. PPH3/pph3Δ::HIS3, RAD53/rad53(R605A)::KanMX6*
2550	S288C	*ura3-52/ura3-52, trp1-63/trp1-63, his3-200/his3-200, MUS81/mus81Δ::URA3. PPH3/pph3Δ::HIS3, RAD53/rad53(R605A)::KanMX6*
2589	S288C	*ura3-52, trp1-63, his3-200, sml1Δ::TRP1, pph3Δ::natMX*
2590	S288C	*ura3-52, trp1-63, his3-200, sml1Δ::TRP1, pph3Δ::natMX*
2591	S288C	*ura3-52, trp1-63, his3-200, sml1Δ::TRP1, fun30Δ::KanMX6, pph3Δ::natMX*
2592	S288C	*ura3-52, trp1-63, his3-200, sml1Δ::TRP1, fun30Δ::KanMX6, pph3Δ::natMX*

2593	S288C	*ura3-52, trp1-63, his3-200, sml1Δ::TRP1, exo1Δ::URA3, pph3Δ::natMX*
2594	S288C	*ura3-52, trp1-63, his3-200, sml1Δ::TRP1, exo1Δ::URA3, pph3Δ::natMX*
2595	S288C	*ura3-52, trp1-63, his3-200, sml1Δ::TRP1, exo1Δ::URA3, fun30Δ::KanMX6, pph3Δ::natMX*
2596	S288C	*ura3-52, trp1-63, his3-200, sml1Δ::TRP1, exo1Δ::URA3, fun30Δ::KanMX6, pph3Δ::natMX*
2597	S288C	*ura3-52, trp1-63, his3-200*
2598	S288C	*ura3-52, trp1-63, his3-200, pph3Δ::HIS3*
2599	S288C	*ura3-52, trp1-63, his3-200, mus81Δ::URA3*
2600	S288C	*ura3-52, trp1-63, his3-200, rad53(R605A)::KanMX6*
2601	S288C	*ura3-52, trp1-63, his3-200, pph3Δ::HIS3, rad53(R605A)::KanMX6*
2602	S288C	*ura3-52, trp1-63, his3-200, pph3Δ::HIS3, mus81Δ::URA3*
2603	S288C	*ura3-52, trp1-63, his3-200, mus81Δ::URA3, rad53(R605A)::KanMX6*
2604	S288C	*ura3-52, trp1-63, his3-200, mus81Δ::URA3, rad53(R605A)::KanMX6*
2605	S288C	*ura3-52, trp1-63, his3-200, mus81Δ::URA3, rad53(R605A)::KanMX6, pph3Δ::natMX*
2606	S288C	*ura3-52, trp1-63, his3-200, mus81Δ::URA3, rad53(R605A)::KanMX6, pph3Δ::natMX*
2607	S288C	*ura3-52, trp1-63, his3-200, mus81Δ::URA3, rad53(R605A)::KanMX6, pph3Δ::HIS3*
2608	S288C	*ura3-52, trp1-63, his3-200, mus81Δ::URA3, rad53(R605A)::KanMX6, pph3Δ::HIS3*
2635	S288C	*MATa, ura3-52, leu2∆1, trp1∆63, his3∆200, lys2∆Bgl, hom3-10, ade2∆1, ade8, arg4∆, sml1∆::TRP1, bar1∆::HIS3, psy4∆::KanMX6*
2636	S288C	*MATa, ura3-52, leu2∆1, trp1∆63, his3∆200, lys2∆Bgl, hom3-10, ade2∆1, ade8, arg4∆, sml1∆::TRP1, bar1∆::HIS3, psy4∆::KanMX6*
2637	S288C	*MATa, ura3-52, leu2∆1, trp1∆63, his3∆200, lys2∆Bgl, hom3-10, ade2∆1, ade8, arg4∆, sml1∆::TRP1, bar1∆::HIS3, pph3Δ::natMX, psy4∆::KanMX6*
2638	S288C	*MATa, ura3-52, leu2∆1, trp1∆63, his3∆200, lys2∆Bgl, hom3-10, ade2∆1, ade8, arg4∆, sml1∆::TRP1, bar1∆::HIS3, pph3Δ::natMX, psy4∆::KanMX6*
2639	W303	*MATa ade2-1 trp1-1 can1-100 leu2-3, 112 his3-11, 15 ura3-1 GAL+ psi+ ssd1-d2 RAD5+, pph3∆::TRP1*
2640	W303	*MATa hta1-S129A hta2-S129A leu2-3, 112 his3-11, 15 ade2-1 ura3-1 trp1-1 can1-100 RAD5+ , pph3∆::TRP1*

2641	W303	*MATa hta1-S129A hta2-S129A leu2-3, 112 his3-11, 15 ade2-1 ura3-1 trp1-1 can1-100 RAD5+, pph3Δ::TRP1*
2642	W303	*MATa ade2-1 trp1-1 can1-100 leu2-3, 112 his3-11, 15 ura3-1 GAL+ psi+ ssd1-d2 RAD5+, slx4Δ::HIS3, pph3Δ::natMX*
2643	W303	*MATa ade2-1 trp1-1 can1-100 leu2-3, 112 his3-11, 15 ura3-1 GAL+ psi+ ssd1-d2 RAD5+, slx4Δ::HIS3, pph3Δ::natMX*
2644	W303	*MATa hta1-S129A hta2-S129A leu2-3, 112 his3-11, 15 ade2-1 ura3-1 trp1-1 can1-100 RAD5+ slx4Δ::HIS3, pph3Δ::TRP1*
2645	S288C	*ura3-52, trp1-63, his3-200, mus81Δ::HIS3*
2646	S288C	*MATa, ura3-52, leu2Δ1, trp1Δ63, his3Δ200, lys2ΔBgl, hom3-10, ade2Δ1, ade8, arg4Δ, sml1Δ::TRP1, bar1Δ::HIS3, mrc1Δ::KanMX6*
2647	S288C	*MATa, ura3-52, leu2Δ1, trp1Δ63, his3Δ200, lys2ΔBgl, hom3-10, ade2Δ1, ade8, arg4Δ, sml1Δ::TRP1, bar1Δ::HIS3, mrc1Δ::KanMX6*
2648	S288C	*MATa, ura3-52, leu2Δ1, trp1Δ63, his3Δ200, lys2ΔBgl, hom3-10, ade2Δ1, ade8, arg4Δ, sml1Δ::TRP1, bar1Δ::HIS3, pph3Δ::natMX, mrc1Δ::KanMX6*
2649	S288C	*MATa, ura3-52, leu2Δ1, trp1Δ63, his3Δ200, lys2ΔBgl, hom3-10, ade2Δ1, ade8, arg4Δ, sml1Δ::TRP1, bar1Δ::HIS3, pph3Δ::natMX, mrc1Δ::KanMX6*
2657	S288C	*ura3-52, trp1-63, his3-200, sgs1Δ::KanMX6*
2658	S288C	*ura3-52, trp1-63, his3-200, sgs1Δ::KanMX6*
2659	S288C	*ura3-52, trp1-63, his3-200, pph3Δ::HIS3, sgs1Δ::KanMX6*
2660	S288C	*ura3-52, trp1-63, his3-200, pph3Δ::HIS3, sgs1Δ::KanMX6*
2661	S288C	*MATa, ura3-52, trp1-63, his3-200, bar1Δ::HIS3, slx4Δ::KanMX6*
2662	S288C	*MATa, ura3-52, trp1-63, his3-200, bar1Δ::HIS3, slx4Δ::KanMX6*
2663	S288C	*MATa, ura3-52, trp1-63, his3-200, bar1Δ::HIS3, pph3Δ::URA3, slx4Δ::KanMX6*
2664	S288C	*MATa, ura3-52, trp1-63, his3-200, bar1Δ::HIS3, pph3Δ::URA3, slx4Δ::KanMX6*
2669	S288C	*MATa, ura3-52, trp1-63, his3-200, bar1Δ::HIS3, psy4Δ::natMX*
2670	S288C	*MATa, ura3-52, trp1-63, his3-200, bar1Δ::HIS3, psy4Δ::natMX*
2671	S288C	*MATa, ura3-52, trp1-63, his3-200, bar1Δ::HIS3, pph3Δ::URA3, psy4Δ::natMX*

2672	S288C	*MATa, ura3-52, trp1-63, his3-200, bar1Δ::HIS3, slx4Δ::KanMX6, psy4Δ::TRP1*
2673	S288C	*MATa, ura3-52, trp1-63, his3-200, bar1Δ::HIS3, slx4Δ::KanMX6, psy4Δ::TRP1*
2674	S288C	*MATa, ura3-52, trp1-63, his3-200, bar1Δ::HIS3, pph3Δ::URA3, slx4Δ::KanMX6, psy4Δ::natMX*
2681	S288C	*ura3-52/ura3-52, trp1-63/trp1-63, his3-200/his3-200, PPH3/pph3Δ::HIS3, SLX4/slx4(S486A)::KanMX6*
2682	S288C	*MATa, ura3-52, trp1-63, his3-200, pph3Δ::HIS3*
2683	S288C	*MATα, ura3-52, trp1-63, his3-200, sgs1Δ::KanMX6*
2684	S288C	*MATa, ura3-52, trp1-63, his3-200, pph3Δ::HIS3*
2685	S288C	*MATα, ura3-52, trp1-63, his3-200*
2686	S288C	*MATα, ura3-52, trp1-63, his3-200, pph3Δ::HIS3*
2687	S288C	*MATa, ura3-52, trp1-63, his3-200, mus81Δ::URA3.*
2688	S288C	*MATα, ura3-52, trp1-63, his3-200, pph3Δ::HIS3, mus81Δ::URA3*
2689	S288C	*MATa, ura3-52, trp1-63, his3-200, pph3Δ::HIS3, sgs1Δ::KanMX*
2690	S288C	*ura3-52/ura3-52, trp1-63/trp1-63, his3-200/his3-200, PPH3/pph3Δ::HIS3, SGS1/sgs1Δ::KanMX6*
2691	S288C	*ura3-52/ura3-52, trp1-63/trp1-63, his3-200/his3-200, PPH3/pph3Δhis, SLX4/slx4Δ::KanMX6*
2692	S288C	*ura3-52/ura3-52, trp1-63/trp1-63, his3-200/his3-200, PPH3/pph3ΔURA3, PTC2/ptc2Δ::TRP1, PTC3/ptc3Δ::natMX, SLX4/slx4Δ::KanMX6, BAR1/bar1Δ::HIS3*
2693	S288C	*ura3-52/ura3-52, trp1-63/trp1-63, his3-200/his3-200, PPH3/pph3Δ::URA3, PTC2/ptc2Δ::TRP1, PTC3/ptc3Δ::natMX, SLX4/slx4(S486A)::KanMX6, BAR1/bar1Δ::HIS3*
2706	S288C	*MATα_ura3-52, trp1-63, his3-200,*
2707	S288C	*MATα_ura3-52, trp1-63, his3-200, rad53(R605A)::KanMX6*
2708	S288C	*MATα_ura3-52, trp1-63, his3-200, pph3Δ::HIS3*
2709	S288C	*MATα_ura3-52, trp1-63, his3-200, mus81Δ::URA3 rad53(R605A)::KanMX6*
2710	S288C	*MATa_ura3-52, trp1-63, his3-200, mus81Δ::URA3. pph3Δ::HIS3, rad53(R605A)::KanMX*
2711	S288C	*MATα_ura3-52, trp1-63, his3-200, pph3Δ::HIS3, slx4Δ::URA3*
2712	S288C	*MATα_ura3-52, trp1-63, his3-200, pph3Δ::HIS3, slx4Δ::URA3*
2713	S288C	*ura3-52, trp1-63, his3-200, pph3Δ::HIS3, rad53(R605A)::KanMX6, slx4Δ::URA3*

2720	S288C	*ura3-52, trp1-63, his3-200*
2721	S288C	*ura3-52, trp1-63, his3-200, rad53(R605A)::KanMX6*
2722	S288C	*ura3-52, trp1-63, his3-200, pph3Δ::HIS3, slx4Δ:URA3*
2723	S288C	*ura3-52, trp1-63, his3-200, pph3Δ::HIS3, slx4Δ:URA3, rad53(R605A)::KanMX6*
2724	S288C	*ura3-52, trp1-63, his3-200, pph3Δ::HIS3, slx4Δ:URA3, rad53(R605A)::KanMX6*
2725	S288C	*MATa, ura3-52, trp1-63, his3-200, bar1Δ::HIS3, pph3Δ::URA3, slx4Δ::natMX*
2726	S288C	*MATa, ura3-52, trp1-63, his3-200, bar1Δ::HIS3, pph3Δ::URA3, slx4Δ::natMX*
2732	S288C	*MATa, ura3-52, trp1-63, his3-200, bar1∆::HIS3, rad53(R605A)::KanMX6*
2733	S288C	*MATa, ura3-52, trp1-63, his3-200, bar1Δ::HIS3, pph3Δ::URA3, slx4Δ::natMX, rad53(R605A)::KanMX6*
2738	S288C	*ura3-52, trp1-63, his3-200, pph3Δ::HIS3, mus81Δ::URA3, rad53(R605A)::KanMX*
2739	S288C	*ura3-52, trp1-63, his3-200, pph3Δ::HIS3, mus81Δ::URA3, rad53(R605A)::KanMX*
2740	S288C	*ura3-52, trp1-63, his3-200, bar1Δ::HIS3*
2741	S288C	*ura3-52, trp1-63, his3-200, ptc2∆::TRP1, ptc3∆::natMX, bar1Δ::HIS3*
2742	S288C	*ura3-52, trp1-63, his3-200, pph3Δ::URA3, bar1Δ::HIS3*
2743	S288C	*ura3-52, trp1-63, his3-200, slx4(S486A)::KanMX6, bar1Δ::HIS3*
2744	S288C	*ura3-52, trp1-63, his3-200, pph3Δ::URA3, ptc2∆::TRP1, ptc3∆::natMX, bar1Δ::HIS3*
2745	S288C	*ura3-52, trp1-63, his3-200, ptc2∆::TRP1, ptc3∆::natMX, slx4(S486A)::KanMX6, bar1Δ::HIS3*
2746	S288C	*ura3-52, trp1-63, his3-200, pph3ΔURA3, ptc2∆::TRP1, ptc3∆::natMX, slx4(S486A)::KanMX6, bar1Δ::HIS3*
2747	S288C	*ura3-52, trp1-63, his3-200, pph3ΔURA3, ptc2∆::TRP1, ptc3∆::natMX, slx4(S486A)::KanMX6, bar1Δ::HIS3*
2748	S288C	*ura3-52/ura3-52, trp1-63/trp1-63, his3-200/his3-200, PPH3/pph3Δ::URA3, ptc2∆::TRP1/ptc2∆::TRP1, PTC3/ptc3∆::natMX, slx4(S486A)::KanMX/slx4(S486A)::KanMX6, BAR1/bar1Δ::HIS3*
2749	S288C	*ura3-52/ura3-52, trp1-63/trp1-63, his3-200/his3-200, PPH3/pph3ΔURA3, ptc2∆::TRP1/ptc2∆::TRP1, ptc3∆::natMX/ptc3∆::natMX, SLX4/slx4∆::KanMX6, BAR1/bar1Δ::HIS3*
2750	S288C	*ura3-52/ura3-52, trp1-63/trp1-63, his3-200/his3-200, BAR1/bar1∆::HIS3, PPH3/pph3Δ::URA3, SLX4/slx4(S486A)::KanMX6*

2751	S288C	*ura3-52/ura3-52, trp1-63/trp1-63, his3-200/his3-200, bar1Δ::HIS3/bar1Δ::HIS3, PPH3/pph3Δ::URA3, SLX4/slx4Δ::KanMX6*
2752	S288C	*ura3-52/ura3-52, trp1-63/trp1-63, his3-200/his3-200, bar1Δ::HIS3/bar1Δ::HIS3, PPH3/pph3ΔURA3, SGS1/sgs1Δ::KanMX6, PTC3/ptc3ΔnatMX, PTC2/ptc2Δ::TRP1*
2786	S288C	*ura3-52/ura3-52, trp1-63/trp1-63, his3-200/his3-200, BAR1/bar1Δ::HIS3, PPH3/pph3Δ::URA3, SLX4/slx4(S486A)::KanMX6, SGS1/sgs1Δ::natMX*
2787	S288C	*ura3-52/ura3-52, trp1-63/trp1-63, his3-200/his3-200, BAR1/bar1Δ::HIS3, PPH3/pph3Δ::URA3, SLX4/slx4(S486A)::KanMX6, SGS1/sgs1Δ::natMX*
2788	S288C	*MATa_ura3-52, trp1-63, his3-200*
2789	S288C	*MATa_ura3-52, trp1-63, his3-200, pph3Δ::URA3,*
2790	S288C	*MATα_ura3-52, trp1-63, his3-200, slx4(S486A)::KanMX*
2791	S288C	*MATa_ura3-52, trp1-63, his3-200, bar1Δ::HIS3, sgs1Δ::natMX*
2792	S288C	*MATa_ura3-52, trp1-63, his3-200, bar1Δ::HIS3*
2793	S288C	*MATα_ura3-52, trp1-63, his3-200, bar1Δ::HIS3, slx4(S486A)::KanMX6, sgs1Δ::natMX*
2794	S288C	*MATα_ura3-52, trp1-63, his3-200, slx4(S486A)::KanMX6, sgs1Δ::natMX*
2795	S288C	*MATα_ura3-52, trp1-63, his3-200, sgs1Δ::natMX*
2796	S288C	*MATa_ura3-52, trp1-63, his3-200, pph3Δ::URA3, slx4(S486A)::KanMX6,*
2797	S288C	*MATα_ura3-52, trp1-63, his3-200, pph3Δ::URA3, sgs1Δ::natMX*
2798	S288C	*MATa_ura3-52, trp1-63, his3-200, slx4(S486A)::KanMX6, sgs1Δ::natMX*
2799	S288C	*MATa_ura3-52, trp1-63, his3-200, bar1Δ::HIS3, pph3Δ::URA3, sgs1Δ::natMX*
2800	S288C	*MATa_ura3-52, trp1-63, his3-200, pph3Δ::URA3, slx4(S486A)::KanMX6, sgs1Δ::natMX*
2801	S288C	*MATa_ura3-52, trp1-63, his3-200, slx4(S486A)::KanMX6, sgs1Δ::natMX*
2802	S288C	*MATa_ura3-52, trp1-63, his3-200, bar1Δ::HIS3, sgs1Δ::natMX*
2803	S288C	*MATa_ura3-52, trp1-63, his3-200, bar1Δ::HIS3, pph3Δ::URA3, sgs1Δ::natMX*
2804	S288C	*MATa_ura3-52, trp1-63, his3-200, bar1Δ::HIS3, pph3Δ::URA3, sgs1Δ::natMX*
2805	S288C	*MATa_ura3-52, trp1-63, his3-200, bar1Δ::HIS3, slx4(S486A)::KanMX6, sgs1Δ::natMX*

2806	S288C	*MATa_ura3-52, trp1-63, his3-200, bar1Δ::HIS3, pph3Δ::URA3, slx4(S486A)::KanMX6, sgs1Δ::natMX*
2807	S288C	*MATa_ura3-52, trp1-63, his3-200, bar1Δ::HIS3, pph3Δ::URA3, slx4(S486A)::KanMX6, sgs1Δ::natMX*
2808	S288C	*MATα_ura3-52, trp1-63, his3-200, bar1Δ::HIS3, pph3Δ::URA3, slx4(S486A)::KanMX6, sgs1Δ::natMX*
2831	S288C	*MATa, ura3-52, leu2Δ1, trp1Δ63, his3Δ200, lys2ΔBgl, hom3-10, ade2Δ1, ade8, arg4Δ, sml1Δ::TRP1 bar1Δ::HIS3, slx4Δ::KanMX6*
2832	S288C	*MATa, ura3-52, leu2Δ1, trp1Δ63, his3Δ200, lys2ΔBgl, hom3-10, ade2Δ1, ade8, arg4Δ, sml1Δ:TRP1 bar1Δ:HIS3, slx4Δ::KanMX6*
2833	S288C	*MATa, ura3-52, leu2Δ1, trp1Δ63, his3Δ200, lys2ΔBgl, hom3-10, ade2Δ1, ade8, arg4Δ, sml1Δ::TRP1 bar1Δ::HIS3, dot1Δ::URA3, slx4Δ::natMX*
2834	S288C	*MATa, ura3-52, leu2Δ1, trp1Δ63, his3Δ200, lys2ΔBgl, hom3-10, ade2Δ1, ade8, arg4Δ, sml1Δ::TRP1 bar1Δ::HIS3, dot1Δ::URA3, slx4Δ::natMX*
2835	S288C	*MATa_ura3-52, trp1-63, his3-200, bar1Δ::HIS3, pph3Δ::TRP1, sgs1Δ::natMX*
2836	S288C	*MATa_ura3-52, trp1-63, his3-200, bar1Δ::HIS3, pph3Δ::TRP1, sgs1Δ::natMX*
2837	S288C	*MATa_ura3-52, trp1-63, his3-200, bar1Δ::HIS3, pph3Δ::TRP1, slx4(S486A)::KanMX6, sgs1Δ::natMX*
2838	S288C	*MATa, ura3-52, trp1-63, his3-200, bar1Δ::HIS3, pph3Δ::URA3, slx4Δ::KanMX6, mus81Δ::TRP1*
2839	S288C	*MATa, ura3-52, trp1-63, his3-200, bar1Δ::HIS3, pph3Δ::URA3, slx4Δ::KanMX6, mus81Δ::TRP1*
2840	S288C	*MATa, ura3-52, trp1-63, his3-200, bar1Δ::HIS3, pph3Δ::URA3, slx4Δ::natMX, rad53(R605A)::KanMX6, mus81Δ::TRP1*
2841	S288C	*ura3-52, trp1-63, his3-200, mus81Δ::URA3, rad53(R605A)::KanMX6, slx4Δ::TRP1*
2842	S288C	*ura3-52, trp1-63, his3-200, mus81Δ::URA3, slx4Δ::TRP1*

Table 6. *S. cerevisiae* strains generated.

APPENDIX iv

DETAILED PROTOCOLS

Protocol: Pulse Field Gel Electrophoresis of Yeast Chromosomes

Materials:

- Solution 1: 100mM EDTA (pH 7.5)
- Solution 2: 10mM KPO_4, pH 7.5 for Zymolyase solution.
    - Prepare this solution by mixing KH_2PO_4 with K_2HPO_4 to get pH 7.5.
    - ~11mL of 50mM KH_2PO_4 + 50mL of K_2HPO_4, check pH and adjust to 7.5 by adding more of one or he other solution. Then dilute to 10mM and filter sterilize.
- Low Melting Point (LMP) agarose. 0.75% in 100mM EDTA pH7.5.
    - Cool to 42C before adding to cells. Prepare several 1.7mL aliquots and store at 4C until ready to use. DO NOT reuse aliquots that have been melted earlier.
    - Final pH is VERY IMPORTANT.
- Zymolyase 20T. 2mg/mL in solution 2. Store at 4C.
- Zym solution: 500mM EDTA, 10mM Tris, pH7.5
- Prot K solution: 5% Sarcosyl, 5mg/ml proteinase K in 500mM EDTA pH7.5
    - Prepare 1mL aliquots and store at -20C.
- Wash solution. 20mM Tris, 50mM EDTA, pH8.0
- Storage solution: 2mM Tris, 1mM EDTA, pH8.0.
- 'Disposable' plug molds
- 5X TBE buffer
    - 54g of Tris base
    - 27.5g boric acid
    - 20mL of 0.5M EDTA (pH 8.0)
    - **Working solution is 0.5X. Dilute 1L of above buffer with 9L water in carboy.**
- Pulse Field Certified Agarose, Biorad.

Method:

- This protocol will take anywhere between 1.5-2 weeks from start to finish. The first day (Day 2 in protocol) will be very long and time consuming.
- Your experiment may vary slightly, but generally you will have either 3 or 4 different strains and will likely have 4-5 different 'time points'. For example, each strain may follow like:

  ASY –asynchronous, before treatment.

  +MMS – (Just following MMS treatment, for example, 0.033% MMS for 2 hours)

1 hour recov – Cells are washed with fresh media and allow to recover for 1 hour.

3 hours rec. – after 3 hours of recovery

5 hours rec. – after 5 hours of recovery

Day 1.

1. Start a 200mL YPD or dropout media overnight for each culture to be studied. From a liquid culture, dilute to an OD of 0.001 the night before.

Day 2.

2. The next morning, if the culture is saturated, dilute down to OD= 0.1 and allow to reach log phase again.
    a. If the cells are not saturated, proceed immediately.
3. Adjust a water bath to 50C.
4. Melt several LMP agarose aliquots in the 95C and allow to 'cool' in the 50C water bath until use.
5. Determine the weight of 1mL of each culture. Isolate 50mg of cell pellet.
    a. Label 4 1.7 tubes. Weigh each empty tube and record this empty weight.
    b. Take out 1mL of each asynchronous culture into these 1.7mL tubes and spin at top speed for 3 minutes.
    c. Immediately, aspirate media while the pellet is still hard.
    d. Spin down again at top speed for 3 more minutes
    e. Remove the residual media.
    f. Weigh tubes again.
    g. Subtract empty tube weight from +1mL weight. Divide 50 by this number. This is the number of mL to spin down from each culture.

	Strain/treatment description	Empty tube (mg)	+1mL (mg)	Net (mg)	50/net = (mL to spin)
1	626 ASY (i.e.)				
2	2422 ASY (i.e.)				
3					
4					

(You will do this for each time point)

6. Spin down cells in a 50mL plastic centrifuge tube for 5min/4C/4000rpm.
7. Resuspend each cell pellet in 1mL solution 1 in a 1.7mL tube and spin again 1min/13,000rpm.
8. Aspirate liquid.
9. Lay each tube on its side, and place a 20uL droplet of the zymolyase solution to the wall of the tube away from the cell pellet.

10. Add 450uL of the melted LMP agarose to the cell pellet, mixing the zymolyase in with the cells. Quickly and completely resuspend the cell pellet into a homogenous mixture.
11. Transfer ~100uL of this mixture (quickly) to the plug molds. This should fill about 5 wells. Make sure you label these molds.
12. Allow these plugs to COMPLETELY solidify. You may need to loosely wrap with plastic wrap and place in fridge for a while.
13. You will perform steps 5-12 for each 'time point'.

MMS treatment

14. Before adding MMS, you may need to restore final volume to 200mL (preferred) and dilute cells. Ideally I like to have an OD of about 0.2-0.3 before MMS treatment.
15. Calculate the amount of MMS to add to each flask and add the drug. I've used concentrations ranging from 0.001%-0.033% MMS for anywhere between 1.5 and 3 hours.
16. At the end of the treatment, collect your +MMS (or '0') time point by following steps 4-11 again.

Recovery of cells.

17. After collecting your time point, spin the rest of the cells down at 1000xG/5min.
18. Prepare 200mL of fresh media.
19. Remove MMS media and resuspend in the fresh media.
20. Subsequently follow steps 5-12 for each desired time point of recovery. I suggest 1, 3 and 5 hours of recovery.

Zymolyase Digestion

21. Once each set of plugs are completely solidified, remove the sticky backing and gently push each plug into a 2mL snapcap tube with 1.2mL of Zym solution. 5 of the same plugs per tube. Invert a few times to prevent plugs from sticking together.
22. Incubate overnight at 37C.

Day 3

23. The next morning, add 400uL of Prot K solution to each tube. Invert tube a few times to homogenize the solution.
24. Incubate at 50C for at least 5 hours, inverting the tubes at least twice during incubation.
25. Wash the plugs for 30 minutes in 4.5mL of Wash solution by adding 4.5mL to 15mL conical tubes and transferring plugs. All the plugs to rock at RT. Small spatulas work for this. Do not try to aspirate media. You will destroy the plugs.

26. Remove the Wash solution and replace with 10mL fresh Wash solution. Rock overnight at RT. I like to strain with the back of a plastic fork gently. Whatever works.

Days 4-?

27. Replace Wash solution 1-2 times a day for anywhere between 5-8 days. The more you wash, the less detergent (sarcosyl) persists and the cleaner the gel.
28. You can store the plugs in 5mL Storage solution at 4C for at least a month.

Setting up the gel

29. Prepare 225mL of 1% Pulse Field Certified Agarose in 0.5% TBE buffer.
30. Melt the agarose in the microwave and allow it to sit on a bench while you set up the plugs.
31. Assemble gel cast with black iron plate seated snugly within the grooves of the casting tray.
32. Use a clean 20-well comb (free of EtBr, if possible) and rest it flat across casting try.
33. Remove one plug per sample/time point/strain and lightly remove the bulk of the buffer by touching the spatula (with the plug on it) onto a kimwipe. Cut using a cutting tool (example below). You can make a cutting tool using two razor blades, a binder clip, and a spacer (I used a piece of a plastic knife).

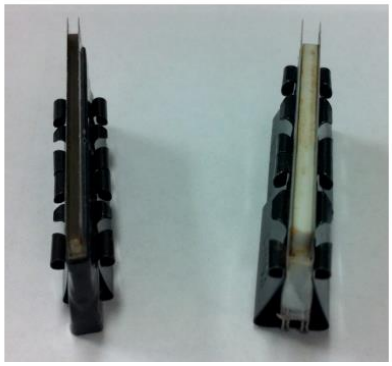

34. Place the cut plug piece at the bottom of the well teeth on the comb. Do this with each plug sample. Put remainder of plug back in the buffer.
35. To prevent 'floating' (plug pieces rising/displacing once the melted agarose is added), place ~5uL of the melted agarose on the comb directly above the plug as a stopper/attachment point.

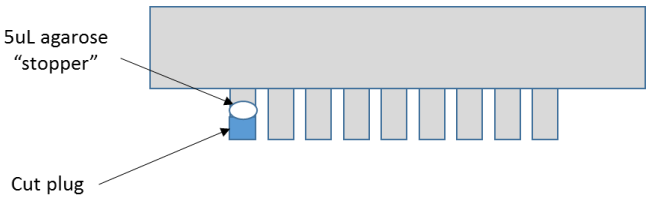

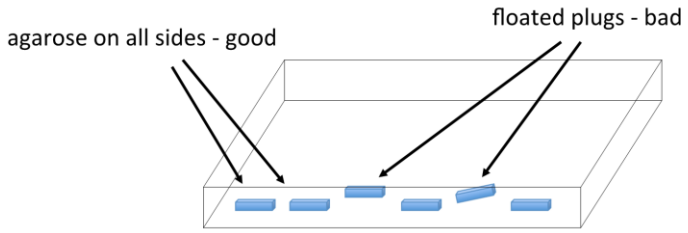

36. Once stopper agarose is solid, place comb (with plugs) right side up in gel caster. Because the combs don't go with the gel caster system, you may need to jerririg a way to suspend the comb so that the bottom of the comb teeth are about 2cm above the iron plate. I used 3 white screw caps taped together.
37. Once the bulk agarose is cool but still liquid (you don't want to remelt the plugs), gently pour the agarose in the gel caster completely surrounding the plugs/comb. Fill the caster as much as you can. It is VERY IMPORTANT the plugs are completely covered by the agarose.

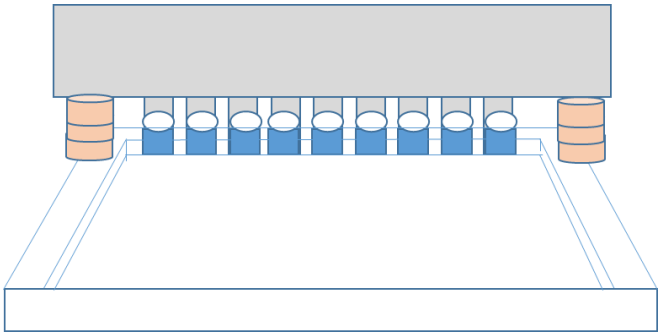

38. Allow to cool on your bench. It will become opaque.
39. After agarose turns opaque, loosely cover the caster/gel/comb with plastic wrap and place in 4C for ~4 hours so that the gel completely solidifies. If you don't allow it to COMPLETELY solidify, you will rip the gel apart trying to take the comb out.
40. Gently remove comb. No need to fill in holes.
41. Remove gel-iron plate from caster. **DO NOT disassemble gel from iron plate.** You need it attached so that it will keep the gel at the bottom of the running chamber.

Preparing for Electrophoresis

42. Fill running chamber with about 1L dH20.
43. In this order,
    a. Power switch ON,
    b. Pump switch ON,
    c. Turn on chiller,
    d. Make sure temperature is set to 14C
    e. Set pump to 70
44. Allow 1L of dH20 to drain out, rinsing tubing and running chamber.
45. Rinse running chamber with ~1L 0.5X TBE. Allow to drain out.
46. Once rinsed, clamp off tubing with binder clip.
47. Place black frame in empty running chamber with plastic pins in holes to keep it in place.
48. Use a level to make sure running chamber is PERFECTLY LEVEL. You can adjust the tilt via adjusting the legs of the chamber. Non-level gels will have more diffuse bands.

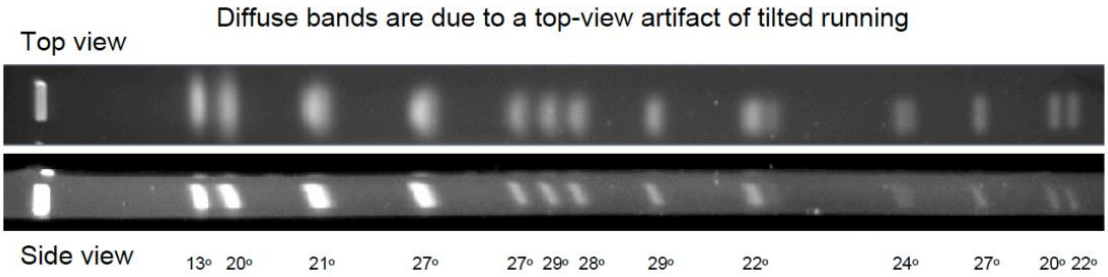

49. Fit the gel with the iron plate snuggly into the black frame.

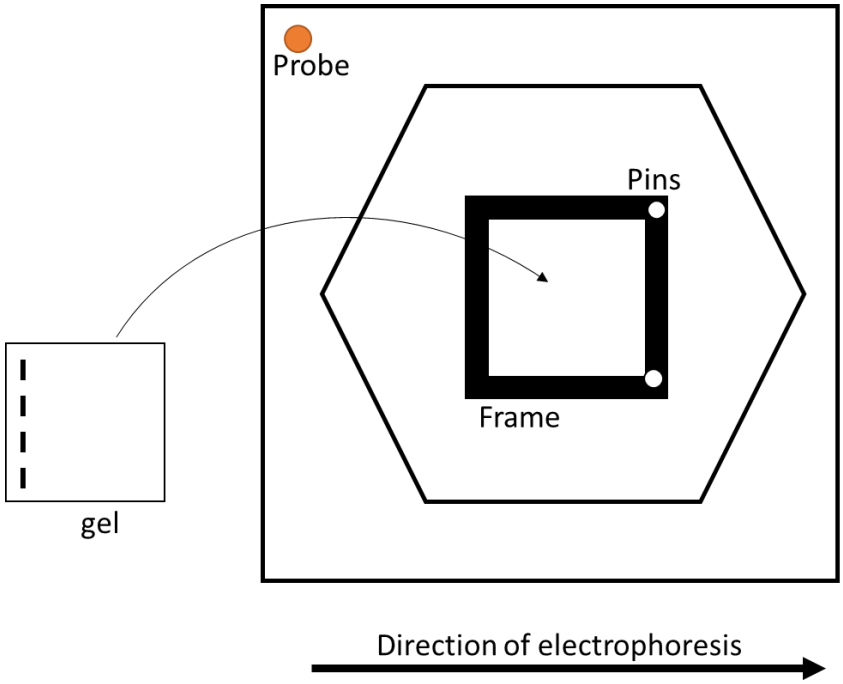

50. Fill the running chamber with ~3.5L of fresh 0.5X TBE buffer.
51. Attach chamber lid.
52. Enter running conditions:
    a. 2 state mode
    b. Gradient: 6.0v/cm + ENTER
    c. Run time: 24 hours 00 min + ENTER
    d. Included angle: 120 + ENTER
    e. Initial switch time: 60 sec + ENTER
    f. Final switch time: 120 sec + ENTER
    g. Ramping factor (a): press ENTER for LINEAR.
53. Gel will run continuously for at least 24 hours. If running for longer than 24 hours, it is wise to change the buffer each additional day.

Stain/Destain the Gel

54. The next day, carefully remove gel from frame and iron plate and place in a glass dish.
55. Add 500mL of dH_20 and 25uL of Ethidium Bromide (EtBr).
56. Cover with plastic wrap and completely cover top and bottom of dish with aluminum foil.
57. Allow to gently rock at room temp for 20 minutes.
58. Destain by removing dH_20+EtBr, and replacing with 500mL of fresh dH_20 2x 20 minutes with rocking.
59. Take to gel imager. (After a few minutes of exposure, the bands will start to fade. Make sure the first few pictures are good ones!)

Protocol: Yeast Mating: Creating a diploid

At a Glance:

1. Resuspend 1 colony of your MATa and MATα in 100uL of sterile water.
2. Mix them together.
3. Plate 20uL of mixture in a single, large droplet on a YPD plate O/N.
4. Next day, streak some cells onto a double dropout plate in which only the mated diploid can grow.
5. In 2 days, pick a single colony and grow O/N in 5mL of either dropout liquid media or YPD.
6. Confirm by PCR (or comparable method) the presence of both alleles (indicative of a diploid).

Detailed Protocol:

1. To mate two yeast strains, you need to make sure:
    a. You have one MATa strain and one MATα strain. (To determine mating type, see TESTING MATING TYPE below).
    b. You do not have different mutations using the same marker. (Same gene deleted with the same marker in both cells is OK and may be advantageous. For example, mating *bar1::HIS3* with *bar1::HIS3* would generate a homozygous diploid. You wouldn't want to mate a *bar1::HIS3* with an *slx4::HIS3,* though).
    c. The strains you are mating need to be isogenic (from the same background strain). You should not mate a silac strain with a non-silac, or a S288C with a W303 strain.
2. Resuspend a single colony of each of your MATa and your MATα strain, separately, in 100uL of sterile dH20 in their own Eppendorf tube.
3. Mix 100uL of each colony together in a single tube and vortex.
4. Plate 20uL of this cell mixture as a single droplet onto a YPD plate. You may need to allow the plate to dry overnight faceup. This allows the two strains to mingle in high density in optimal growth conditions.
5. The next day, either:
    a. (Preferred) Restreak some of these cells onto a double dropout plate that has one marker from each strain. For instance, if you are mating a *yfg1::NatMX* with a *yfg2::URA3*, streak out on –URA +NatMX plates. **You may wish to make these plates ahead of time the day before.**
    b. Restreak on one dropout plate, and then in two days, replica-plate on another dropout plate. (with a's example, restreak on –URA plates, then in 2 days, replica-plate on +NatMX plates.) Pick only single colonies that grew in both plates.
6. Pick single colonies and grow up overnight in 5mL fresh media.

7. Prepare genomic preps and confirm that these cells are diploids by PCR to confirm that both the marker and the gene are present (both alleles, if heterozygous for a deletion, for example).
8. Save this diploid in the yeast collection.
9. To obtain different combinations of haploids with this mutant, follow protocol #18 Sporulation and Tetrad Dissection.

The Ultimate SILAC Phosphoproteome - IMAC/HILIC/MS - Yeast

Light: strain:_____

Volume:_____mL

Treatment?: _____

Heavy: strain:_____

Volume:_____mL

Treatment?: _____

MATERIALS:

- Trypsin – TPCK treated (Wortington, # LS003741)

SOLUTIONS:

- Lysis buffer 1: 50mM Tris-HCl (pH 8.0), 0.2% Tergitol, 150mM NaCl, 5mM EDTA. Add protease inhibitors "complete" EDTA-free from Roche (cat # 05 056 489 001), 1mM PMSF and phosphatase inhibitors (5mM NaF, 10mM B-glycerol-phosphate);

- PPT solution: 50 % acetone, 49.9 % ethanol, 0.1 % acetic acid;

- Urea/tris solution (make fresh): 8 M urea, 100 mM Tris-HCl (pH 8.0);

- Tris/NaCl solution: 50 mM Tris-HCl (pH 8.0), 150 mM NaCl;

- C18-buffer A: 0.1 % TFA;

- C18-buffer C: 0.1 % acetic acid;

- C18-buffer D: 80 % acetonitrile, 0.1 % acetic acid;

- IMAC washing solution 1: 0.1 M NaCl, 0.1 % acetic acid, 25 % acetonitrile;

- IMAC washing solution 2: 1 % acetic acid;

- IMAC eluting solution: 12 % ammonia, 10 % acetonitrile

DAY 1:

I. Cell growth (MBS164 derived strains) – for approx. 1g cell pellet/50mg of WCE

1. Grow a fresh 5 mL stock culture from 10 am to 8 pm. Measure OD at 8 pm (want it to be as close to OD=1 as possible, should not be saturated);
2. Pre-warm **800 mL** of SILAC media to a 2.8L Erlenmeyer;
3. Calculate the amount of stock culture to be added to SILAC media to have OD of 0.001 (for MBS164). Before adding, spin stock culture to remove the YPD; 0.015 for 188
4. Grow overnight at 30C/250rpm
5. Next morning, OD of culture should be around OD 0.2-0.4. Dilute to OD=0.1;
   Light: _____

   Heavy: _____
6. Grow until OD= 0.2 (if doing a treatment) or 0.4 if just spinning down/freezing.
   Light: _____

   Heavy: _____

II. Alpha-factor arrest

7. Add alpha factor (stock = 10.000X) to culture and arrest cells for 2h.

III. Release and HU/MMS treatment

8. Spin cells at 1000g for 5min at RT;
9. Quickly resuspend cells in **400mL** of pre-warmed SILAC media (in 2000-2800mL flask with grooves) with 1000X pronase; Add appropriate desired treatment (HU, MMS,…)
   Treatment: _____
10. After incubation check OD, mix equal amounts (based on the OD) of heavy and light cells.
    Duration of treatment: _____

    Light: _____

    Heavy: _____
11. Spin at 4500 rpm; 4C for 5min. Wash pellet with 20mL of cold TE buffer + fresh 100X PMSF.
12. Split cells in ~20 equal aliquots in 2mL screw cap eppendorfs. Spin, remove TE and store at -80C.

DAY 2

IV. Cell lysis (for 1G pellet/40 to 50mg WCE)

13. Cell pellet should be around 250mg each;
14. Separate the amount of tubes to give you ~ 1G of cell pellet.
    a. add 600 uL glass beads to each tube,
    b. add 1.2mL of lysis buffer to each tube and break for 20 minutes at 4 C;
        i. Lysis buffer + 100X PMSF +100X complet + 100X Phos.Inh.
15. Transfer the lysate together with glass beads to a falcon tube and leave it on ice until beads decant.
16. Using a 5ml pipette, transfer as much as you can from the lysate to a 50mL polycarbonate centrifuge tube.
17. Rinse the beads left on the falcon tube 2x5mL of lysis buffer and transfer it to the polycarbonate centrifuge tube together with the rest of the lysate;
18. Centrifuge at 45,000G at 4C for 20' and transfer supernatant to a 50mL falcon tube.
19. Save 10uL for Bradford.

BSA		Sample	
1.5 (3mg)		0.5uL	
2 (4mg)		1uL	
2.5 (5mg)		2uL	
3 (6mg)			
3.5 (7mg)			
4 (8mg)			

20. Transfer to 50mL falcon tube. Volume = _____mL
    _____mg/mL x _____mL = _____mg total
21. Protein concentration should be around 4-5mg/mL; total ~ 40mg of proteins. Keep sample at 4C until proceeding to the next step;

V. Protein extract preparation and trypsin digestion

22. Add 1% SDS (1mL of 10% stock) and reduce disulfides by 5mM DTT (55µL of 1M stock) at 55-65C for 10 min;
SDS: _____

DTT: _____

23. Alkylate cysteines by 15mM Iodoacetamide (add 330µL of a 33X solution [0.5M: 90mg in 1mL of 1 M Tris-HCL, pH 8.0]) at RT for 15 min;

    45mg = _____

    500mL

    _____uL /33 = _____ uL of iodoacetamide to add

24. Transfer the solution to 50mL falcon tubes (~12mL per tube). Precipitate proteins with 3 volumes (~ 36mL) of PPT solution. Add solution at room temperature, mix it and keep on ice for at least 10 minutes;
25. Spin for 10 minutes at 4,500RPM (4,700G) at RT;
26. Pour supernatant out. Keep tube upside down for 2 minutes to drain PPT solution. There should be no acetone smell.
27. Prepare 10mL of 8M urea/100mM Tris-HCl, pH 8
    (4.8G of urea + 1mL of Tris-HCL pH 8 + water to 9mL)
28. Add 4.5 mL of H2O + 45µL of 8M urea/100mM Tris-HCl, pH 8 and resuspend protein pellet using pipet-aid (avoid the formation of foam). The solution will be “milky” as most proteins are not soluble.
29. Transfer the solution to a 50mL polycarbonate centrifuge tube;
30. Centrifuge proteins again at 45,000G for 4’.
31. Carefully remove supernatant with a vacuum pump. Wash the walls 2x1mL of water without disturbing the pellet and remove the water by aspiration. This is a critical step to help remove hydrophilic contaminants as much as possible;
32. To the protein pellet, add 6mL of Urea 8M/Tris 100mM pH 8.0 to solubilize it. Use douncer to homogenize.
33. Pour back into a 50mL falcon tube and add 18mL of Tris/NaCl solution (this is important to dilute urea to 2 M before trypsin digestion). Can double/triple 6mL and 18mL depending on protein concentration. 6/18 is suggested for 40mg of protein. Keep ratios the same.
34. Add 400µg of TPCK treated trypsin (40µl of a 10µg/µl stock). Let digest overnight at 37C under constant rotation.

    (____mg protein/ 200) x 100 = _____uL of TPCK-treated trypsin to add.

DAY 3

35. Next morning, using glass micro-syringes, add 0.2% formic acid and 0.2% TFA (use 0.5mL of 10% stock solutions of these acids);
    ____mL of 10% FA

    ____mL of 10% TFA

36. To remove insoluble material centrifuge tubes for 5 minutes at 4,500 RPM.
37. Separate (keep) supernatant. Can freeze at -80C if necessary.

VI. Sample Clean-Up (max capacity for 1 x C18 $_{200mG}$ is 6mG) – Use 8 columns for 40-50mG

**for 20mg protein – 1g column clean up. Elute with 3mL (4x750uL)

38. 200mg column ~5mg protein
    1g column ~ 20mg protein

    2g column ~ 40mg protein

    Condition ____(number) of _____ columns depending on amount of proteins with C18-buffer D until column is completely wet (use a bulb to help),

39. Wash column with C18-buffer A. Do not let column dry at any time;
40. Load peptides equally among columns and let it flow by gravity;
41. Wash with C18-buffer C and let it flow by gravity X2.
42. Elute bound peptides from each C18 column in a glass tube tube with:

    0.75 mL for 200mg column

    3.5mL for 1g column

    7mL for 2g column

    of C18-buffer D (50% CAN, 0.1%HAc), mix the elutions and add 750uL to glass vials.

43. Dry elutions in a speed-vac at 45 C for approx. 2h30;
44. Add 100µL of 1 % acetic acid (pH 2.3) to each tube. Cap the tubes and vortex each one for exactly 1 minute. Transfer the volumes to a 1.7mL micro centrifuge tube. Avoid remove pellets on the walls of glass tubes by scratching. Transfer only what it is soluble. Centrifuge in a bench top centrifuge for 1 minute @14.000 RPM and collect supernatant;
45. Preclean supernatant with 4uL imac resin (pellet) beater 10min.

VII. Phosphopeptide purification / agarose IMAC (0.5mL of IMAC for 50mG of WCE)

46. Prepare IMAC resin. 30uL IMAC each column. After packing column, equilibrate in 1% HAc.
47. Apply flow through to 0.5 mL of a fresh agarose IMAC resin (for agarose IMAC resin preparation see **Appendix_I**) packed in a 10mL Bio-Rad column. Run sample through resin by gravity. Load 100uL sample at a time. Collect flow through;
48. Wash with 1 column volume (CV) of IMAC **washing solution 1** (add 100uL and remove 70uL);
49. Wash with 2 x CV of IMAC **washing solution 2** (add 100ul, remove 40ul);
50. Wash with 1 x CV of deionized water (add 100uL, remove 70uL);
51. Elute phosphopeptides directly in a silanized flat bottom glass tube with 3 x CV of IMAC eluting solution (90uL);
52. Take out 4.5uL (5%) and dry separately.

53. Resuspend in 6uL 0.1P and shoot 1% and 3%
    a. 1% - 1uL _____ (method)
    b. 3% - 3uL _____ (method)
54. To the 95%, resuspend in 15uL water, until deciding to do HILIC.

IX. Fractionation of phosphopeptides by HILIC chromatography

55. Prepare HILIC.
    a. Blank
    b. Angio
56. Add 10µl of 10% formic acid and 60 uL of ACN mix well with 100uL micropipette and spin for 1 minute at to remove insoluble material. Transfer supernatant to a small silanized tube and apply it to HILIC fractionation;
57. Use program Hillic_newgrad_collection (14 fraction of 1 min each);
58. Collect fractions 1 to 11;
59. Dry fractions for 45' @ 45C;
60. Add 7 uL of C18 buffer A (TFA 0.1 % with 0.1pmol/uL) to each tube;;

X. Shooting sample for LC-MS/MS analysis of phosphopeptides

HILIC fraction	**MS method**

IP/MS of Acetylated Peptides (SILAC)

Project Name:

Strains:

Treatment (optional):

Quantitative

LIGHT:

HEAVY:

MATERIALS NEEDED:

- TE pH8.0
- α-factor (stock 50ng/mL)
- SILAC media
- Lysis buffer pH8.0
- TSA (4mM stock)
- 100X complet
- 100X Phos. Inh.
- BSA 2ug/uL
- SDS (10% stock)
- DTT (1M stock)
- Iodoacetamide
- 1M Tris pH8.0
- PPT solution (50% acetone, 49.9% ethanol, 0.1% acetic acid)
- Urea
-
- 50mM Tris pH8.0, 150mM NaCl
- TPCK-treated trypsin
- 10% Formic acid
- 10% TFA
- C18 column(s)
- 80% Acetonitrile(ACN)/0.1%HAc
- 0.1% TFA
- 0.1% Acetic acid (HAc)
- Glass vials
- 50% ACN
- Immunoprecipitation buffer (50mM MOPS, pH7.2, 10mM Sodium phosphate, 50mM sodium chloride)

*NOTE: when using acetone, acetonitrile, formic acid, TFA, do not use plastic!

DAY 1

Growing cells

1. Calculate the amount of stock culture to be added to SILAC media to have an OD of 0.001.
2. From a liquid culture inoculate 800mL each of heavy and light SILAC media (prewarmed) and inc O/N at 30C (should get about 100mg protein each). **Try to aim for cells to be ready in the morning**
3. If overgrown, dilute cells to 0.1 in a total volume of 800mL SILAC media each.
4. Grow until 0.4. If arresting, grow until 0.2.

Arresting cells with α-factor (G1 arrest) -optional

5. At OD= 0.2, add 20,000X α-factor for 2 hours. Amount of α-factor added = _____
6. If releasing, spin down cells at 30C/4,000RPM/5MIN.
7. Resuspend in fresh, pre-warmed SILAC media and add 100X pronase to degrade leftover α-factor.
8. If releasing, release for _____ (light) and _____ (heavy).

Treatment with MMS

9. Treat with MMS for 3 hours.
10. Concentration of MMS = _____% (add _____uL).

Pellet

1. Take ODs.
    a. Light =
    b. Heavy =
2. Mix heavy and light cells together evenly.
3. Pellet cells at 4,000RPM/4C/5MIN
4. Wash with 25mL (for 800+800mL of cells) of cold TE and transfer to 2mL screw cap. ~22-24 tubes
5. Spin again
6. Aspirate TE.
7. Weigh pellet. Should have ~0.2g cell pellet. Can stop and store at -80C.

DAY 2

Lyse

1. Add 600uL of glass bead to cell pellet(s)
2. Add 1.2mL of Lysis buffer (Stock lysis buffer at pH8.0, with 5uM TSA, 100X complet, and 100X Phos Inh.)
3. Bead beat at 4C 3X 10 minutes (1 minute interval)
4. Spin 10MIN/4C/13,000RPM
5. Remove supernatant and mix them together appropriately into a 15mL centrifuge tube. _____mL (volume) ~20-24mL
6. Take out 10uL for Bradford

BSA (2ug/uL)	ABS600	Sample	ABS600
1.5uL (3ug)		0.5uL	
2uL (4ug)		1uL	
2.5uL (5ug)			
3uL (6ug)			
3.5uL (7ug)			
4uL (8ug)			

_____ ug/uL sample = mg/mL

____ (vol) x _____mg/mL = _____mg protein (total)

Preparing protein

1. Immediately add SDS to rest of supernatant to final conc of 1%. **SDS denatures proteins**
   _____uL of 10% SDS
2. Keep at RT while mixing.
3. (also quickly) Add DTT (1M stock) to final concentration of 5mM. **DTT reduces disulfide bonds**
   _____uL of 1M DTT
4. Leave at 65C for 5 mins, then take out and let cool at RT before adding Iodoacetamide.
5. Prepare iodoacetamide (light sensitive). Will need a final concentration of 15mM iodoacetamide. **Iodoacetamide alkylates cysteines so that disulfide bonds won't reform.**

   (45mg iodoacetamide in 500uL 1M Tris pH8.0…= 33X solution)

   Volume = _____mL

   _____mL/33 = _____uL Iodo.

6. Leave at RT for 10mins.

7. Add 3X volume of PPT and mix well at RT. (may need to transfer to 50mL falcon tube)
8. Leave on ice for 10 minutes.
9. Spin 5MIN/4,500RPM
10. Prepare 8M Urea/0.1M Tris:

    1.92g Urea +400uL 1M Tris pH8.0 (urea takes long time to dissolve)
    Add water to 4mL
    Recipe is for ~30mg protein…adjust as needed
11. Pour out supernatant.
12. Invert tube and leave tube inverted to drain pellet. Do not move on until acetone smell is gone.
13. Add 2mL of the 8M urea/tris per 30mg protein. Amount added = _____mL
14. Get Douncer and wash with water.
15. Resuspend pellet with a P1000 (never pipet all the way up)
16. Pour into Douncer.
17. Homogenize (try to avoid foaming).
18. Add 6mL of 50mM Tris pH8.0, 150mM NaCl for every 2mL Urea/Tris added to dilute 8M urea to 2M urea (trypsin won't work in 8M). Amount added= _____mL
19. Prepare TPCK-treated trypsin solution (TPCK prevents autodegradation)

    1:10 trypsin:0.1% HAc (if going to freeze and store for future use, use 0.3% HAc)
    e.g. 1mg trypsin in 100uL, 0.7mg in 70uL, etc.
    = 10ug/uL
20. Add trypsin 1:200 (1ug trypsin: 200ug protein) dilution overnight at 37C with constant rotation.

    ~____mg protein total

    $\frac{\text{\_\_\_\_\_mg protein}}{\text{X mg trypsin}} = \frac{200}{1}$

    X = _____mg (____ug) trypsin needed

    $\text{\_\_\_\_ug trypsin} \times \frac{1\text{uL}}{10\text{ug}} =$ _____uL trypsin solution

DAY 3

21. Using a glass syringe add formic acid and TFA (from 10% stocks) to make a final concentration of 0.2%. Dilution = 50. *precipitation is normal.

    Amount to add (each) = _____

22. Wash syringe 2-3X's with water. Mix well.
23. Spin 4,500RPM/5MIN.

C18 column clean up.

We use the C18 column to remove bulk trypsin and urea. Binds hydrophobic things.

1. Each 200mg C18 column can handle ~6mg protein.

   Each 1g C18 column can handle ~35mg protein.

   Each 2g C18 column can handle ~70mg protein. (above 30mg protein, use these)

   Mg of protein = _____mg
   Amount of columns to use = ____ (quantity) of _____ (C18 type)
2. Condition the columns with 80%ACN/0.1% HAc. Use bulb.
   IMPORTANT: Don't let air into the column!
3. Wash column with 0.1% TFA (TFA makes C18 more 'sticky'). Use bulb.
4. Add protein solution. (use liquid, discard pellet). Let flow by gravity.
5. Wash column with 0.1% HAc. Use bulb.
6. Add more of HAc. Invert tube and dump out HAc.
7. Wash again with 0.1% HAc. Use bulb.
8. Cut a new yellow tip for eluting.
9. Flick tip of the column to remove any residual liquid before eluting.
10. Elute with ~4 volumes (~750uL for each 200mg C18, 3.5mL for each 1g C18 column) of 50% acetonitrile into glass vials. If using 1g columns, elute together in single glass culture tube. Dry column completely with bulb.
11. Mix with pipet (eluate often forms aqueous and ACN layers which need to be mixed).
12. Dry completely in speed vac for ~ 100 minutes.
13. Once dry, add 500uL of Immunoprecipitation buffer to glass vials. (can stop and store at -20C)

	Beads 1 (binds FT)	Beads 2 (binds elution)
IP-1	2 hours	2 hours
IP-2	6 hours	O/N
IP-3	O/N	6 hours

Immunoprecipitation A – Beads 1 with FT

1. Need 100uL for IP so take out ~200uL resin. (mix well before washing)
2. Wash beads with 600uL Immunoprecipitation (IP) buffer 3 times. Remove extra liquid.
3. Transfer peptides to 15mL falcon tube.
4. Add beads to peptides by washing beads with combined peptide fractions and transferring to 15mL tube.
5. Nutate at 4C for 2 (first time with peptide solution), then 6 hours (with FT), then O/N (with used FT).

Elution A

1. Spin down beads and remove extra liquid. If in 15mL tube, transfer solution in increments into 1.7mL eppe and spin. Remember to save FT.
2. Wash beads 2-3X's with 600uL IP buffer.
    a. FOR SMALL VOLUMES-Use gel-loading tip as a column to drain beads. Use a syringe to force liquid down (do not dry beads!)
3. Wash beads with 300uL water (3X volumes of beads) twice. (removes salt)
4. Elute bound peptides with 300uL (3X beads) of 0.1%TFA. Tap eppe for a few minutes. Quick spin, and remove supernatant (elution) into a clean 1.7mL eppe.
5. Using IP buffer, recapture and wash beads and save. (BEADS_1).

Immunoprecipitation B - Beads 2 with elutions

1. Wash 100uL beads (200uL slurry) of new resin 3X with IP buffer.
2. Add ~1mL IP buffer directly to elution (~300uL). **pH should be the same as just IP buffer.**
3. Add elution to beads and transfer to 2mL centrifuge tube. Aim for 1.5mL of beads+elution+buffer in a 2mL centrifuge tube ← this nutates well.
4. Bind for 2 (with first elution), or O/N (with second elution), or 6 hours (with 3rd elution) at 4C.

Elution B

1. Spin down beads and remove extra liquid. (should be already in 1.7mL eppe)
2. Wash beads 2-3X's with 600uL IP buffer.
    a. FOR SMALL VOLUMES-Use gel-loading tip as a column to drain beads. Use a syringe to force liquid down (do not dry beads!)
3. Wash beads with 300uL water (3X volumes of beads) twice. (removes salt)
4. Elute bound peptides with 300uL (3X beads) of 0.1%TFA. Tap eppe for a few minutes. Quick spin, and remove supernatant (elution) into a clean 1.7mL eppe.
5. Using IP buffer, recapture and wash beads and save. (BEADS_2).

C18 Column Clean-up (pre-HILIC)

1. Use smaller column (54955)
2. Condition with 80%ACN/0.1%HAc
3. Equilibrate with 0.1%TFA
4. Load peptides/combined elutions
5. Wash with 0.1%HAc
6. Fill up column with 0.1%HAc, invert a couple of times, and discard HAc.
7. Wash again with 0.1HAc.
8. Flick residual volume off syringe tip
9. Elute in silanized vial with 200uL 50%ACN.
10. Pipette up and down to mix
11. Collect ____uL (usually 20uL – 10% *INPUT*)
12. Dry both 20uL and 180uL fractions.
13. Resuspend INPUT in ___ (8uL 0.1P) Shoot ____(2uL) in MS.
    a. MS run = _____ (usually 40min, 1 MS - 8 MS/MS program)
14. Resuspend rest in 15uL water
15. Just before shooting into HILIC, add 10uL 10%FA and 60uL of 100%ACN.
16. Dry HILIC fractions and resuspend in ____ (7uL) of 0.1P (0.1pmol angiotensin).
17. Shoot varying amounts of HILIC fractions depending on HILIC fraction profile.

HILIC fraction	**Amount to shoot in MS**	**MS program/duration**

PREPARATION OF IMAC RESIN

Materials:

-Ni-NTA spin columns (Qiagen, cat #31014)

-Ferric chloride: $FeCl_3$-$_6H_2O$ (Sigma, cat #F-1513)

Solutions:

Stripping solution: 50mM EDTA, 1M NaCl.

10X Iron stock solution: 1M $FeCl_3$ in 0.3% acetic acid (make 0.5L and let it sit for at least 1 month, then use supernatant).

Iron solution: (make fresh) 100mM $FeCl_3$ in 0.3% acetic acid. Use 10X solution above and dilute in 0.3% acetic acid

IMAC washing solution: 25% acetonitrile, 0.1M NaCl, 0.1% acetic acid.

Method:

Stripping Ni:

1. Add the resid of 1 spin column (~60mg) to 25mL of Stripping solution (in a 50mL falcon tube), and shake on a nutator for 40 minutes at RT;
2. Spin resin for 60 seconds 1,500RPM at RT;
3. Remove most of the liquid using a glass pipette coupled to a vacuum (always keep resin moist by leaving a fine layer of liquid covering the resin).
4. Add 25mL dH_2O
5. Repeat steps 2 and 3;
6. Add 25mL of 0.6% acetic acid
7. Repeat steps 2 and 3.
8. Transfer resin to a sterile Eppendorf using 1mL of 0.1% acetic acid. After resin settles, remove enough liquid to reach the 600uL mark. This 10 to 1 slurry can be stored at 4C for 1 week. On the top of the Eppendorf write: “Stripped NTA, date”

Adding Fe:

1. Use 300uL of slurry (30mg resin) from step 8. In a 50mL falcon tube, add 300uL slurry to 20mL of iron solution (18mL of 0.3% acetic acid and 2mL of 100mM $FeCl_3$ solution). Shake on a nutator for 40 minutes at RT.
2. Repeat steps 2 and 3;
3. Add 20mL of 0.6% acetic acid
4. Repeat steps 2 and 3;

5. Add 20mL of IMAC washing solution 1. Shake for 1 minute.
6. Repeat steps 2 and 3;
7. Add 20mL 0.1% acetic acid.
8. Repeat steps 2 and 3;
9. Transfer resin to a sterile Eppendorf using 1mL of 0.1% acetic acid. After resin settles, remove enough liquid to reach the 100uL mark. This 3 to 1 slurry can be stored at 4C for 3 days. On the top of the Eppendorf, write “IMAC, date”.

REFERENCES

Adams, K.E.; Medhurst, A.L.; Dart, D.; Lakin, N.D. (2006). Recruitment of ATR to sites of ionizing radiation-induced DNA damage requires ATM and components of the MRN protein complex. Oncogene *25,* 3894-3904.

Agarwal, R.; Tang, Z.; Yu, H.; Cohen-Fix, O. (2003). Two distinct pathways for inhibiting Pds1 ubiquitination in response to DNA damage. J. Biol. Chem. *278,* 45027-45033.

Ahn, J.Y.; Schwarz, J.K.; Piwnica-Worms, H.; Canman, C.E. (2000). Threonine 68 phosphorylation by ataxia telangiectasia mutated is required for efficient activation of Chk2 in response to ionizing radiation. Cancer Res. *60,* 5934-5936.

Ahn, J.; Prives, C. (2002). Checkpoint kinase 2 (Chk2) monomers or dimers phosphorylate Cdc25C after DNA damage regardless of Threonine 68 phosphorylation. J. Biol. Chem. *277,* 48418-48426.

Ahn, J.; Urist, M.; Prives, C. (2004). The Chk2 protein kinase. DNA Repair *3,* 1039-1047.

Alabert, C.; Bianco, J.N.; Pasero, P. (2009). Differential regulation of homologous recombination at DNA breaks and replication forks by the Mrc1 branch of the S-phase checkpoint. EMBO J. *28,* 1131-1141.

Alani, E.; Thresher, R.; Griffith, J.D.; Kolodner, R.D. (1992). Characterization of DNA-binding and strand-exchange stimulation properties of y-RPA, a yeast single-strand-DNA-binding protein. J. Mol. Biol. *227,* 54-71.

Alcasabas, A.A.; Osborn, A.J.; Bachant, J.; Hu, F.; Werler, P.J.; Bousset, K.; Furuya, K.; Diffley, J.F.; Carr, A.M. Elledge, S.J. (2001). Mrc1 transduces the signals of DNA replication stress to activate Rad53. Cell Biol. *3,* 958-965.

Alexandru, G.; Ulhmann, F.; Mechtler, K.; Poupart, M.; Nasmyth, K. (2001). Phosphorylation of the cohesion subunit Scc1 by polo/Cdc5 kinase regulates sister chromatid separation in yeast. Cell *105,* 459-472.

Ali, A.; Zhang, J.; Bao, S.; Liu, I.; Otterness, D.; Dean, N.M.; Abraham, R.T.; Wang, X.F. (2004). Requirement of protein phosphatase 5 in DNA-damage-induced ATM activation. Genes Dev. *18,* 249-254.

Allen, J.B.; Zhou, Z.; Siede, W.; Friedberg, E.C.; Elledge, S.J. (1994). The SAD1/RAD53 protein kinase controls multiple checkpoints and DNA damage-induced transcription in yeast. Genes Dev. *8,* 2401-2415.

Ammazzalorso, F.; Pirzio, L.M.; Bignami, M.; Franchitto, A.; Pichierri, P. (2010). ATR and ATM differently regulate WRN to prevent DSBs at stalled replication forks and promote replication fork recovery. EMBO J. *29,* 3156-3169.

Amon, A.; Surana, U.; Muroff, I.; Nasmyth, K. (1992). Regulation of p34CDC28 tyrosine phosphorylation is not required for entry into mitosis in *S. cerevisiae.* Nature *355,* 368-371.

Andreas, S.; Schmidt, K.; Lim, Y.A.; Ittner, L.M.; Hemmings, B.A.; Götz, J.

Archambault, J.; Pan, G.; Dahmus, G.K.; Carrier, M.; Marshall, N.; Zhang, S.; Dahmus, M.E.; Greenblatt, J. (1998). FCP1, the RAP74-interacting subunit of a human protein phosphatase that dephosphorylates the carboxyl-terminal domain of RNA polymerase IIO. J. Biol. Chem. *273,* 27593-27601.

Aylon, Y.; Kupiec, M. (2003). The checkpoint protein Rad24 of *Saccharomyces cerevisiae* is involved in processing double-strand break ends and in recombination partner choice. Mol. Cell. Biol. *23,* 6585-6596.

Baber-Furnari, B.A.; Rhind, N.; Boddy, M.N.; Shanahan, P.; Lopez-Girona, A.; Russell, P. (2000). Regulation of mitotic inhibitor Mik1 helps to enforce the DNA damage checkpoint. Mol. Biol. Cell *11,* 1-11.

Bähler, J.; Wu, J.Q.; Longtine, M.S.; Shah, N.G.; McKenzie, A.; Steever, A.B.; Wach, A.; Phillippsen, P.; Pringle, J.R. (1998). Heterologous modules for efficient and versatile PCR-based gene targeting in *Schizosaccharomyces pombe.* Yeast *14,* 943-951.

Balakrishnan, L.; Brandt, P.D.; Lindsey-Boltz, L.A.; Sancar, A.; Bambara, R.A. (2009). Long patch base excision repair proceeds via coordinated stimulation of the multienzyme DNA repair complex. J. Biol. Chem. *284,* 15158-15172.

Balint, A.; Kim, T.; Gallo, D.; Cussiol, J.R.; Bastos de Oliveira, F.M.; Yimit, A.; Ou, J.; Nakato, R.; Gurevich, A.; Shirahige, K.; Smolka, M.B.; Zhang, Z.; Brown, G.W. (2015). Assembly of Slx4 signaling complexes behind DNA replication forks. EMBO J. *34,* 2182-2197.

Ball, H.L.; Myers, J.S.; Cortez, D. (2005). ATRIP binding to replication protein A-single-stranded DNA promotes ATR-ATRIP localization but is dispensible for Chk1 phosphorylation. Mol. Biol. Cell *16,* 2372-2381.

Bando, M.; Katou, Y.; Komata, M.; Tanaka, H.; Itoh, T.; Sutani, T.; Shirahige, K. (2009). Csm3, Tof1, and Mrc1 form a heterotrimeric mediator complex that associates with DNA replication forks. J. Biol. Chem. *284,* 34355-34365.

Barberis, M.; Spiesser, T.W.; Klipp, E. (2010). Replication origins and timing of temporal replication in budding yeast: How to solve the conundrum? Curr. Genomics *11,* 199-211.

Bardin, A.J.; Visintin, R.; Amon, A. (2000). A mechanism for coupling exit from mitosis to partitioning of the nucleus. Cell *102,* 21-31.

Barlow, J.H.; Rothstein, R. (2009). Rad53 recruitment is DNA replication independent and regulated by Cdc28 and the Mec1 kinase. EMBO J. *28,* 1121-1130.

Baroni, E.; Viscardi, V.; Cartagena-Lirola, H.; Lucchini, G.; Longhese, M.P. (2004). The functions of budding yeast Sae2 in the DNA damage response require Mec1- and Tel1-dependent phosphorylation. Mol. Cell. Biol. *24,* 4151-4165.

Bartkova, J.; Horejsi, Z.; Koed, K.; Kramer, A.; Tort, F.; Sieger, K.; Guldberg, P.; Sehested, M.; Nesland, J.M.; Lukas, C. Ørntoft, T.; Lukas, J.; Bartek, J. (2005). DNA damage response as a candidate anti-cancer barrier in early human tumorigenesis. Nature *434*, 864-870.

Bartkova, J.; Rezaei, N.; Liontos, M.; Karakaidos, P.; Kletsas, D.; Issaeva, N.; Vassiliou, L.V.; Kolettas, E.; Niforou, K.; Zoumpourlis, V.C.; Takaoka, Ml; Nakagawa, H.; Tort, F.; Fugger, K.; Johansson, F.; Sehested, M.; Andersen, C.L.; Dyrskjot, L.; Orntoft, T.; Lukas, J.; Kittas, C.; Helleday, T.; Halazonetis, T.D.; Bartek, J.; Gorgoulis, V.G. (2006). Oncogene-induced senescence is part of the tumorigenesis barrier imposed by DNA damage checkpoints. Nature *444,* 633-637.

Bastos de Oliveira, F.M.; Harris, M.R.; Brazauskas, P.; de Bruin, R.A.; Smolka, M.B. (2012). Linking DNA replication checkpoint to MBF cell-cycle transcription reveals a distinct class of G1/S genes. EMBO J. *31,* 1798-1810.

Bastos de Oliveira, F.M.; Kim, D.; Cussiol, J.R.; Das, J.; Jeong, M.C.; Doerfler, L.; Schmidt, K.H.; Yu, H.; Smolka, M.B. (2015). Phosphoproteomics reveal distinct modes of Mec1/ATR signaling during DNA replication. Mol. Cell *57,* 1124-1132.

Bazzi, M.; Mantiero D.; Trovesi, C.; Lucchini, G.; Longhese, M.P. (2010). Dephosphorylation of γH2A by Glc7/protein phosphatase 1 promotes recovery from inhibition of DNA replication. Mol. Cell. Biol. *30,* 131-145.

Beckman, R.A.; Loeb, L.A. (2006). Efficiency of carcinogenesis with and without a mutator mutation. Proc. Natl. Acad. Sci. USA *103,* 14140-14145.

Benton, M.G.; Somasundaram, S.; Glasner, J.D.; Palecek, S.P. (2006). Analyzing the dose-dependence of the *Saccharomyces cerevisiae* global transcriptional response to methyl methanesulfonate and ionizing radiation. BMC Genomics *7,* 305.

Berens, T.J.; Toczyski, D.P. (2012). Colocalization of Mec1 and Mrc1 is sufficient for Rad53 phosphorylation *in vivo*. Mol. Biol. Cell *23,* 1058-1067.

Bloecher, A.; Venturi, G.M.; Tatchell, K. (2000). Anaphase spindle position is monitored by the BUB2 checkpoint. Nat. Cell Biol. *2,* 556-558.

Bjergbaek, L.; Cobb, J.A.; Tsai-Pflugfelder, M.; Gasser, S.M. (2005). Mechanistically distinct roles for Sgs1p in checkpoint activation and replication fork maintenance. EMBO J. *24,* 405-417.

Boiteux, S.; Jinks-Robertson, S. (2013). DNA repair mechanisms and the bypass of DNA damage in *Saccharomyces cerevisiae.* Genetics *193,* 1025-1064.

Bolderson, E.; Tomimatsu, N.; Richard, D.J.; Boucher, D.; Kumar, R.; Pandita, T.K.; Burma, S.; Khanna, K.K. (2010). Phosphorylation of Exo1 modulates homologous recombination repair of DNA double-strand breaks. Nucleic Acids Res. *38,* 1821-1831.

Bonilla, C.Y.; Melo, J.A.; Toczyski, D.P. (2008). Colocalization of sensors is sufficient to activate te DNA damage checkpoint in the absence of damage. Mol. Cell *30,* 267-276.

Bosotti, R.; Isacchi, A.; Sonnhammer, E.L. (2000). FAT: A novel domain in PIK-related kinases. Trends Biochem. Sci. *25,* 225-227.

Botuyan, M.V.; Lee, J.; Ward, I.M.; Kim, J.E.; Thompson, J.R.; Chen, J.; Mer, G. (2006). Structural basis for the methylation state-specific recognition of histone H4-K20 by 53BP1 and Crb2 in DNA repair. Cell *127,* 1361-1373.

Brown, E.J.; Baltimore, D. (2000). ATR disruption leads to chromosomal fragmentation and early embryonic lethality. Genes Dev. *14,* 397-402.

Branzei, D.; Vanoli, F.; Foiani, M. (2008). SUMOylation regulates Rad18-mediated template switch. Nature *456,* 915-920.

Branzei, D.; Foiani, M. (2009). The checkpoint response to replication stress. DNA Repair *8,* 1038-1046.

Branzei, D.; Foiani, M. (2010). Maintaining genome stability at the replication fork. Nat. Rev. Mol. Cell Biol. *11,* 208-219.

Burrell, R.A.; McGranahan, N.; Bartek, J.; Swanton, C. (2013). The causes and consequences of genetic heterogeneity in cancer evolution. Nature *501,* 338-345.

Busino, L.; Donzelli, M.; Chiesa, M.; Guardavaccaro, D.; Ganoth, D.; Dorello, N.V.; Hershko, A.; Pagano, M.; Draetta, G.F. (2003). Degradation of Cdc25S by beta-TrCP during S phase and in response to DNA damage. Nature *426,* 87-91.

Callebaut, I.; Mornon, J. P. (1997). From BRCA1 to RAP1, a widespread BRCT module closely associated with DNA repair *1,* FEBS Lett. *400*, 25-30.

Carnegie, G.K.; Sleeman, J.E.; Morrice, N.; Hastie, C.J.; Peggie, M.W.; Philp, A.; Lamond, A.I.; Cohen, P.T. (2003). Protein phosphatase 4 interacts with the Survival of Motor Neurons complex and enhances the temportal localization of snRNPs. J. Cell Sci. *116,* 1905-1913.

Carr, A.M. (2002). DNA structure dependent checkpoints as regulators of DNA repair. DNA Repair *1.* 983-994.

Chabes, A.; Georgieva, B.; Domkin, B.; Zhao, X.; Rothstein, R.; Thelander, L. (2003). Survival of DNA damage in yeast directly depends on increased dNTP levels allowed by relaxed feedback inhibition on ribonucleotide reductase. Cell *112,* 391-401.

Chan, D.W.; Ye, R.; Veillette, C.J.; Lees-Miller, S.P. (1999). DNA-dependent protein kinase phosphorylation sites in Ku 70/80 heterodimer. Biochemistry *38,* 1819-1828.

Chang, M.; Bellaoui, M.; Boone, C.; Brown, G.W. (2002). A genome-wide screen for methyl methanesulfonate-sensitive mutants reveals genes required for S phase progression in the presence of DNA damage. Proc. Natl. Acad. Sci. USA *99,* 16934-16939.

Chang, D.Y.; Lu, A.L. (2005). Interaction of checkpoint proteins Hus1/Rad1/Rad9 with DNA base excision repair enzyme MutY homolog in fission yeast. *Schizosaccharomyces pombe.* J. Biol. Chem. *280,* 408-417.

Chen, C.; Kolodner, R.D. (1999). Gross chromosomal rearrangements in *Saccharomyces cerevisiae* replication and recombination defective mutants. Nature Genetics *23,* 81-85.

Chen, P.; Luo, C.; Deng, Y.; Ryan, K.; Register, J.; Margosiak, S.; Tempcyzk-Russell, A.; Nguyen, B.; Myers, P.; Lundgren, K.; Kan, C.C.; O'Connor, P.M. (2000). The 1.7 A crystal structure of human cell cycle checkpoint kinase Chk1: implications for Chk1 regulation. Cell *100,* 681-692.

Chen, L.; Trujillo, K.; Ramos, W.; Sung, P.; Tomkinson, A.E. (2001). Promotion of Dnl4-catalyzed DNA end-joining by the Rad50/Mre11/Xrs2 and Hdf1/Hdf2 complexes. Mol. Cell *8,* 1105-1115.

Chen, L.; Trujillo, K.; Ramos, W.; Sung, P.; Tomkinson, A.E. (2001). Promotion of Dnl4-catalyzed DNA end-joining by the Rad50/Mre11/Xrs2 and Hdf1/Hdf2 complexes. Mol. Cell *8,* 1105-1115.

Chen, S.; Zhou, H. (2009). Reconstitution of Rad53 activation by Mec1 through adaptor protein Mrc1. J. Biol. Chem. *284,* 18593-18604.

Cheng, L.; Hunke, L.; Hardy, C.F. (1998). Cell cycle regulation of the *Saccharomyces cerevisiae* polo-like kinase Cdc5p. Mol. Cell. Biol. *18,* 7360-7370.

Cho, H.; Kim, T.K.; Mancebo, H.; Lane, W.S.; Flores, O.; Reinberg, D. (1999). A protein phosphatase functions to recycle RNA polymerase II. Genes Dev. *13,* 1540-1552.

Ciccia, A.; McDonald, N.; West, S.C. (2008). Structural and functional relationships of the XPF/MUS81 family of proteins. Annu. Rev. Biochem. *77,* 259-287.

Cimprich, K.A.; Cortez, D. (2008). ATR: An essential regulator of genome integrity. Nat. Rev. Mol. Cell Biol. *9,* 616-627.

Ciosk, R.; Zachariae, W.; Michaelis, C.; Shevchenko, A.; Mann, M.; Nasmyth, K. (1998). An ESP1/PDS1 complex regulates loss of sister chromatid cohesion at the metaphase to anaphase transition in yeast. Cell *93,* 1067-1076.

Cobb, J.; Bjergbaek, L.; Shimada, K.; Frei, C.; Gasser, S. (2003). DNA polymerase stabilization at stalled replication forks requires Mec1 and the RecQ helicase Sgs1. EMBO J. *22,* 4325-4336.

Cobb, J.; Schleker, T.; Rojas, V.; Bjergbaek, L.; Tercero, J.A.; Gasser, S.M. (2005). Replisome instability, fork collapse, and gross chromosomal rearrangements arise synergistically from Mec1 kinase and RecQ helicase mutations. Genes Dev. *19,* 3055-3069.

Cohen-Fix, O.; Koshland, D. (1997). The anaphase inhibitor of *Saccharomyces cerevisiae* Pds1p is a target of the DNA damage checkpoint pathway. Proc. Natl. Acad. Sci. USA *94,* 14361-14366.

Cortez, D.; Wang, Y.; Qin, J.; Elledge, S.J. (1999). Requirement of ATM-dependent phosphorylation of brca1 in the DNA damage response to double-strand breaks. Science *286,* 1162-1166.

Cortez, D.; Guntuku, S.; Qin, S.; Elledge, S. (2001). ATR and ATRIP: partners in checkpoint signaling. Science *294,* 1713-1716.

Costanzo, V.; Robertson, K.; Bibikova, M.; Kim, E.; Grieco, D.; Gottesman, M.; Carroll, D.; Gautier, J. (2001). Mre11 protein complex prevents double-strand break accumulation during chromosomal DNA replication. Mol. Cell *8,* 137-147.

Costanzo, V.; Shecter, D.; Lupardus, P.J.; Cimprich, K.A.; Gottesman, M.; Gautier, J. (2003). An ATR- and Cdc7-dependent DNA damage checkpoint that inhibits initiation of DNA replication. Mol. Cell *11,* 203-213.

Coulon, S.; Gaillard, P.H.; Chahwan, C.; McDonald, W.H.; Yates, J.R., 3rd; Russell, P. (2004). Slx1-Slx4 are subunits of a structure-specific endonuclease that maintains ribosomal DNA in fission yeast. Mol. Biol. Cell *15*, 71-80.

Cotta-Ramusino, C.; Fachinetti, D.; Lucca, C.; Doksani, Y.; Lopes, M.; Sogo, J.; Foiani, M. (2005). Exo1 processes stalled replication forks and counteracts fork reversal in checkpoint-defective cells. Mol. Cell *17,* 153-159.

Cotta-Ramusino, C.; McDonald, E.R. 3rd; Hurov, K.; Sowa, M.E.; Harper, J.W.; Elledge, S.J. (2011). A DNA damage response screen identifies RHINO, a 9-1-1 and TopBP1 interacting protein required for ATR signaling. Science *332,* 1313-1317.

Courcelle, J.; Hanawalt, P.C. (2003). RecA-dependent recovery of arrested DNA replication forks. Ann. Rev. Genetics *37,* 611-646.

Cox, M.M. (2001). Recombinational DNArepair of damaged replication forks in *Escherichia coli:* questions. Ann. Rev. Genetics *35,* 53-82.

Critchlow, S.E.; Jackson, S.P. (1998). DNA end-joining: from yeast to man. Trends Bio. Sci. *23,* 394-398.

Cuadrado, M.; Martinez-Pastor, B.; Murga, M.; Toledo, L.I.; Guierrez-Martinez, P.; Lopez, E.; Fernandez-Capetillo, O. (2006). ATM regulates ATR chromatin loading in response to DNA double-strand breaks. J. Exp. Med. *203,* 297-303.

Cui, D.Y.; Brown, C.R.; Chiang, H.L. (2004). The type 1 phosphatase Reg1p-Glc7p is required for the glucose-induced degradation of fructose-1,6-bisphosphatase in the vacuole. J. Biol. Chem. *279,* 9713-9724.

Cussiol, J.R.; Jablonowski, C.M.; Yimit, A.; Brown, G.W.; Smolka, M.B. (2015). Dampening DNA damage checkpoint signaling via coordinated BRCT domain interactions. EMBO J. *34,* 1704-1717.

Dart, D.A.; Adams, K.E.; Akerman, I.; Lakin, N.D. (2004). Recruitment of the cell cycle checkpoint kinase ATR to chromatin during S-phase. J. Biol. Chem. *279,* 16433-16440.

Davidson, M.B.; Katou, Y.; Keszthelyi, A.; Sing, T.L.; Xia, T.; Ou, J.; Vaisica, J.A.; Thevakumaran, N.; Marjavaara, L.; Myers, C.L.; Chabes, A.; Shirahige, K.; Brown, G.W. (2012). Endogenous DNA replication stress results in expansion of dNTP pools and a mutator phenotype. EMBO J. *31,* 895-907.

Davies, S.L.; North, P.S.; Dart, A.; Lakin, N.D.; Hickson, I.D. (2004). Phosphorylation of the Bloom's syndrome helicase and its role in recovery from S-phase arrest. Mol. Cell. Biol. *24,* 1279-1291.

Davies, S.L.; North, P.S.; Hickson, I.D. (2007). Role for BLM in replication-fork restart and suppression of origin firing after replicative stress. Nat. Struct. Mol. Biol. *14,* 677-679.

Davis, A.P.; Symington, L.S. (2004). RAD51-dependent break-induced replication in yeast. Mol. Cell. Biol. *24,* 2344-2351.

De Klein, A.; Muijtjens, M.; van Os, R.; Verhoeven, Y.; Smit, B.; Carr, A.M.; Lehmann, A.R.; Hoeijmakers, J.H. (2000). Targeted disruption of the cell-cycle checkpoint gene ATR leads to early embryonic lethality in mice. Curr. Biol. *10,* 479-482.

de la Torre-Ruiz, M.; Green, C.M.; Lowndes, N.F. (1998). *RAD9* and *RAD24* define two additive, interacting branches of the DNA damage checkpoint pathway in budding yeast normally required for Rad53 modification and activation. EMBO J. *17,* 2687-2698.

Delacroix, S.; Wagner, J.M.; Kobayashi, M.; Yamamoto, K.; Karnitz, L.M. (2007). The Rad9-Hus1-Rad1 (9-1-1) clamp activates checkpoint signaling via TopBP1. Genes Dev. *21,* 1472-1477.

Deng, C.; Brown, J.A.; You, D.; Brown, J.M. (2005). Multiple endonucleases function to repair covalent topoisomerase I complexes in *Saccharomyces cerevisiae*. Genetics *170*, 591-600.

Dozier, C.; Bonyadi, M.; Baricault, L.; Tonasso, L.; Darbon, J.M. (2004). Regulation of Chk2 phosphorylation by interaction with protein phosphatase 2A via its B' regulatory subunit. Biol. Cell *96,* 509-517.

den Elzen, N.R.; O'Connell, M.J. (2004). Recovery from DNA damage checkpoint arrest by PP1-mediated inhibition of Chk1. EMBO J. *23,* 908-918.

Desany, B.A.; Alcasabas, A.A.; Bachant, J.B.; Elledge, S.J. (1998). Recovery from DNA replicational stress is the essential function of the S-phase checkpoint pathway. Genes Dev. *12,* 2956-2970.

Doil, C.; Mailand, N.; Bekker-Jensen, S.; Menard, P.; Larsen, D.H.; Pepperkok, R.; Ellenberg, J.; Panier, S.; Durocher, D.; Bartek, J.; Lukas, J.; Lukas, C. (2009). RNF168 binds and amplifies ubiquitin conjugates on damaged chromosomes to allow accumulation of repair proteins. Cell *136,* 435-446.

Downs, J.A.; Lowndes, N.F.; Jackson, S.P. (2000). A role for *Saccharomyces cerevisiae* histone H2A in DNA repair. Nature *408,* 1001-1004.

Drablos, F.; Feyzi, E.; Aas, P.A.; Vaagbo, C.B.; Kavli, B.; et al. (2004). Alkylation damage in DNA and RNA-repair mechanisms and medical significance. DNA Repair *3,* 1389-1407.

Dubrana, K.; van Attikum, H.; Hediger, F.; Gasser, S.M. (2007). The processing of double-strand breaks and binding of single-strand-binding proteins RPA and Rad51 modulate the formation of ATR-kinase foci in yeast. J. Cell Sci. *120,* 4209-4220.

Duro, E.; Vaisica, J.; Brown, G.; Rouse, J. (2008). Budding yeast Mms22 and Mms1 regulate homologous recombination induced by replisome blockage. DNA Repair (Amst) *7,* 811-818.

Durocher, D.; Jackson, S.P. (2002). The FHA domain. FEBS Letters *513,* 58-66.

Duursma, A.M.; Driscoll, R.; Elias, J.E.; Cimprich, K.A. (2013) A role for the MRN complex in ATR activation via TOPBP1 recruitment. Mol. Cell *50,* 116-122.

El-Shemerly, M.; Hess, D.; Pyakurel, A.K.; Moselhy, S.; Ferrari, S. (2008). ATR-dependent pathways control hEXO1 stability in response to stalled forks. Nucleic Acids Res. *36,* 511-519.

Ellison, V.; Stillman, B. (2003). Biochemical characterization of DNA damage checkpoint complexes: clamp loader and clamp complexes with specificity for 5' recessed DNA. PLoS Biol. *1,* 231-241.

Emili, A. (1998). *MEC1*-dependent phosphorylation of Rad9p in response to DNA damage. Mol. Cell *2,* 183-189.

Enoch, T.; Nurse, P. (1990). Mutation of fission yeast cell cycle control genes abolishes dependence of mitosis on DNA replication. Cell *60,* 665-673.

Falbo, K.B.; Alabert, C.; Katou, Y.; Wu, S.; Han, J.; Wehr, T.; Xiao, J.; He, X.; Zhang, Z.; Shi, Y.; Shirahige, K.; Pasero, P.; Shen, X. (2009). Involvement of a chromatin remodeling complex in damage tolerance during DNA replication. Nat. Struct. Mol. Biol. *16,* 1167-1173.

Fekairi, S.; Scaglione, S.; Chahwan, C.; Taylor, E.R.; Tissier, A.; Coulon, S.; Dong, M.Q.; Ruse, C.; Yates, J.R. 3rd; Russell, P.; Fuchs, R.P.; McGowan, C.H.; Gaillard, P.H. (2009). Human SLX4 is a Holliday junction resolvase subunit that binds multiple DNA repair/recombination endonucleases. Cell *138,* 78-89.

Finn, K.; Lowndes, N.F.; Grenon, M. (2012). Eukaryotic DNA damage checkpoint activation in response to double-strand breaks. Cell. Mol. Life Sci. *69,* 1447-1473.

Fiscella, M.; Zhang, H.; Fan, S.; Sakaguchi, K.; Shen, S.; Mercer, W.E.; *et al.* (1997). Wip1, a novel human protein phosphatase that is induced in response to ionizing radiation in a p53-dependent manner. Proc. Natl. Acad. Sci. USA *94,* 6048-6053.

Flott, S.; Alabert, C.; Toh, G.W.; Toth, R.; Sugawara, N.; Campbell, D.G.; Haber, J.E.; Pasero, P.; Rouse, J. (2007). Phosphorylation of Slx4 by Mec1 and Tel1 regulates the single-strand annealing mode of DNA repair in budding yeast. Mol. Cell. Biol. *27,* 6433-6445.

Flott, S.; Rouse, J. (2005). Slx4 becomes phosphorylated after DNA damage in a Mec1/Tel1-dependent manner and is required for repair of DNA alkylation damage. Biochem. J. *391,* 325-333.

Foiani, M.; Pellicioli, A.; Lopes, M.; Lucca, C.; Ferrari, M.; Liberi, G.; Muzi Falconi, M.; Plevani, P. (2000). DNA damage checkpoints and DNA replication controls in *Saccharomyces cerevisiae.* Mutat. Res. *451,* 187-196.

Frei, C.; Gasser, S.M. (2000). The yeast Sgs1p helicase acts upstream of Rad53p in the DNA replication checkpoint and colocalizes with Rad53p in S-phase-specific foci. Genes Dev. *14,* 81-96.

Fricke, W.M., and Brill, S.J. (2003). Slx1-Slx4 is a second structure-specific endonuclease functionally redundant with Sgs1-Top3. Genes Dev. *17,* 1768-1778.

Friedel, A.M.; Pike, B.L.; Gasser, S.M. (2009). ATR/Mec1: Coordinating fork stability and repair. Curr. Opin. Cell. Biol. *21,* 237-244.

Fry, A.M.; Nigg, E.A. (1995). The NIMA kinase joins forces with Cdc2. Curr. Biol. *5,* 1122-1125.

Fujimoto, H.; Onishi, N.; Kato, N.; Takekawa, M.; Xu, X.Z.; Kosugi, A.; Kondo, T.; Imamura, M.; Oishi, I.; Yoda, A.; Minami, Y. (2006). Regulation of the antioncogenic Chk2 kinase by the oncogenic Wip1 phosphatase. Cell Death Diff. *13,* 1170-1180.

Furuya, K.; Poitelea, M.; Guo, L.; Caspari, T.; Carr, A.M. (2004). Chk1 activation requires Rad9 S/TQ-site phosphorylation to promote association with C-terminal BRCT domains of Rad4TOPBP1. Genes Dev. *18,* 1154-1164.

Gallina, I.; Colding, C.; Henriksen, P.; Beli, P.; Nakamura, K.; et al. (2015). Cmr/WDR76 defines a nuclear genotoxic stress body linking genome integrity and protein quality control. Nat. Commun. *6,* 6533.

Gallo-Fernández, M.; Saugar, I.; Ortiz-Bazán, M.A.; Vázquez, M.V.; Tercero, J.A. (2012). Cell cycle-dependent regulation of the nuclease activity of Mus81-Eme1/Mms4. Nucleic Acids Res. *40,* 8325-8335.

Gasch, A.P.; Huang, M.; Metzner, S.; Botstein, D.; Elledge, S.J.; Brown, P.O. (2001). Genomic expression responses to DNA-damaging agents and the regulatory role of the yeast ATR homolog Mec1p. Mol. Biol. Cell *12,* 2987-3003.

Gembka, A.; Toueille, M.; Smirnova, E.; Poltz, R.; Ferrari, E.; Villani, G.; Hübscher, U. (2007). The checkpoint clamp, Rad9-Rad1-Hus1 complex, preferentially stimulates the activity of apurinic/apyrimidinic endonuclease 1 and DNA polymerase β in long patch base excision repair. *35,* 2596-2608.

Giannattasio, M.; Lazzaro, F.; Plevani, P; Muzi-Falconi, M. (2005). The DNA damage checkpoint response requires histone H2B ubiquitination by Rad6-Bre1 and H3 methylation by Dot1. J. Biol. Chem. *280,* 9879-9886.

Gietz, D.; Jean, S.A.; Woods, R.A.; Schiestl, R.H. (1992). Improved method for high efficiency transformation of intact yeast cells. Nucleic Acids Res. *20,* 1425.

Gilbert, C.S.; Green, C.M.; Lowndes, N.F. (2001). Budding yeast Rad9 is an ATP-dependent Rad53 activating machine. Mol. Cell *8,* 129-136.

Gilbert, D.M.; Takebayashi, S.I.; Ryba, T.; Lu, J.; Pope, B.D.; Wilson, K.A.; Kiratani, I. (2010). Space and time in the nucleus: Developmental control of replication timing and chromosome architecture. Cold Spring Harbor Symp. *75,* 143-153.

Gingras, A.C.; Caballero, M.; Zarske, M.; Sanchez, A.; Hazbun, T.R.; Fields, S.; Sonenberg, N.; Hafen, E.; Raught, B.; Aebersold, R. (2005). A novel, evolutionarily conserved protein phosphatase complex involved in cisplatin sensitivity. Mol. Cell Proteomics *4,* 1725-1740.

Glover, D.M.; Hagan, I.M.; Tavares, A.A. (1998). Polo-like kinases: a team that plays throughout mitosis. Genes Dev. *12,* 3777-3787.

Goodarzi, A.A.; Jonnalagadda, J.C.; Douglas, P.; Young, D.; Ye, R.; Moorhead, G.B.; Lees-Miller, S.P.; Khanna, K.K. (2004). Autophosphorylation of ataxia-telangiectasia mutated is regulated by protein phosphatase 2A. EMBO J. *23,* 4451-4461.

Gorgoulis, V. G.; Vassiliou, L.V.; Karakaidos, P.; Zacharatos, P.; Kotsinas, A.; Liloglou, T.; Venere, M.; Ditullio, R.A. Jr.; Kastrinakis, N.G.; Levy, B.; Kletsas, D.; Yoneta, A.; Herlyn, M.; Kittas, C.; Halazonetis, T.D. (2005). Activation of the DNA damage checkpoint and genomic instability in human precancerous lesions. Nature *434,* 907-913.

Gottlieb, T.M.; Jackson, S.P. (1993). The DNA-dependent protein kinase: requirement for DNA ends and association with Ku antigen. Cell *72,* 131-142.

Gould, K.L.; Nurse, P. (1989). Tyrosine phosphorylation of the fission yeast *cdc2+* protein kinase regulates entry into mitosis. Nature *342,* 39-45.

Gould, K.L.; Moreno, S.; Owen, D.J.; Sazer, S.; Nurse, P. (1991). Phosphorylation at Thr167 is required for *Schizosaccharomyces pombe* p34(cdc2) function. EMBO J. *10,* 3297-3309.

Granata, M.; Lazzaro, F.; Novarina, D.; Panigada, D.; Puddu, F.; et al. (2010). Dynamics of Rad9 chromatin binding and checkpoint function are mediated by its dimerization and are cell cycle-regulated by CDK1 activity. PLoS Genet. *6,* e1001047.

Gravel, S.; Larrivee, M.; Labrecque, P.; Wellinger, R.J. (1998). Yeast Ku as a regulator of chromosomal DNA end structure. Science *280,* 741-744.

Grenon, M.; Gilbert, C.; Lowndes, N.F. (2001). Checkpoint activation in response to double-strand breaks requires the Mre11/Rad50/Xrs2 complex. Nat. Cell Biol. *3,* 844-847.

Grenon, M.; Costelloe, T.; Jimeno, S.; O'Shaughnessy, A.; Fitzgerald, J.; Zgheib, O.; Lowndes, N.F. (2007). Docking onto chromatin via the *Saccharomyces cerevisiae* Rad9 Tudor domain. Yeast *24,* 105-119.

Gritenaite, D.; Princz, L.N.; Szakal, B.; Bantele, S.C.; Wendeler, L.; Schilbach, S.; Habermann, B.H.; Matos, J.; Lisby, M.; Branzei, D.; Pfander, B. (2014). A cell cycle-regulated Slx4-Dpb11 complex promotes the resolution of DNA repair intermediates linked to stalled replication. Genes Dev. *28,* 1604-1619.

Guan, X.; Madabushi, A.; Chang, D.; Fitzgerald, M.E.; Shi, G.; Drohat, A.C.; Lu, A. (2007). The human checkpoint sensor Rad9-Rad1-Hus1 interacts with and stimulates DNA repair enzyme TDG glycosylase. Nucleic Acids Res. *35,* 6207-6218.

Guillermain, G.; Ma, E.; Mauger, S.; Miron, S.; Thai, R.; Guerois, R.; Ochsenbein, F.; Marsolier-Kergoat, M.C. (2007). Mechanisms of checkpoint kinase Rad53 inactivation after a double-strand break in *Saccharomyces cerevisiae.* Mol. Cell Biol. *27,* 3378-3389.

Halazonetis, T.D.; Gorgoulis, V.G.; Bartek, J. (2008). An oncogene-induced DNA damage model for cancer development. Science *319,* 1352-1355.

Hammet, A.; Magill, C.; Heierhorst, J.; Jackson, S.P. (2007). Rad9 BRCT domain interaction with phosphorylation H2AX regulates the G1 checkpoint in budding yeast. EMBO Rep. *8,* 851-857.

Hanahan, D.; Weinberg, R.A. (2011). Hallmarks of cancer: the next generation. Cell *144,* 646-674.

Harper, J.W.; Elledge, S.J. (2007). The DNA damage response: ten years after. Mol. Cell *28,* 739-745.

Harrison, J.C.; Haber, J.E. (2006). Surviving the breakup: the DNA damage checkpoint. Annu. Rev. Genet. *40,* 209-235.

Hartwell, L.H.; Weinert, T.A. (1989). Checkpoints: Controls that ensure the order of cell cycle events. Science *246,* 629-634.

Hegnauer, A.M.; Hustedt, N.; Shimada, K.; Pike, B.L.; Vogel, M.; Amsler, P.; Rubin, S.M.; van Leeuwen, F.; Guenole, A.; van Attikum, H.; Thoma, N.H.; Gasser, S.M. (2012). An N-terminal acidic region of Sgs1 interacts with Rpa70 and recruits Rad53 kinase to stalled forks. EMBO J. *31,* 3768-3783.

Hekmat-Nejad, M.; You, Z.; Ye, M.C.; Newport, J.W.; Cimprich, K.A. (2000). Xenopus ATR is a replication-dependent chromatin-binding protein required for the DNA replication checkpoint. Curr. Biol. *10,* 1565-1573.

Helt, C.E.; Wang, W.; Keng, P.C.; Bambara, R.A. (2005). Evidence that DNA damage detection machinery participates in DNA repair. Cell Cycle *4,* 529-532.

Hennessy, K.M.; Lee, A.; Chen, E.; Botstein, D. (1991). A group of interacting yeast DNA replication genes. Genes Dev. *5,* 958-969.

Herzinger, T.; Funk, J.O.; Hillmer, K.; Eick, D.; Wolf, D.A.; Kind, P. (1995). Ultraviolet B irradiation-induced G2 cell cycle arrest in human keratinocytes by inhibitory phosphorylation of the cdc2 cell cycle kinase. Oncogene *11,* 2151-2156.

Hickson, I.D.; Mankouri, H.W. (2011). Processing of homologous recombination repair intermediates by the Sgs1-Top3-Rmi1 and Mus81-Mms4 complexes. Cell Cycle *10,* 3078-3085.

Hoege, C.; Pfander, B.; Moldovan, G.L.; Pyrowolakis, G.; Jentsch, S. (2002). RAD6-dependent DNA repair is linked to modification of PCNA by ubiquitin and SUMO. Nature *419,* 135-141.

Hoeijmakers, J.H. (2009). DNA damage, aging, and cancer. N. Engl. J. Med. *361,* 1475-1485.

Hoglund, A.; Nilsson, L.M.; Muralidharan, S.V.; Hasvold, L.A.; Merta, P.; Rudelius, M.; Nikolova, V.; Keller, U.; Nilsson, J.A. (2011). Therapeutic implications for the induced levels of Chk1 in Myc-expressing cancer cells. Clin. Cancer Res. *17,* 7067-7079.

Hoyt, M.A.; Totis, L.; Roberts, B.T. (1991). *S. cerevisiae* genes required for cell cycle arrest in response to loss of microtubule function. Cell *66,* 507-517.

Hu, J.; Sun, L.; Shen, F.; Chen, Y.; Hua, Y.; Zhang, M.; Hu, Y.; Wang, Q.; Xu, W.; Sun, F.; Ji, J.; Murray, J.M.; Carr, A.M.; Kong, D. (2012). The intra-S phase checkpoint targets Dna2 to prevent stalled replication forks from reversing. Cell *149,* 1221-1232.

Hu, M.C.; Tang-Oxley, Q.; Qiu, W.R.; Wang, Y.P.; Mihindukulasuriya, K.A.; Afshar, R.; Tan, T.H. (1998). Protein phosphatase X interacts with c-Rel and stimulates c-Rel/nuclear factor kappaB activity. J. Biol. Chem. *273,* 33561-33565.

Hu, F.; Wang, Y.; Liu, D.; Li, Y.; Qin, J.; Elledge, S.J. (2001). Regulation of the Bub2/Bfa1 GAP complex by Cdc5 and cell cycle checkpoints. Cell *107,* 655-665.

Huang, J.C.; Svoboda, D.L.; Reardon, J.T.; Sancar, A. (1992). Human nucleotide excision nuclease removes thymine dimers from DNA by incising the 22nd phosphodiester bond 5' and the 6th phosphodiester bond 3' to the photodimer. Proc. Nat. Acad. Sci. USA *89,* 3664-3668.

Huang, M.; Zhou, Z.; Elledge, S.J. (1998). The DNA replication and damage checkpoint pathways induce transcription by inhibition of the Crt1 repressor. Cell *94,* 595-605.

Huang, R.Y.; Eddy, M.; Vujcic, M.; Kowalski, D. (2005). Genome-wide screen identifies genes whose inactivation confer resistance to cisplatin in *Saccharomyces cerevisiae*. Cancer Res. *65,* 5890-5897.

Huang, M.; Miao, Z.; Zhu, H.; Cai, Y.; Lu, W.; Ding, J. (2008). Chk1 and Chk2 are differentially involved in homologous recombination repair and cell cycle arrest in response to NA double-strand breaks induced by camptothecins. Mol. Cancer. Ther. *7,* 1440-1449.

Huen, M.S.; Grant, R.; Manke, I,; Minn, K.; Yu, X.; Yaffe, M.B.; Chen, J. (2007). RNF8 transduces the DNA-damage signal via histone ubiquitylation and checkpoint protein assembly. Cell *131,* 901-914.

Hustedt, N.; Seeber, A.; Sack, M.; Tsai-Pflufelder, M.; Bhullar, B.; Vlaming, H.; van Leeuwen, F.; Guénolé, A.; van Attikum, H.; Srivas, R.; Ideker, T.; Shimada, K.; Gasser, S.M. (2015). Yeast PP4 interacts with ATR homolog Ddc2-Mec1 and regulates checkpoint signaling. Mol. Cell *57,* 273-289.

Huyen, Y.; Zgheib, O.; Ditullio, R.A. Jr.; Gorgoulis, V.G.; Zacharatos, P.; Petty, T.J.; Sheston, E.A.; Mellert, H.S.; Stavridi, E.S.; Halazonetis, T.D. (2004). Methylated lysine 79 of histone H3 targets 53BP1 to DNA double-strand breaks. Nature *432,* 406-411.

Ira, G.; Pellicioli, A.; Balijja, A.; Wang, X.; Fiorani, S.; Carotenuto, W.; Liberi, G.; Bressan, D.; Wan, L.; Hollingsworth, N.M.; Haber, J.E.; Foiani, M. (2004). DNA end resection, homologous recombination and DNA damage checkpoint activation require CDK1. Nature *431,* 1011-1017.

Jazayeri, A.; Falck, J.; Lukas, C.; Bartek, J.; Smith, G.C.; Lukas, J.; Jackson, S.P. (2006). ATM- and cell cycle-dependent regulation of ATR in response to DNA double-strand breaks. Nat. Cell Biol. *8,* 37-45.

Jelinsky, S.A.; Samson, L.D. (1999). Global response of *Saccharomyces cerevisiae* to a alkylating agent. Proc. Nat. Acad. Sci. USA *96,* 1486-1491.

Jin, J.; Shirogane, T.; Xu, L.; Nalepa, G.; Qin, J.; Elledge, S.J.; Harper, J.W. (2003). SCFbeta-TRCP links Chk1 signaling to degradation of the Cdc25A protein phosphatase. Genes Dev. *17,* 3062-3074.

Jiricny, J. (2006). The multifaceted mismatch-repair system. Nat. Rev. Mol. Cell Biol. *7,* 335-346.

Kai, M.; Boddy, M.N.; Russell, P.; Wang, T.S. (2005). Replication checkpoint kinase Cds1 regulates Mus81 to preserve genome integrity during replication stress. Genes Dev. *19,* 919-932.

Kanke, M.; Kodama, Y.; Takahashi, T.S.; Nakagawa, T.; Masukata, H. (2012). Mcm10 plays an essential role in origin DNA unwinding after loading of the CMG components. EMBO J. *31,* 2182-2194.

Karlsson-Rosenthal, C.; Millar, J.B. (2006). Cdc25: Mechanisms of checkpoint inhibition and recovery. Trends Cell Biol. *16,* 285-292.

Karras, G.I.; Fumasoni, M.; Sienski, G.; Vanoli, F.; Branzei, D.; Jentsch, S. (2013). Noncanonical role of the 9-1-1 clamp in the error-free DNA damage tolerance pathway. Mol. Cell *49,* 536-546.

Kastan, M. B., and Bartek, J. (2004). Cell-cycle checkpoints and cancer. Nature *432,* 316-323.

Katou, Y.; Kanoh, Y.; Bando, M.; Noguchi, H.; Tanaka, H.; Ashikari, T.; Sugimoto, K.; Shirahige, K. (2003). S-phase checkpoint proteins Tof1 and Mrc1 form a stable replication-pausing complex. Nature *424,* 1078-1083.

Katsuragi, Y.; Sagata, N. (2004). Regulation of Chk1 kinase by autoinhibition and ATR-mediated phosphorylation. Mol. Biol. Cell *15,* 1680-1689.

Keogh, M.C.; Kim, J.A.; Downey, M.; Fillingham, J.; Chowdhury, D.; Harrison, J.C.; Onishi, M.; Datta, N.; Galicia, S.; Emili, A.; Lieberman, J.; Shen, X.; Buratowski, S.; Haber, J.E.; Durocher, D.; Greenblatt, J.F.; Krogan, N.J. (2006). A phosphatase complex that dephosphorylates gammaH2AX regulates DNA damage checkpoint recovery. Nature *439,* 497-501.

Kim, S.T.; Lim, D.S.; Canman, C.E.; Kastan, M.B. (1999). Substrate specificities and identification of putative substrates of ATM kinase family members. J. Biol. Chem. *274,* 37538-37543.

Kim, J.-A. A.; Hicks, W.M.; Li, J.; Tay, S.Y.; Haber, J.E. (2011). Protein phosphatases Pph3, Ptc2, and Ptc3 play redundant roles in DNA double-strand break repair by homologous recombination. Mol. Cell. Biol. *31,* 507-516.

Koboldt, D.C.; Zhang, Q.; Larson, D.E.; Shen, D.; McLellan, M.D. Lin, L.; Miller, C.A.; Mardis, E.R.; Ding, L.; Wilson, R.K (2012). VarScan 2: somatic mutation and copy number alteration discovery in cancer by exome sequencing. Genome Res. *22,* 568-576.

Kolas, N.K.; Chapman, J.R.; Nakada, S.; Ylanko, J.; Chahwan, R.; Sweeney, F.D; Panier, S.; Mendez, M.; Wildenhain, J.; Thomson, T.M; Pelletier, L.; Jackson, S.P.; Durocher, D. (2007). Orchestration of the DNA-damage response by the RNF8 ubiquitin ligase. Science *318,* 1637-1640.

Kozubowski L.; Panek H.; Rosenthal, A.; Bloecher, A.; DeMarini, D.J.; Tatchell, K. (2003). A Bni4-Glc7 phosphatase complex that recruits chitin synthase to the site of bud emergence. Mol. Biol. Cell *14,* 26-39.

Kumagai, A.; Lee, J.; Yoo, H.Y.; Dunphy, W.G. (2006). TopBP1 activates the ATR-ATRIP complex. Cell *124,* 943-955.

Kumar, S.; Burgers, P.M. (2013). Lagging strand maturation factor Dna2 is a component of the replication checkpoint initiation machinery. Genes Dev. *27,* 313-321.

Larson, J.R.; Bharucha, J.P.; Ceasar, S.; Salamon, J.; Richardson, C.J.; Rivera, S.M.; Tatchell, K. (2008). Protein phosphatase type 1 directs chitin synthesis at the bud neck in *Saccharomyces cerevisiae.* Mol. Biol. Cell *19,* 3040-3051.

Lavin, M.F.; Kozlov, S. (2007). ATM activation and DNA damage response. Cell Cycle *6,* 931-942.

Lee, C.; Chung, J.H. (2001). The hCds1 (Chk2)-FHA domain is essential for a chain of phosphorylation events on hCds1 that is induced by ionizing radiation. J. Biol. Chem. *276,* 30537-30541.

Lee, S.J.; Schwartz, M.F.; Duong, J.K.; Stern, D.F. (2003). Rad53 phosphorylation site clusters are important for Rad53 regulation and signaling. Mol. Cell Biol. *23,* 6300-6314.

Lee, J.; Kumagai, A.; Dunphy, W.G. (2007). The Rad9-Hus1-Rad1 checkpoint clamp regulates interaction of TopBP1 with ATR. J. Biol. Chem. *282,* 28036-28044.

Lee, Y.D.; Wang, J.; Stubbe, J.; Elledge, S.J. (2008). Dif1 is a DNA-damage-regulated facilitator of nuclear import for ribonucleotide reductatase. Mol. Cell *32,* 70-80.

Lenssen, E.; James, N.; Pedruzzi, I.; Dubouloz, F.; Cameroni, E.; Bisig, R.; Maillet, L.; Werner, M.; Rossen, J.; Petrovic, K.; Winderickx, J.; Collart, M.; De Virgilio, C. (2005). The Ccr-Not complex independently controls both Msn2-dependent transcriptional activation-via a newly identified Glc7/Bud14 type 1 protein phosphatase module- and TFIID promoter distribution. Mol. Cell. Biol. *25,* 488-498.

Leroy, C., Lee, S.E. Vaze, M. B., Ochsenbien, F., Guerois, R., Haber, J. E., and Marsolier-Kergoat, M. C. (2003). PP2C phosphatases Ptc2 and Ptc3 are required for DNA checkpoint inactivation after a double-strand break. Mol. Cell *11,* 827-835.

Leung-Pineda, V.; Ryan, C.E.; Piwnica-Worms, H. (2006). Phosphorylation of Chk1 by ATR is antagonized by a Chk1-regulated protein phosphatase 2A circuit. Mol. Cell Biol. *26,* 7529-7538.

Li, H.H.; Cai, X.; Shouse, G.P.; Piluso, L.G.; Liu, X. (2007). A specific PP2A regulatory subunit, B56gamma, mediates DNA damaged-induced dephosphorylation of p53 at Thr55. EMBO J. *26,* 402-411.

Li, N.; Jablonowski, C.; Jin, H.; Zhong, W. (2009). Stand-alone rolling circle amplification combined with capillary electrophoresis for specific detection of small RNA. Anal. Chem. *81,* 4906-4913.

Li, X.; Liu, K.; Li, F.; Wang, J.; Huang, H.; Wu, J.; Shi, Y. (2012). Structure of C-terminal tandem BRCT repeats of Rtt107 protein reveals critical role in interaction with phosphorylated histone H2A during DNA damage response. J. Biol. Chem. *287,* 9137-9146.

Lindahl, T. (1993). Recovery of antediluvian DNA. Nature 362, 709-715.

Lisby, M.; Barlow, J.H.; Burgess, R.C.; Rothstein, R. (2004). Choreography of the DNA damage response: spatiotemporal relationships among checkpoint and repair proteins. Cell *118,* 699-713.

Lisby, M.; Rothstein, R. (2009). Choreography of recombination proteins during the DNA damage response. DNA Repair *8,* 1068-1076.

Liu, Q.; Guntuku, S.; Cui, X.S.; Matsuoka, S.; Cortez, D.; Tamai, K.; Luo, G.; Carattini-Rivera, S.; DeMayo, F.; Bradley, A.; et al. (2000). Chk1 is an essential kinase thatis regulated by ATR and required for the G(2)/M DNA damage checkpoint. Genes Dev. *14,* 1448-1459.

Liu, Y.; West, S. (2004). Happy Hollidays: 40th anniversary of the Holliday junction. Nat. Rev. Mol. Cell Biol. *5,* 937-944.

Liang, X.; Reed, E.; Yu, J.J. (2006). Protein phosphatase 2A interacts with Chk2 and regulates phosphorylation at Thr-68 after cisplatin treatment of human ovarian cancer cells. Int. J. Mol. Med. *17,* 703-708.

Longtine, M.S.; McKenzie, A. 3rd.; Demarini, D.J.; Shah, N.G.; Wach, A.; et al. (1998). Additional modules for versatile and economical PCR-based gene deletion and modification in *Saccharomyces cerevisiae*. Yeast *14,* 953-961.

Lopes, M.; Cotta-Ramusino, C.; Pellicioli, A.; Liberi, G.; Plevani, P.; Muzi-Falconi, M.; Newlon, C.S.; Foiani, M. (2001). The DNA replication checkpoint response stabilizes stalled replication forks. Nature *412,* 557-561.

Lopez-Mosqueda, J.; Maas, N.L.; Jonsson, Z.O.; DeFazio-Eli, L.G.; Wohlschlegel, J.; Toczyski, D.P. (2010). Damage-induced phosphorylation of Sld3 is important to block late origin firing. Nature *467,* 479-485.

Lowe, S.W.; Cepero, E.; Evan, G. (2004). Intrinsic tumour suppression. Nature *432,* 307-315.

Lu, K.P.; Hunter, T. (1995). Evidence for a NIMA-like mitotic pathway in vertebrate cells. Cell *81,* 30530-30537.

Lu, X.; Nguyen, T.A.; Donehower, L.A. (2005). Reversal of the ATM/ATR-mediated DNA damage response by the oncogenic phosphatase PPM1D. Cell Cycle *4,* 1060-1064. (a)

Lu, X.; Nannenga, B.; Donehower, L.A. (2005). PPM1D dephosphorylates Chk1 and p53 and abrogates cell cycle checkpoints. Genes Dev. *19,* 1162-1174. (b)

Lucca, C.; Vanoli, F.; Cotta-Ramusino, C.; Pellicioli, A.; Liberi, G.; Haber, J.; Foiani, M. (2004). Checkpoint-mediated control of replisome-fork association and signalling in response to replication pausing. Oncogene *23,* 1206-1213.

Lukas, C.; Falck, J.; Bartkova, J.; Bartek, J.; Lukas, J. (2003). Distinct spatiotemporal dynamics of mammalian checkpoint regulators induced by DNA damage. Nat. Cell Biol. *5,* 255-260.

Lundgren, K.; Walworth, N.; Booher, R.; Dembski, M.; Kirschner, M.; Beach, D. (1991). *mik1* and *wee1* cooperate in the inhibitor tyrosine phosphorylation of *cdc2*. Cell *64,* 1111-1122.

Ma, J.L.; Lee, S.J.; Duong, J.K.; Stern, D.F. (2006). Activation of the checkpoint kinase Rad53 by the phosphatidyl inositol kinase-like kinase Mec1. J. Biol. Chem. *281,* 3954-3963.

MacDougall, C.A.; Byun, T.S.; van, C.; Yee, M.C.; Cimprich, K.A. (2007). The structural determinants of checkpoint activation. Genes Dev. *21,* 898-903.

Mailand, N.; Bekker-Jensen, S.; Faustrup, H.; Melander, F.; Bartek, J.; Lukas, C.; Lukas, J. (2007). RNF8 ubiquitylates histones at DNA double-strand breaks and promotes assembly of repair proteins. Cell *131,* 887-900.

Majka, J.; Binz, S.K.; Wold, M.S.; Burgers, P.M. (2006). Replication protein A directs loading of the DNA damage checkpoint clamp to 5'-DNA junctions. J. Biol. Chem. *281,* 27855-27861. (a)

Majka, J.; Niedziela-Majka, A.; Burgers, P.M. (2006). The checkpoint clamp activates Mec1 kinase during initiation of the DNA damage checkpoint. Mol. Cell *24,* 891-901. (b)

Mantiero, D.; Clerici, M.; Lucchini, G.; Longhese, M.P. (2007). Dual role for *Saccharomyces cerevisiae* Tel1 in the checkpoint response to double-strand breaks. EMBO Rep. *8,* 380-387.

Mantiero, D.; Mackenzie, A.; Donaldson, A.; Zegerman, P. (2011). Limiting replication initiation factors execute the temporal programme of origin firing in budding yeast. EMBO J. *30,* 4805-4814.

Martin, S.G.; Laroche, T.; Suka, N.; Grunstein, M.; Gasser, S.M. (1999). Relocalization of telomeric Ku and SIR proteins in response to DNA strand breaks in yeast. Cell *97,* 621-633.

Masumoto, H.; Muramatsu, S.; Kamimura, Y.; Araki, H. (2002). S-Cdk-dependent phosphorylation of Sld2 essential for chromosomal DNA replication in budding yeast. Nature *415,* 651-655.

Matsuoka, S.; Roman, G.; Ogawa, A.; Shiloh, Y.; Tamai, K.; Elledge, S.J. (2000). Ataxia telangiectasia-mutated phosphorylates Chk2 *in vivo* and *in vitro.* Proc. Natl. Acad. Sci. USA *97,* 10389-10394.

McGowan, C.H.; Russell, P. (1993). Human Wee1 kinase inhibits cell division by phosphorylating p34(cdc2) on Tyr15. EMBO J. *12,* 75-85.

Meister, P.; Taddei, A.; Vernis, L.; Poidevin, M.; Gasser, S.M.; Baldacci, G. (2005). Temporal separation of replication and recombination requires the intra-S checkpoint. J. Cell Biol. *168,* 537-544.

Melchionna, R.; Chen, X.B.; Blasina, A.; McGowan, C.H. (2000). Threonine 68 is required for radiation-induced phosphorylation and activation of Cds1. Nat. Cell. Biol. *2,* 762-765.

Melo, J., and Toczyski, T. (2002). A unified view of the DNA-damage checkpoint. Curr. Opin. Cell Biol. *14,* 237-245.

Michaelis, C.; Ciosk, R.; Nasmyth, K. (1997). Cohesins: chromosomal proteins that prevent premature separatin of sister chromatids. Cell *91*, 32-46.

Michel, B.; Ehrlich, S.D.; et al. (1997). DNA double-strand breaks caused by replication arrest. EMBO J. *16,* 430-438.

Moorhead, G.B.; Trinkle-Mulcahy, L.; Ulke-Lemee, A. (2007). Emerging roles of nuclear protein phosphatases. Nat. Rev. Mol. Cell Biol. *8,* 234-244.

Mordes, D.A.; Glick, G.G.; Zhao, R.; Cortez, D. (2008). TopBP1 activates ATR through ATRIP and a PIKK regulatory domain. Genes Dev. *22,* 1478-1489. (a)

Mordes, D.A.; Nam, E.A.; Cortez, D. (2008). Dpb11 activates the Mec1-Ddc2 complex. Proc. Nat. Acad. Sci. USA *105,* 18730-18734. (b)

Morgan, D.O. (1999). Regulation of the APC and the exit from mitosis. Nat. Cell Biol. *1,* E47-E53.

Morin, I.; Ngo, H.P.; Greenall, A.; Zubko, M.K.; Morrice, N.; Lydall, D. (2008). Checkpoint-dependent phosphorylation of Exo1 modulates the DNA damage response. EMBO J. *27,* 2400-2410.

Mose, S.; Class, R.; Weber, H.W.; Oszyald, A.; Rahn, A.; Brady, L.W.; Bottcher, H.D. (2002). Combined radiotherapy and gemcitabine. Evaluation of clinical data based on experimental knowledge. Strahlenther Onkol. *178,* 59-70.

Mullen, J.R.; Kaliraman, V.; Ibrahim, S.S.; Brill, S. J. (2001). Requirement for three novel protein complexes in the absence of the Sgs1 DNA helicase in *Saccharomyces cerevisiae*. Genetics *157,* 103-118.

Muñoz, I.M.; Déclais, A.C.; Gardiner, M.; Toh, G.W.; Sanchez-Pulido, L.; Heuckmann, J.M.; Toth, R.; Macartney, T.; Eppink, B.; Kanaar, R.; Ponting, C.P.; Lilley, D.M.; Rouse, J. (2009). Coordination of structure-specific nucleases by human SLX4/BTBD12 is required for DNA repair. Mol. Cell *35,* 116-127.

Murga, M.; Campaner, S.; Lopez-Contreras, A.J.; Toledo, L.I.; Soria, R.; Montana, M.F.; D'Artista, L.; Schleker, T.; Guerra, C.; Garcia, E.; Barbacid, M.; Hidalgo, M.; Amati, B.; Fernandez-Capetillo, O. (2011). Exploiting oncogene-induced replicative stress for the selective killing of Myc-driven tumors. Nat. Struct. Mol. Biol. *18,* 1331-1335.

Mustelin, T. (2007). A brief introduction to the protein phosphatase families. Methods Mol. Biol. *365,* 9-22.

Myers, J.S.; Cortez, D. (2006). Rapid activation of ATR by ionizing radiation requires ATM and Mre11. J. Biol. Chem. *281,* 9346-9350.

Myung, K.; Datta, A.; Kolodner, R.D. (2001). Suppression of spontaneous chromosomal rearrangements by S phase checkpoint functions in *Saccharomyces cerevisiae*. Cell *104,* 397-408.

Myung, K.; Chen, C.; Kolodner, R.D. (2001). Multiple pathways cooperate in the suppression of genome instability in *Saccharomyces cerevisiae*. Nature *411,* 1073-1076. (b).

Myung, K.; Kolodner, R. (2002). Suppression of genome instability by redundant S-phase checkpoint pathways in *Saccharomyces cerevisiae*. Proc. Natl. Acad. Sci. USA *99,* 4500-4507.

Nakada, D.; Hirano, Y.; Tanaka, Y.; Sugimoto, K. (2005). Role of the C terminus of Mec1 checkpoint kinase in its localization to sites of DNA damage. Mol. Biol. Cell *16,* 5227-5235.

Navadgi-Patil, V.M.; Burgers, P.M. (2009). The unstructured C-terminal tail of the 9-1-1 clamp subunit Ddc1 activates Mec1/ATR via two distinct mechanisms. Mol. Cell *36,* 743-753.

Navadgi-Patil, V.M.; Burgers, P.M. (2011). Cell-cycle=specific activators of the Mec1/ATR checkpoint kinase. Biochem. Soc. Trans. *39,* 600-605.

Navadgi-Patil, V.M.; Kumar, S.; Burgers, P.M. (2011). The unstructured C-terminal tai of yeast Dpb11 (human TopBP1) protein is dispensable for DNA replication and the S phase checkpoint but required for the G2/M checkpoint. J. Biol. Chem. *286,* 40999-41007.

Navas, T.A.; Sanchez, Y.; Elledge, S.J. (1996). *RAD9* and DNA polymerase epsilon form parallel sensory branches for transducing the DNA damage checkpoint signal in *Saccharomyces cerevisiae.* Genes Dev. *15,* 2632-2643.

Naylor, M.L.; Li, J.; Osborn, A.J.; Elledge, S.J. (2009). Proc. Natl. Acad. Sci. *106,* 12765-12770.

Nielson, O.; Løbner-Olesen, A. (2008). Once in a lifetime: Strategies for preventing re-replication in prokaryotic and eukaryotic cells. EMBO Rep. *9,* 151-156.

Nigg, E.A. (1998). Polo-like kinases: positive regulators of cell division from start to finish. Curr. Opin. Cell Biol. *10,* 776-783.

Nordlund, P.; Reichard, P. (2006). Ribonucleotide reductases. Annu. Rev. Biochem. *75,* 681-706.

O'Connor, P.M.; Ferris, D.K.; Hoffmann, I.; Jackman, J.; Draetta, G.; Kohn, K.W. (1994). Role of the cdc25 phosphatase in G2 arrest induced by nitrogen mustard. Proc. Natl. Acad. Sci. *91,* 9480-9484.

O'Neill, B.M.; Hanway, D.; winzeler, F.A.; Romesberg, F.E. (2004). Coordinated functions of WSS1, PSY2, and TOF1 in the DNA damage response. Nucleic Acids *32,* 6519-6530.

O'Neill, B.M.; Szyjka, S.J.; Lis, E.T.; Bailey, A.O.; Yates IIIrd, J.R.; Aparicio, O.M.; Romesberg, F.E. (2007). Pph3-Psy2 is a phosphatase complex required for Rad53 dephosphorylation and replication fork restart during recovery from DNA damage. Proc. Natl. Acad. Sci. U.S.A. *104*, 9290-9295.

Oe, T.; Nakajo, N.; Katsuragi, Y.; Okazaki, K.; Sagata, N. (2001). Cytoplasmic occurrence of the Chk1/Cdc25 pathway and regulation of Chk1 in Xenopus oocytes. Dev. Biol. *229,* 250-261.

Ohouo, P.Y.; Bastos de Oliveira, F.M.; Almeida, B.S.; Smolka, M.B. (2010). DNA damage signaling recruits the Rt107-Slx4 scaffolds via Dpb11 to mediate replication stress response. Mol. Cell *39,* 300-306.

Ohouo, P.Y.; Smolka, M.B. (2012). The many roads to checkpoint activation. Cell Cycle *11,* 4495.

Ohouo, P.Y.; Bastos de Oliveira, F.M.; Liu, Y.; Ma, C.J.; Smolka, M.B. (2013). DNA-repair scaffolds dampen checkpoint signalling by counteracting the adaptor Rad9. Nature *493,* 120-124.

Oliva-Trastoy, M. Berthonaud, V.; Chevalier, A.; Ducrot, C.; Marsolier-Kergoat, M.C.; Mann, C.; Leteurtre, F. (2007). The Wip1 phosphatase (PPM1D) antagonizes activation of the Chk2 tumour suppressor kinase. Oncogene *26,* 1449-1458.

Osborn, A.J.; Elledge, S.J. (2003). Mrc1 is a replication fork component whose phosphorylation in response to DNA replication stress activates Rad53. Genes Dev. *17,* 1755-1767.

Paciotti, V.; Lucchini, G.; Plevani, P.; Longhese, M.P. (1998). Mec1p is essential for phosphorylation of the yeast DNA damage checkpoint protein Ddc1p, which physically interacts with Mec3p. EMBO J. *17,* 4199-4209.

Palou, G.; Palou, R.; Zeng, F.; Vashisht, A.A.; Wohlschlegel, J.A.; Quintana, D.G. (2015). Three different pathways prevent chromosome segregation in the presence of DNA damage or replication stress in budding yeast. PLoS Genet. *11,* e1005468.

Paques, F.; Haber, J.E. (1999). Multiple pathways of recombination induced by double-strand breaks in *Saccharomyces cerevisiae.* Microbiol. Mol. Biol. Rev. *63,* 349-404.

Paull, T.T.; Gellert, M. (2000). A mechanistic basis for Mre11-directed DNA joining at microhomologies. PNAS *97,* 6409-6414.

Paulovich, A.G.; Armour, C.D.; Hartwell, L.H. (1998). The *Saccharmyces cerevisiae RAD9, RAD17, RAD24,* and *MEC3* genes are required for tolerating irreparable, ultraviolet-induced DNA damage. Genetics *150,* 75-93.

Peggie MW, et al. (2002) Essential functions of Sds22p in chromosome stability and nuclear localization of PP1. J Cell Sci *115*, 195-206.

Pei, H.; Zhang, L.; Luo, K.; Qin, Y.; Chesi, M.; Fei, F.; Bergsagel, P.L.; Wang, L.; You, Z.; Lou, Z. (2011). MMSET regulates histone H4K20 methylation and 53BP1 accumulation at DNA damage sites. Nature *470,* 124-128.

Pellicioli, A.; Lucca, C.; Liberi, G.; Marini, F.; Lopes, M.; et al. (1999). Activation of Rad53 kinase in response to DNA damage and its effect in modulating phosphorylation of the lagging strand DNA polymerase. EMBO J. *18,* 6561-6572.

Pellicioli, A.; Lee, S.E.; Lucca, C.; Foiani, M.; Haber, J.E. (2001). Regulation of *Saccharomyces* Rad53 checkpoint kinase during adaptation from DNA damage-induced G2/M arrest. Mol. Cell *7,* 293-300.

Pellicioli, A.; Foiani, M. (2005). Signal transduction: how Rad53 kinase is activated. Curr. Biol. *15,* R769-R771.

Peng, C.Y.; Graves, P.R.; Thoma, R.S.; Wu, Z.; Shaw, A.S.; Piwnica-Worms, H. (1997). Mitotic and G2 checkpoint control: Regulation of 14-3-3 protein binding by phosphorylation of Cdc25C on serine-216. Science *277,* 1501-1505.

Pereira, G.; Hofken, T.; Grindlay, J.; Manson, C.; Schiebel, E. (2000). The Bub2p spindle checkpoint links nuclear migration with mitotic exit. Mol. Cell *6,* 1-10.

Petukhova, G.; Sung, P.; Klein, H. (2000). Promotion of Rad51-dependent D-loop formation by yeast recombination factor Rdh54/Tid1. Genes Dev. *14,* 2206-2215.

Pfander, B.; Diffley, J.F. (2011). Dpb11 coordinates Mec1 kinase activations with cell cycle-regulated Rad9 recruitment. EMBO J. *30,* 4897-4907.

Phillips, D.H.; Hewer, A.; Martin, C.N.; Colin, R.; King, M.M. (1988). Correlation of DNA adduct levels in human lung with cigarette smoking. Nature *336,* 790-792.

Pike, B.I.; Yongkiettrakul, S.; Tsai, M.; Heierhorst, J. (2003). Diverse but overlapping functions of the two forkhead-associated (FHA) domains in Rad53 checkpoint kinase activation. J. Biol. Chem. *278,* 30421-30424.

Pike, B.I.; Tenis, N.; Heierhorst, J. (2004). Rad53 kinase activation-independent replication checkpoint function of the N-terminal forkhead-associated (FHA1) domain. J. Biol. Chem. *279,* 39636-39644.

Puddu, F.; Granata, M.; di Nola, L.; Balestrini, A.; Piergiovanni, G.; Lazzaro, F.; Giannattasio, M.; Plevani, P.; Muzi-Falconi, M. (2008). Phosphorylation of the budding yeast 9-1-1 complex is required for Dpb11 function in the full activation of the UV-induced DNA damage checkpoint. Mol. Cell. Biol. *28,* 4782-4793.

Puddu, F.; Piergiovanni, G.; Plevani, P.; Muzi-Falconi, M. (2011). Sensing of replication stress and Mec1 activation act throught two independent pathways involving the 9-1-1 complex and DNA polymerase epsilon. PLoS Genet. *7,* e1002022.

Qu, M.; Rappas, M.; Wardlaw, C.P.; Garcia, V.; Ren, J.; Day, M.; Carr, A.M.; Oliver, A.W.; Du, L.; Pearl, L.H. (2013). Phosphorylation-dependent assembly and coordination of the DNA damage checkpoint apparatus by Rad4/TopBP1. Mol. Cell *51,* 723-736.

Randall, J.C.; Fan, A.; Chan, C.; Francis, L.I.; Heller, R.C.; Galani, K.; Bell, S.P. (2010). Mec1 is one of multiple kinases that prime the Mcm2-7 helicase for phosphorylation by Cdc7. Mol. Cell *40,* 353-363.

Reaper, P.M.; Griffiths, M.R.; Long, J.M.; Charrier, J.D.; Maccormick, S.; Charlton, P.A.; Golec, J.M.; Pollard, J.R. (2011). Selective killing of ATM- or p53-deficient cancer cells through inhibition of ATR. Nat. Chem. Biol. *7,* 428-430.

Rhind, N.; Furnari, B.; Russell, P. (1997). Cdc2 tyrosine phosphorylation is required for the DNA damage checkpoint in fission yeast. Genes Dev. *11,* 504-511.

Rhind, N.; Russell, P. (1998). Tyrosine phosphorylation of cdc2 is required for the replication checkpoint in *Schizosaccharomyces pombe*. Mol. Cell. Biol. *18,* 3782-3787.

Roberts, T. M.; Kobor, M. S.; Bastin-Shanower, S. A.; Ii, M.; Horte, S. A.; Gin, J. W.; Emili, A.; Rine, J.; Brill, S. J.; Brown, G. W. (2006). Slx4 regulated DNA damage checkpoint-dependent phosphorylation of the BRCT domain protein Rtt107/Esc4. Mol. Biol. Cell *17,* 539-548.

Roberts, T.; Zaidi, I.; Vaisica, J.; Peter, M.; Brown, G. (2008). Regulation of Rtt107 recruitment to stalled DNA replication forks by the cullin Rtt101 and the Rtt109 acetyltransferase. Mol. Biol. Cell *19,* 171-180.

Rouse, J. (2004). Esc4p, a new target of Mec1p (ATR), promotes resumption of DNA synthesis after DNA damage. EMBO J. *23,* 1188-1197.

Rouse, J. (2009). Control of genome stability by Slx protein complexes. Biochem. Soc. Trans. *37,* 495-510.

Sancar, A.; Lindsey-Boltz, L.A.; Unsal-Kacmaz, K.; Linn, S. (2004). Molecular mechanisms of mammalian DNA repair and the DNA damage checkpoints. Annu. Rev. Biochem. *73,* 39-85.

Sanchez, Y.; Desany, B.A.; Jones, W.J.; Liu, Q.; Wang, B.; Elledge, S.J. (1996). Regulation of *RAD53* by the *ATM*-like kinases *MEC1* and *TEL1* in yeast cell cycle checkpoint pathways. Science *271,* 357-360.

Sanchez, Y.; Wong, C.; Thoma, R.S.; Richman, R.; Wu, Z.; Piwnica-Worms, H. Elledge, S.J. (1997). Conservation of the Chk1 checkpoint pathway in mammals: linkage of DNA damage to Cdk1 rgulation through Cdc25. Science *277,* 1497-1501.

Sanchez, Y.; Bachant, J.; Wang, H.; Hu, F.; Liu, D.; Tetzlaff, M.; Elledge, S.J. (1999). Control of the DNA damage checkpoint by Chk1 and Rad53 protein kinases through distinct mechanisms. Science *286,* 1166-1171.

Santocanale, C.; Diffley, J.F. (1998). A Mec1- and Rad53-dependent checkpoint controls late-firing origins of DNA replication

Sanz, M.; Castrejon, F; Duran, A.; Roncero, C. (2004) *Saccharomyces cerevisiae* Bni4p directs the formation of the chitin ring and also participates in the correct assembly of the septum structure. Microbiology 150(Pt 10):3229-41

Sarbajna, S.; West, S.C. (2014). Holliday junction processing enzymes as guardians of genome stability. Trends Biochem. Sci. *39,* 409-419.

Saugar, I.; Vazquez, M.V.; Gallo-Fernandez, M.; Ortiz-Bazan, M.A.; Segurado, M.; Calzada, A.; Tercero, J.A. (2013). Temporal regulation of the Mus81-Mms4 endonuclease ensures cell survival under conditions of DNA damage. Nucleic Acids Res. *41,* 8943-8958.

Scholes, D.T.; Banerjee, M.; Bowen, B.; Curcio, M. J. (2001). Multiple regulators of Ty1 transposition in *Saccharomyces cerevisiae* have conserved roles in genome maintenance. Genetics *159,* 1449-1465.

Schwartz M.F.; Duong, J.K.; Sun, Z.; Morrow, J.S.; Pradhan, D.; Stern, D.F. (2002). Rad9 phosphorylation sites couple Rad53 to the *Saccharomyces cerevisiae* DNA damage checkpoint. Mol. Cell *9,* 1055-1065.

Schwarz, J.K.; Lovly, C.M.; Piwnica-Worms, H. (2003). Regulation of the Chk2 protein kinase by oligomerization-mediated cis- and trans-phosphorylation. Mol. Cancer Res. *1,* 598-609.

Segurado, M.; Diffley, J.F. (2008). Separate roles for the DNA damage checkpoint protein kinases in stabilizing DNA replication forks. Genes Dev. *22,* 1816-1827.

Shen, X.; Mizuguchi, G.; Hamiche, A.; Wu, C. (2000). A chromatin remodelling complex involved in transcription and DNA processing. Nature *406,* 541-544.

Shimada, K.; Oma, Y.; Schleker, T.; Kugou, K.; Ohta, K.; Harata, M.; Gasser, S.M. (2008). Ino80 chromatin remodeling complex promotes recovery of stalled replication forks. Curr. Biol. *18,* 566-575.

Shiotani, B.; Zou, L. (2009). Single-stranded DNA orchestrates and ATM-to-ATR switch at DNA breaks. Mol. Cell *33,* 547-558.

Shirahige, K.; Hori, Y.; Shiraishi, K.; Yamashita, M.; Takahashi, K.; Obuse, C.; Tsurimoto, T.; Yoshikawa, H. (1998). Regulation of DNA-replication origins during cell-cycle progression. Nature *395,* 618-621.

Shirayama, M.; Zachariae, W.; Ciosk, R.; Nasmyth, K. (1998). The polo-like kinase Cdc5p and the WD-repeat protein Cdc20/fizzy are regulators and substrates of the anaphase promoting complex in *Saccharomyces cerevisiae.* EMBO J. *17,* 1336-1349.

Shroff, R.; Arbel-Eden, A.; Pilch, D.; Ira, G.; Bonner, W.M. (2004). Distribution and dynamics of chromatin modification induced by a defined DNA double-strand break. Curr. Biol. *14,* 1703-1711.

Sirbu, B.M.; Lachmayer, S.J.; Wulfing, V.; Marten, L.M.; Clarkson, K.E.; Lee, L.W.; Gheorghiu, L.; Zou, L.; Powell, S.N.; Dahm-Daphi, J.; Willers, H. (2011). ATR-p53 restricts homologous recombination in response to replicative stress but does not limit DNA interstrand crosslink repair in lung cancer cells. PLoS ONE *6,* e23053.

Smith, G.C.; Divecha, N.; Lakin, N.D.; Jackson, S.P. (1999). DNA-dependent protein kinase and related proteins. Biochem. Soc. Symp. *64,* 91-104.

Smolka, M.B.; Albuquerque, C.P.; Chen, S.H.; Schmidt, K.H.; Wei, X.X.; Kolodner, R.D. Zhou, H. (2005). Dynamic changes in protein-protein interaction and protein phosphorylation probed with amine-reactive isotope tag. Mol. Cell Proteomics *4,* 1358-1369.

Smolka, M.B.; Albuquerque, C.P.; Chen, S.; Zhou, H. (2007). Proteome-wide identification of *in vivo* targets of DNA damage checkpoint kinases. Proc. Natl. Acad. Sci. USA *104,* 10364-10369.

Sogo, J.M.; Lopes, M.; Foiani, M. (2002). Fork reversal and ssDNA accumulation at stalled replication forks owing to checkpoint defects. Science *297,* 599-602.

Sørensen, C.S.; Hansen, L.T.; Dziegielewski, J.; Syljuasen, R.G.; Lundlin, C.; Bartek, J.; Helleday, T. (2005). The cell-cycle checkpoint kinase Chk1 is required for mammalian homologous recombination repair. Nat. Cell Biol. *7,* 195-201.

Sørensen, C.S.; Syljuasen, R.G. (2012). Safeguarding genome integrity: The checkpoint kinases ATR, CHK1 and WEE1 restrain CDK activity during normal DNA replication. Nucl. Acid. Res. *40,* 477-486.

Sorger, P.K.; Murray, A.W. (1992). S-phase feedback control in budding yeast independent of tyrosine phosphorylation of p34(cdc28). Nature *355,* 365-368.

Spagnolo, L.; Rivera-Calzada, A.; Pearl, L.H.; Llorca, O. (2006). Three-dimensional structure of the human DNA-PKcs/Ku70/Ku80 complex assembled on DNA and its implications for DNA DSB repair. Mol. Cell *22,* 511-519.

Stern, A.; Privman, E.; Rasis, M.; Lavi S.; Pupko, T. (2007). Evolution of the metazoan protein phosphatase 2C superfamily. J. Mol. Evol. *64,* 61-70.

Stewart, G.S.; Panier, S.; Townsend, K.; Al-Hakim, A.K.; Kolas, N.K.; Miller, E.S.; Nakada, S.: Ylanko, J.; Olivarius, S.; Mendez, M.; Oldreive, C.; Wildenhain, J.; Tagliaferro, A.; Pelletier, L.; Taubenheim, N.; Durandy, A.; Byrd, P.J.; Stankovic, T.; Taylor, A.M.; Durocher, D. (2009). The RIDDLE syndrome protein mediates a ubiquitin-dependent signaling cascade at sites of DNA damage. Cell *136,* 420-434.

Stracker, T.H.; Usui, T.; Petrini, J.H. (2009). Taking time to make important decisions: the checkpoint effector kinases Chk1 and Chk2 and the DNA damage response. DNA Repair *8,* 1047-1054.

Stueland, C.S.; Lew, D.J.; Cismowski, M.J.; Reed, S.I. (1993). Full activation of p34CDC28 histone H1 kinase activity is unable to promote entry into mitosis in checkpoint-arrested cells of the yeast *Saccharomyces cerevisiae*. Mol. Cell Biol. *13,* 3744-3755.

Sugawara, N.; Wang, X.; Haber, J.E. (2003). *In vivo* roles of Rad52, Rad54, and Rad55 proteins in Rad51-mediated recombination. Mol. Cell *12,* 209-219.

Sun, Z.; Fay, D.S.; Marini, F.; Foiani, M.; Stern, D.F. (1996). Spk1/Rad53 is regulated by Mec1-dependent protein phosphorylation in DNA replication and damage checkpoint pathways. Genes Dev. *10,* 395-406.

Sun, Z.; Hsiao, J.; Fay, D.S.; Stern, D.F. (1998). Rad53 FHA domain associated with phosphorylated Rad9 in the DNA damage checkpoint. Science *281,* 272-274.

Sung, P.; Krejci, L.; et al. (2003). Rad51 recombinase and recombination mediators. J. Biol. Chem. *278,* 42729-42732.

Svendsen, J.M.; Smogorzewska, A.; Sowa, M.E.; O'Connell, B.; Gygi, S.P.; Elledge, S.J. (2009). Mammalian BTBD12/SLX4 assembles a Holliday junction resolvase and is required for DNA repair. Cell *138,* 63-77.

Sweeney, F.D.; Yang, F.; Chi, A.; Shabanowitz, J.; Hunt, D.F.; Durocher, D. (2005). *Saccharomyces cerevisiae* Rad9 acts as a Mec1 adaptor to allow Rad53 activation. Curr. Biol. *15,* 1364-1375.

Szakal, B.; Branzei, D. (2013). Premature Cdk1/Cdc5/Mus81 pathway activation induces aberrant replication and deleterious crossover. EMBO J. *32,* 1155-1167.

Szilard, R.K.; Jacques, P.E.; Laramee, L.; Cheng, B.; Galicia, S.; Bataille, A.R.; Yeung, M.; Mendez, M.; Bergeron, M.; Robert, F.; Durocher, D. (2010). Systematic identification

of fragile sites via genome-wide location analysis of gamma-H2AX. Nat. Struc. Mol. Biol. *17,* 299-305.

Szyjka, S.J.; Aparicio, J.G.; Viggiani, C.J.; Knott, S.; Xu, W.; Tavaré, S.; Aparicio, O.M. (2008). Rad53 regulates replication fork restart after DNA damage in *Saccharomyces cerevisiae*. Genes Dev. *22,* 1906-1920.

Tacar, O.; Sriamomsak, P.; Dass, C.R. (2013). Doxorubicin: an update on anticancer molecular action, toxicity and novel drug delivery systems. J. Pharm. Pharmacol. *65,* 157-170.

Tak, Y.S.; Tanaka, Y.; Endo, S.; Kamimura, Y.; Araki, H. (2006). A CDK-catalysed regulatory phosphorylation for formation of the DNA replication complex Sld2-Dpb11. EMBO J. *25,* 1987-1996.

Takai, H.; Tominaga, K.; Motoyama, N.; Minamishima, Y.A.; Nagahama, H.; Tsukiyama, T.; Ikeda, K.; Nakayama, K.; Nakanishi, M.; Nakayama, K. (2000). Aberrant cell cycle checkpoint function and early embryonic death in Chk1 (-/-) mice. Genes Dev. *14*, 1439-1447.

Takekawa, M.; Adachi, M.; Nakahata, A.; Nakayama, I.; Itoh, F.; Tsukuda, H.; Taya, Y.; Imai, K. (2000). p53-inducible Wip1 phosphatase mediates a negative feedback regulation of p38 MAPK-p53 signaling in response to UV radiation. EMBO J. *19,* 6517-6526.

Tan, Y.S.; Morcos, P.A.; Cannon, J.F. (2003). Pho85 phosphorylates the Glc7 protein phosphatase regulator Glc8 in vivo. J Biol Chem *278,* 147-153.

Tanaka, K.; Russell, P. (2001). Mrc1 channels the DNA replication arrest signal to checkpoint kinase Cds1. Nat. Cell Biol. *3,* 966-972.

Tanaka, S.; Araki, H. (2010). Regulation of the initiation step of DNA replication by cyclin-dependent kinases. Chromosoma *119,* 565-574.

Tanaka, S.; Nakato, R.; Katou, Y.; Shirahige, K.; Araki, H. (2011). Origin association of Sld3, Sld7, and Cdc45 proteins is a key step for determination of origin-firing timing. Curr. Biol. *21,* 2055-2063.

Tercero, J.A.; Longhese, M.P.; Diffley, J.F. (2003). A central role for DNA replication forks in checkpoint activation and response. Mol. Cell *11,* 1323-1336.

Thiriet, C.; Hayes, J.J. (2005). Replication-independent core histone dynamics at transcriptionally active loci *in vivo.* Genes Dev. *19,* 677-682.

Thompson, J.; Lepikhova, T.; Teixido-Travesa, N.; Whitehead, M.A.; Palvimo, J.J.; Janne, O.A. (2006). Small carboxyl-terminal domain phosphatase 2 attenuates androgen-dependent transcription. EMBO J. *25,* 2757-2767.

Tkach, J.M.; Yimit, A.; Lee, A.Y.; Riffle, M.; Costanzo, M.; Jaschob, D.; Hendry, J.A.; Ou, J.; Moffat, J.; Boone, C.; Davis, T.N.; Nislow, C.; Brown, G.W. (2012). Dissecting DNA damage response pathways by analyzing protein localization and abundance changes during DNA replication stress. Nat. Cell Biol. *14,* 966-976.

Toh, G.W.; O'Shaughnessy, A.M.; Jimeno, S.; Dobbie, I.M.; Grenon, M.; Maffini, S.; O'Rorke, A.; Lowndes, N.F. (2006). Histone H2A phosphorylation and H3 methylation are required for a novel Rad9 DSB repair function following checkpoint activation. DNA Repair *5,* 693-703.

Toledo, L.I.; Murga, M.; Fernandez-Capetillo, O. (2011). Targeting ATR and Chk1 kinases for cancer treatment: a new model for new (and old) drugs. Mol. Oncol. *5,* 368-373. (a)

Toledo, L.I.; Murga, M.; Zur, R.; Soria, R.; Rodriguez, A.; Martinez, S.; Oyarzabal, J.; Pastor, J.; Bischoff, J.R.; Fernandez-Capetillo, O. (2011). A cell-based screen identifies ATR inhibitors with synthetic lethal properties for cancer-associated mutations. Nat. Struct. Mol. Biol. *18,* 721-727. (b)

Toledo, L.I.; Altmeyer, M.; Rask, M.B.; Lukas, C.; Larsen, D.H.; Povlsen, L.K.; Bekker-Jensen, S.; Mailand, N.; Bartek, J.; Lukas, J. (2013). ATR prohibits replication catastrophe by preventing global exhaustion of RPA. Cell *155,* 1088-1103.

Tong, A. H.; Evangelista, M.; Parsons, A.B.; Xu, H.; Bader, G.D.; Pagé, N.; Robinson, M.; Raghibizadeh, S.; Hogue, C.W.; Bussey, H.; Andrews, B.; Tyers, M.; Boone, C. (2001). Systematic genetic analysis with ordered arrays of yeast deletion mutants. Science *294,* 2364-2368.

Tong, A. H.; *et al.* (2004). Global mapping of the yeast genetic interaction network. Science *303,* 808-813.

Toueille, M.; El-Andaloussi, N.; Frouin, I.; Freire, R.; Funk, D.; Shevelev, I.; Friedrich-Heineken, E.; Villani, G.; Hottiger, M.O.; Hübscher, U. (2004). The human Rad9/Rad1/Hus1 damage sensor clamp interacts with DNA polymerase β and increases its DNA substrate utilisation efficiency: implications for DNA repair. Nucleic Acids Res. *32,* 3316-3324.

Tourrière, H.; Versini, G.; Cordón-Preciado, V.; Alabert, C.; Pasero, P. (2005). Mrc1 and Tof1 promote replication fork progression and recovery independently of Rad53. Mol. Cell *19,* 699-706.

Traven, A.; Heierhorst, J. (2005). SQ/TQ cluster domains: concentrated ATM/ATR kinase phosphorylation site regions in DNA-damage-response proteins. BioEssay *27,* 397-407.

Travesa, A.; Duch, A.; Quintana, D.G. (2008). Distinct phosphatases mediate the deactivation of the DNA damage checkpoint kinase Rad53. J. Biol. Chem. *283,* 17123-17130.

Travesa, A.; Kuo, D.; de Bruin, R.A.; Kalashnikova, T.I.; Guaderrama, M.; Thai, K.; Aslanian, A.; Smolka, M.B.; Yates, J.R. 3rd; Ideker, T.; et al (2012). DNA replication stress differentially regulates G1/S genes via Rad53-dependent inactivation of Nrm1. EMBO J. *31.* 1811-1822.

Uhlmann, F.; Lottspeich, F.; Nasmyth, K. (1999). Sister-chromatid separation at anaphase onset is promoted by cleavage of the cohesion subunit Scc1. Nature *400,* 37-42.

van Attikum, H.; Fritsch, O.; Hohn, B.; Gasser, S.M. (2004). Recruitment of the INO80 complex by H2A phosphorylation links ATP-dependent chromatin remodeling with DNA double-strand break repair. *119,* 777-788.

van Attikum, H.; Gasser, S.M. (2009). Crosstalk between histone modifications during the DNA damage response. Trends Cell Biol. *19,* 207-217.

Van Deursen, F.; Sengupta, S.; de Piccoli, G.; Sanchez-Diaz, A.; Labib, K. (2012). Mcm10 associates with the loaded DNA helicase at replication origins and defines a novel step in its activation. EMBO J. *31,* 2195-2206.

van Leeuwen, F.; Gafken, P.R.; Gottschling, D.E. (2002). Dot1p modulates silencing in yeast by methylation of the nucleosome core. Cell *109,* 745-756.

Vaze, M.B., Pellicioli, A., Lee, S. E., Ira, G., Liberi, G., Arbel-Eden, A., Foiani, M., and Haber, J. E. (2002). Recovery from checkpoint-mediated arrest after repair of a double-strand break requires Srs2 helicase. Mol. Cell *10,* 373-385.

Vialard, J.E.; Gilbert, C.S.; Green, C.M.; Lowndes, N.F. (1998). The budding yeast Rad9 checkpoint protein is subject to Mec1/Tel1-dependent hyperphosphorylation and interacts with Rad53 after DNA damage. EMBO J. *17,* 5679-5688.

Vincent, J.A.; Kwong, T.J.; Tsukiyama, T. (2008). ATP-dependent chromatin remodeling shapes the DNA replication landscape. Nat. Struct. Mol. Biol. *15,* 477-484.

Virshup, D.M.; Shenolikar, S. (2009). From promiscuity to precision: protein phosphatases get a makeover. Mol. Cell *33,* 537-545.

Walker, J.R.; Corpina, R.A.; Goldberg, J. (2001). Structure of the Ku heterodimer bound to DNA and its implications for double-strand break repair. Nature *412,* 607-614.

Walker, M.; Black, E.J.; Oehler, V.; Gillespie, D.A.; Scott, M.T. (2009). Chk1 C-terminal regulatory phosphorylation mediates checkpoint activation by de-repression of Chk1 catalytic activity. Oncogene *28,* 2314-2323.

Wang, Y.; Hu, F.; Elledge, S.J. (2000). The Bfa1/Bub2 GAP complex comprises universal checkpoint required to prevent mitotic exit. Curr. Biol. *10,* 1379-1382.

Wang, H.; Elledge, S.J. (2002). Genetic and physical interactions between DPB11 and DDC1 in the yeast DNA damage response pathway. Genetics *160,* 1295-1304.

Wang, J.C. (2002). Cellular roles of DNA topoisomerases: a molecular perspective. Nat. Rev. Mol. Cell Biol. *3,* 430-440.

Wang, W.; Brandt, P.; Rossi, M.L.; Lindsey-Boltz, L.; Podust, V.; Fanning, E.; Sancar, A.; Bambara, R.A. (2004). The human Rad9-Rad1-Hus1 checkpoint complex stimulates flap endonuclease 1. Proc. Natl. Acad. Sci. *101,* 16762-16767.

Wang, G.; Tong, X.; Weng, S.; Zhou, H. (2012). Multiple phosphorylation of Rad9 by CDK is required for DNA damage checkpoint activation. Cell Cycle *11,* 3792-3800.

Wardlaw, C.P.; Carr, A.M.; Oliver, A.W. (2014). TopBP1: A BRCT-scaffold protein functioning in multiple cellular pathways. DNA Repair *22,* 165-174.

Watase, G.; Takisawa, H.; Kanemaki, M.T. (2012). Mcm10 plays a role in functioning of the eukaryotic replicative DNA helicase, Cdc45-Mcm-GINS. Curr. Biol. *22,* 343-349.

Watts, F.Z. (2006). Sumoylation of PCNA: Wrestling with recombination at stalled replication forks. DNA Repair *5,* 399-403.

Weinert, T.A.; Hartwell, L.H. (1988). The *RAD9* gene controls the cell cycle response to DNA damage in *Saccharomyces cerevisiae.* Science *241,* 317-322.

Weinert, T.A.; Kiser, G.L.; Hartwell, L.H. (1994). Mitotic checkpoint genes in budding yeast and the dependence of mitosis on DNA replication and repair. Genes Dev. *8,* 652-665.

Weinreich, M.; Stillman, B. (1999). Cdc7p-Dbf4p kinase binds to chromatin during S phase and is regulated by both the APC and the *RAD53* checkpoint pathway. EMBO J. *18,* 5334-5346.

Weterings, E.; Verkaik, N.S.; Bruggenwirth, H.T.; Hoeijmakers, J.H.; van Gent, D.C. (2003). The role of DNA dependent protein kinase in synapsis of DNA ends. Nucleic Acids Res. *31,* 7238-7246.

Williams, J.S.; Williams, R.S.; Dovery, C.L.; Guenther, G.; Tainer, J.A.; Russell, P. (2010). GammaH2A binds Brc1 to maintain genome integrity during S-phase. EMBO J. *29,* 1136-1148.

Williams-Hart, T.; Wu, X.; Tatchell, K. (2002). Protein phosphatase type 1 regulates ion homeostatis in *Saccharomyces cerevisiae.* Genetics *160,* 1423-1437.

Wold, M.S. (1997). Replication protein A: a heterotrimeric, single-stranded DNA-binding protein required for eukaryotic DNA metabolism. Annu. Rev. Biochem. *66,* 61-92.

Wysocki, R.; Javaheri, A.; Allard, S.; Sha, F.; Cote, J.; *et al.* (2005). Role of Dot1-dependent H3 methylation in G1 and S phase DNA damage checkpoint functions of Rad9. Mol. Cell. Biol. *25,* 8430-8443.

Xu, X.; Tsvetkov, L.M.; Stern, D.F. (2002). Chk2 activation and phosphorylation-dependent oligomerization. Mol. Cell. Biol. *22,* 4419-4432.

Yamamoto, A.; Guacci, V.; Koshland, D. (1996). Pds1p, an inhibitor of anaphase in budding yeast, plays a critical role in the APC and checkpoint pathway(s). J. Cell Biol. *133,* 99-110.

Yeh, P.Y.; Yeh, K.H.; Chuang, S.E.; Song, Y.C.; Cheng, A.I. (2004). Suppression of MEK/ERK signaling pathway enhances cisplatin-induced NF-kappaB activation by protein phosphatase 4-mediated NF-kappaB p65 Thr dephosphorylation. J. Biol. Chem. *279,* 26143-26148.

Yeo, M.; Lee, S.K.; Lee, B.; Ruiz, E.C.; Pfaff, S.L.; Gill, G.N. (2005). Small CTD phosphatases function in silencing neuronal gene expression. Science *307,* 596-600.

Yong, W.; Bao, S.; Chen, H.; Li, D.; Sanchez, E.R.; Shou, W. (2007). Mice lacking protein phosphatase 5 are defective in ataxia telangiectasia mutated (ATM)-mediated cell cycle arrest. J. Biol. Chem. *282,* 14690-14694.

Zegerman, P.; Diffley, J.F. (2009). DNA replication as a target of the DNA damage checkpoint. DNA Repair *8,* 1077-1088.

Zegerman, P.; Diffley, J.F. (2010). Checkpoint-dependent inhibition of DNA replication initiation by Sld3 and Dbf4 phosphorylation. Nature *467,* 474-478.

Zhang, J.; Bao, S.; Furumai, R.; Kucera, K.S.; Ali, A.; Dean, N.M.; Wang, X.F. (2005). Protein phosphatase 5 is required for ATR-mediated checkpoint activation. Mol. Cell Biol. *25,* 9910-9919.

Zhang, T.; Nirantar, S.; Lim, H.H.; Sinha, I.; Surana, U. (2009). DNA damage checkpoint maintains Cdh1 in an active state to inhibit anaphase progression. Dev. Cell *17,* 541-551.

Zhang, X.; Ozawa, Y.; Lee, H.; Wen, Y.D.; Tan, T.H.; Wadzinski, B.E.; Seto, F. (2005). Histone deacetylase 3 (HDAC3) activity is regulated by interaction with protein serine/threonine phosphatase 4. Genes Dev. *19,* 827-839.

Zhao, X.; Chabes, A.; Domkin, V.; Thelander,L.; Rothstein, R. (2001). The ribonucleotide reductase inhibitor Sml1 is a new target of the Mec1/Rad53 kinase cascade during growth and in response to DNA damage. EMBO J. *20,* 3544-3553.

Zhao, X.; Rothstein, R. (2002). The Dun1 checkpoint kinase phosphorylates and regulates the ribonucleotide reductase inhibitor Sml1. Proc. Natl. Acad. Sci. USA *99,* 3746-3751.

Zhao, X.; Blobel, G. (2005). A SUMO ligase is part of a nuclear multiprotein complex that affects DNA repair and chromosomal organization. PNAS *102,* 4777-4782.

Zhao, X.; Muller, E.G.; Rothstein, R. (1998). A suppressor of two essential checkpoint genes identifies a novel protein that negatively affects dNTP pools. Mol. Cell *2,* 329-340.

Zhou, Z.; Elledge, S.J. (1993). *DUN1* encodes a protein kinase that controls the DNA damage response in yeast. Cell *75,* 1119-1127.

Zhu, Z.; Chung, W.H.; Shim, E.Y.; Lee, S.E.; Ira, G. (2008). Sgs1 helicase and two nucleases Dna2 and Exo1 resect DNA double-strand break ends. Cell *134,* 981-994.

Zou, L., and Elledge, S. J. (2003). Sensing DNA damage through ATRIP recognition of RPA-ssDNA complexes. Science *300,* 1542-1548.

Zuo, Z.; Dean, N.M.; Honkanen, R.E. (1998). Serine/threonine protein phosphatase type 5 acts upstream of p53 to regulate the induction of p21 (WAF1/Cip1) and mediate growth arrest. J. Biol. Chem. *273,* 12250-12258.